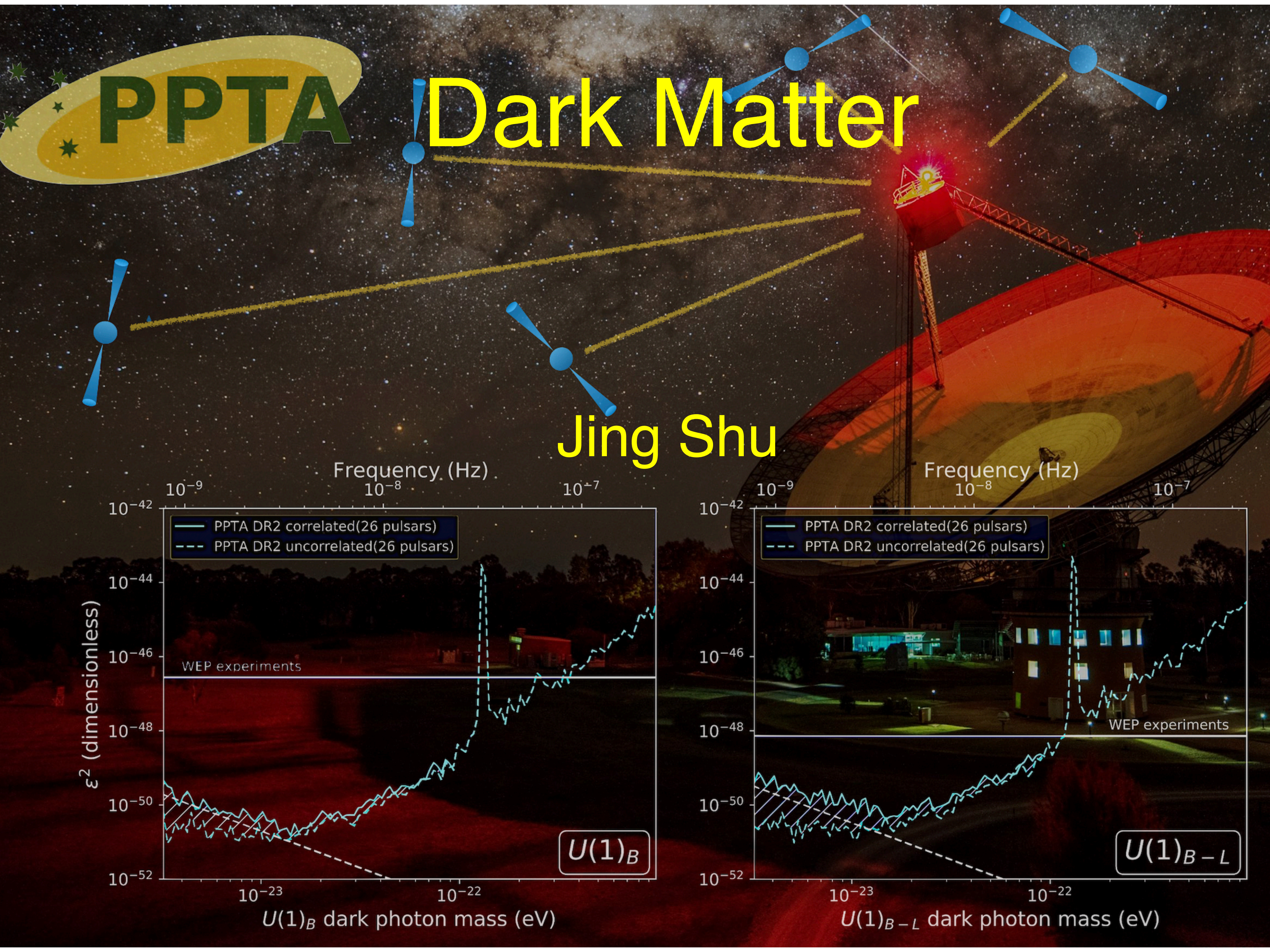
PPTA
Dark Matter
Jing Shu
Frequency (Hz)
10^-9
10^-8
10^-7
10^-42
10^-44
10^-46
10^-48
10^-50
10^-52
ε^2 (dimensionless)
PPTA DR2 correlated(26 pulsars)
PPTA DR2 uncorrelated(26 pulsars)
WEP experiments
U(1)_B
10^-23
10^-22
U(1)_B dark photon mass (eV)
Frequency (Hz)
10^-9
10^-8
10^-7
10^-42
10^-44
10^-46
10^-48
10^-50
10^-52
PPTA DR2 correlated(26 pulsars)
PPTA DR2 uncorrelated(26 pulsars)
WEP experiments
U(1)_B-L
10^-23
10^-22
U(1)_B-L dark photon mass (eV)

Outlines

- Introduction to DM
- Properties of DM
- Detection Methods of DM
  - Particle-like DM Detection
  - Wave-like DM Detection
- Summary and Outlook

Introduction to DM

Hierarchical Structure of the Universe

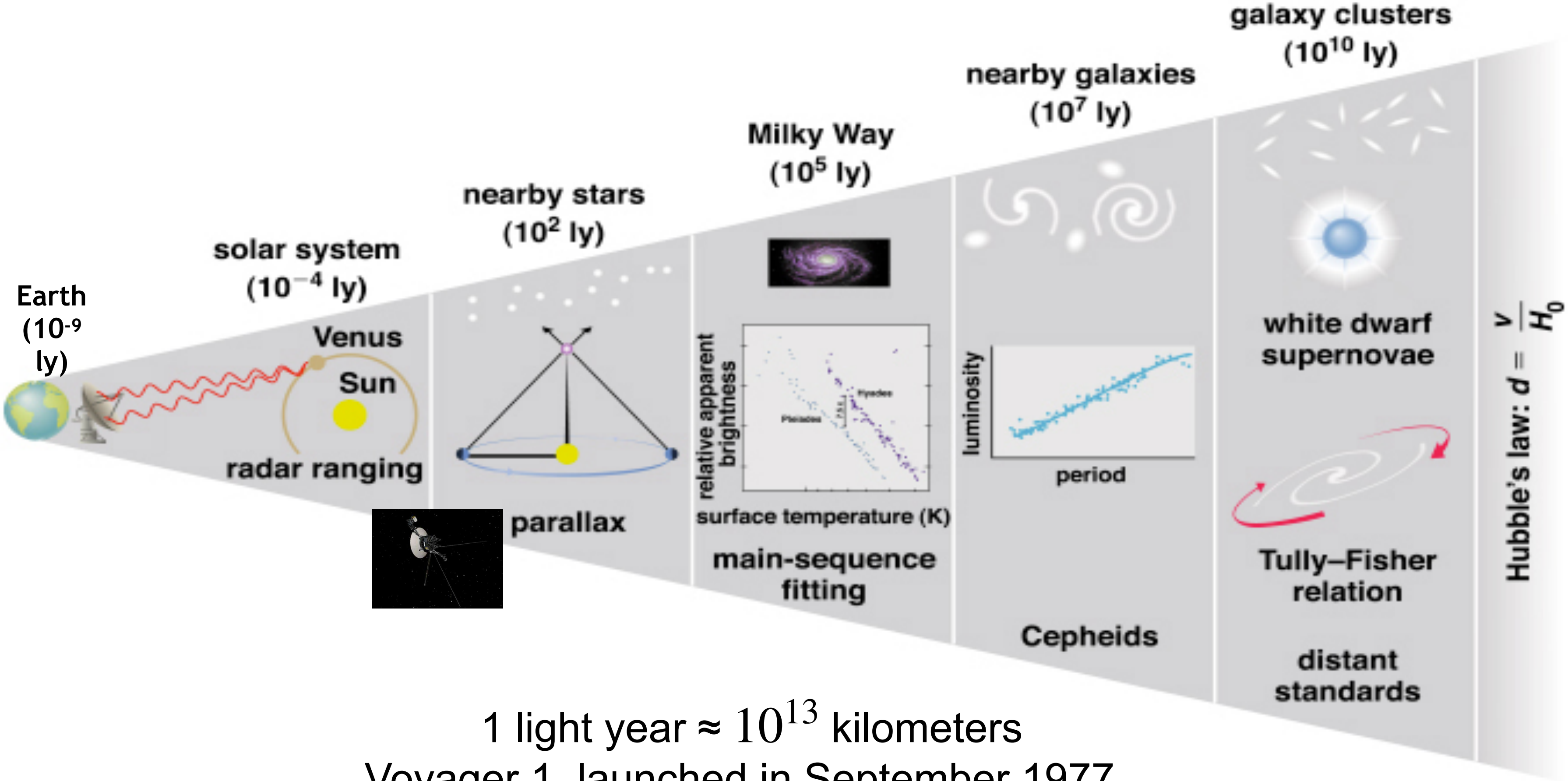

1 light year ≈ 10^{13} kilometers
Voyager 1, launched in September 1977, only exited the solar system in 2012, and is "just" about 20 billion kilometers away from Earth!

How to "Weigh" Celestial Bodies?

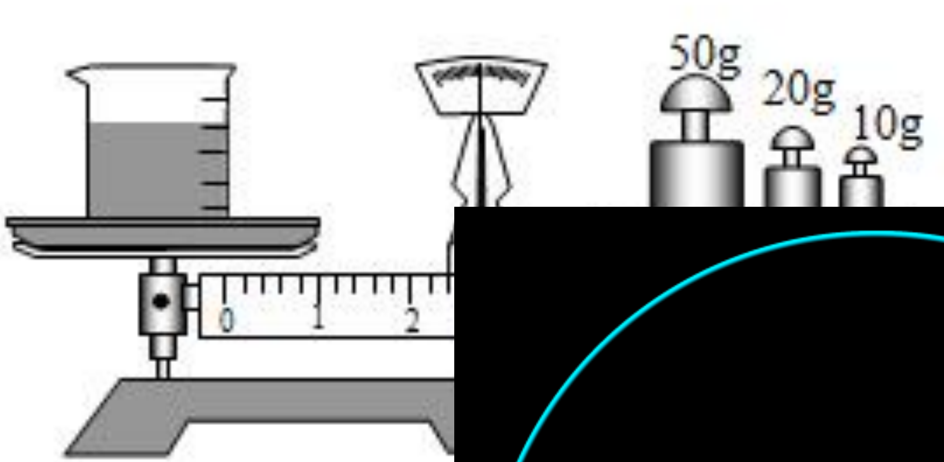

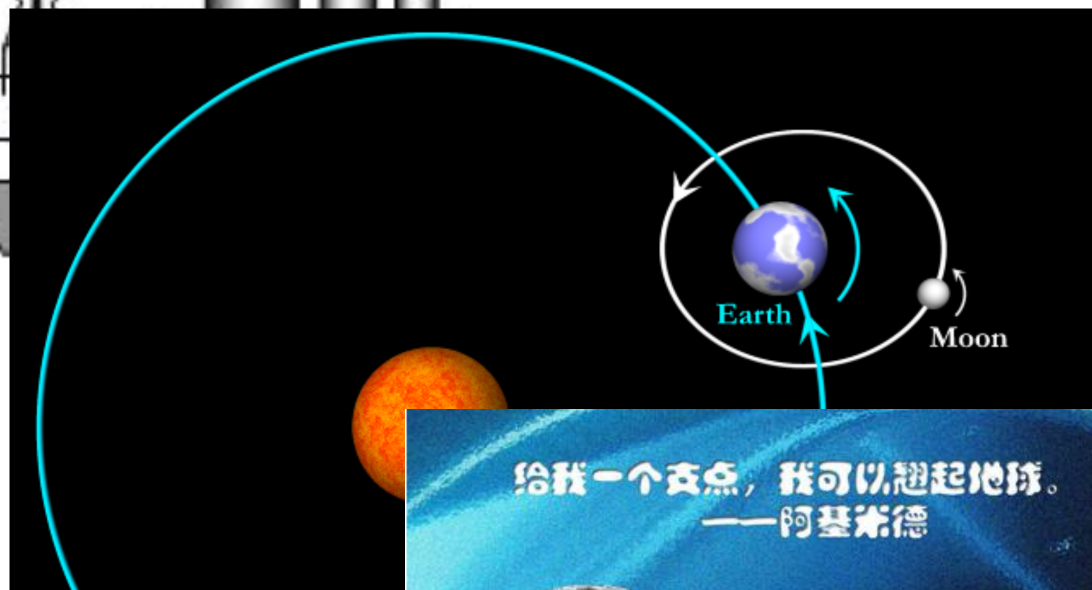

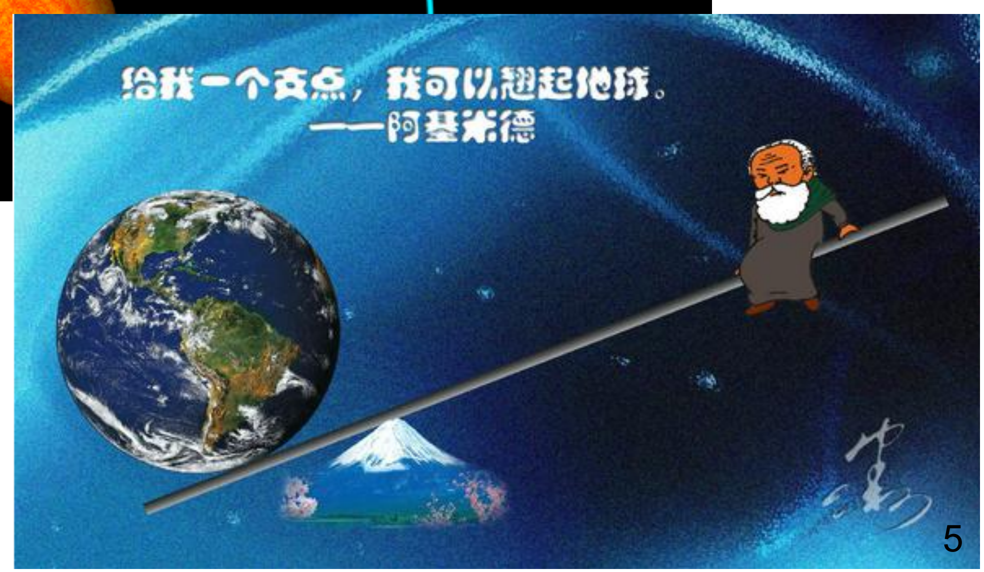

Newton's Laws

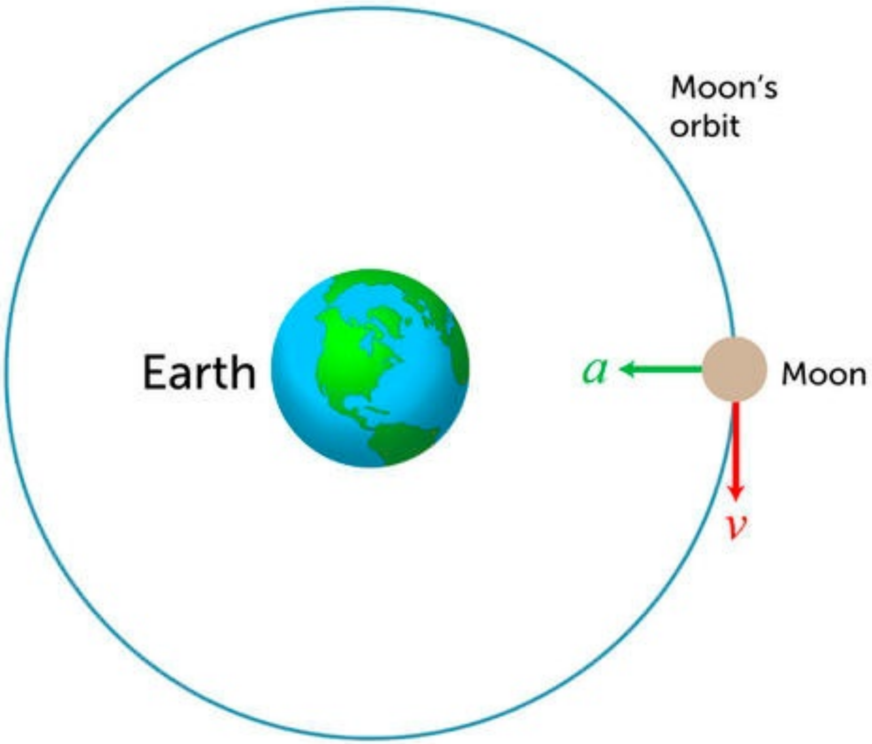

$$\frac{GMm}{r^2} = \frac{mv^2}{r}$$

$$v = \sqrt{\frac{GM}{r}}$$

Rotation Curve in Solar System

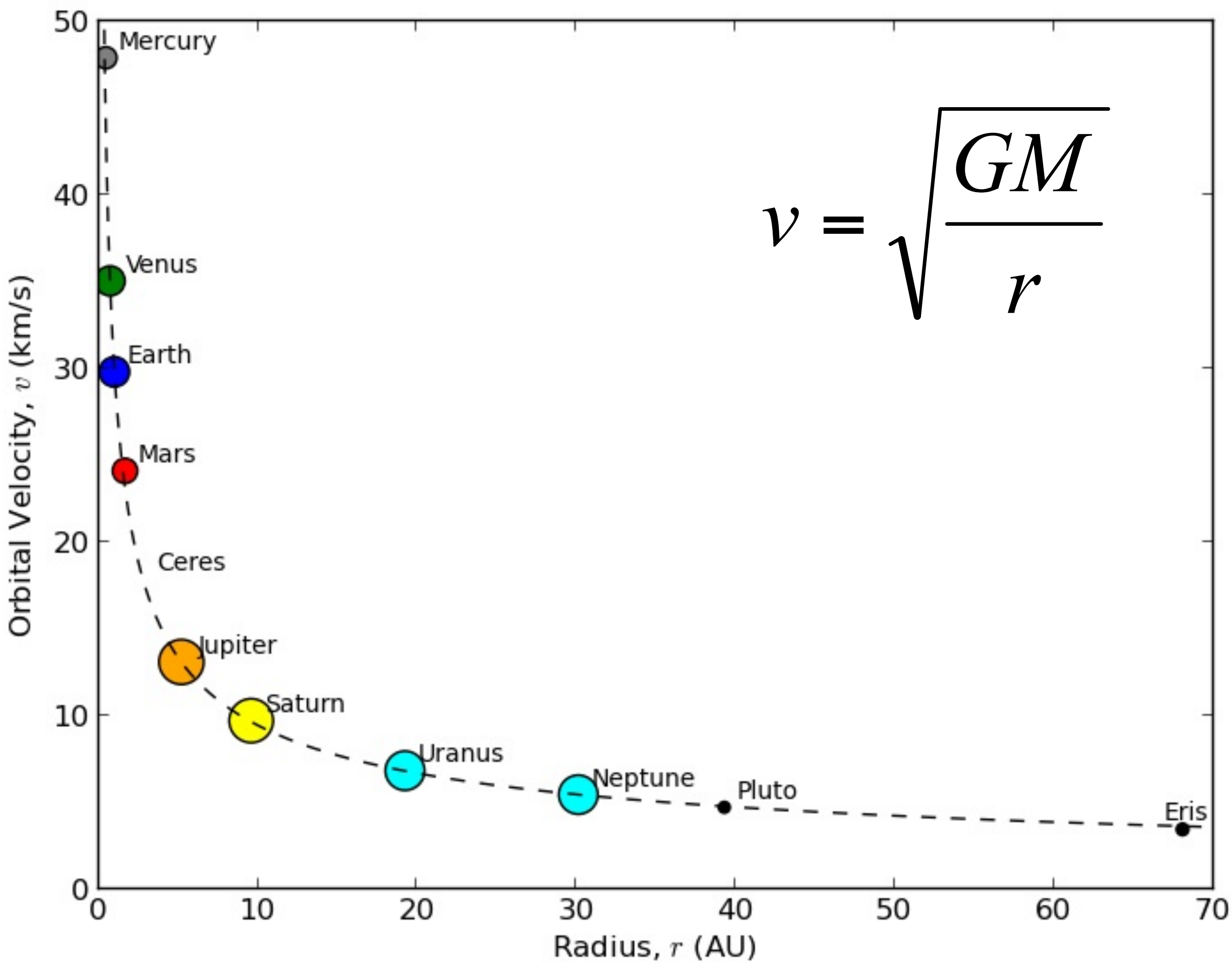

$$v = \sqrt{\frac{GM}{r}}$$

Rotation Curve in Spiral Galaxy

Vera Rubin

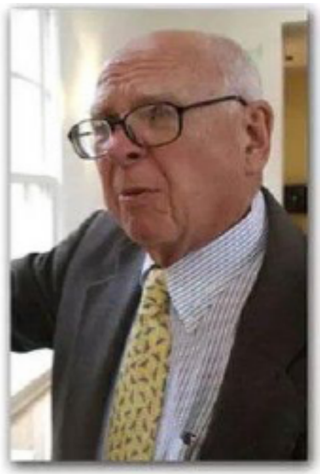

Kent Ford

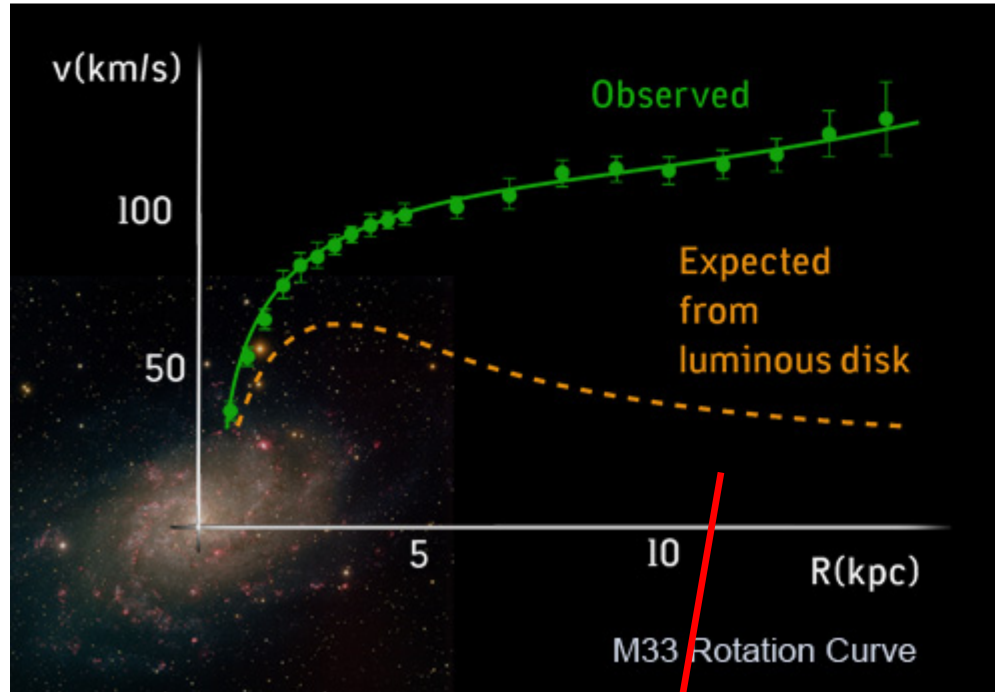

Completely different from the square root decline law (Kepler's laws)!

Possible non-luminous (dark) matter

Gravitational Lensing

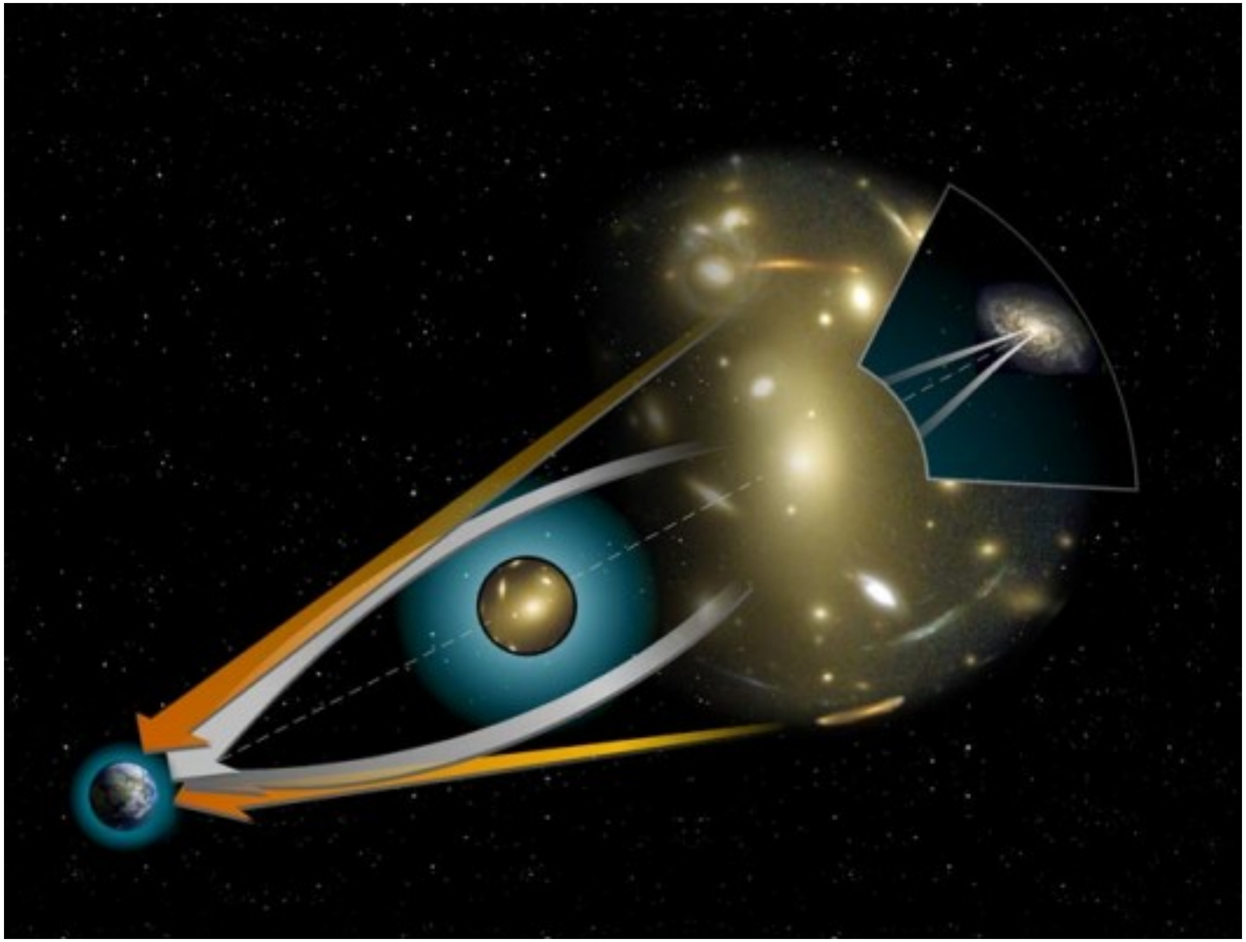

Bullet Cluster: Compelling Evidence for the Existence of Dark Matter

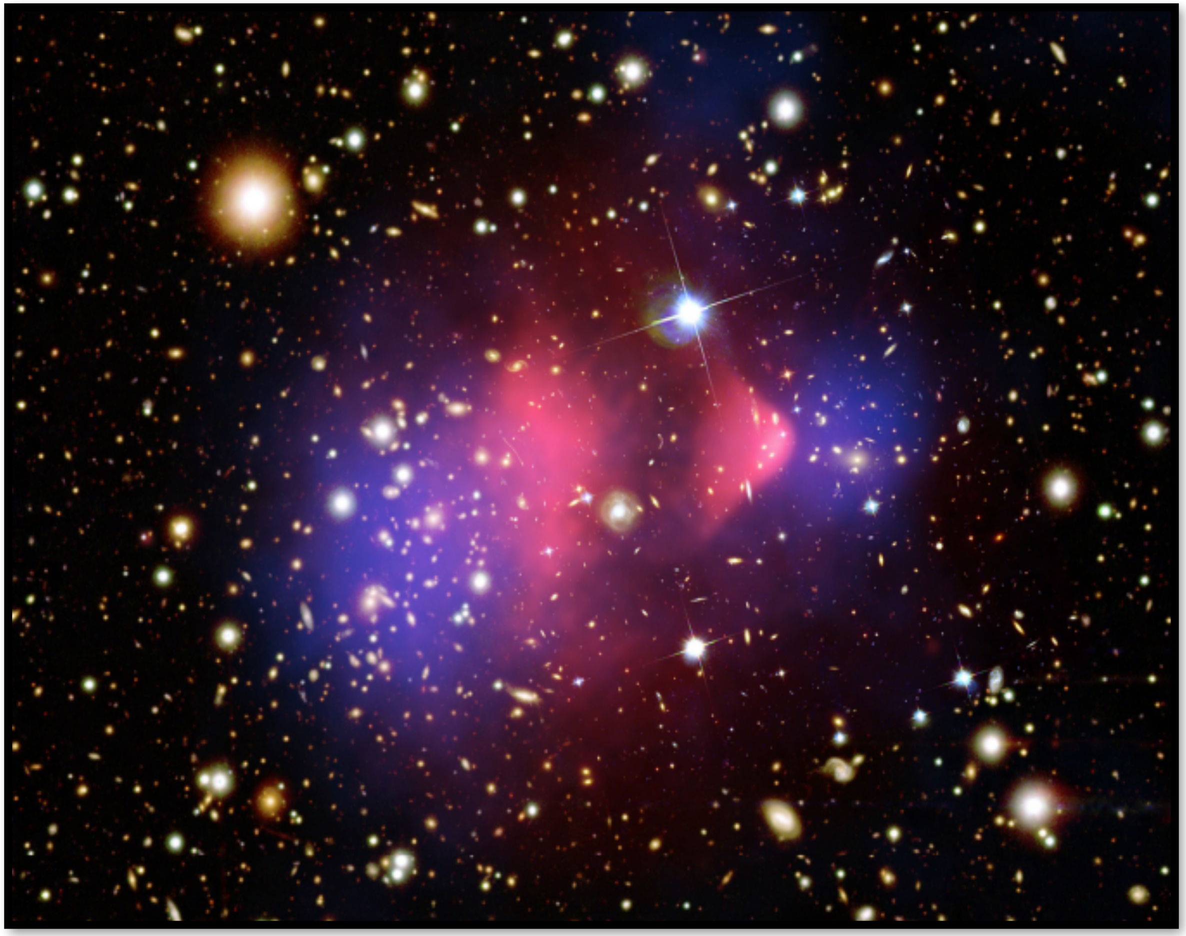

Clowe et al. (2006)

Red: Mass Distribution of X-ray Gas

Blue: Mass Distribution from Gravitational Lensing

Large-Scale Structure: Cold Dark Matter

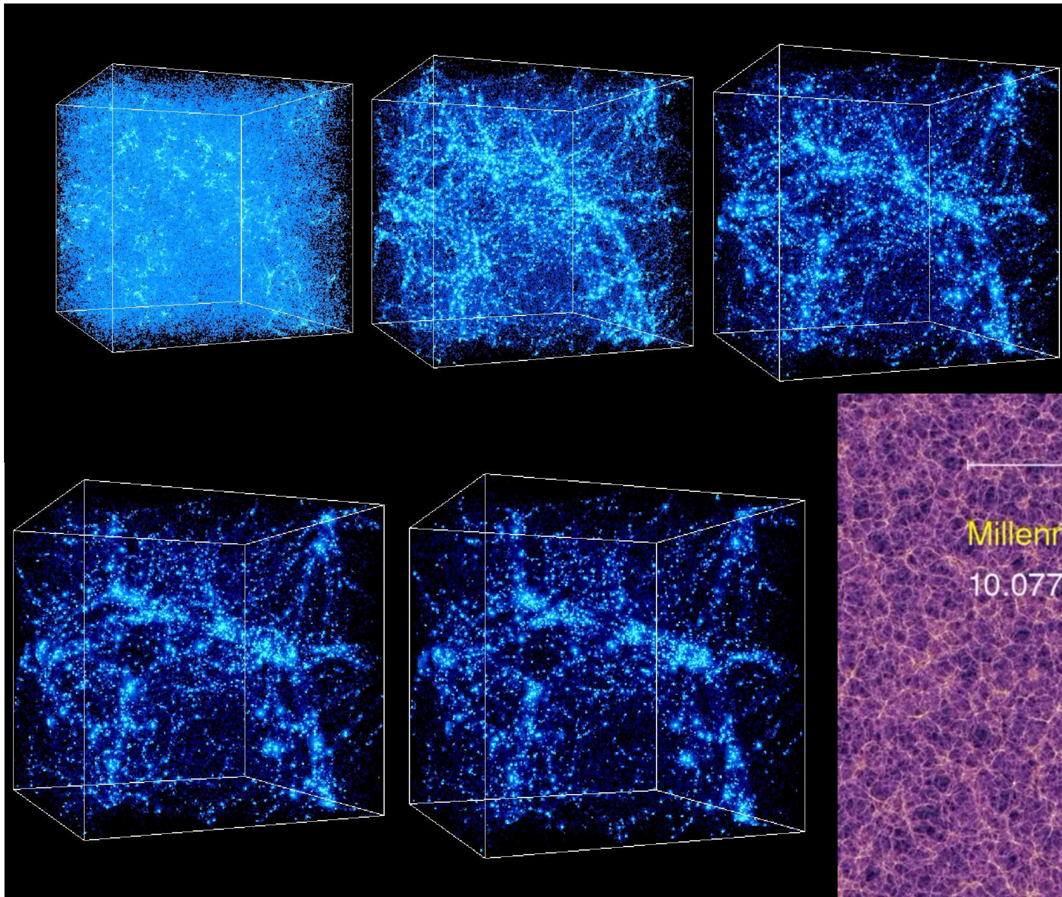

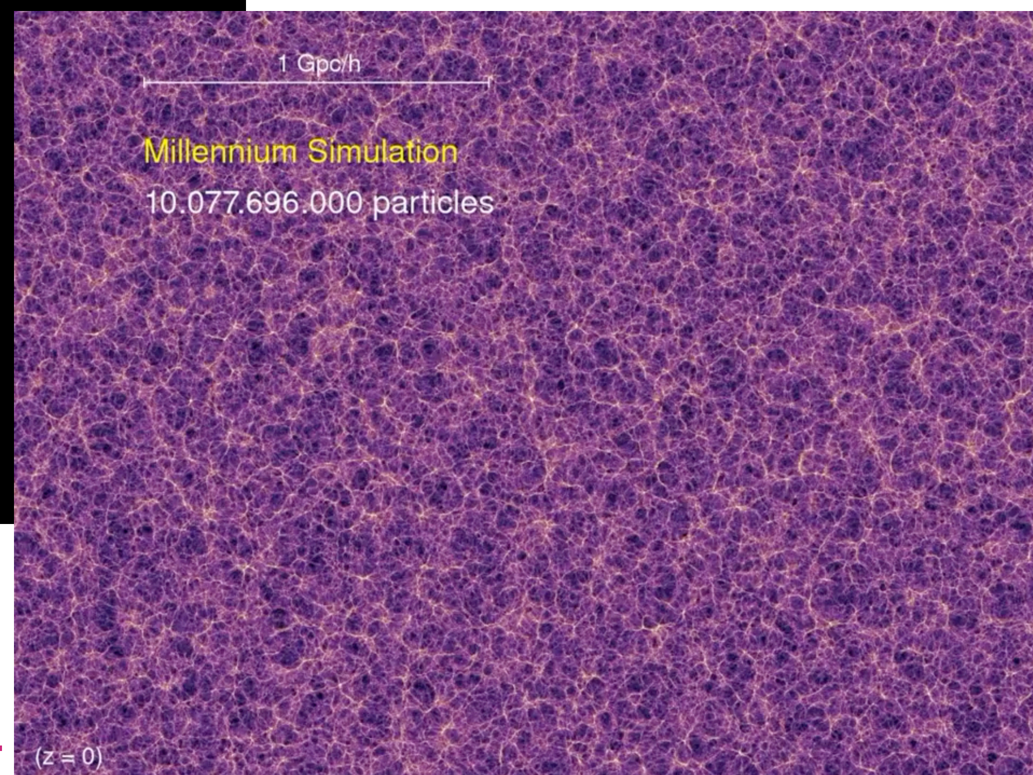

The *Millennium Run* used more than 10 billion particles to trace the evolution of the matter distribution in a cubic region of the Universe over 2 billion light-years on a side.

Composition of the Universe

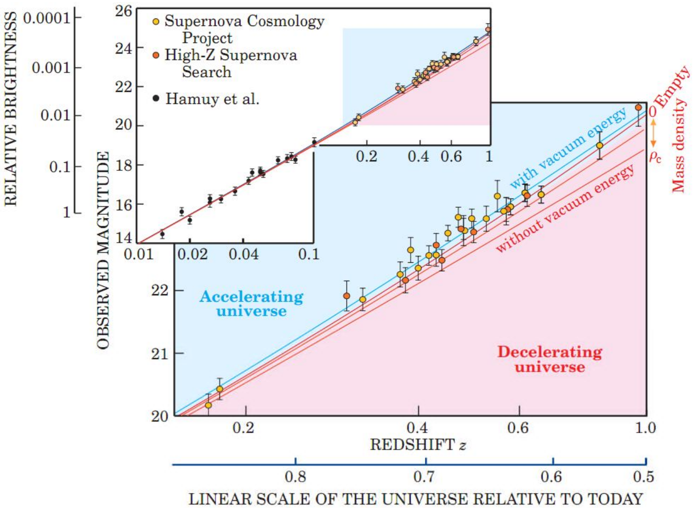

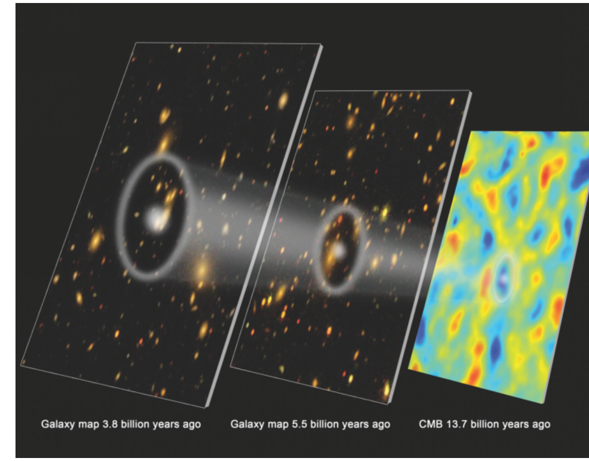

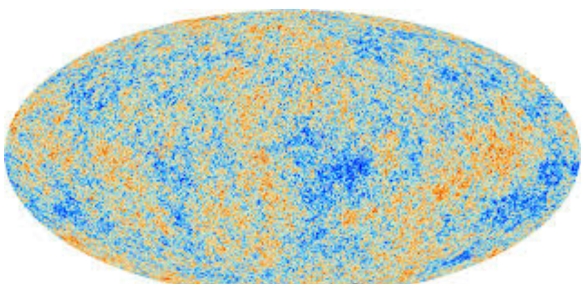

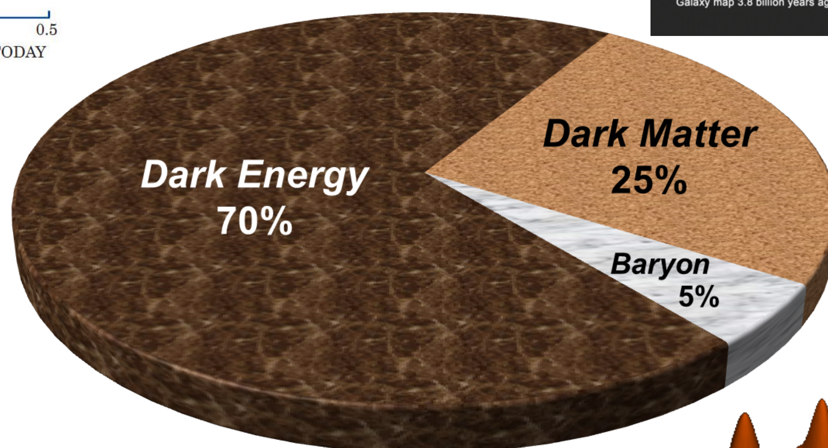

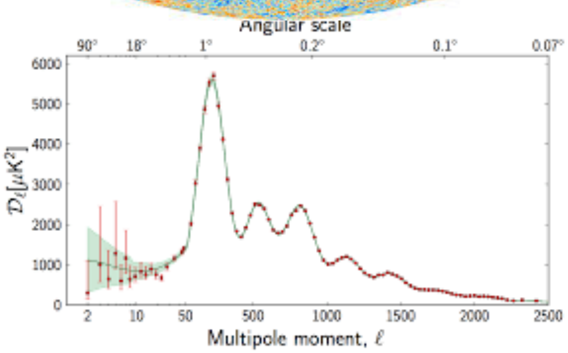

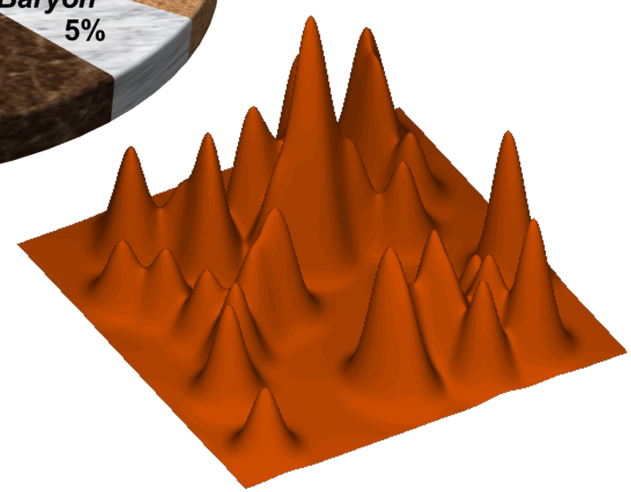

NO!

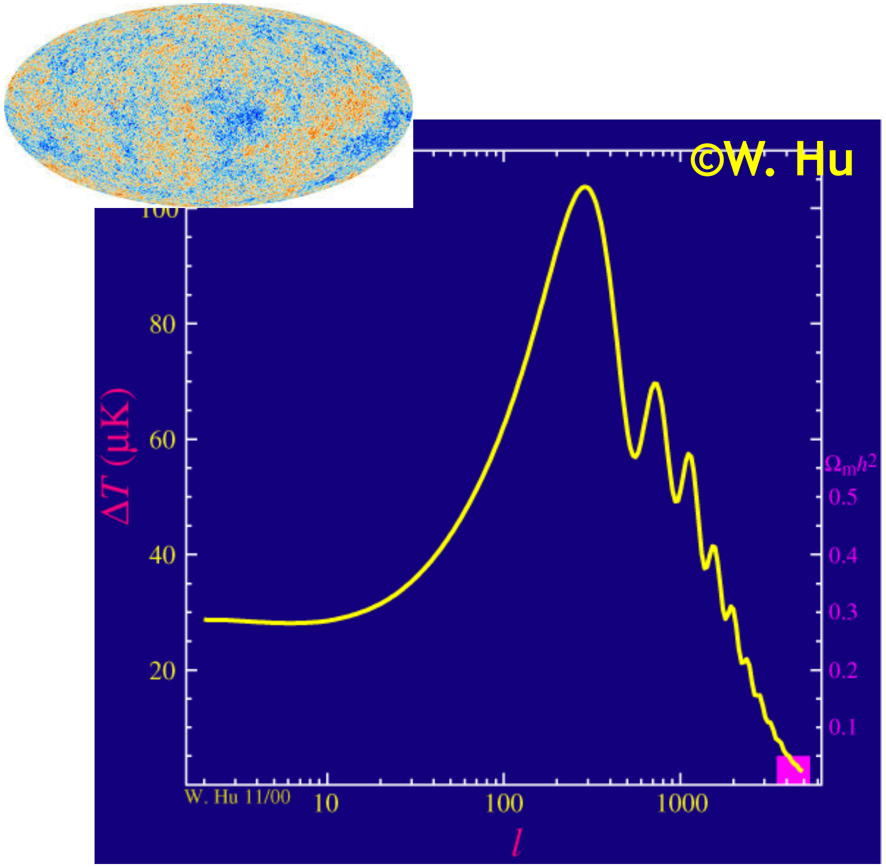

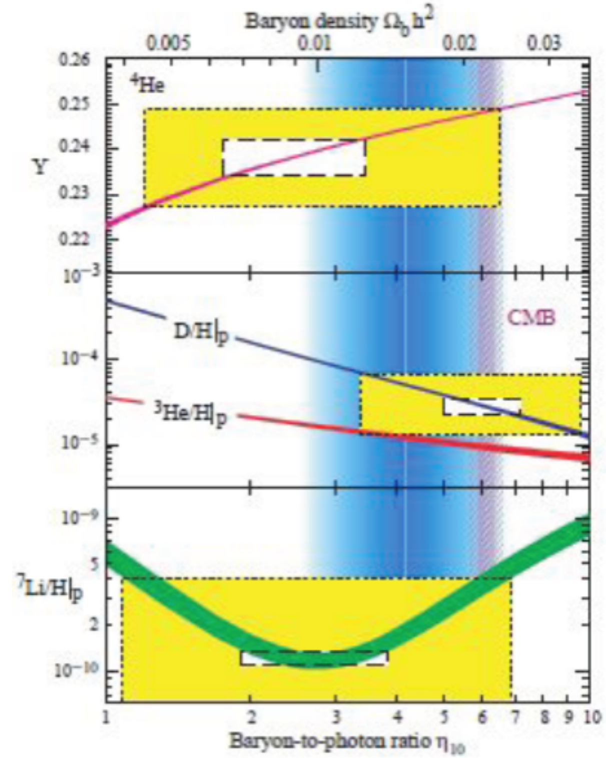

Cosmic Microwave Background(CMB) Radiation Anisotropy:

Ω_b~0.05, Ω_{dm}~0.25

Abundance of light elements predicted by Big Bang Nucleosynthesis(BBN)： Ω_b~0.05 (Fields and Sarkar 2004)

The nature of DM is different from baryonic matter!

Can we see DM with telescopes powerful enough?

Thirty Meter Telescope (TMT)

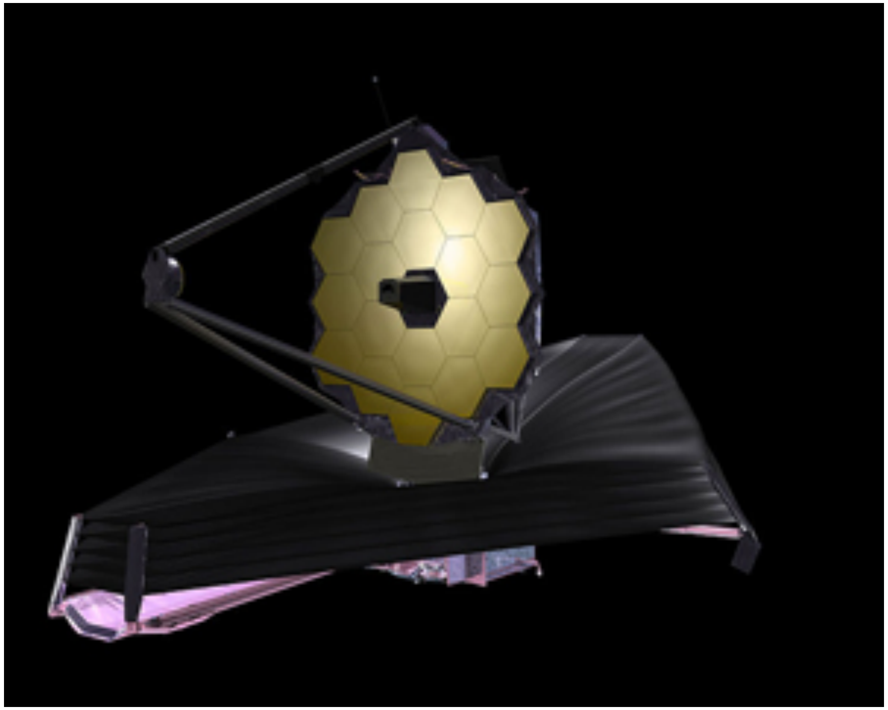

James Webb 6.5-meter Space Telescope

Do the laws of gravity hold true anywhere and anytime?

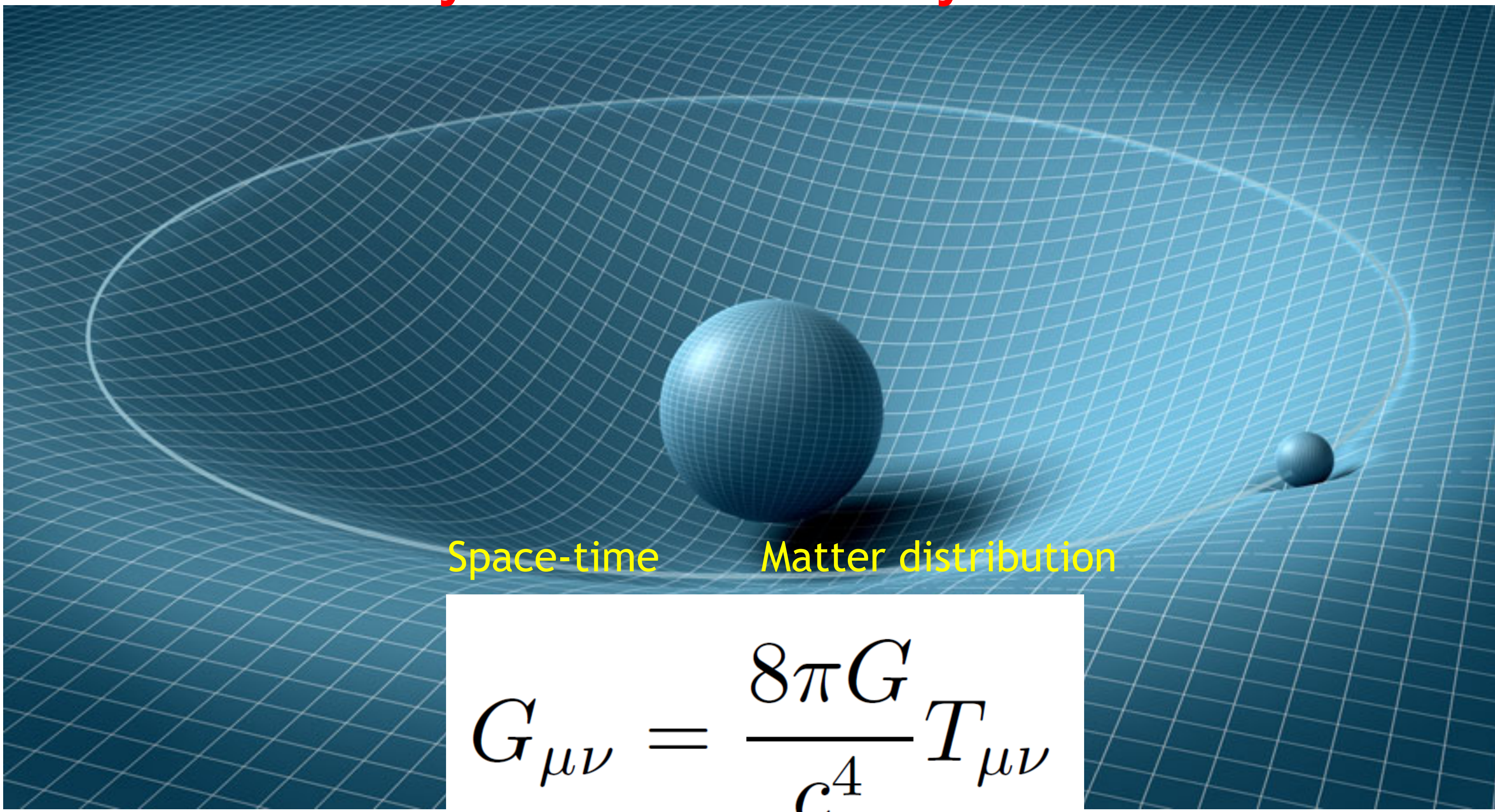

$$G_{\mu\nu} = \frac{8\pi G}{c^4} T_{\mu\nu}$$

Attempts to Modify the Laws of Gravity

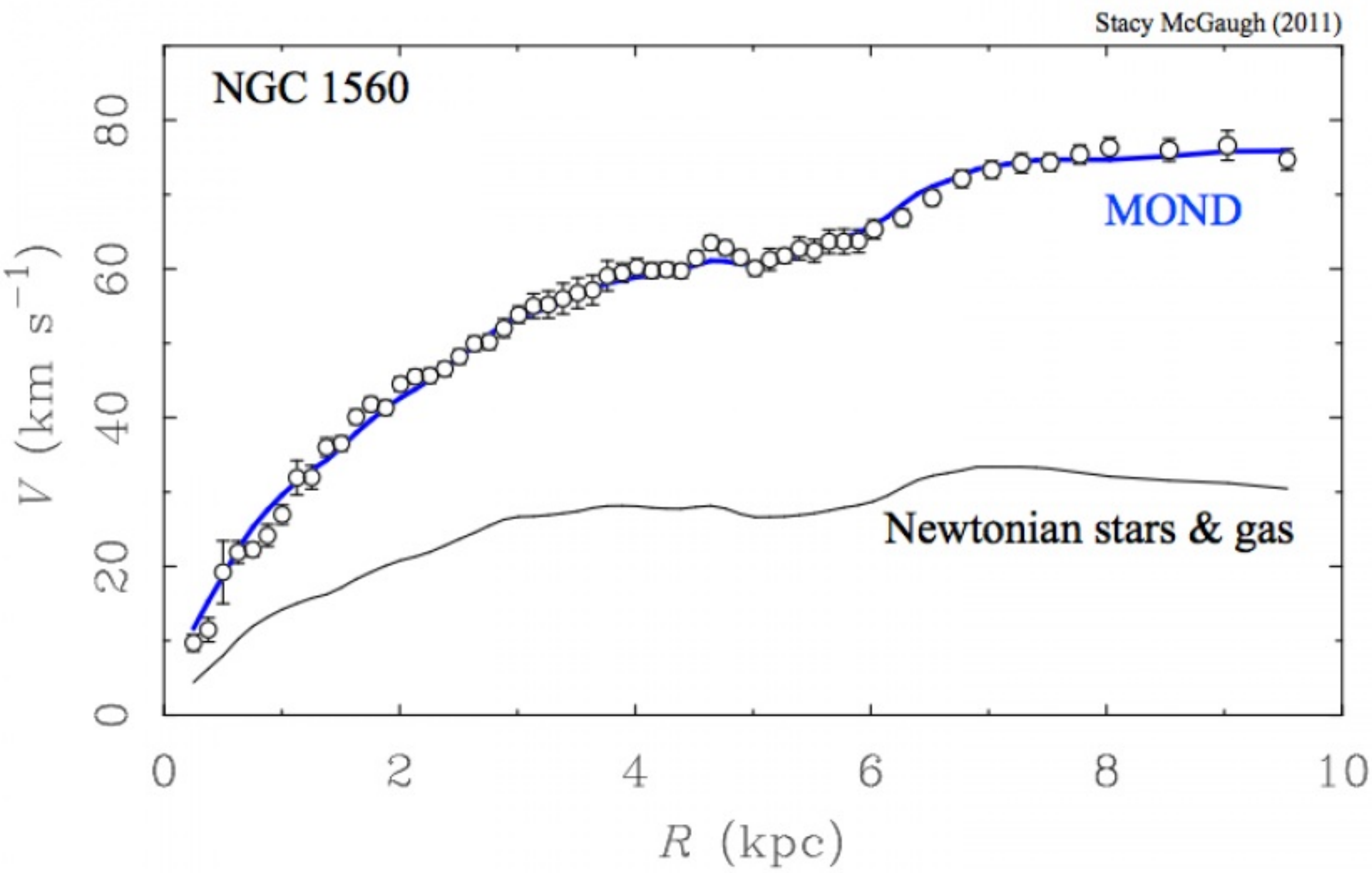

- Sometimes effective, but more often fail.
- Newton/Einstein's laws of gravity have been precisely tested on various scales.

The laws of gravity have undergone rigorous testing.

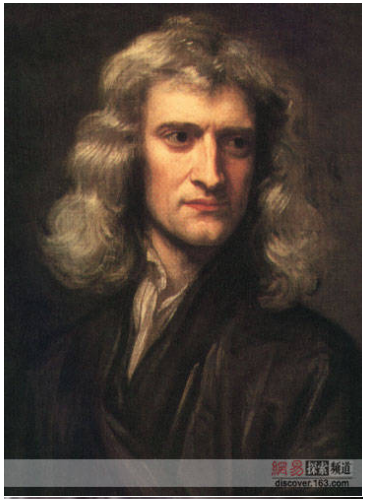

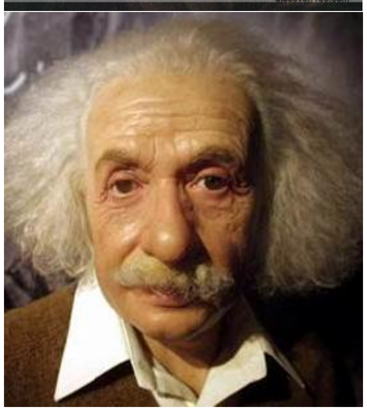

Space-time is swirling around a dead star, proving Einstein right again

News By Charles Q. Choi published January 31, 2020

Space-time is indeed churned by massive rotating bodies, as scientist

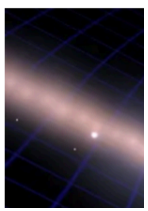

Einstein is right again! Scientists prove that plunging regions exist around black holes - a theory first proposed by the physicist in 1915

- **Scientists have proven the existe**
- **This discovery confirms theoreti**

By WILIAM HUNTER
PUBLISHED: 05:05 EDT, 16 May 2024 | U

Share

Over 100 years on, scientists have f about the nature of black holes.

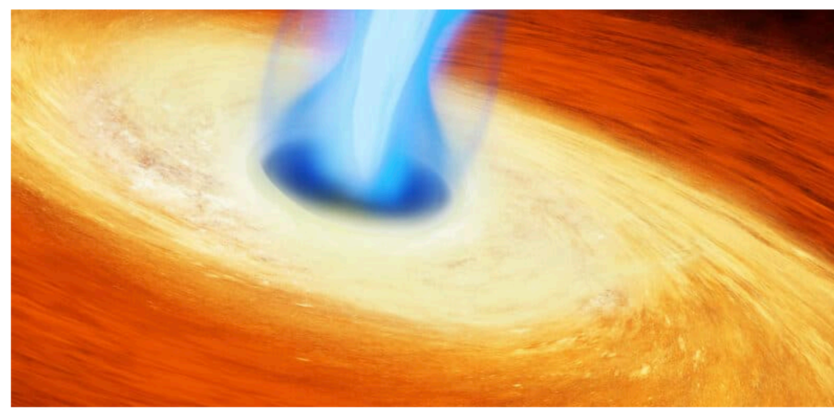

05-23-2024

Black hole "waterfall" discovery proves Einstein right again

By Eric Ralls

General Relativity: Prediction and Confirmation of Gravitational Waves

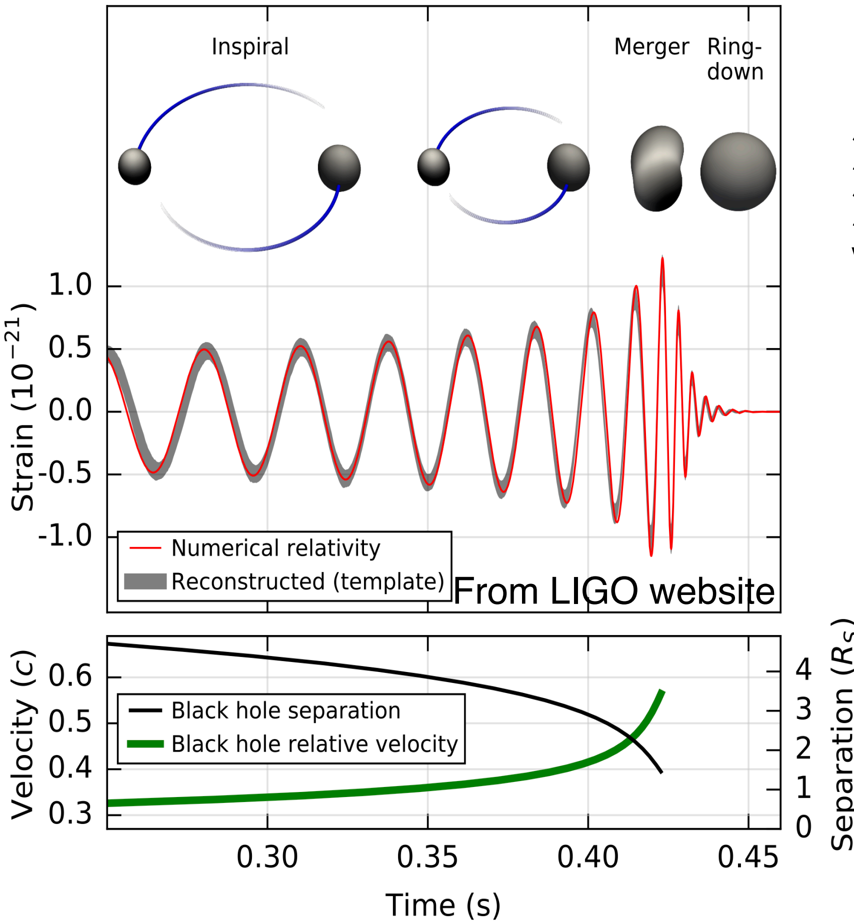

From LIGO website

1916: Einstein predicted gravitational waves based on General Relativity
2015: LIGO/VIRGO detected GW150914
2017: Nobel Prize in Physics awarded to Weiss, Barish, Thorne

General Relativity: Prediction and Confirmation of Black Holes

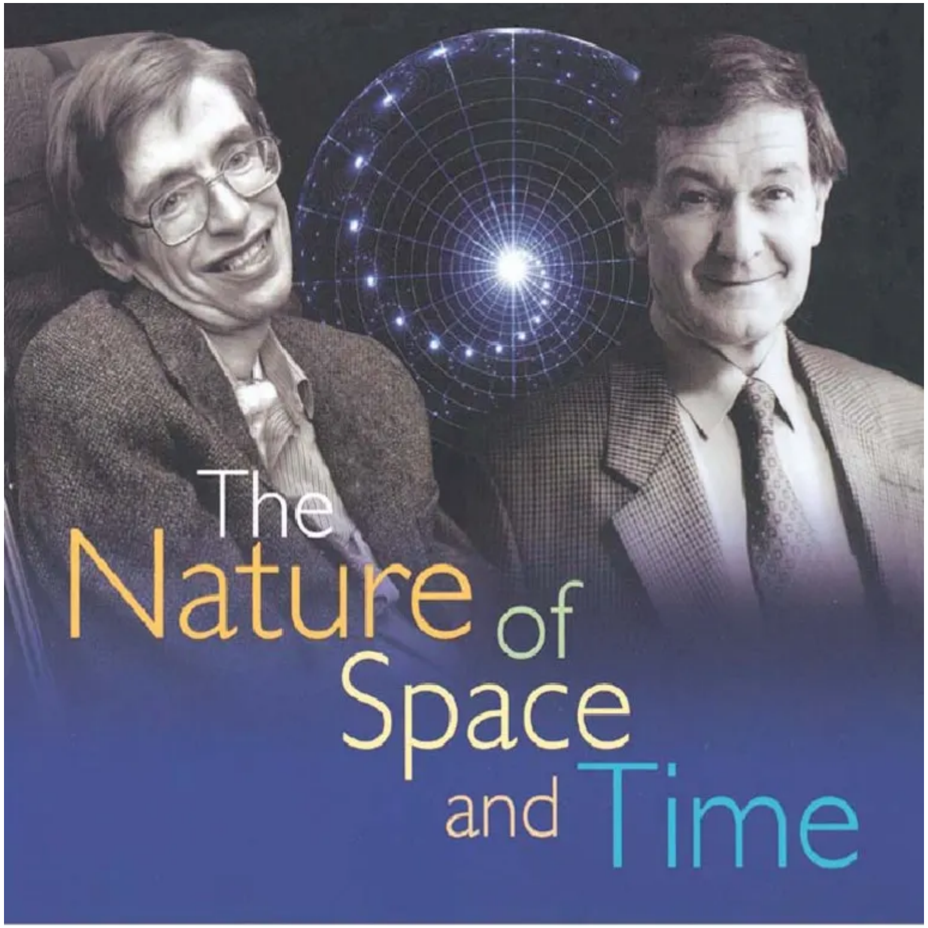

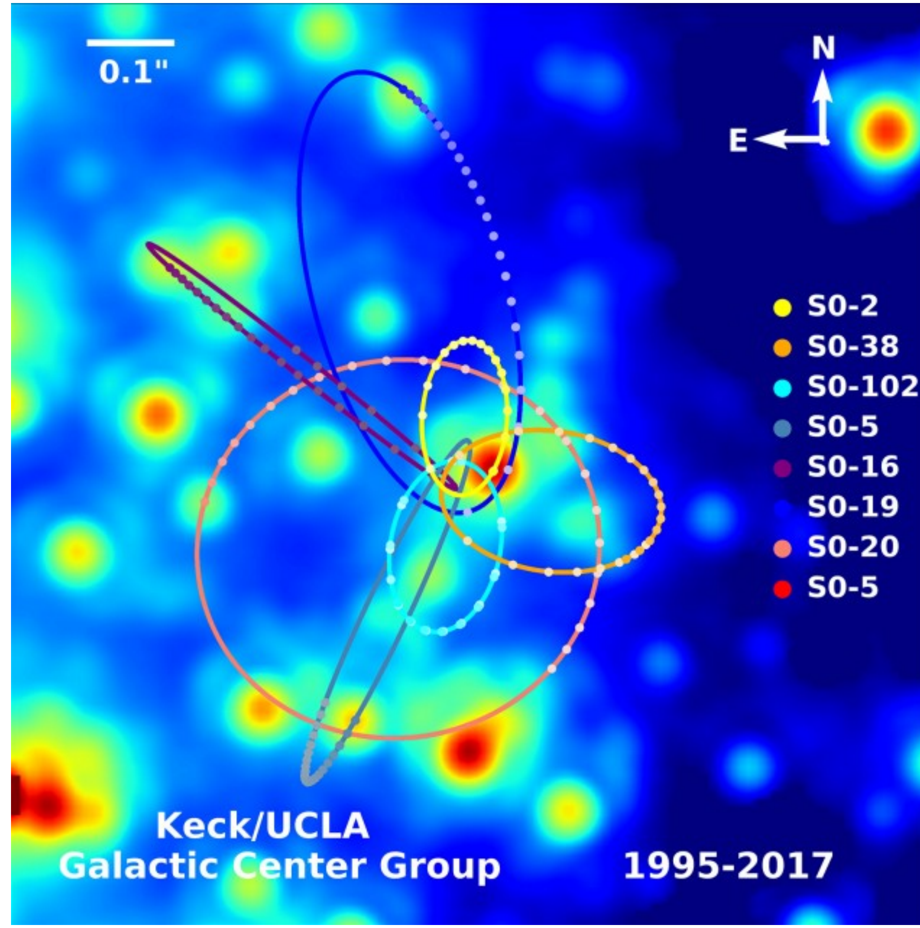

1964-1970: Penrose and Hawking mathematically confirmed the existence of black holes based on General Relativity
1995-2016: Genzel and Ghez discovered and confirmed the supermassive black hole at the center of the Milky Way
2020: Penrose, Genzel, and Ghez received the Nobel Prize in Physics

Precise Testing of General Relativity Near the Galactic Center Black Hole

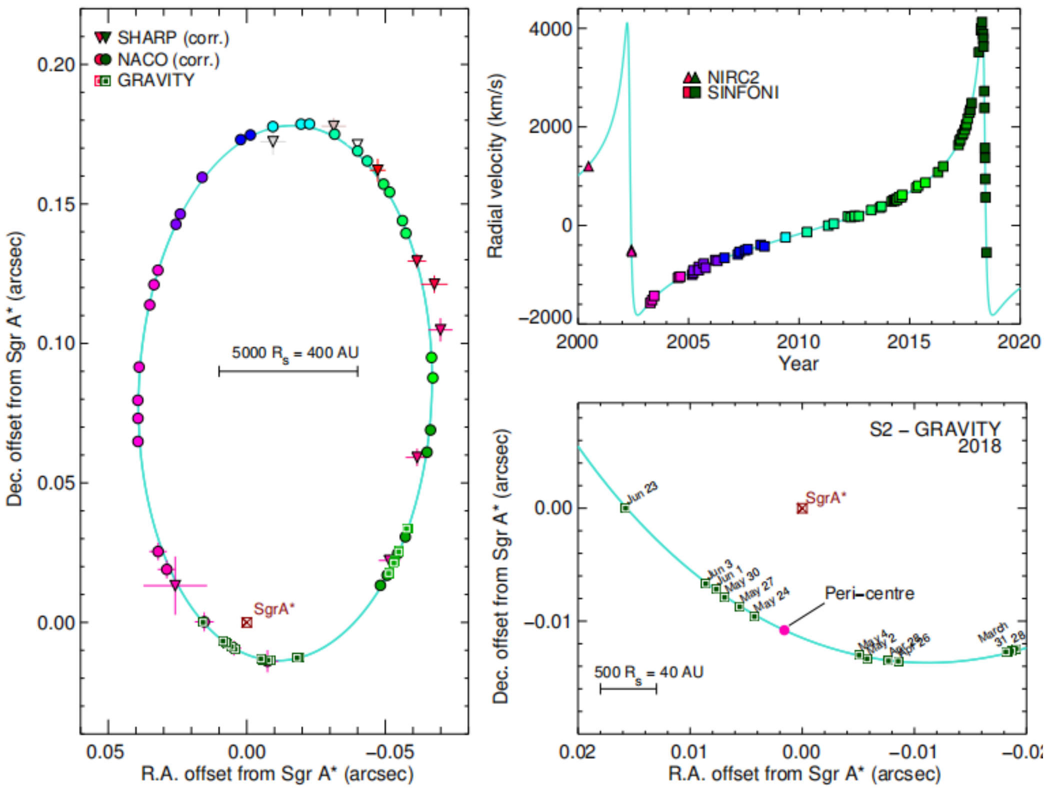

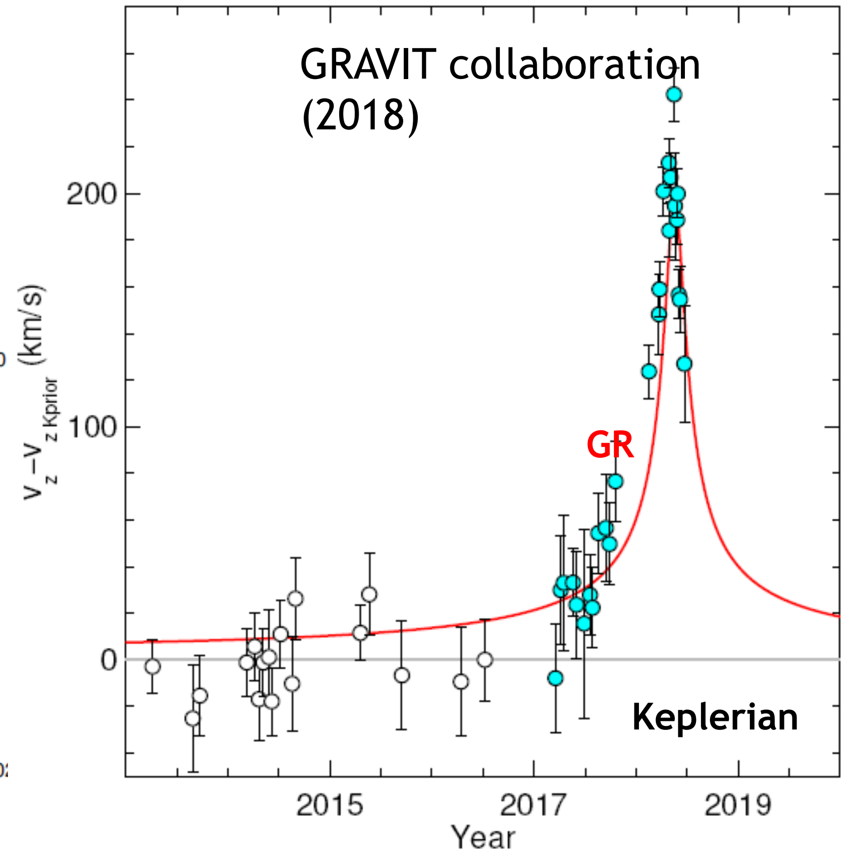

The GRAVITY experiment's measurements of the orbit and velocity of the S2 star around the Galactic Center black hole have precisely validated General Relativity in strong gravitational fields.

Event Horizon Telescope Imaging of a Black Hole

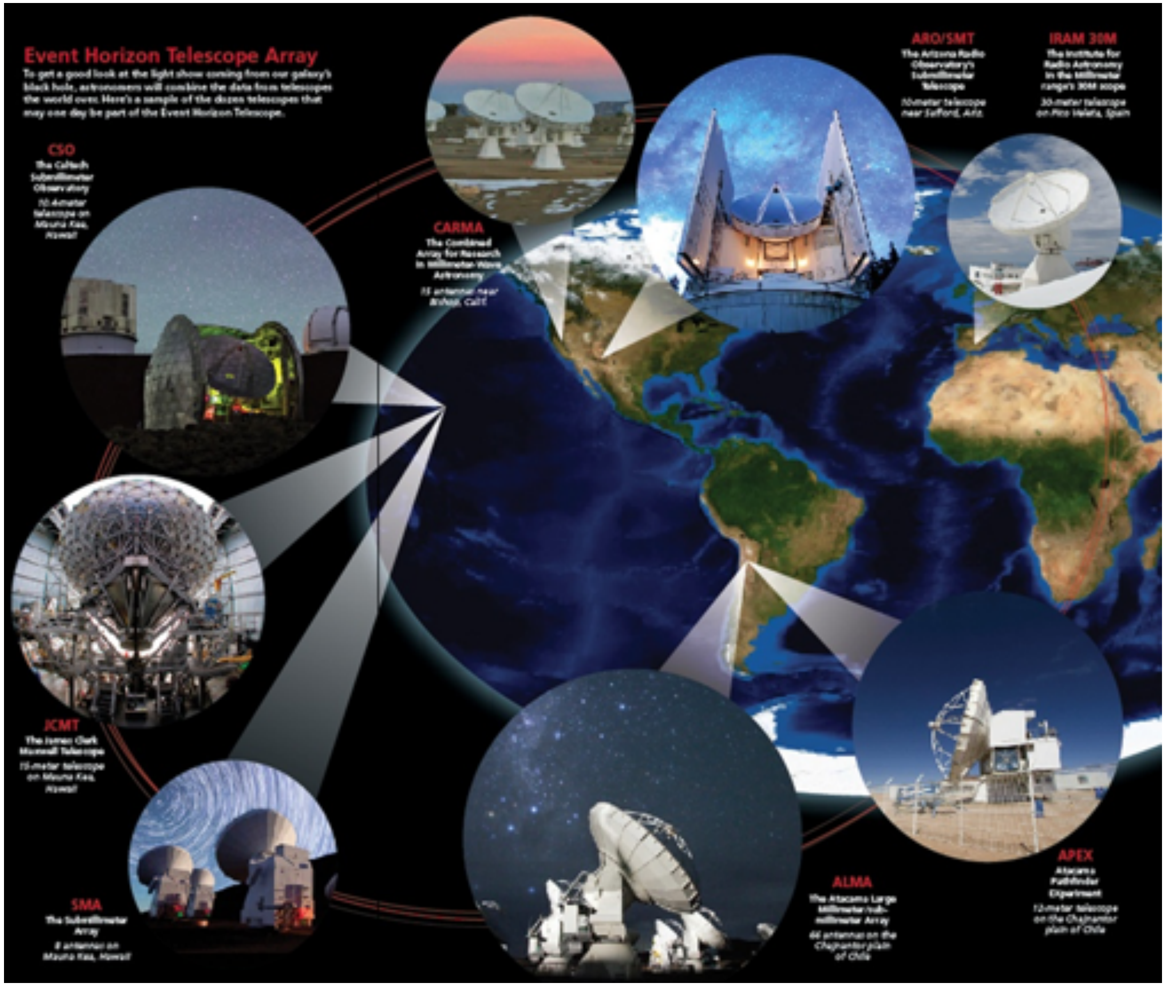

EHT collaboration (2019)

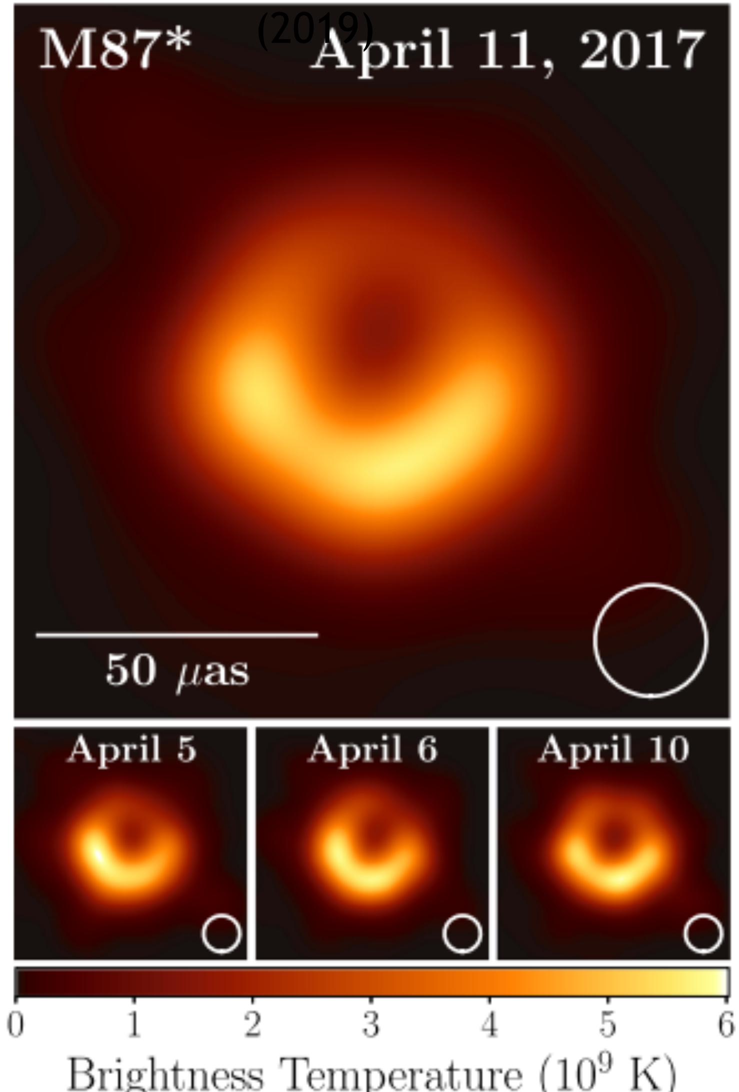

Dark matter matters!

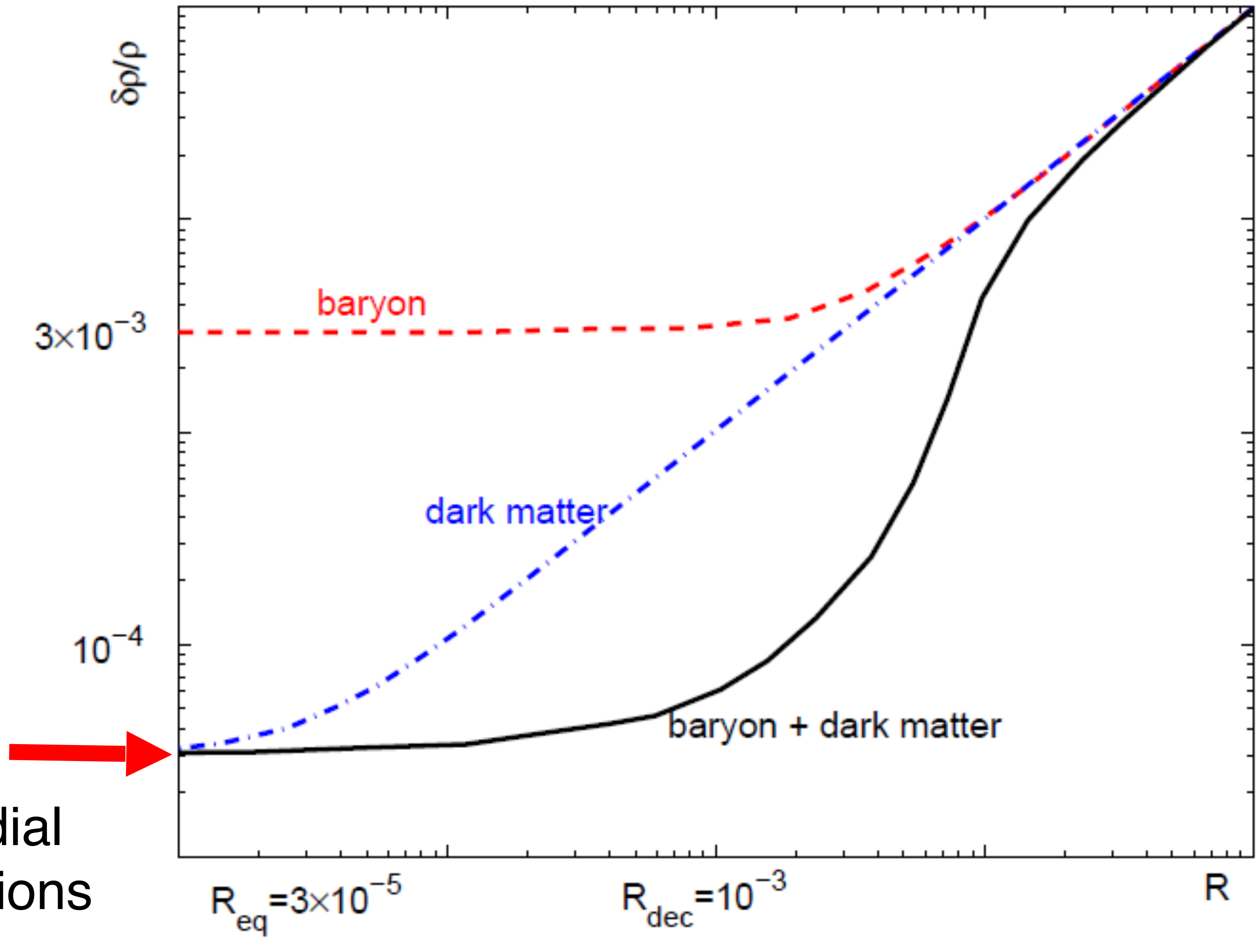

Primordial fluctuations

Without DM, galaxies wouldn't have had enough time to form, so there would be no Milky Way, no Solar System, and likely no you or me!

Properties of DM

What is Dark Matter?

DM is an unknown substance inferred from astronomical observations. It doesn't emit light or electromagnetic waves but affects celestial bodies and the universe through gravity on large scales.

DM is unevenly distributed, forming structures of various sizes. Overall, DM has five times the mass of ordinary matter, but its distribution varies greatly.

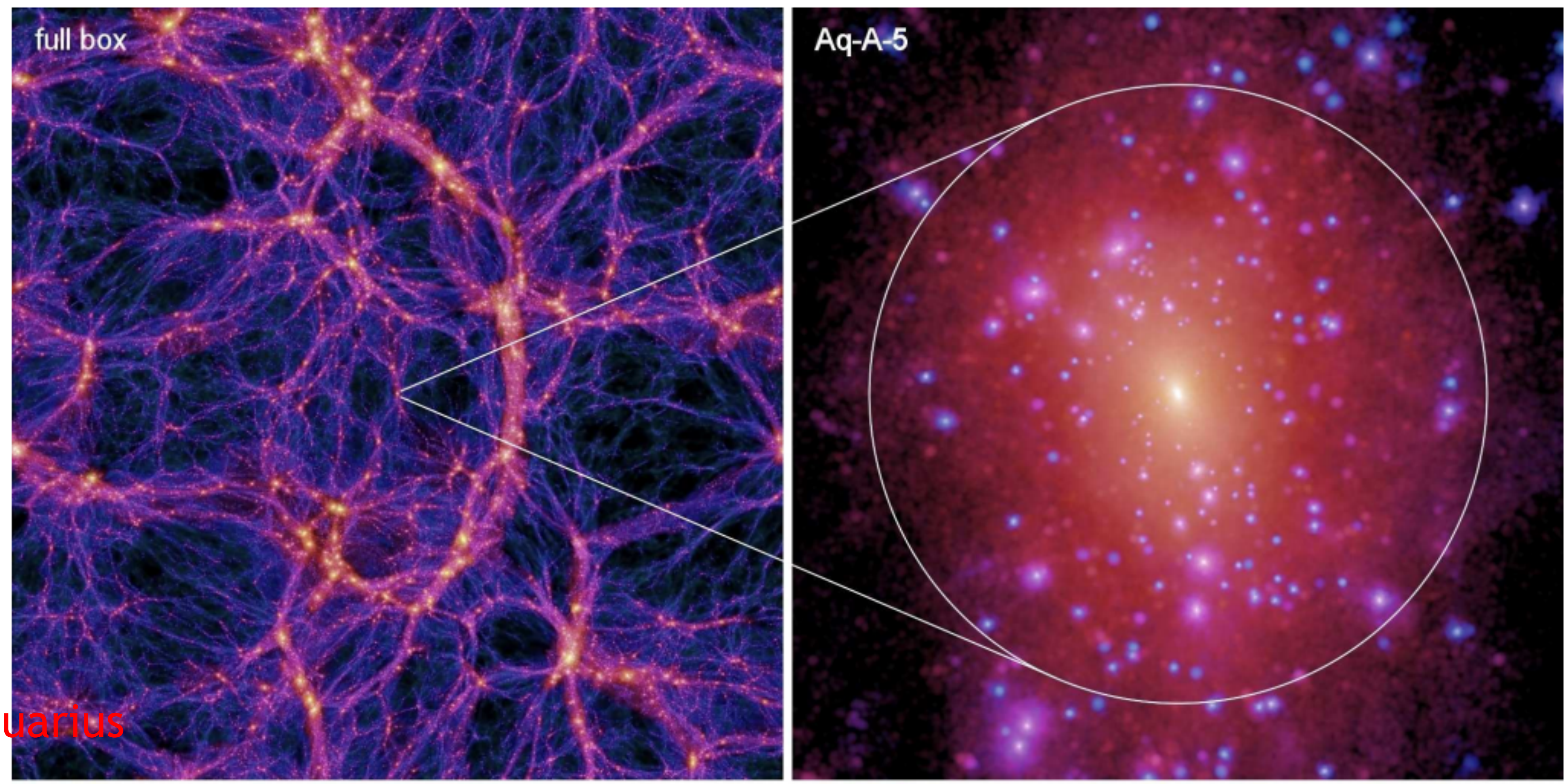

What is Dark Matter?

- Neutral, uncharged
    - Weakly interacts with visible matter
- Stable
- Massive
- Cold

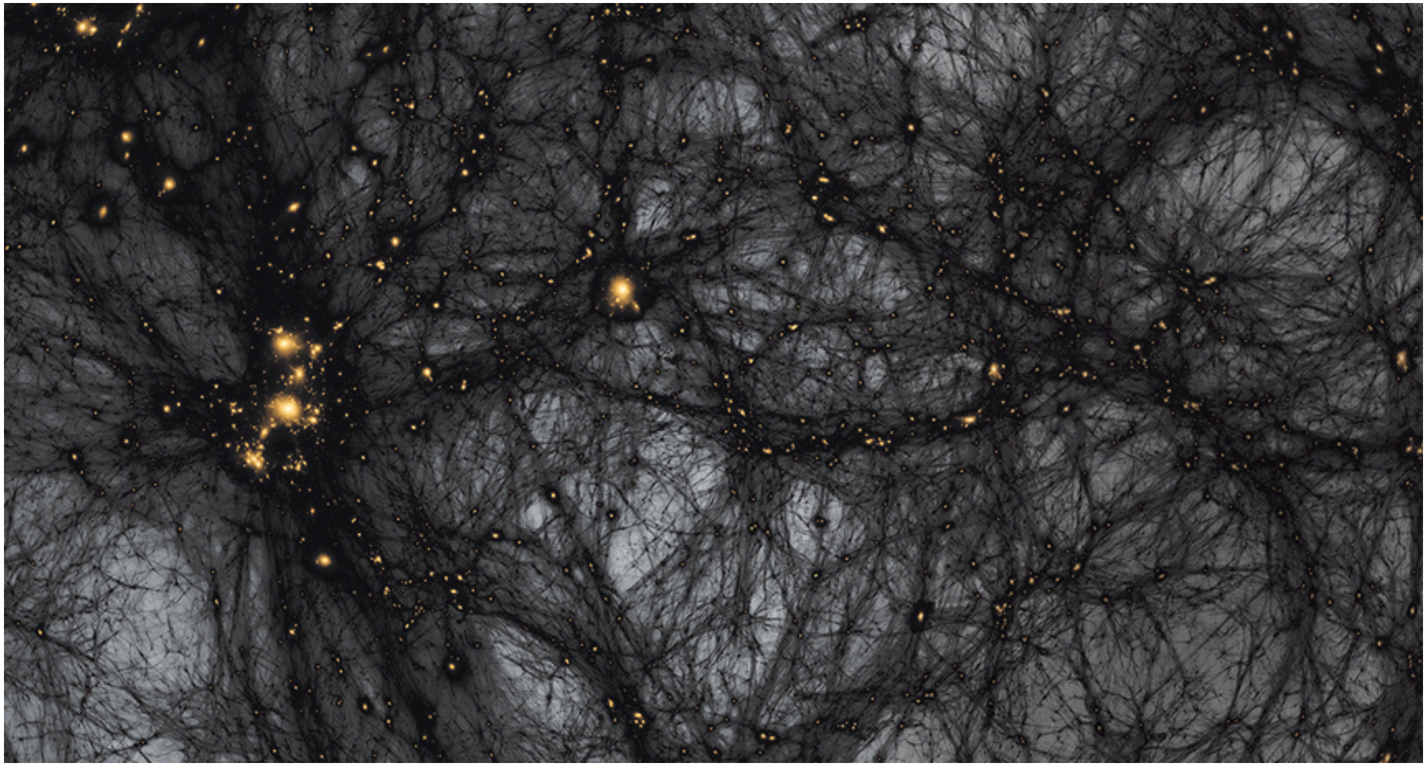

Dark Matter Around Us

- DM density is about 0.3 hydrogen atoms per cm^3.
- Assuming a DM particle mass is 100 times that of a hydrogen atom, there is roughly 1 DM particle in a teacup.
- About 100 million DM particles pass through our bodies every second.
- The total mass of DM within the Earth's volume is approximately 0.5 kilograms.
- In the Milky Way, the mass of DM is about 10 times that of stars and gas.

DM Candidate Models

1904.07915， TASI lecture

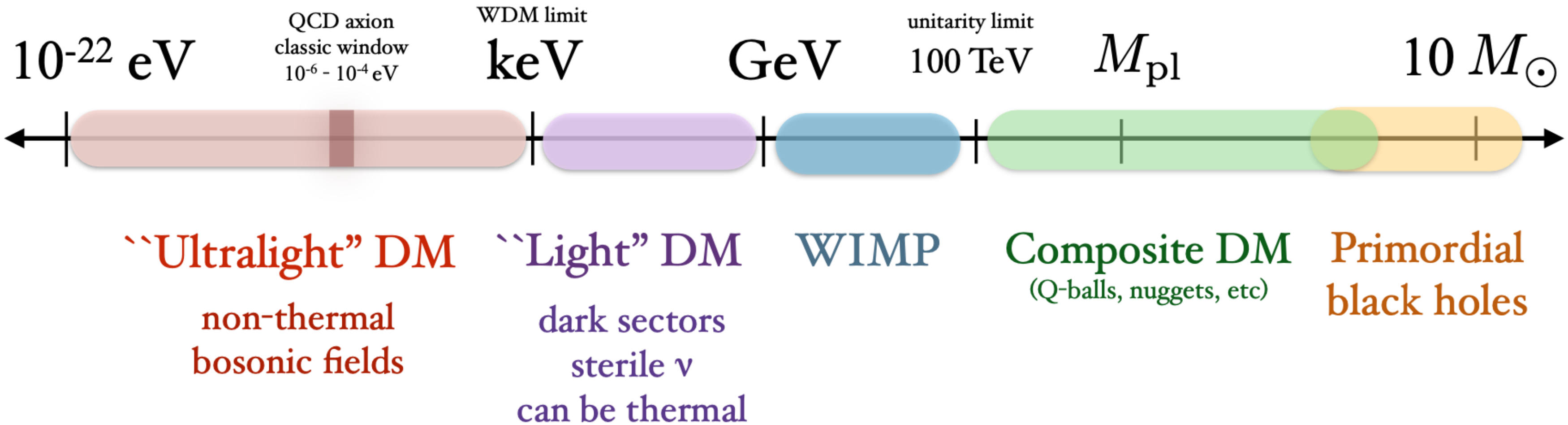

- Primordial Black Hole (PBH)
- Ultralight Dark Matter
- Weakly Interacting Massive Particle (WIMP)

PBH Dark Matter

- Macroscopic Objects
- Primordial Black Holes
- Asteroid-sized primordial black holes could serve as DM.

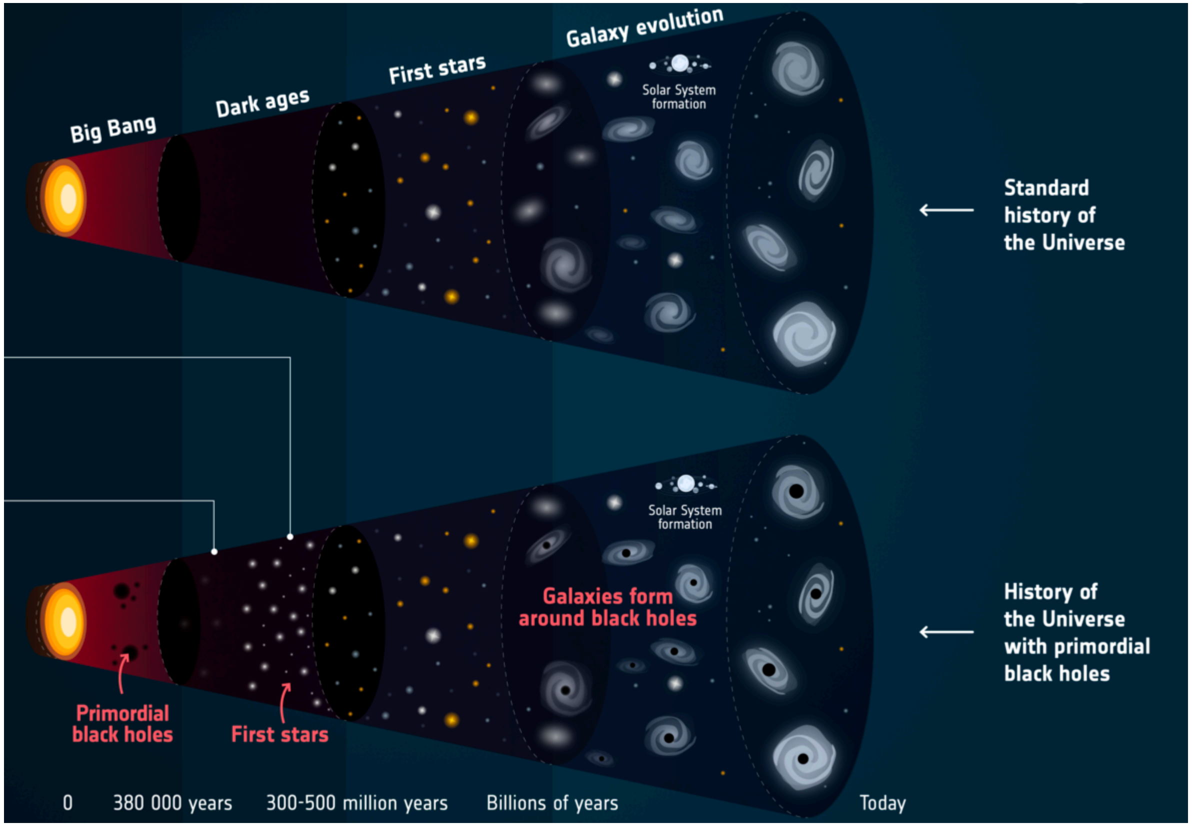

Is DM made of black holes?

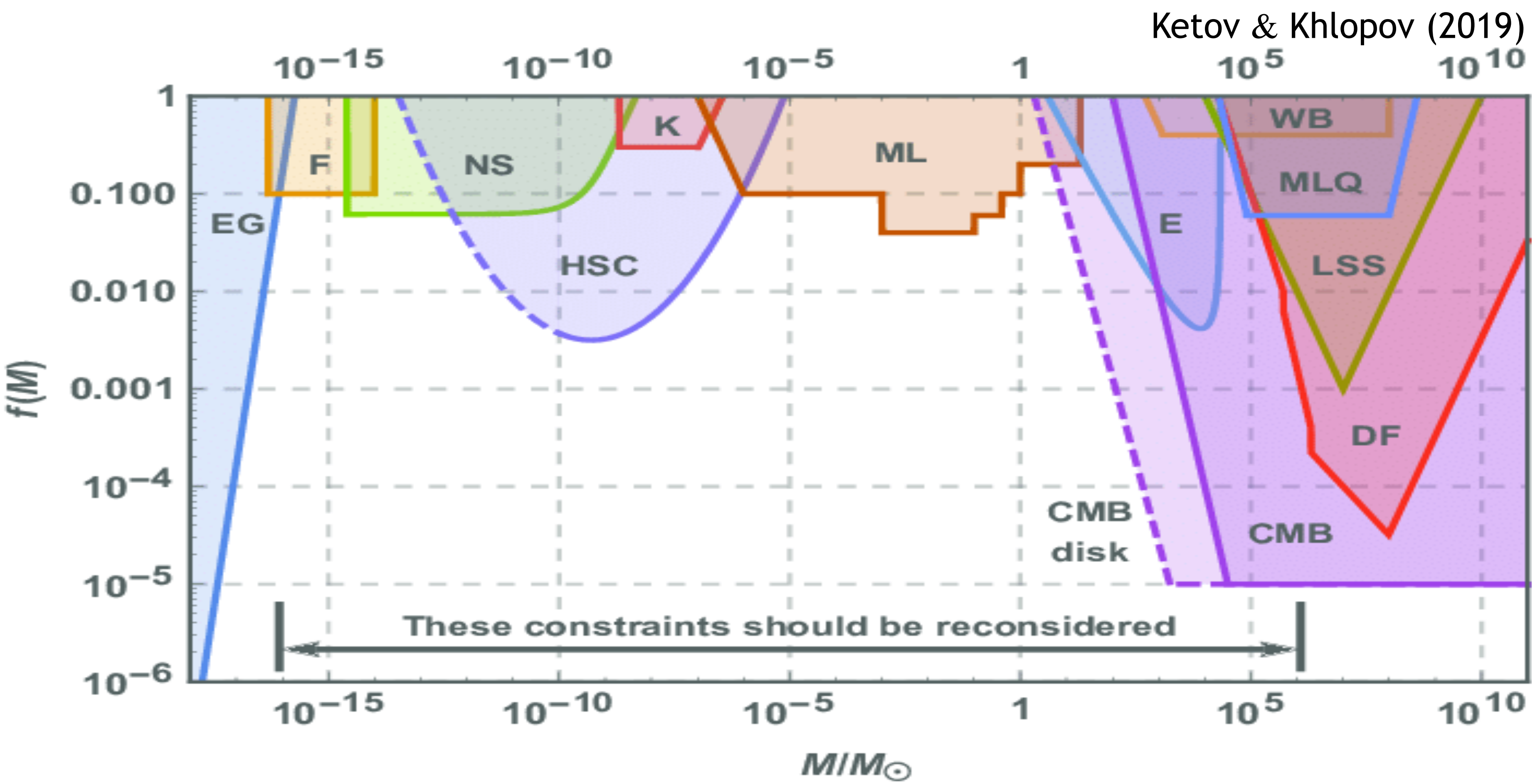

Even if black holes can constitute DM, they can only account for a small fraction of the DM in the universe.

What is Dark Matter?

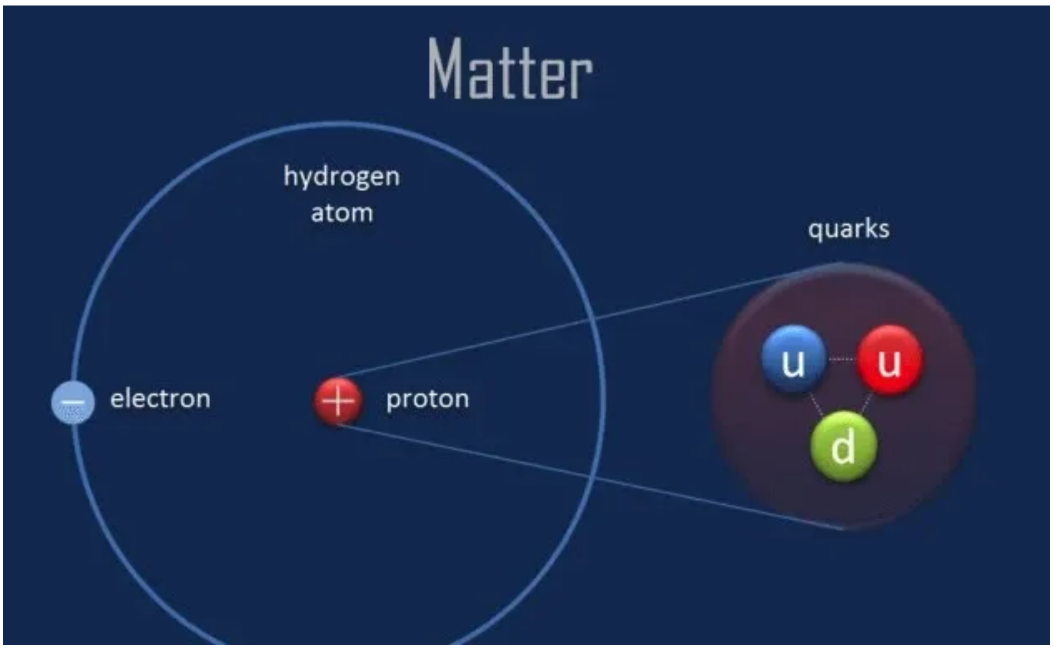

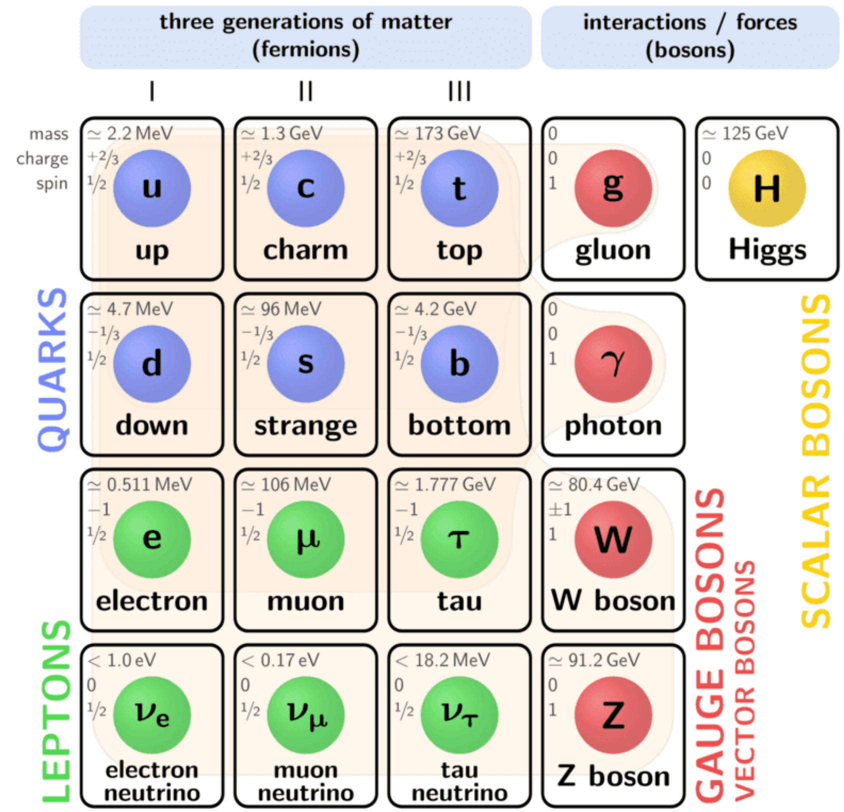

Properties of DM: stable, slow-moving (cold), non-baryonic, weakly interacting

DM is different from any particles in the Standard Model, likely a new particle (or particles) beyond the Standard Model—new physics!

The Standard Model of Particle Physics and DM

- No body knows what DM is
- Not in Standard Model
- There are good guesses

Not neutrinos ✗

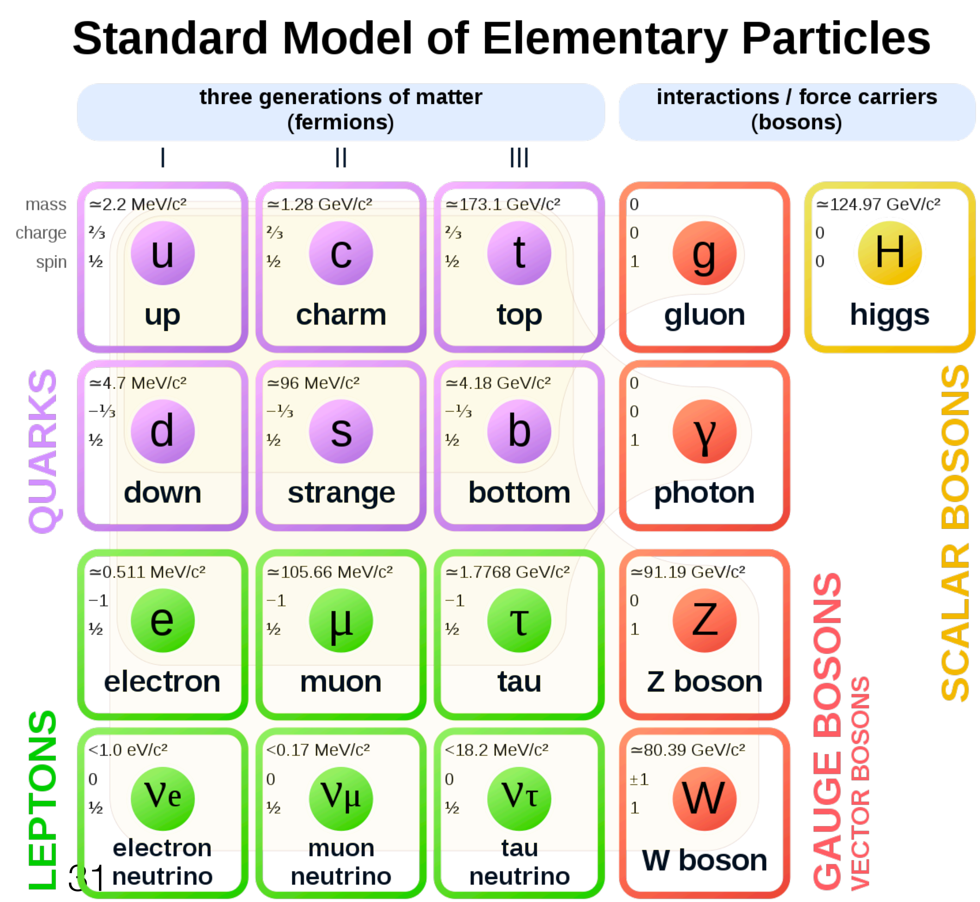

The Standard Model of Particle Physics and DM

- No body knows what DM is
- Not in Standard Model
- There are good guesses

Not neutrinos ✘

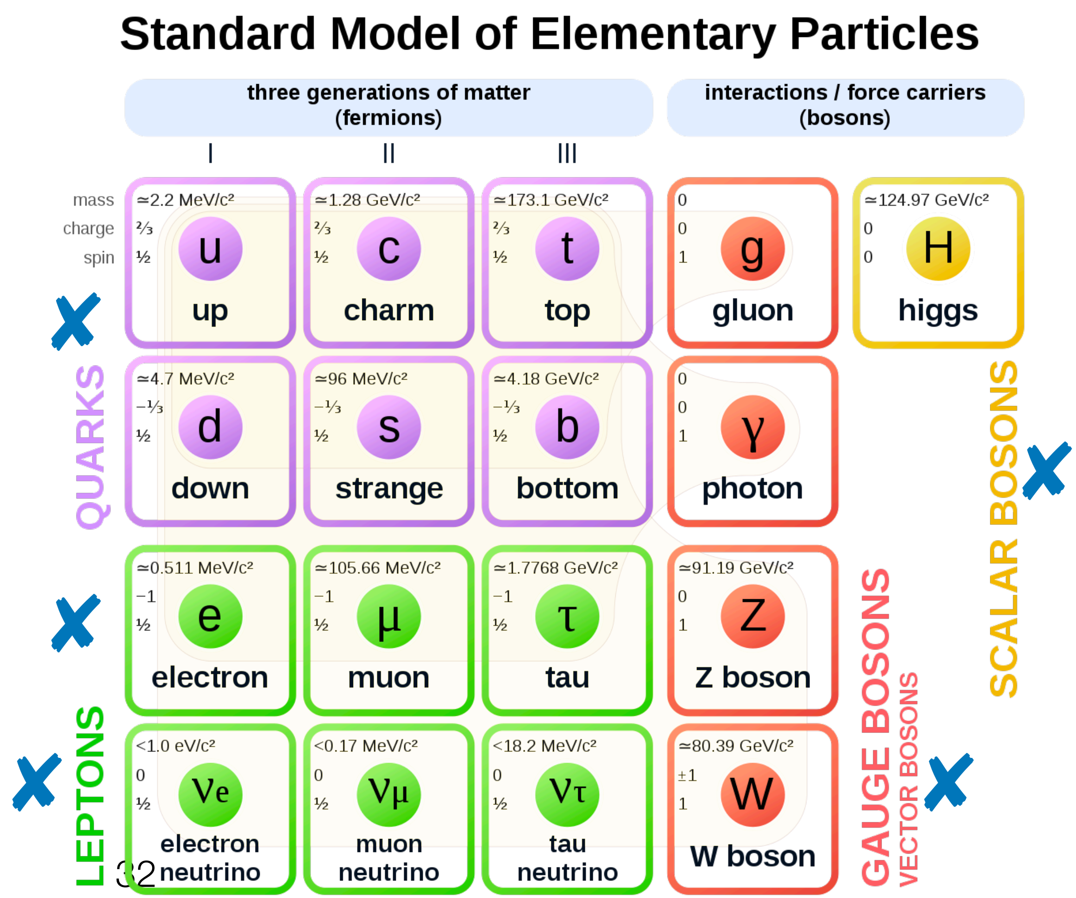

Implications of Large-Scale Structure in the Universe

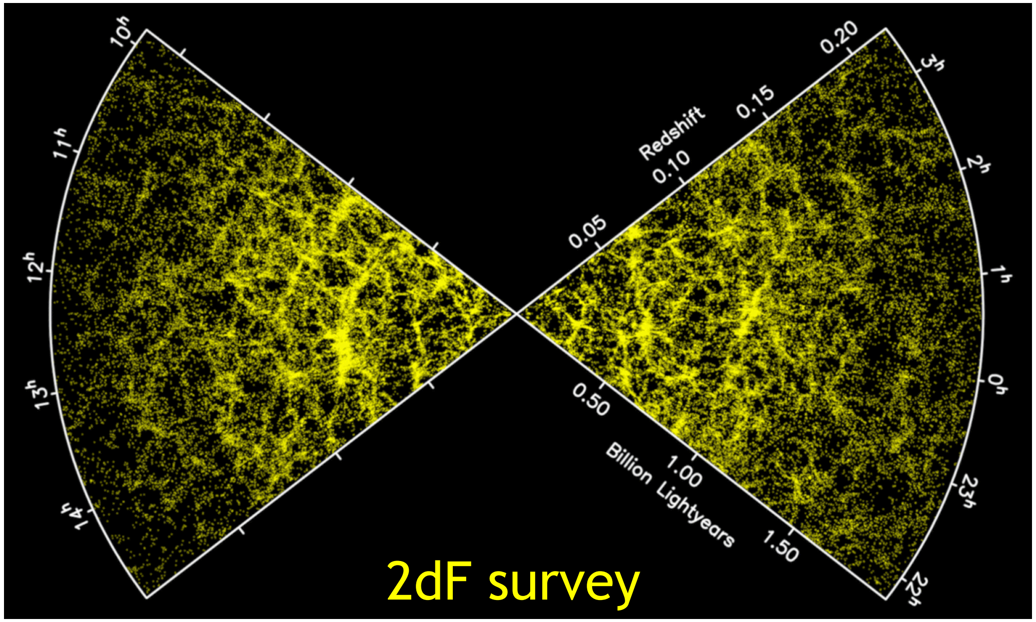

The evolution of structures from small to large implies that DM is cold. ("Cold" means DM has low kinetic energy and short free-streaming distances, forming structures via Jeans instability before spreading out.)

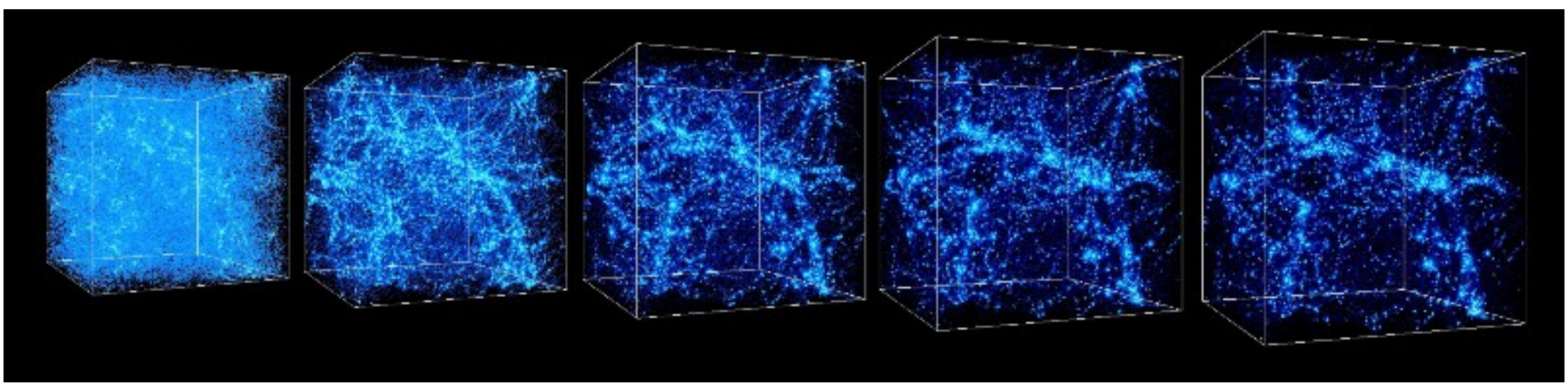

Thermal History of the Universe

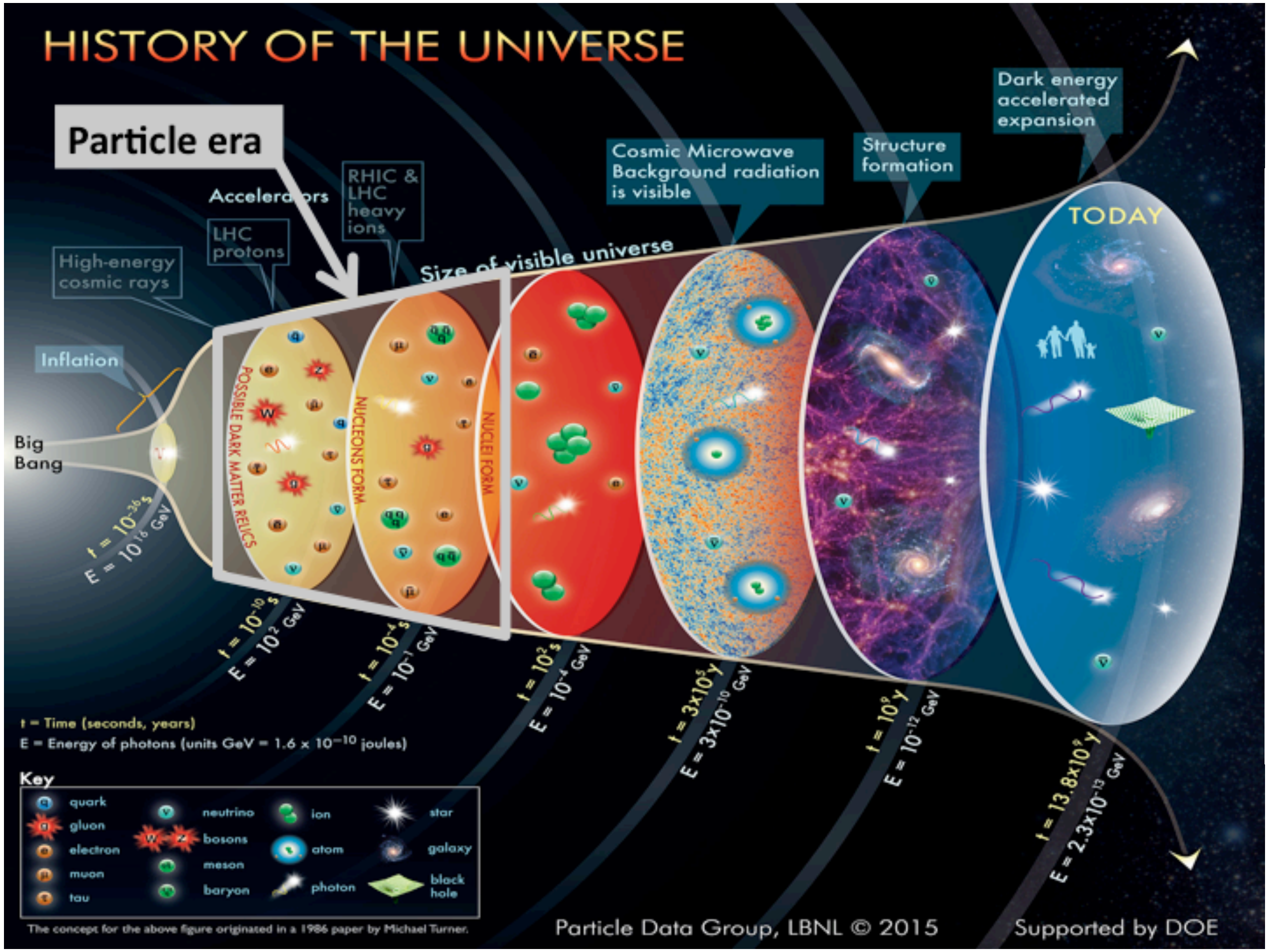

The dark matter distribution

- Astrophysicist knows the distribution of DM by simulation

$$\rho(r) = \frac{\rho_0}{\frac{r}{R_s}\left(1 + \frac{r}{R_s}\right)^2}$$

- Navarro-Frenk-White profile:
- R_s is the “scale radius”, $\{\rho_0, R_s\}$ varies from halo to halo
- Integrated mass:

$$M = \int_0^{R_{\max}} 4\pi r^2 \rho(r)\, dr = 4\pi\rho_0 R_s^3 \left[\ln\left(\frac{R_s + R_{\max}}{R_s}\right) + \frac{R_s}{R_s + R_{\max}} - 1\right]$$

$$M = \int_0^{R_{\rm vir}} 4\pi r^2 \rho(r)\, dr = 4\pi\rho_0 R_s^3 \left[\ln(1+c) - \frac{c}{1+c}\right]$$

The dark matter distribution

- Astrophysicist knows the distribution of DM by N-body simulation

- Navarro-Frenk-White profile:

$$\rho(r) = \frac{\rho_0}{\frac{r}{R_s}\left(1 + \frac{r}{R_s}\right)^2}$$

- Other competing profile: Einasto

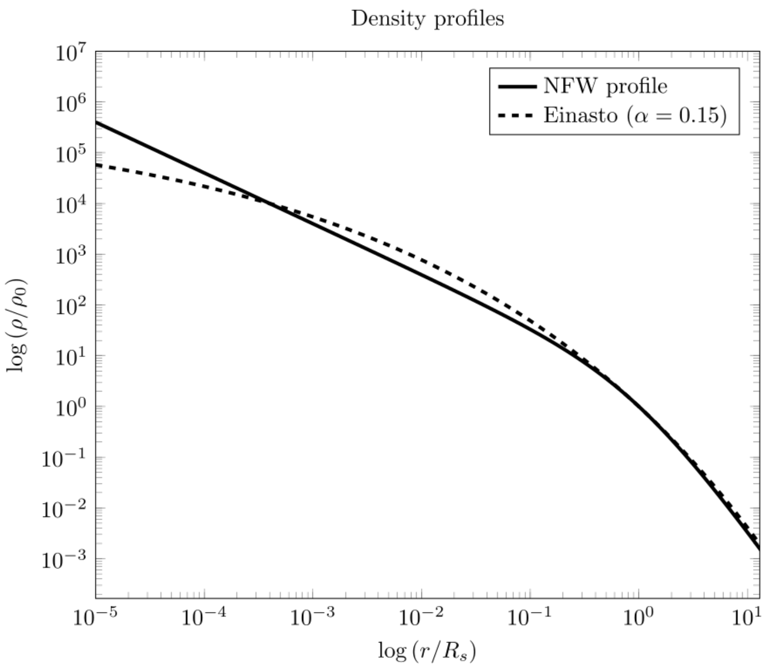

Small-Scale Structure Problem of DM

- Astrophysicist knows the distribution of DM by N-body simulation
- Navarro-Frenk-White profile:
- $$\rho(r) = \frac{\rho_0}{\frac{r}{R_s}\left(1 + \frac{r}{R_s}\right)^2}$$
- CDM: very good for large scale, but problems at galactic scale

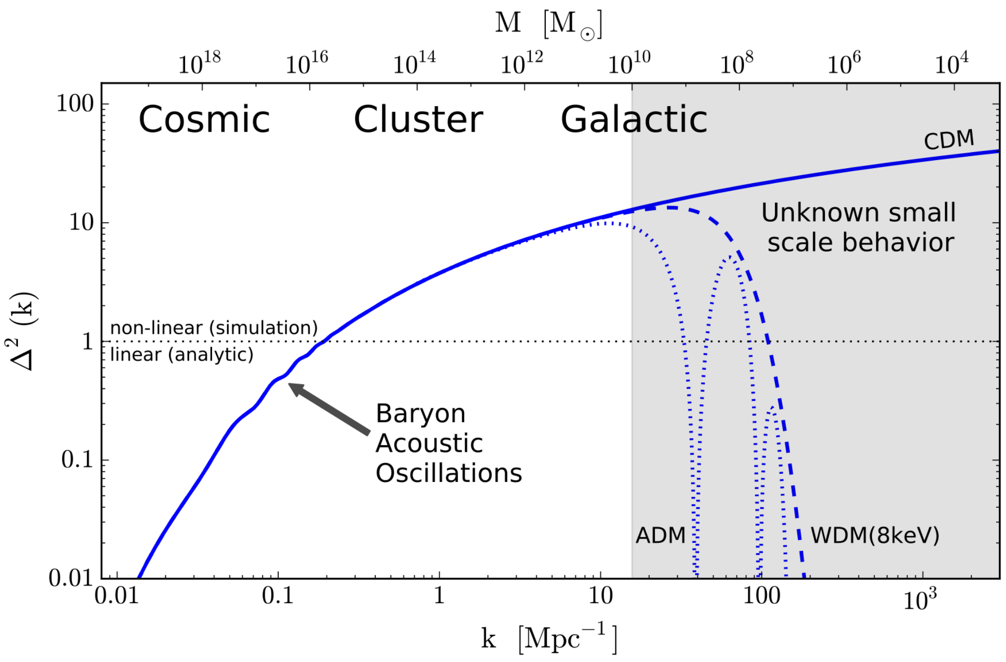

Small-Scale Structure: Cusp-Core Distribution Problem

- Astrophysicist knows the distribution of DM by simulation
- Navarro-Frenk-White profile:
-

$$\rho(r) = \frac{\rho_0}{\frac{r}{R_s}\left(1 + \frac{r}{R_s}\right)^2}$$

- CDM: very good for large scale, but problems at galactic scale
    - Core-Cusp problem of cold dark matter

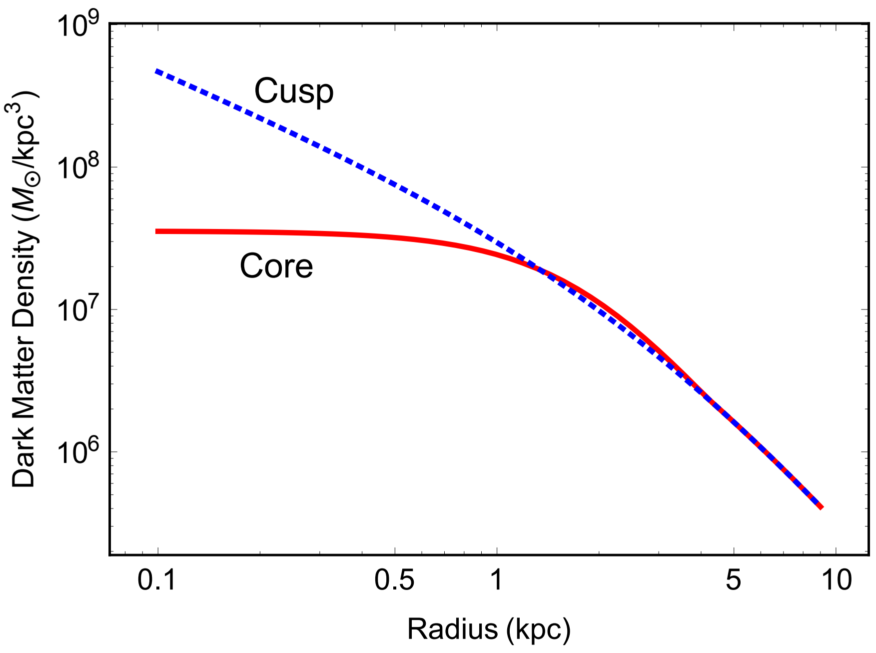

Thermal Evolution History of DM Density

DM+DM $\longleftrightarrow$ SM+SM

Garrett & Duta (2011)

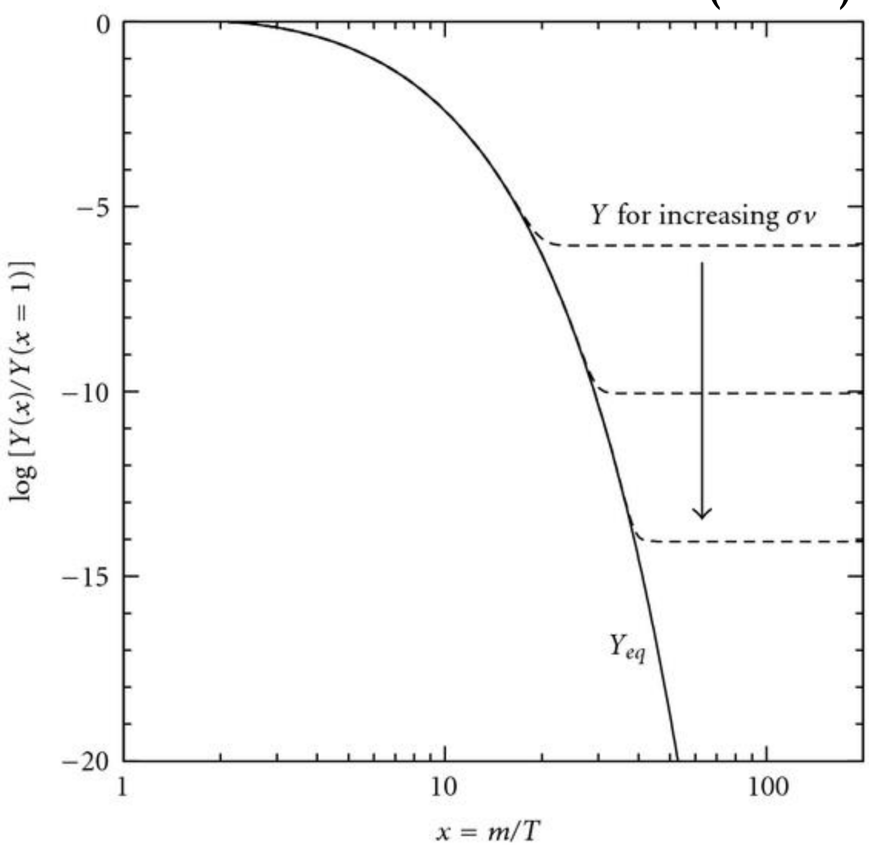

$$\langle \sigma v \rangle \simeq \left(\frac{3 \times 10^{-27} \mathrm{cm}^3 \mathrm{s}^{-1}}{\Omega_\chi h^2} \right)$$

$\sigma \sim 10^{-35} \mathrm{cm}^2$

Weak Interaction Cross-Section!

WIMP Miracle: Weakly Interacting Massive Particles (WIMPs) are the best candidates for DM!

Abundance of Thermal Dark Matter

Excellent Production Mechanism: Thermal Freeze-out

- DM is a massive elementary particle
- DM has an electroweak-scale coupling
    - DM starts with thermal distribution
    - Relic abundance is determined by freeze-out mechanism
    - DM Annihilation into
        - X = Standard Model particles (direct coupling)

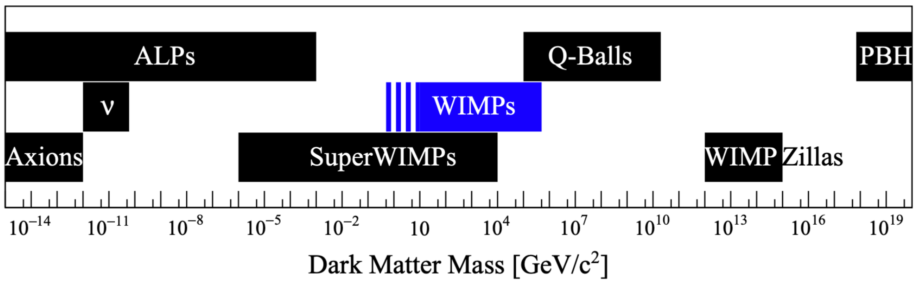

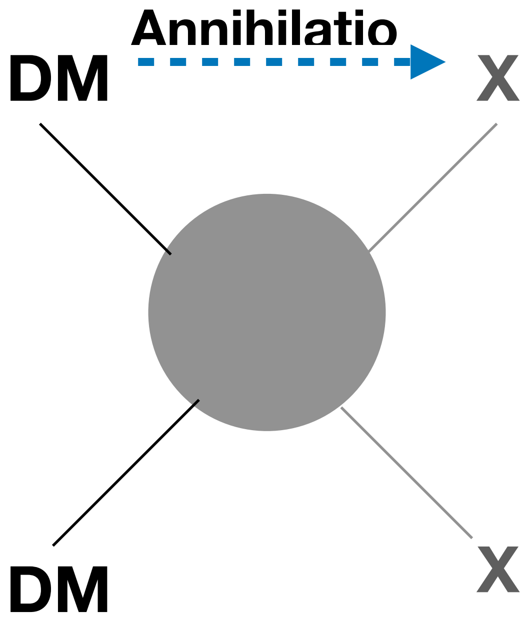

Thermal Decoupling Annihilation Cross-Section of WIMP DM

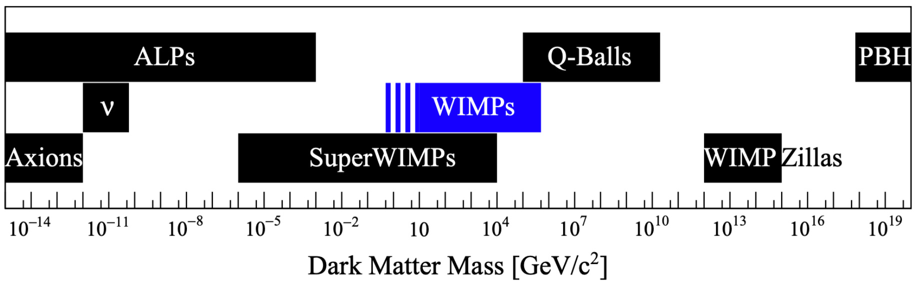

- The thermal decoupling annihilation cross-section matches the strength and scale of electroweak interactions.

$$\langle \sigma v \rangle \sim \frac{\alpha^2}{m_W^2} \sim 3 \times 10^{-26} \mathrm{cm}^3 \mathrm{s}^{-1}$$

Such match is called WIMP miracle

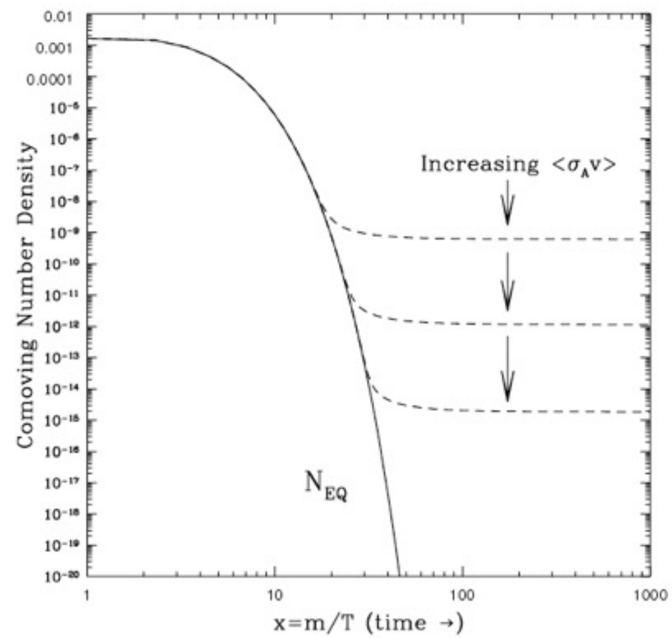

Jungman *et al* hep-ph/9506380

Thermal Freeze-out: Excellent!

- Naturally yields the relic abundance
  - No need for UV information (starts with thermal equilibrium distribution)
  - Annihilation cross-section at the electroweak scale
  - Similar story to other Standard Model particles (decoupling, ratio, nuclear elements)
    - (ν decoupling, n_p/n_n ratio, nuclear elements)
  - Predicts direct/indirect/collider experimental signals

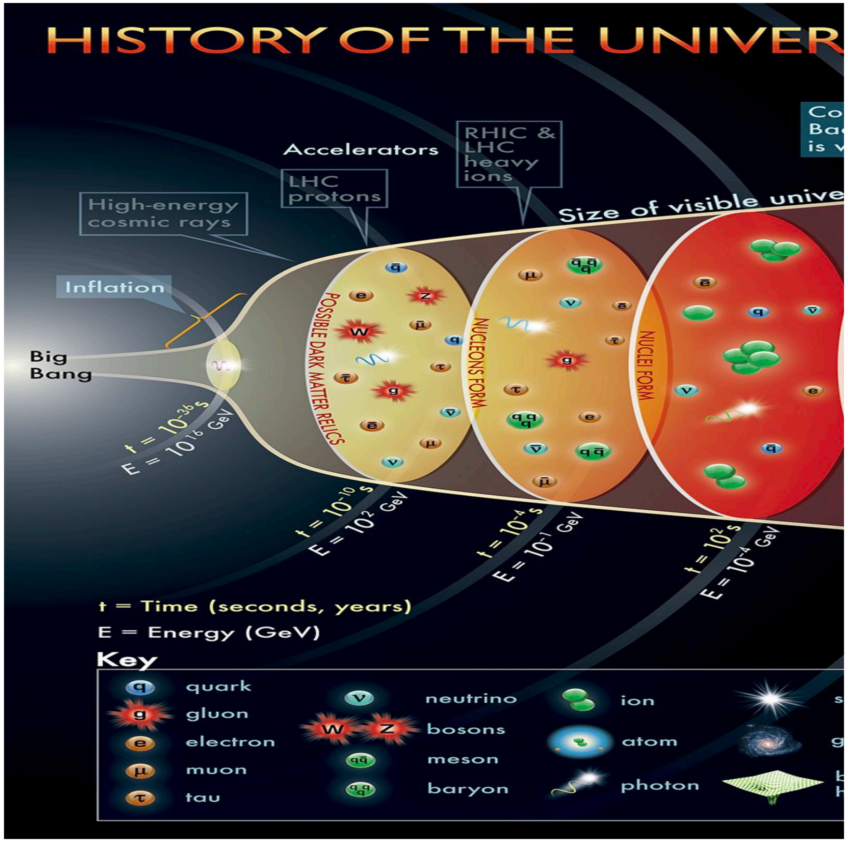

Background Knowledge：
Phase Space and Cross-sections

- Particle's phase space
- 4D Lorentz-invariance： phase-space of a single on-shell particle

$$dPS = \Theta(E)\delta(p \cdot p - m^2)d^4p = \frac{d^3\vec{p}}{(2\pi)^3 2E}$$

  - Why the factor $(2E)^{-1}$?
  - Normalize to 2E particle in the volume

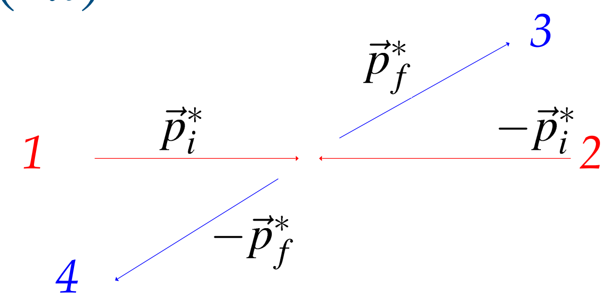

- Interaction Cross-section： $1 + 2 \to 3 + 4$ (DM + DM > SM SM)

$$\sigma = \frac{1}{2E_1 2E_2 \left| v_1 - v_2 \right|} \int \left(\prod_f \frac{d^3 p_f}{(2\pi)^3} \frac{1}{2E_f} \right) \times \left| \mathscr{M} \left(p_1, p_2 \to \left\{ p_f \right\} \right) \right|^2 (2\pi)^4 \delta^{(4)} \left(p_1 + p_2 - \sum p_f \right)$$

Background Knowledge 2：
Phase Space Density of particles

- Phase space distribution function $f(\vec{x}, \vec{p}, t) d\vec{x} d\vec{p}$
- Distribution under thermal equilibrium $f_{\mathrm{eq}} = \dfrac{1}{e^{E/T} \pm 1} \approx e^{-E/T}$
- Number density $n_{\mathrm{eq}} = \int d\vec{p} f_{\mathrm{eq}} = \int \dfrac{d\vec{p}}{(2\pi)^3} e^{-\frac{E}{T}}$
  - High temperature $T \gg m$ limit (relativistic) $n_{\mathrm{eq}} = T^3$
  - High temperature $T \ll m$ limit (non-relativistic) $n_{\mathrm{eq}} = \left(\dfrac{mT}{2\pi}\right)^{3/2} e^{-\frac{m}{T}}$

Background Knowledge 3：
Cosmic Metric and radiation-dominated universe

- Expansion Rate of a Radiation-Dominated Universe

$$H_{\rm rad}^2 = \frac{8\pi^3}{90}\frac{g_* T^4}{m_{\rm PL}^2}$$

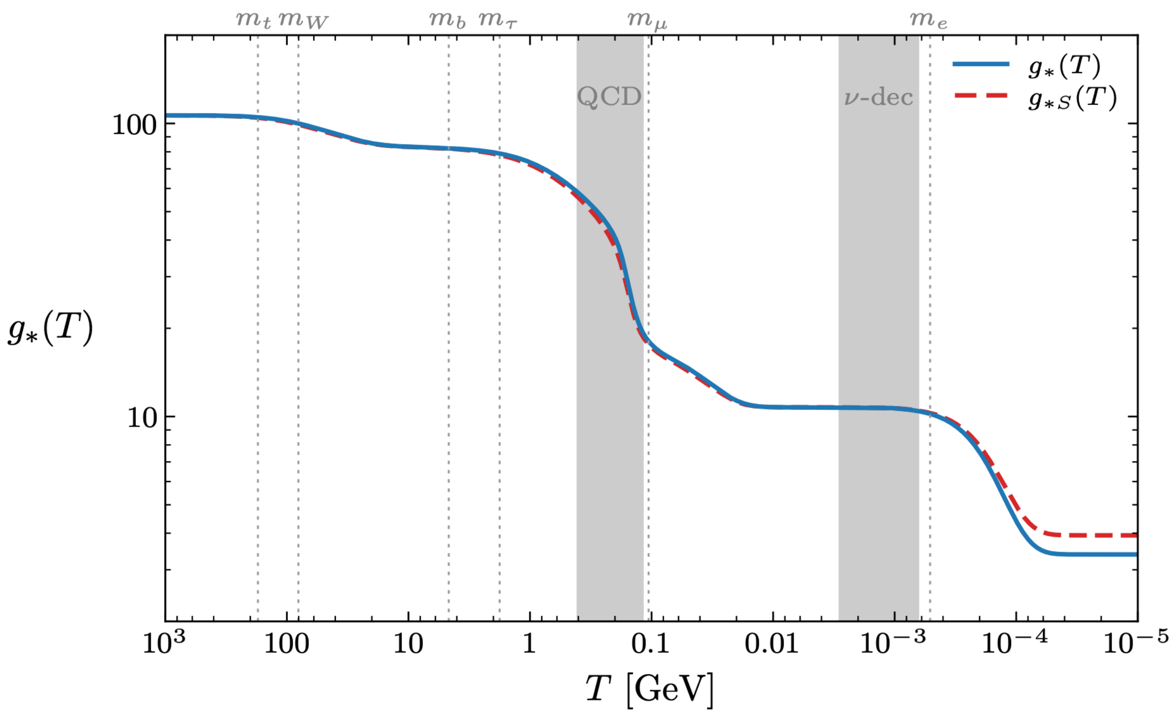

- Temperature Redshift in a Radiation-Dominated Universe

$$T \propto a(t)^{-1}$$

$$\rho_{\rm rad} \propto a(t)^{-4}$$

DM freeze-out: Boltzmann Equation

- Final Evolution of DM: The Boltzmann Equation

$$a^{-3}\frac{d(na^3)}{dt} = n_1^{\rm eq} n_2^{\rm eq} \langle \sigma v \rangle \left(\frac{n_3 n_4}{n_3^{\rm eq} n_4^{\rm eq}} - \frac{n_1 n_2}{n_1^{\rm eq} n_2^{\rm eq}} \right)$$

$$\dot{n} + 3Hn = \langle \sigma v \rangle (n_{\rm eq}^2 - n^2)$$

- Thermally Averaged DM Annihilation Cross-Section

$$\langle \sigma v \rangle \equiv \frac{1}{n_1^{\rm eq} n_2^{\rm eq}} \int \Pi_{i=1}^{4} d{\rm PS}_i \times (2\pi)^4 \delta^4(p_1 + p_2 - p_3 - p_4) \, |\mathscr{M}|^2 \times e^{-\frac{E_1+E_2}{T}}$$

Solving the DM freeze-out Boltzmann Equation

- Behavior of DM number density

$$n_{\rm eq}^{\rm rad} \sim T^3 \sim a^{-3}, \quad n_{\rm eq}^{\rm mat} \sim (mT)^{3/2} e^{-m/T}$$

$$n_{\rm freeze-out} \sim a^{-3}$$

- Useful variable: DM Yield and temperature x

$$Y_{\rm dm} \equiv n_{\rm dm}/s, \quad x \equiv m_{\rm dm}/T$$

- DM Evolution: Boltzmann Equation

$$\frac{dY}{dx} = \frac{\langle \sigma v \rangle x s}{\sqrt{\frac{8\pi^3 g_\star}{90 m_{\rm Pl}^2}}\, m^2} \left(Y_{\rm eq}^2 - Y^2\right) \qquad dx/dt = (8\pi^3 g_\star/(90 m_{\rm Pl}^2))^{1/2} m^2/x$$

Solving the DM freeze-out Boltzmann Equation

- DM Evolution: Boltzmann Equation

$$\frac{dY}{dx} = \frac{\langle \sigma v \rangle x s}{\sqrt{\frac{8\pi^3 g_\star}{90 m_{\rm Pl}^2}}\, m^2} \left(Y_{\rm eq}^2 - Y^2\right)$$

- DM thermal freeze-out temperature

$$n_{\rm fo} \langle \sigma v \rangle \approx H_{\rm fo}$$

$$x_{\rm fo} \sim 25$$

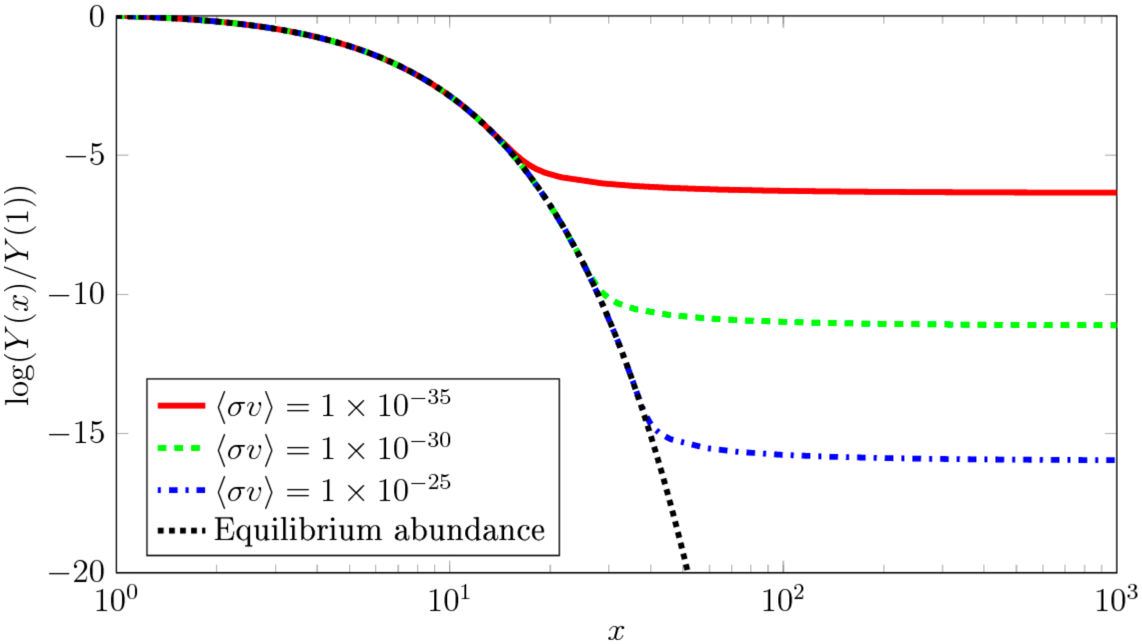

Approximately Solving the DM freeze-out Boltzmann Equation

- Approximately Solving the Boltzmann Equation

$$\frac{dY}{dx} = -\frac{\lambda}{x^2}(Y^2 - Y_{\rm eq}^2)$$

$$\frac{\lambda}{x^2} \equiv \langle \sigma v \rangle \frac{xs}{H_{\rm rad}(T = m_{\rm DM})}$$

- For $x \gg 1$

$$\frac{dY}{dx} \approx -\frac{\lambda}{x^2} Y^2$$

$$\Longrightarrow Y_\infty^{-1} - Y_{\rm fo}^{-1} = \frac{\lambda}{x_{\rm fo}} \Longrightarrow Y_\infty^{-1} = \frac{\lambda}{x_{\rm fo}}$$

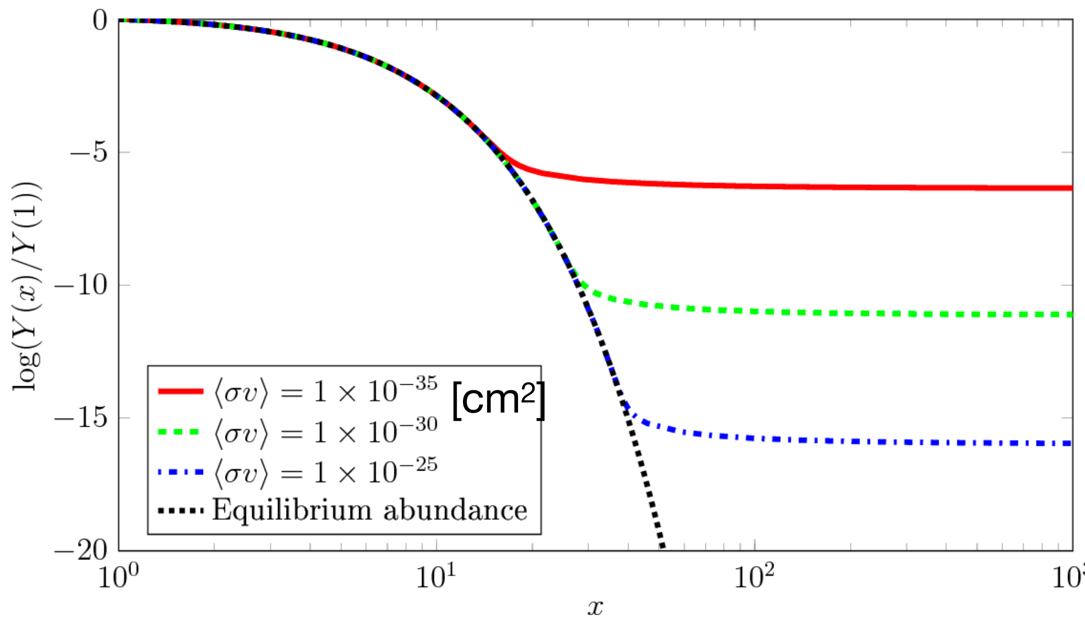

Approximately Solving the DM freeze-out Boltzmann Equation

- Approximately Solving the Boltzmann Equation $Y_\infty^{-1} = \frac{\lambda}{x_{\rm fo}}$

- Today's DM energy fraction $\Omega_{\rm dm} = 26.8\,\%$

$$\Omega_{\rm dm} h^2 = \frac{Y_0 s_0 m_{\rm dm}}{\rho_{\rm cr}} h^2 \approx \frac{Y_\infty s_0 m_{\rm dm}}{\rho_{\rm cr}} h^2 \approx 0.3 \left(\frac{m_{\rm dm}}{\rm eV}\right) Y_\infty$$

$$\rho_{\rm cr} = 3H_0^2 m_{\rm Pl}^2/8\pi \approx 8\times 10^{-47} h^2\,{\rm GeV}^4 \text{ and } s_0 \approx 2970\,{\rm cm}^{-3}$$

- Magnitude of DM Annihilation Cross-Section at Thermal Decoupling

$$\Omega h^2 \approx 0.1 \left(\frac{x_f}{25}\right) \left(\frac{g_\star}{80}\right)^{-1} \left(\frac{3\times 10^{-26}{\rm cm}^3{\rm s}^{-1}}{\langle \sigma v\rangle}\right)$$

WIMP Dark Matter Miracle

- Magnitude of DM Annihilation Cross-Section at Thermal Decoupling

$$\Omega h^2 \approx 0.1 \left(\frac{x_f}{25}\right) \left(\frac{g_\star}{80}\right)^{-1} \left(\frac{3 \times 10^{-26}\mathrm{cm}^3\mathrm{s}^{-1}}{\langle \sigma v \rangle}\right)$$

$$\langle \sigma v \rangle \sim 3 \times 10^{-26} cm^3/s$$

$$\sim 10^{-8}\ \mathrm{GeV}^{-2} \sim \frac{\alpha^2}{m_W^2}$$

- DM might be associated with the electroweak interaction scale.

The WIMP Miracle

- WIMP miracle is properly a statement about perturbative thermal relics:
  - upper bound on m: $g^2 < 4\pi$

    $\Rightarrow \; m \lesssim 40\,\mathrm{TeV}$

  - lower bound on m: freezeout must happen when DM is relativistic...

    $\Rightarrow \; m \gtrsim 10\,\mathrm{eV}$

  - but in practice packing DM into galaxies is more stringent

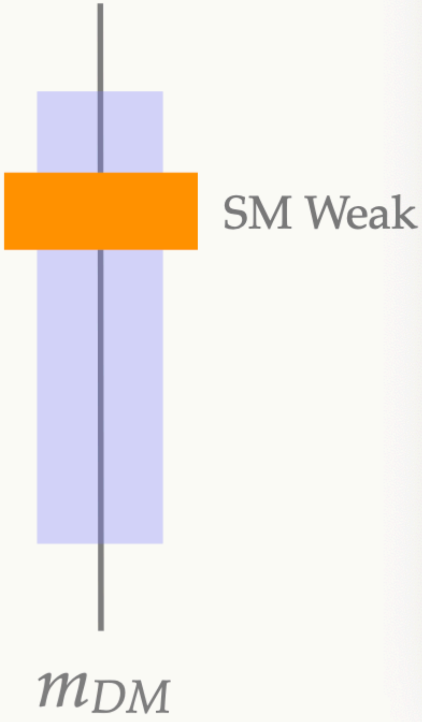

Why weak scale DM popular in the past?

- DM stability as an extension to solve the gauge hierarchy problem （higgs quadratic divergence)

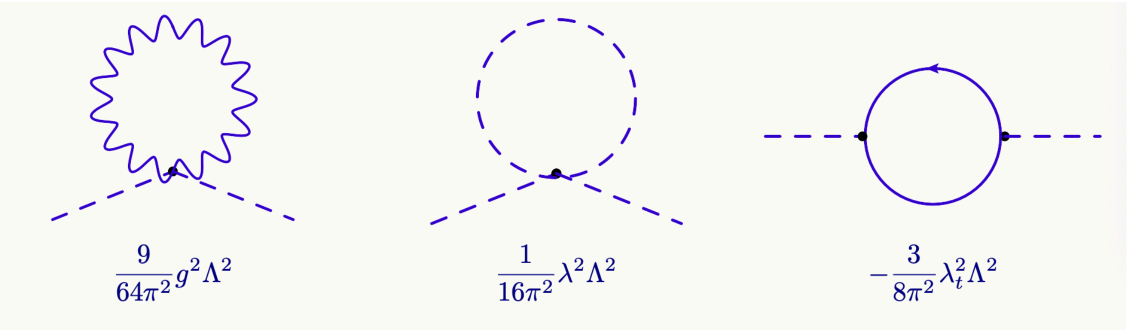

- SUSY models
- Little Higgs/Twin Higgs
- UED

However， we do not see new particles at the LHC………

WIMP DM crisis

- Null result from direct detection
    - Maybe discovery in the corner?
    - Neutrino floor and beyond: directional ..
    - The rise of light dark matter ($\lesssim$ 10 GeV)

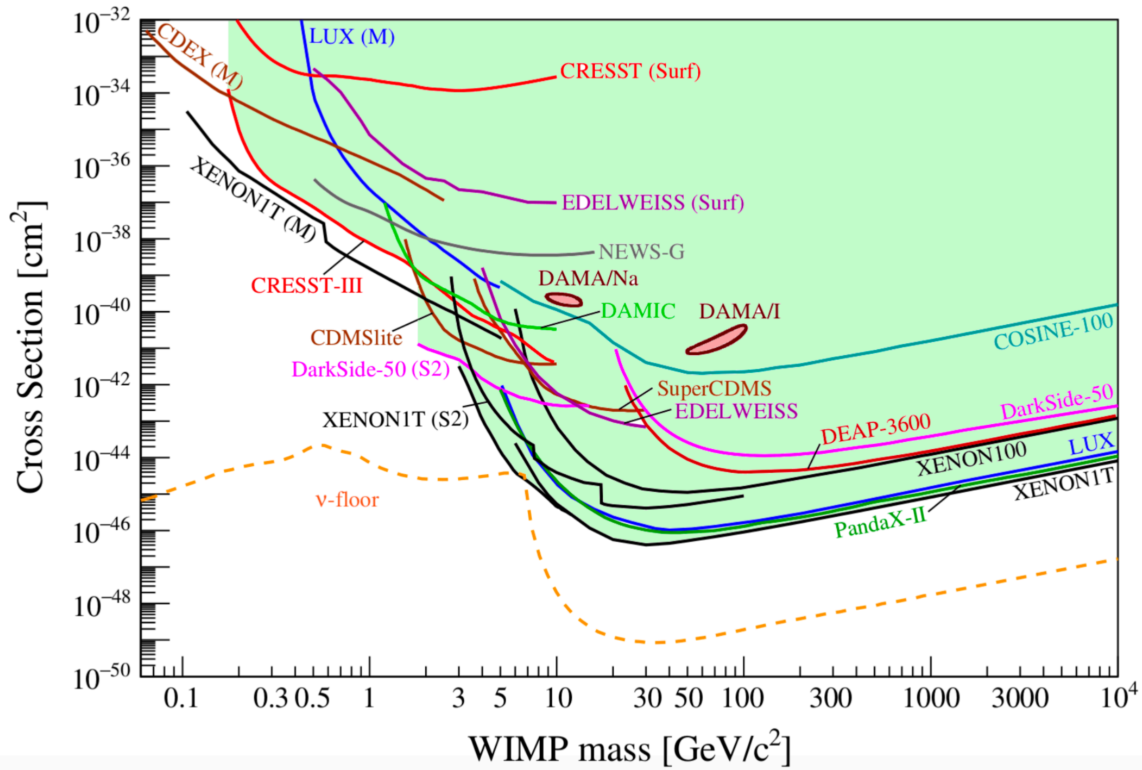

APPEC Committee Report: 2104.07634

Detection Methods of DM

Particle-like DM Detection

Theorists' View of DM

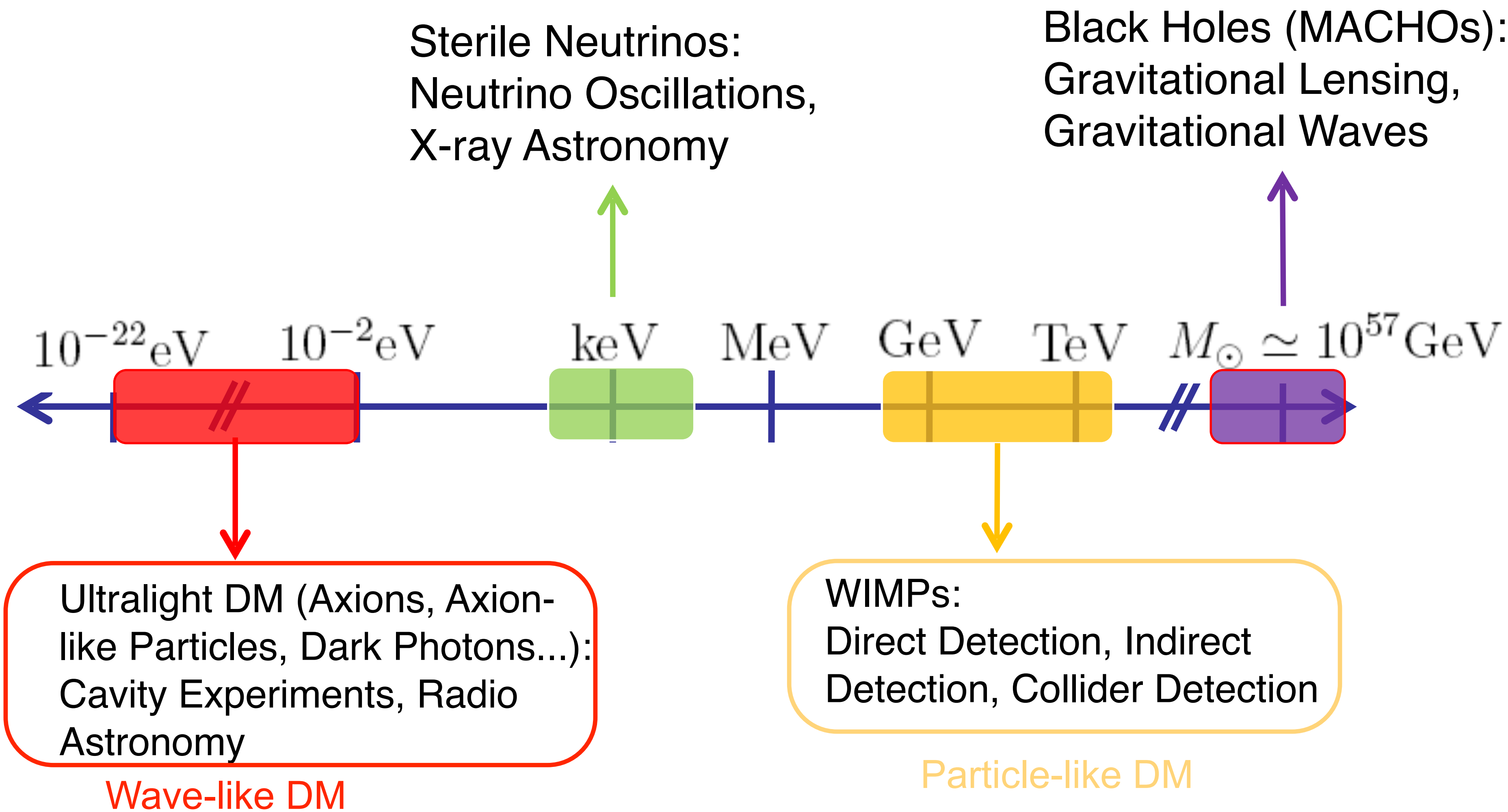

Theoretical possibilities for DM are numerous, spanning a wide range of masses and interaction cross-sections, making experimental detection highly challenging.

Detecting WIMP DM from Underground to Space

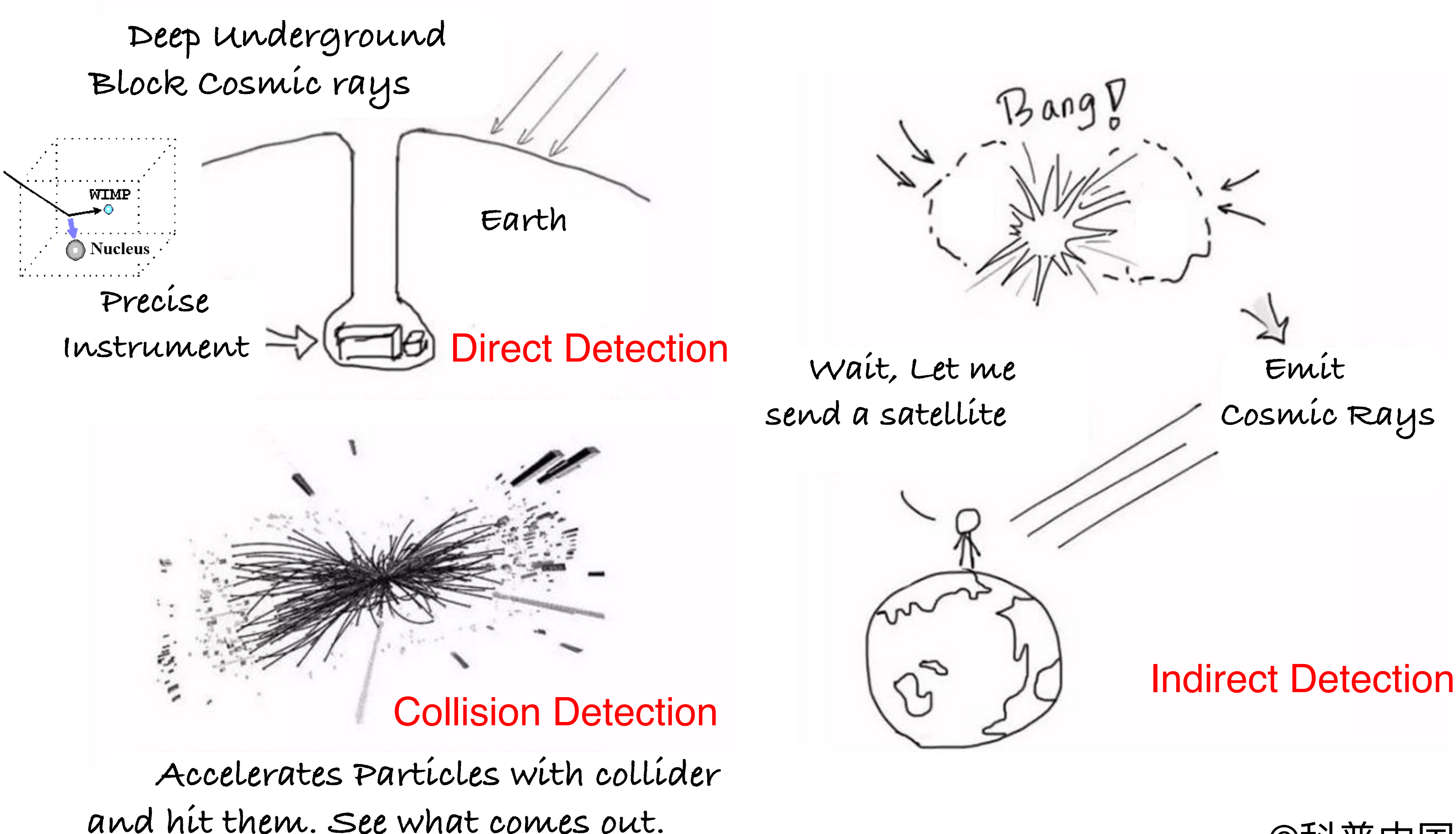

Direct Detection of Dark Matter

- Measuring the recoil signal of nuclei after collisions with DM
  - Proposed in 1985 (Goodman & Witten), detection sensitivity has improved by six orders of magnitude over 30 years.

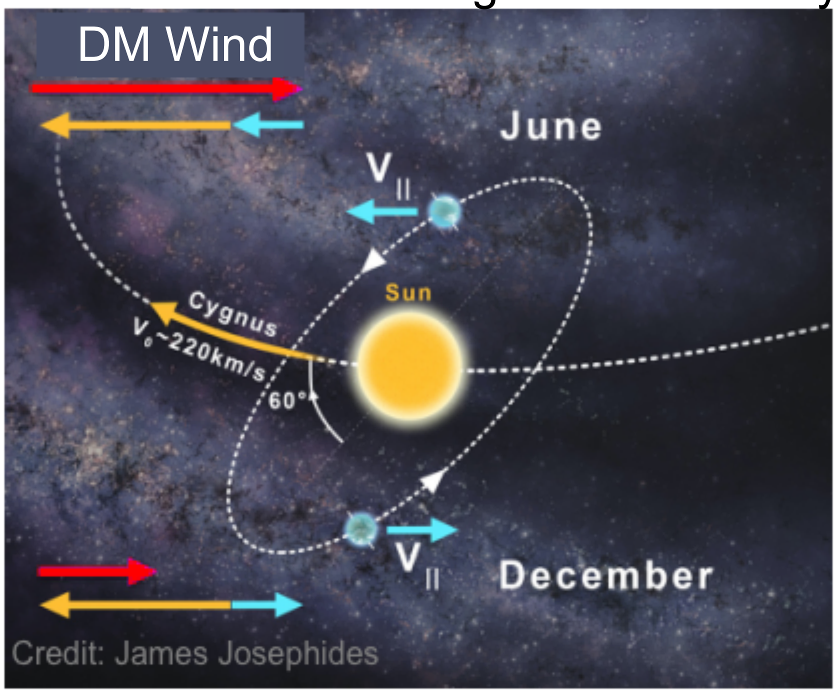

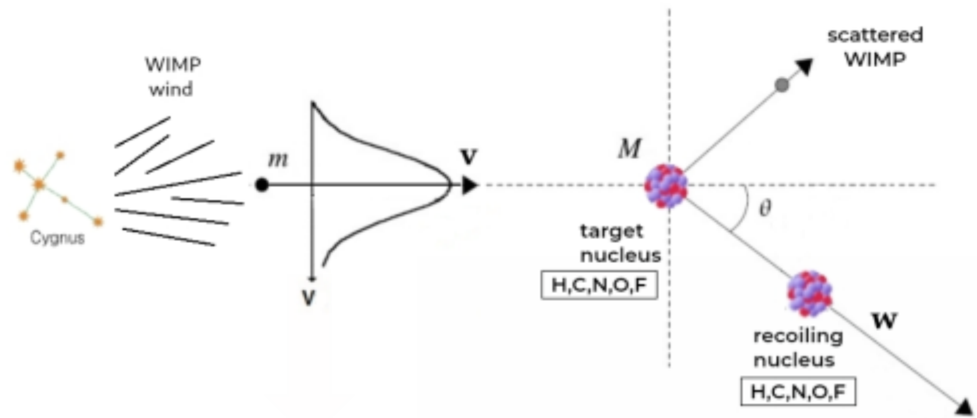

Direct Detection of WIMP DM

What is collision?

- Particle Physicist's language
  - Interaction

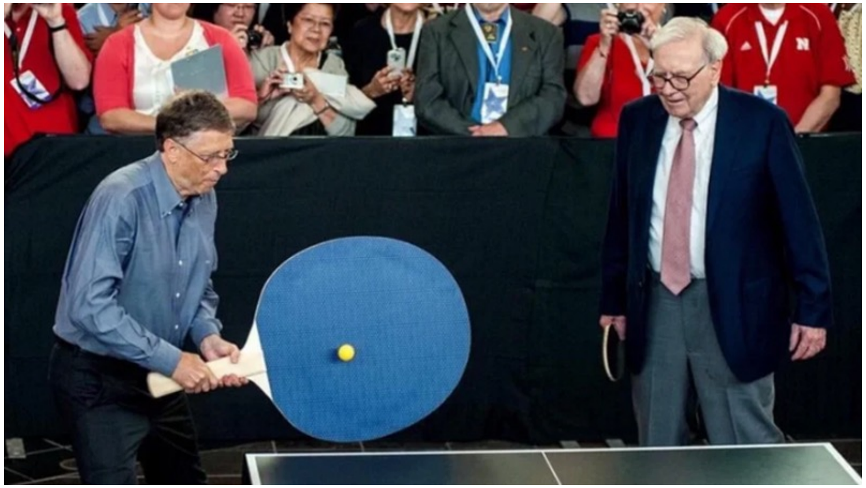

- When a ping-pong ball and paddle collide => interaction occurs
  - Dark matter and ordinary matter can interact: collision!
- The stronger the interaction: the easier the collision
  - The size of the paddle hints the strength of interaction: cross-section

Direct Detection of WIMP DM

What is the target matter

- How to detect such weak “interactions”
  - Large amount of atoms => One big piece of ordinary matter
  - Everyone has 100000000000000000000000000000(10^{29}) atoms

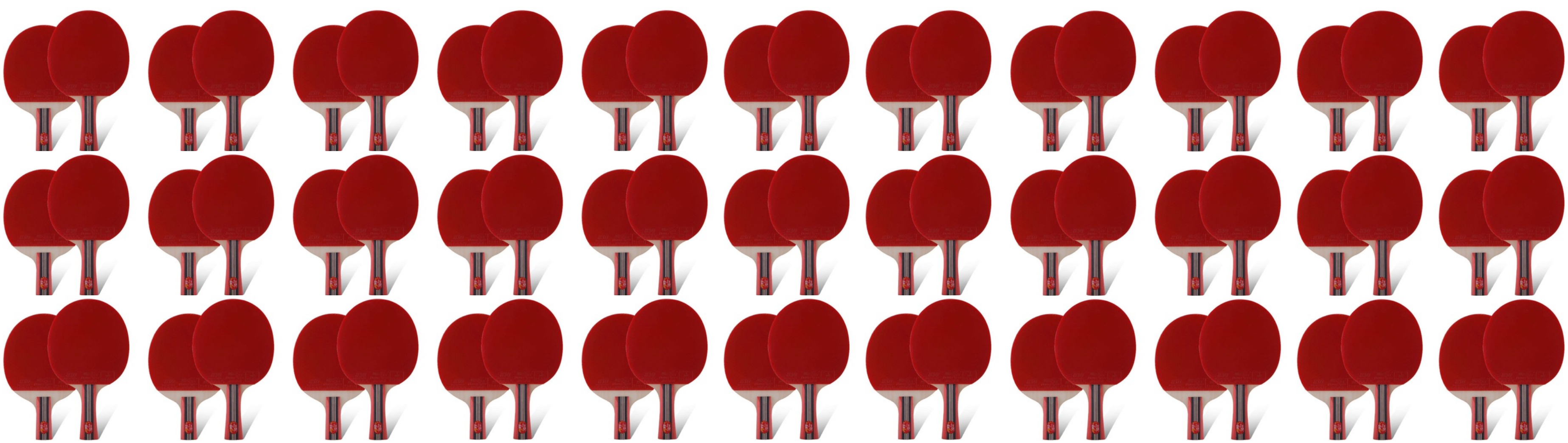

Direct Detection of WIMP DM

What is recoil

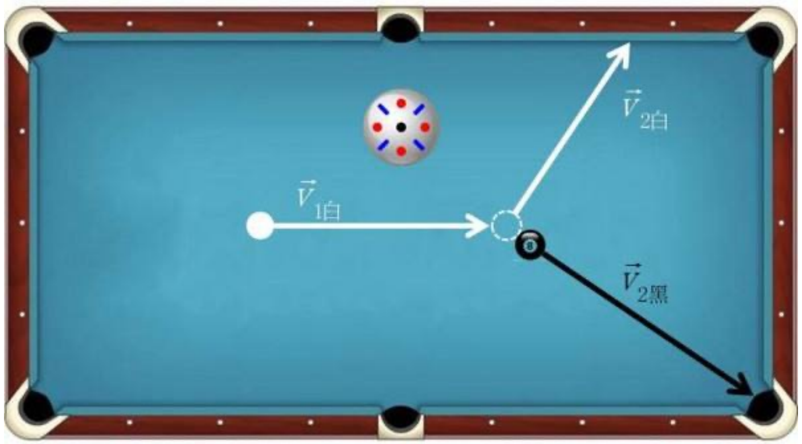

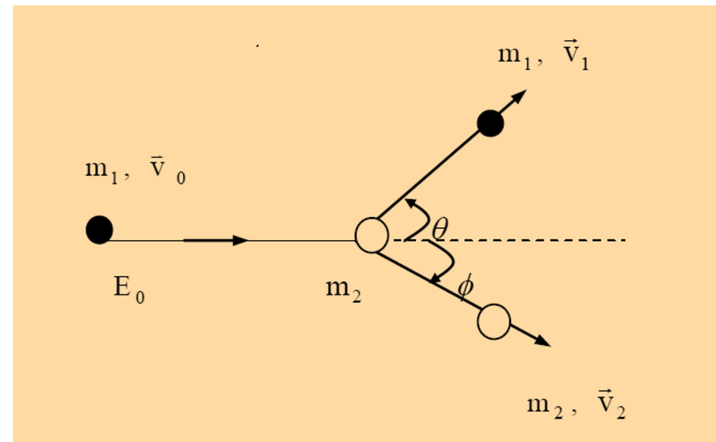

- The recoiled atoms carry energy
- Direct Detection of DM can change recoil into observable signals
  - Infer the mass of the DM particles
  - Measure the interaction strength with ordinary matter

Direct Detection of WIMP DM

Can DM easily collide with ordinary matter

- 100000000(10^8) DM particles travel through us each second
- Each person has 10^{29} target particles
- Each person collides with dark matter < 1 time each year

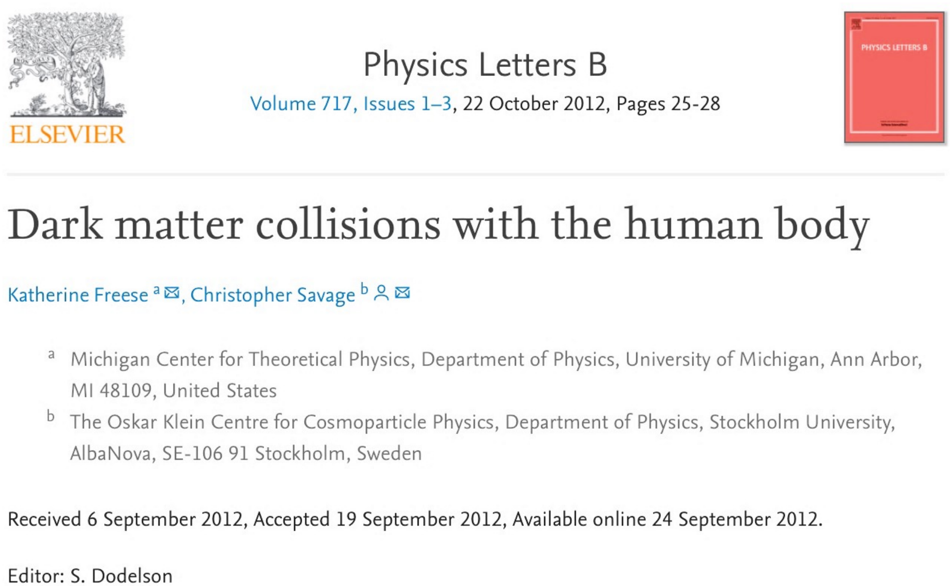
ELSEVIER

Physics Letters B

Volume 717, Issues 1–3, 22 October 2012, Pages 25-28

PHYSICS LETTERS B

Dark matter collisions with the human body

Katherine Freese [a], Christopher Savage [b]

[a] Michigan Center for Theoretical Physics, Department of Physics, University of Michigan, Ann Arbor, MI 48109, United States

[b] The Oskar Klein Centre for Cosmoparticle Physics, Department of Physics, Stockholm University, AlbaNova, SE-106 91 Stockholm, Sweden

Received 6 September 2012, Accepted 19 September 2012, Available online 24 September 2012.

Editor: S. Dodelson

Current Direct Detection of WIMP DM

Calculate the DM Event Rate

- For a 1ton Xenon Detector
- Assumptions for DM
  - DM mass-100GeV
  - DM cross-section with xenon nucleus-$10^{-38}\mathrm{cm}^2$
  - DM relative velocity-200km/s
  - DM density near the earth-0.3GeV/cm^3
- Please estimate, how many collision signals on the device each year?

1

Direct Detection of WIMP DM

Where to find the Dark Matter

- Our body collides with cosmic rays and gamma rays 10^8 times each day
  - Cosmic rays: high energy particles from the universe
  - Gamma rays: from adjacent nucleus decay
  - Those fake signals are called "background noise"

- Hide the detector into deep underground, and cover the detector with thick screening material

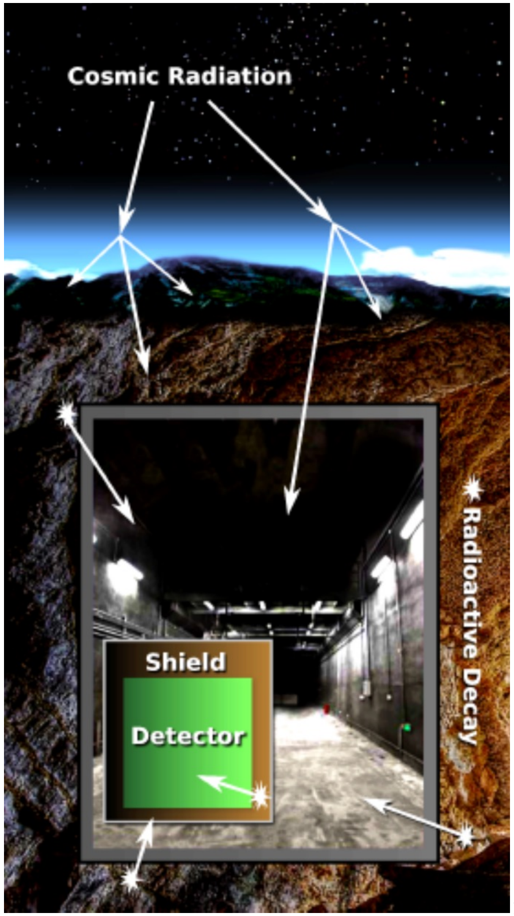

Direct Detection of WIMP DM

DM scatter with nucleus of atoms

- DM particles elastically scatter with target nucleus
- Recoil energy of nucleus $E_R = \frac{4m_\chi m_N}{(m_\chi + m_N)^2} E_\chi^{kin}$
  - $E_\chi^{kin} \sim \frac{1}{2} m_\chi v^2 \sim 50\ \mathrm{keV} \frac{m_\chi}{100\ \mathrm{GeV}}$

Low detection threshold

- Event Rate of unit target mass scattering with DM
  - $\frac{dR}{dE_R} \propto \sigma_N \frac{\rho_{DM}}{m_{DM}} \int_{v_{min}}^{v_{esc}} \frac{dv}{v} f(v)$
- Spin-unrelated $\sigma_N^{SI}(E_R) \propto \boldsymbol{A}^2 F^2(E_R) \sigma_n$

Heavy target nucleus

- Spin-related $\sigma_N^{SD}(E_R) \propto \frac{1}{2\boldsymbol{J}+1} S(E_R) \sigma_n$

Target nucleus with spin

Direct Detection of WIMP DM

Calculate signatures of DM signal

- Assumptions for DM
  - DM mass-100GeV
  - DM cross-section with xenon nucleus-$10^{-38}\mathrm{cm}^2$
  - DM relative velocity-200km/s
  - DM density near the earth-0.3GeV/cm^3
- Please estimate the recoil energy of nucleus scattering with DM

Direct Detection of WIMP DM

Signatures of DM signal

- **Scattering cross section on nuclei**
  - Spin-independent, $\propto A^2$, Form factor
  - Spin-dependent, spin structure factor

$$\frac{dR}{dE_R} = \frac{\rho_0}{m_\chi m_N} \int_{v_{min}}^{v_{esc}} \frac{d\sigma_{\chi N}}{dE_R}(v, E_R) v f(v) dv$$

$$\frac{d\sigma_{\chi N}}{dE_R} = \frac{m_N}{2\mu_N^2 v^2}(\sigma_0^{SI} F_{SI}^2(E_R) + \sigma_0^{SD} F_{SD}^2(E_R))$$

Recoil energy spectrum

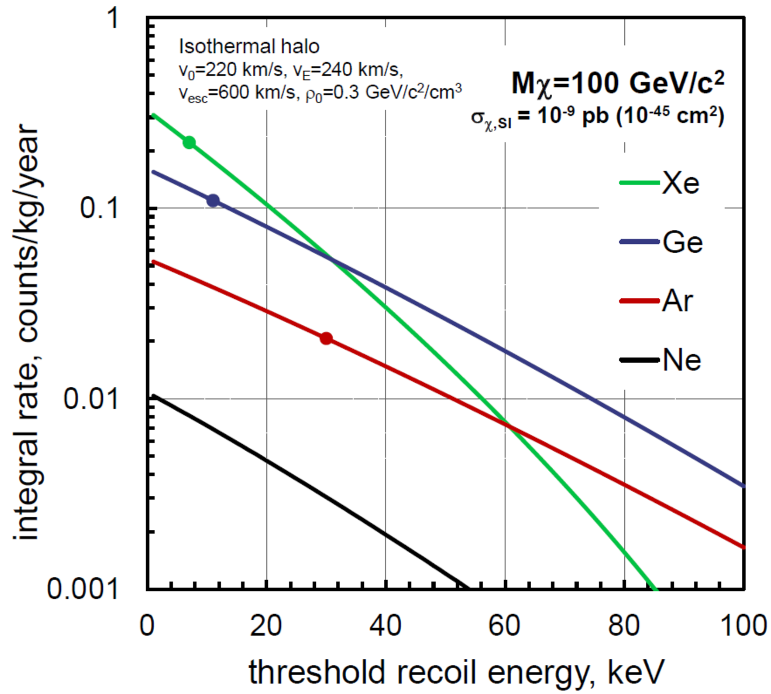

19

Underground Direct Detection

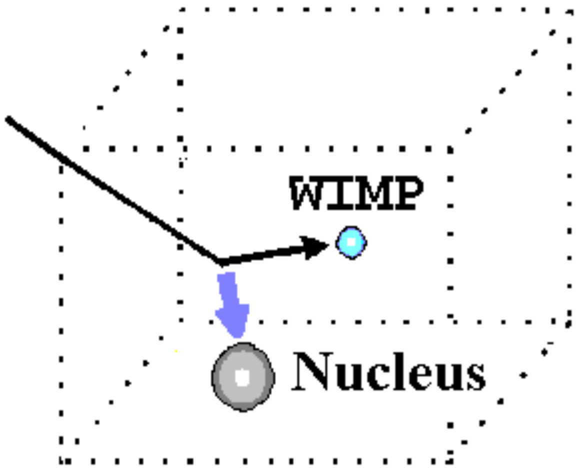

- ➢ Detect the recoil energy of nucleus scattered by DM
- ➢ Deep underground, to block the cosmic ray background

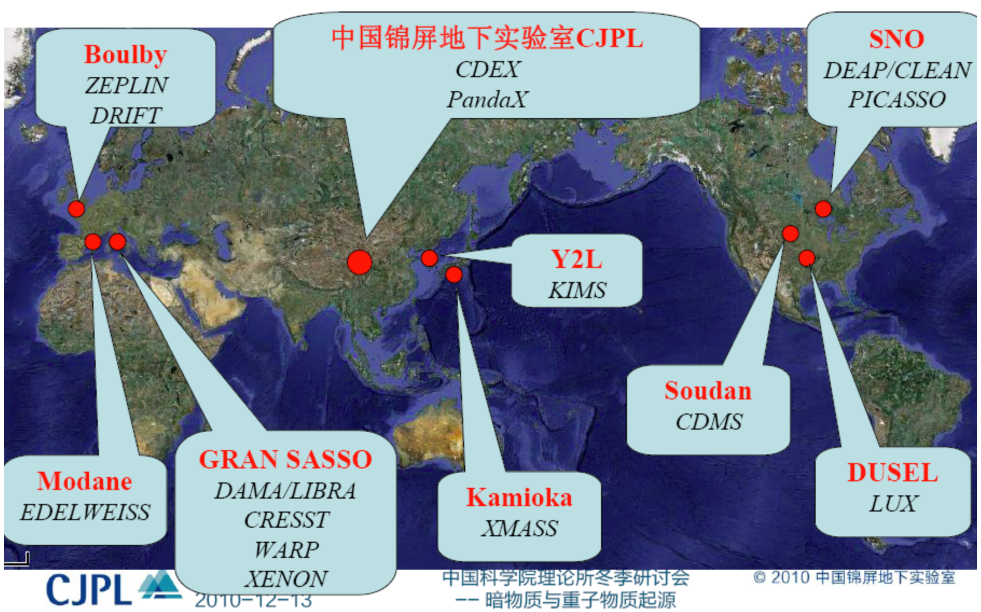

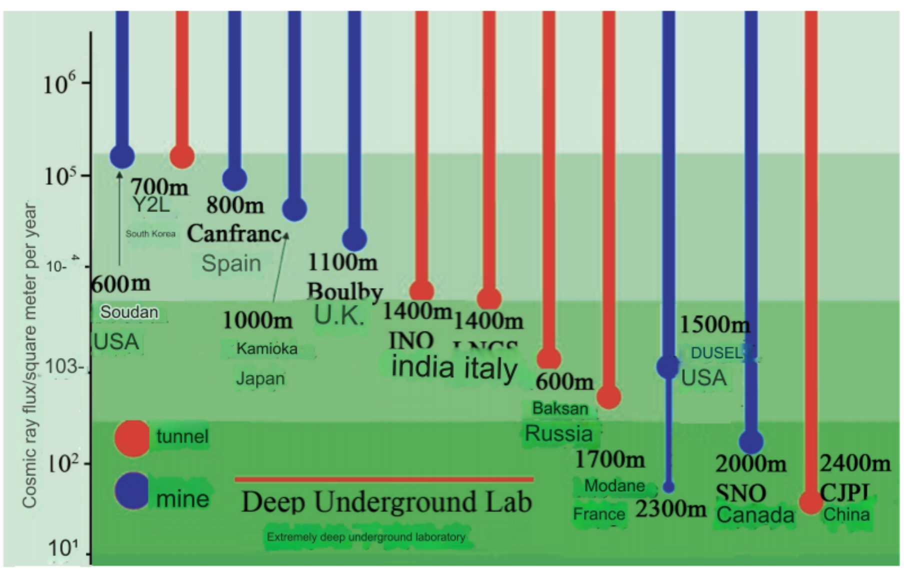

Annual modulation observed by DAMA

DAMA (2008)

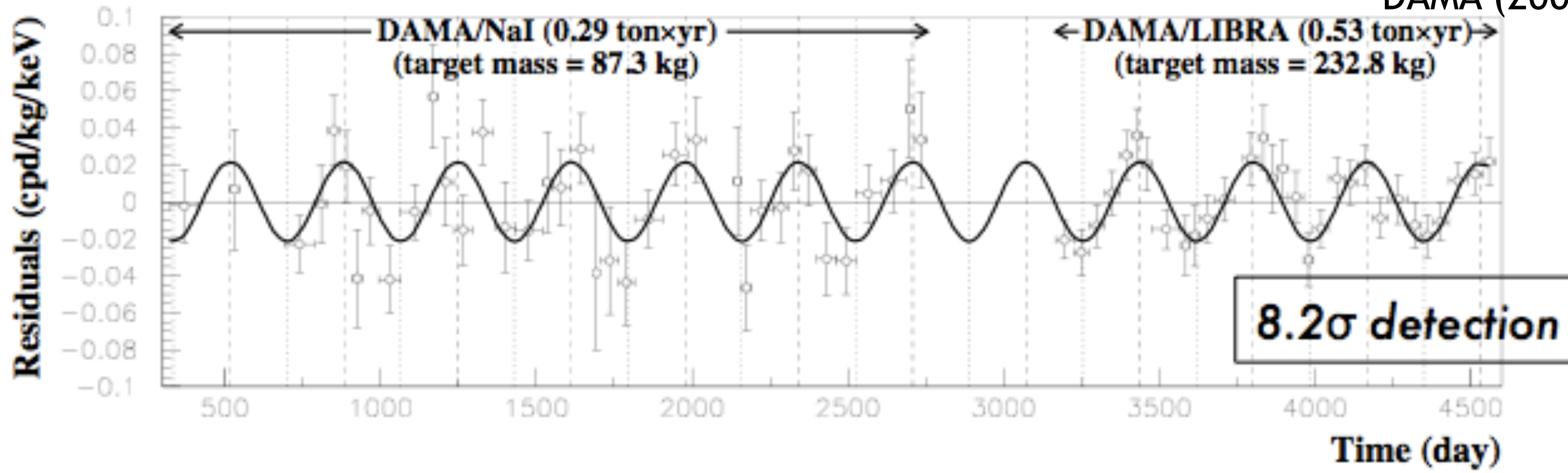

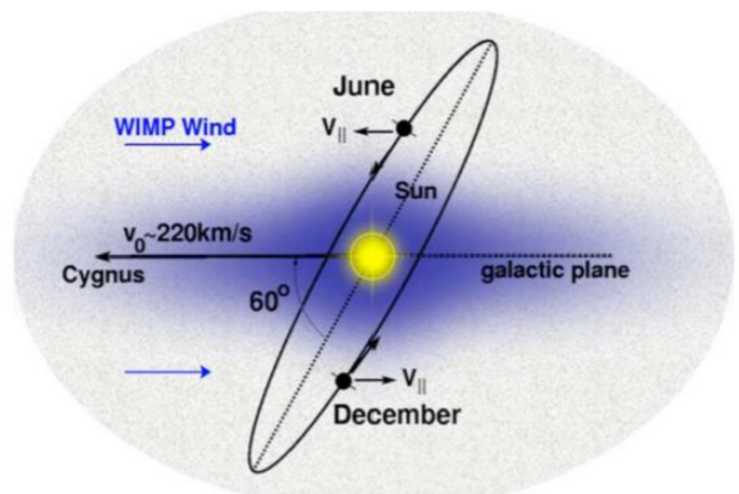

COSINE (2018)

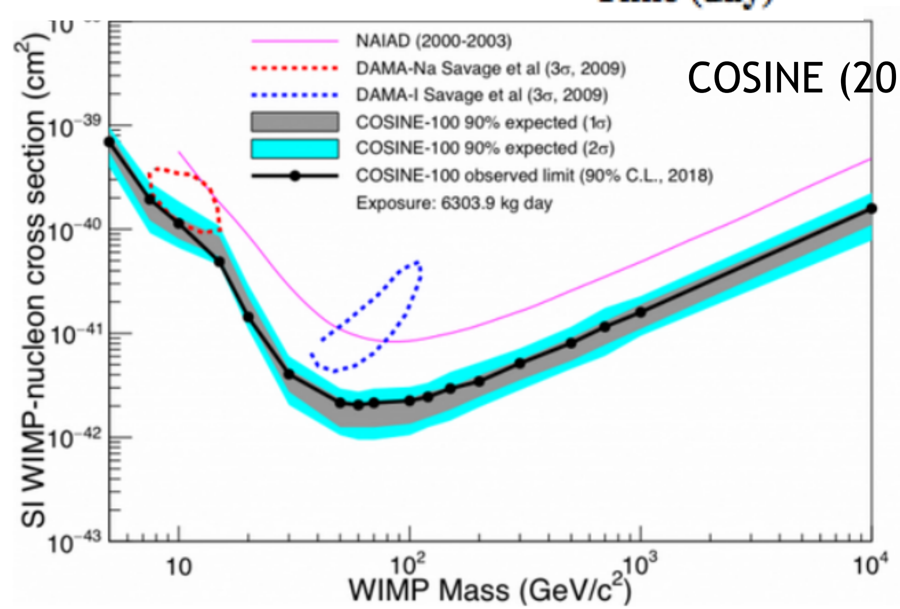

Inconsistent with other experiments!

PandaX in Jinping

Direct DM detection in PandaX

PandaX-4T (2021)

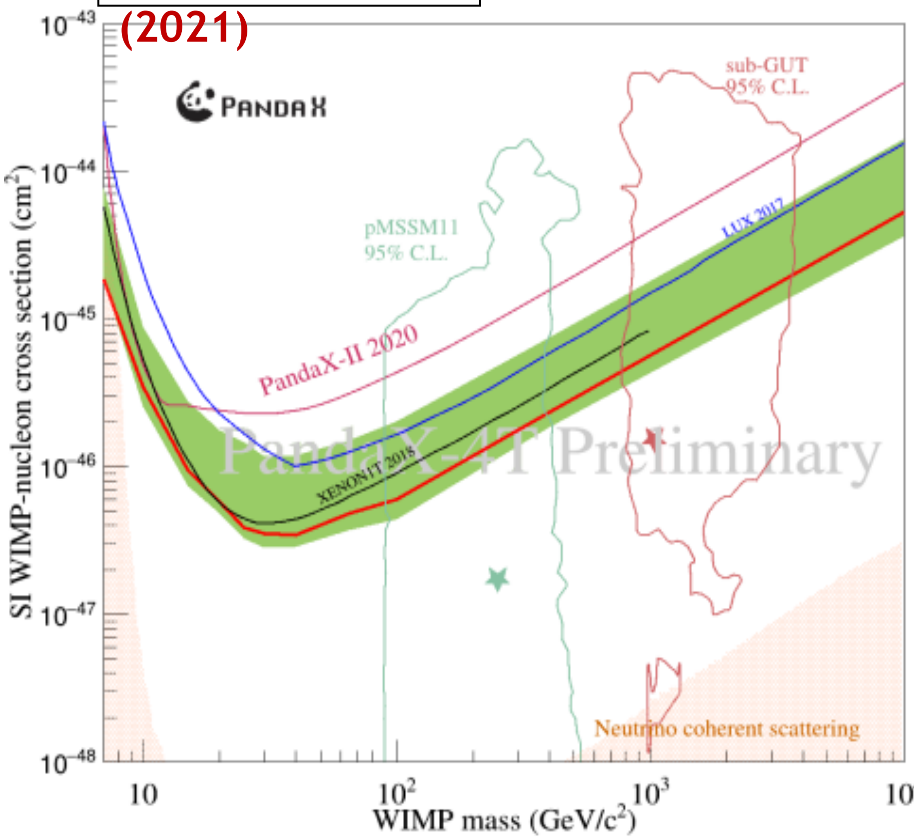

CDEX (2018)

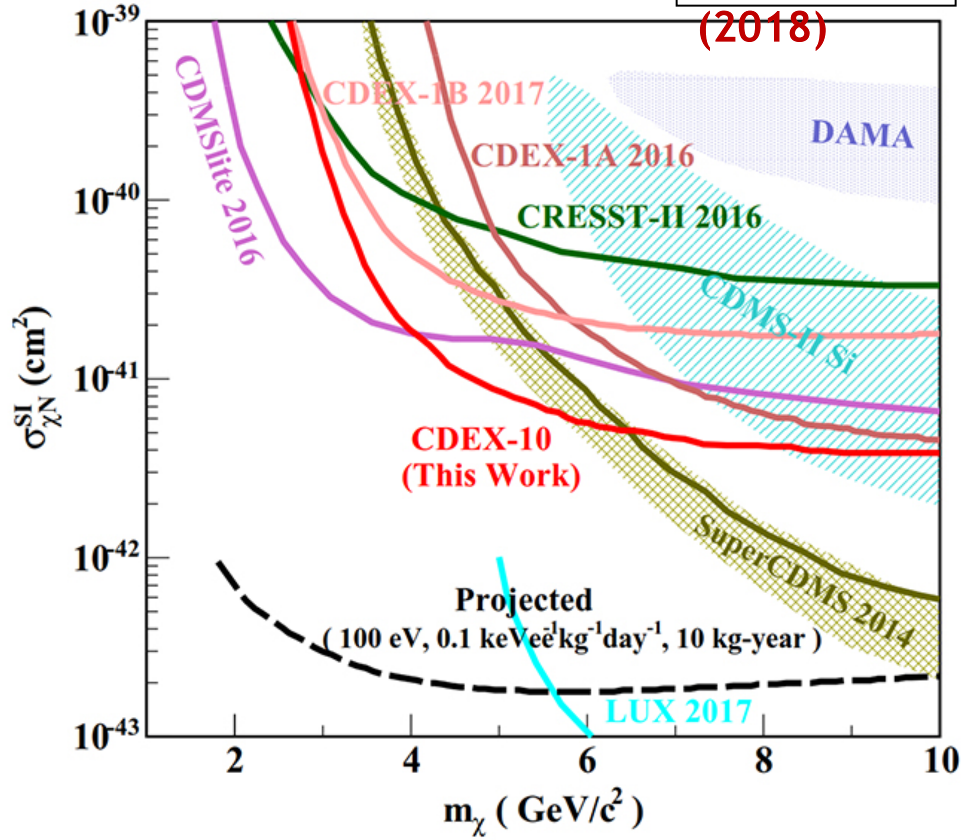

XENON1T excess of electron recoil

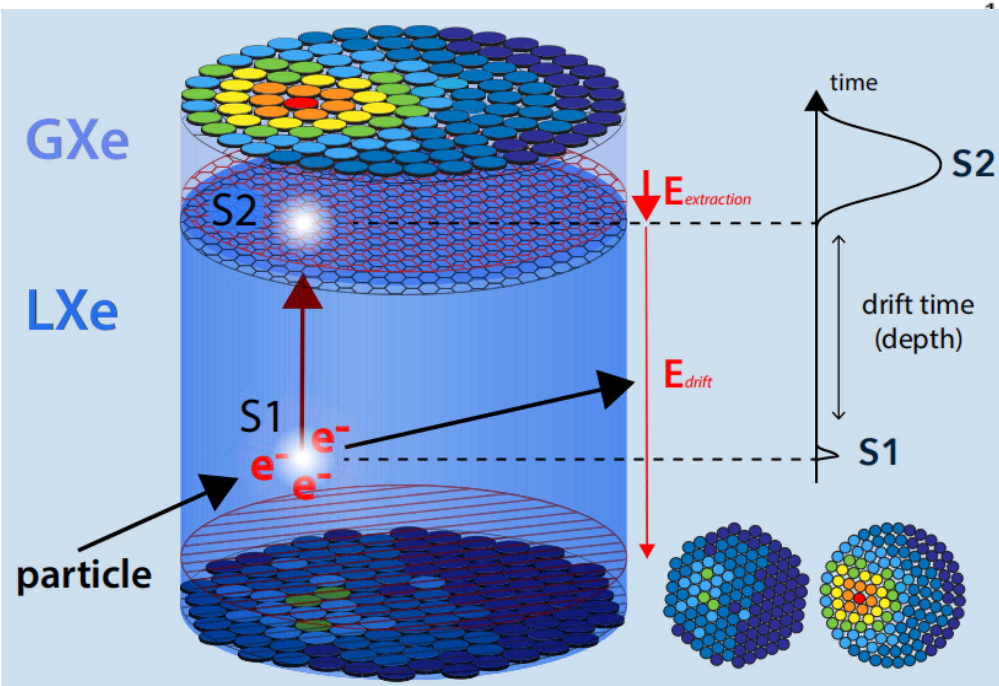

Aprile et al., PRD, 102, 072004 (2020)

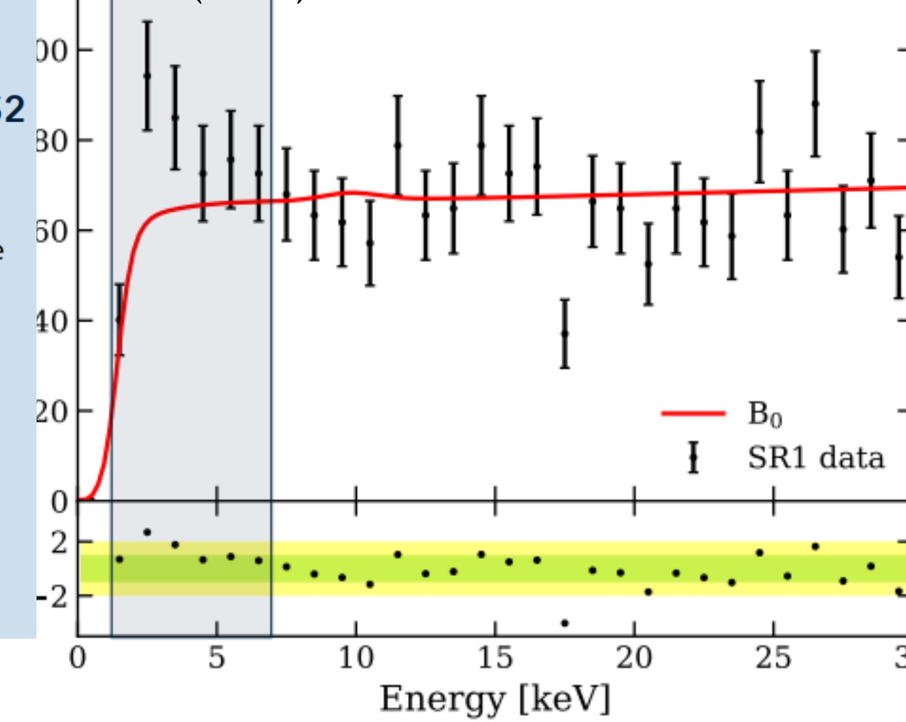

XENON1T reported its latest analysis results of electron recoil events in June 2020, finding an excess of about 3.5σ in the 2-7 keV energy range. Possible explanations include tritium background, solar axions, neutrino magnetic moment, dark matter, etc.

PandaX-II results of electron recoil

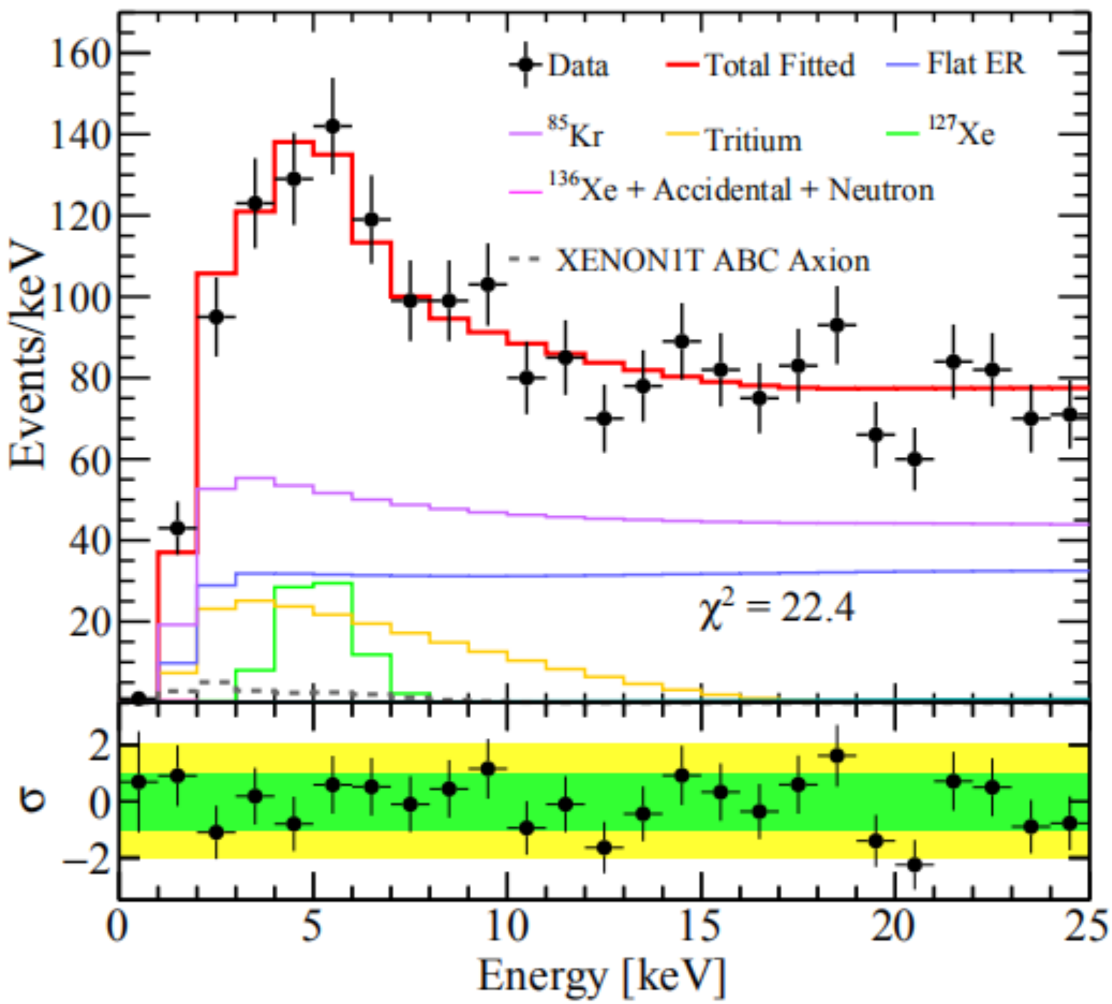

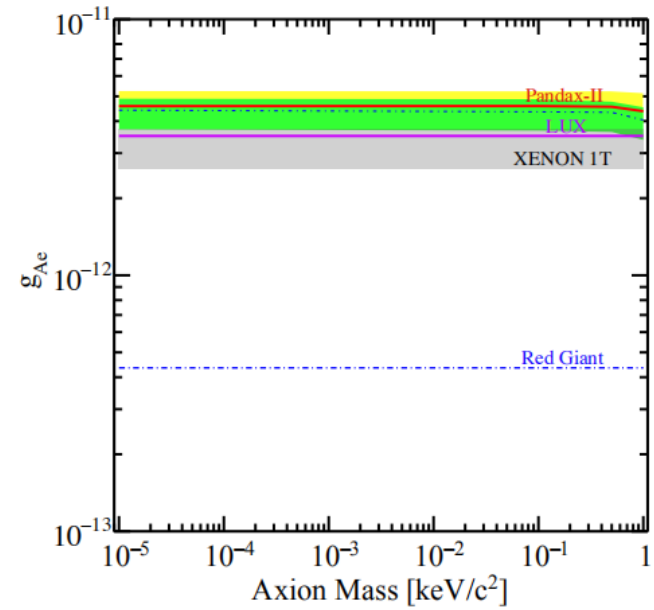

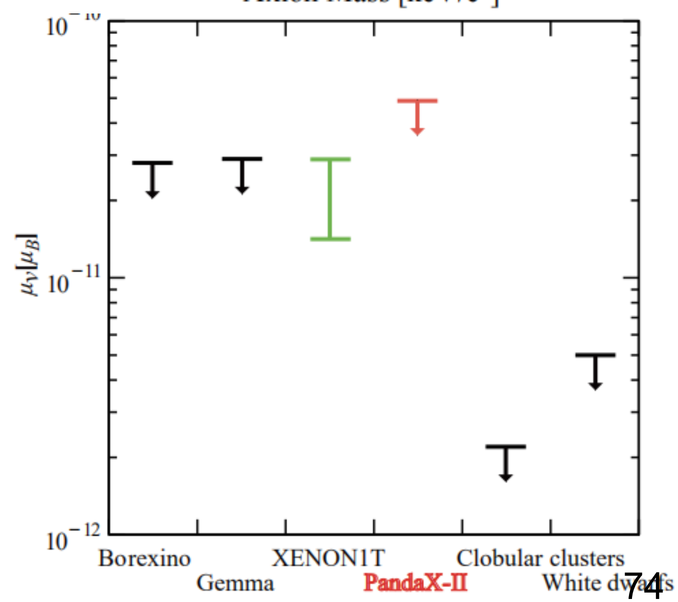

Consistent with expected background, but can't exclude the XENON1T results. Zhou et al., Chin. Phys. Lett., 38, 011301 (2020)

Current Direct Detection of WIMP DM

- ➢ Lower threshold
- ➢ Boosted DM

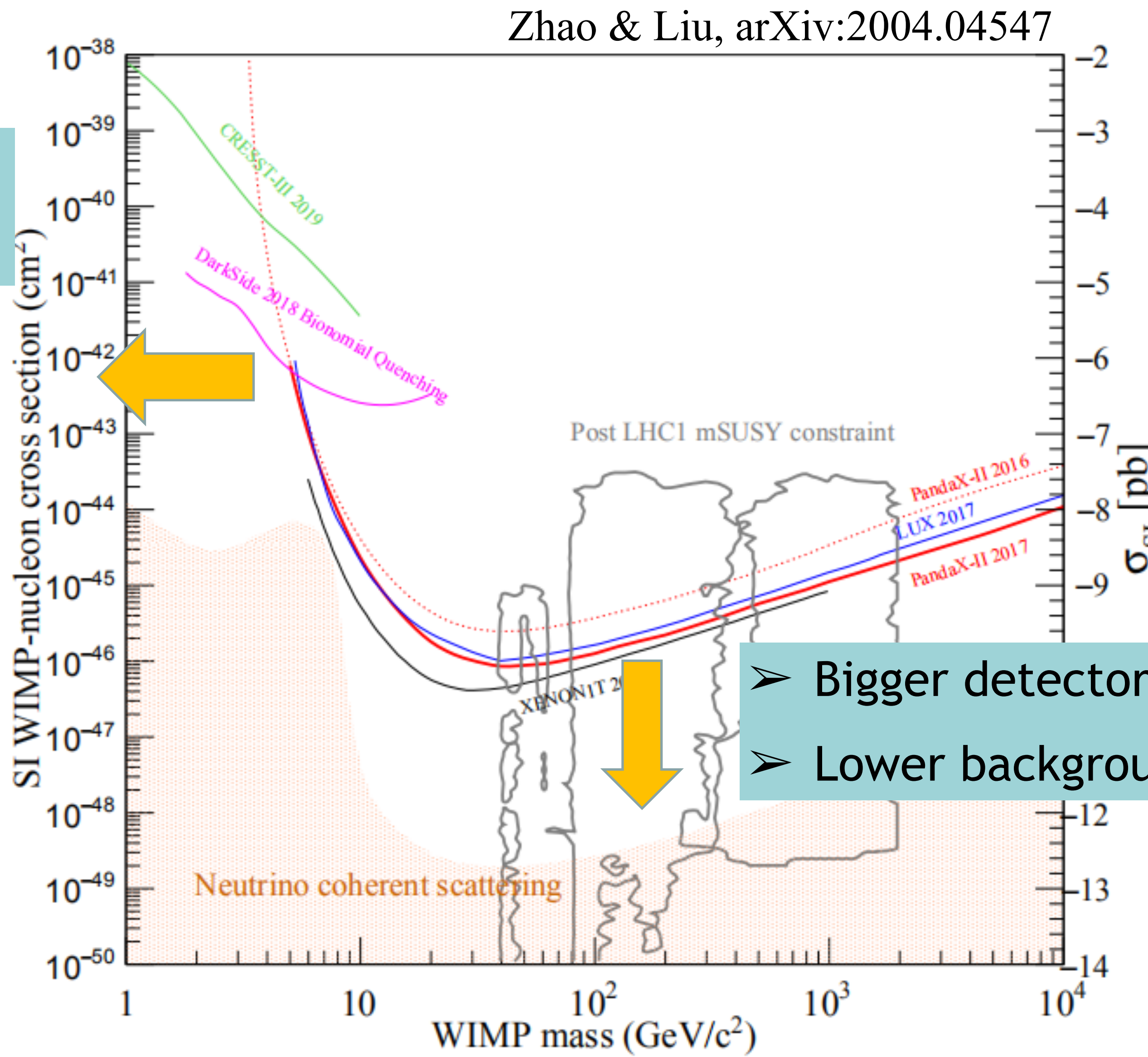

- ➢ Bigger detector
- ➢ Lower background

Detect DM from Large particle collision experiment

dark matter production in association with X

- dark matter escape detection
- X: visible particles
- E_T^{miss}: momentum imbalance in transverse plane

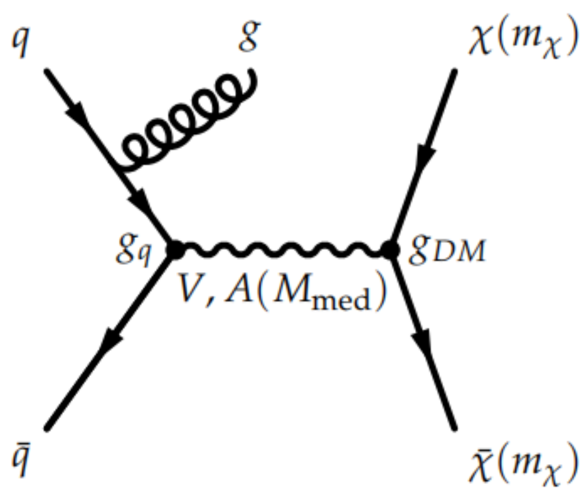

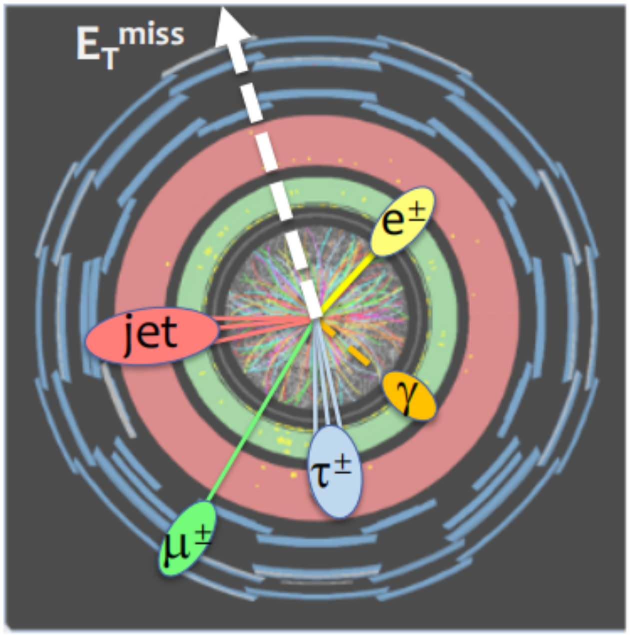

Detect DM from Large particle collision experiment

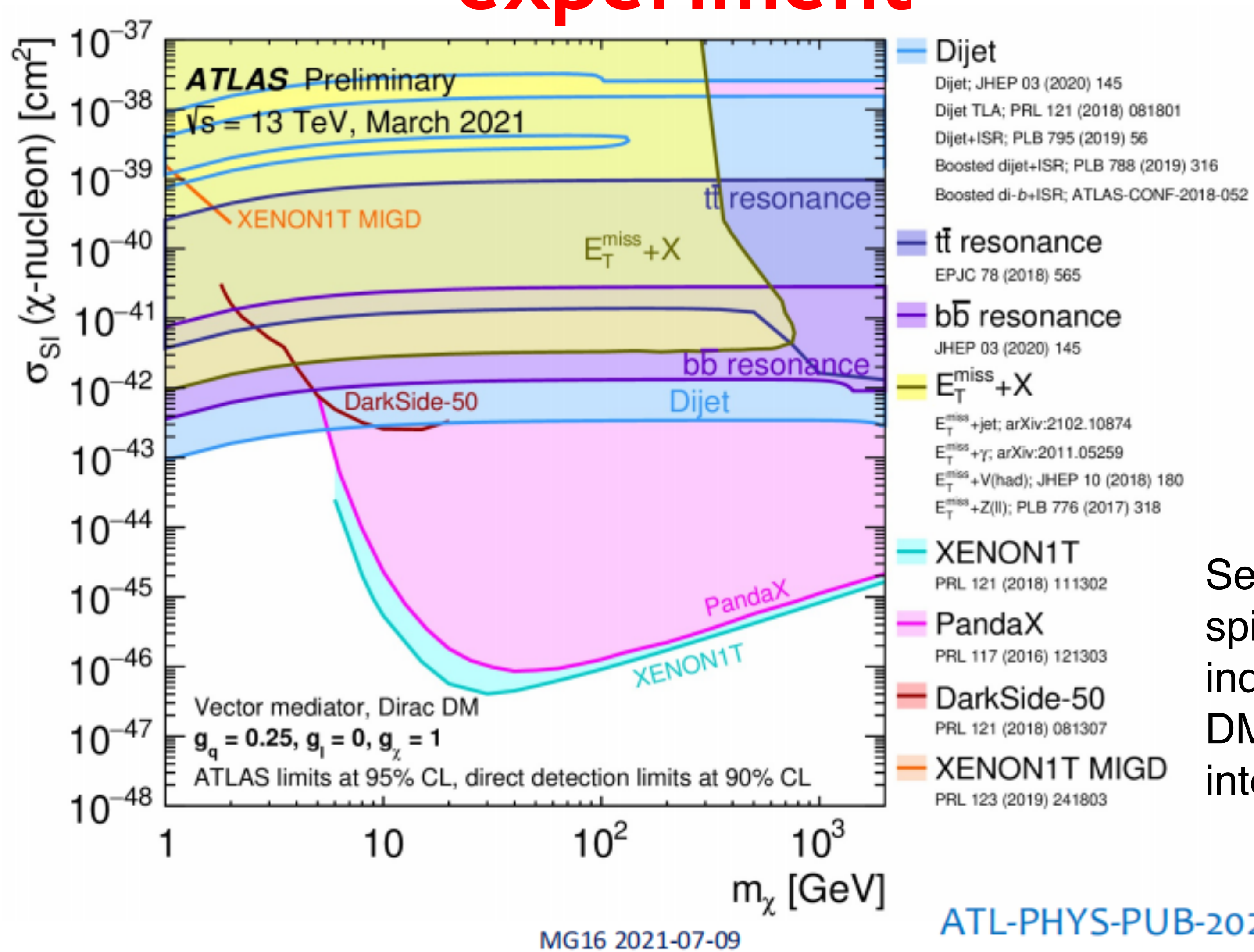

Search for spin-independent DM-nucleus interaction

ATL-PHYS-PUB-2021-006

Detect DM from Large particle collision experiment

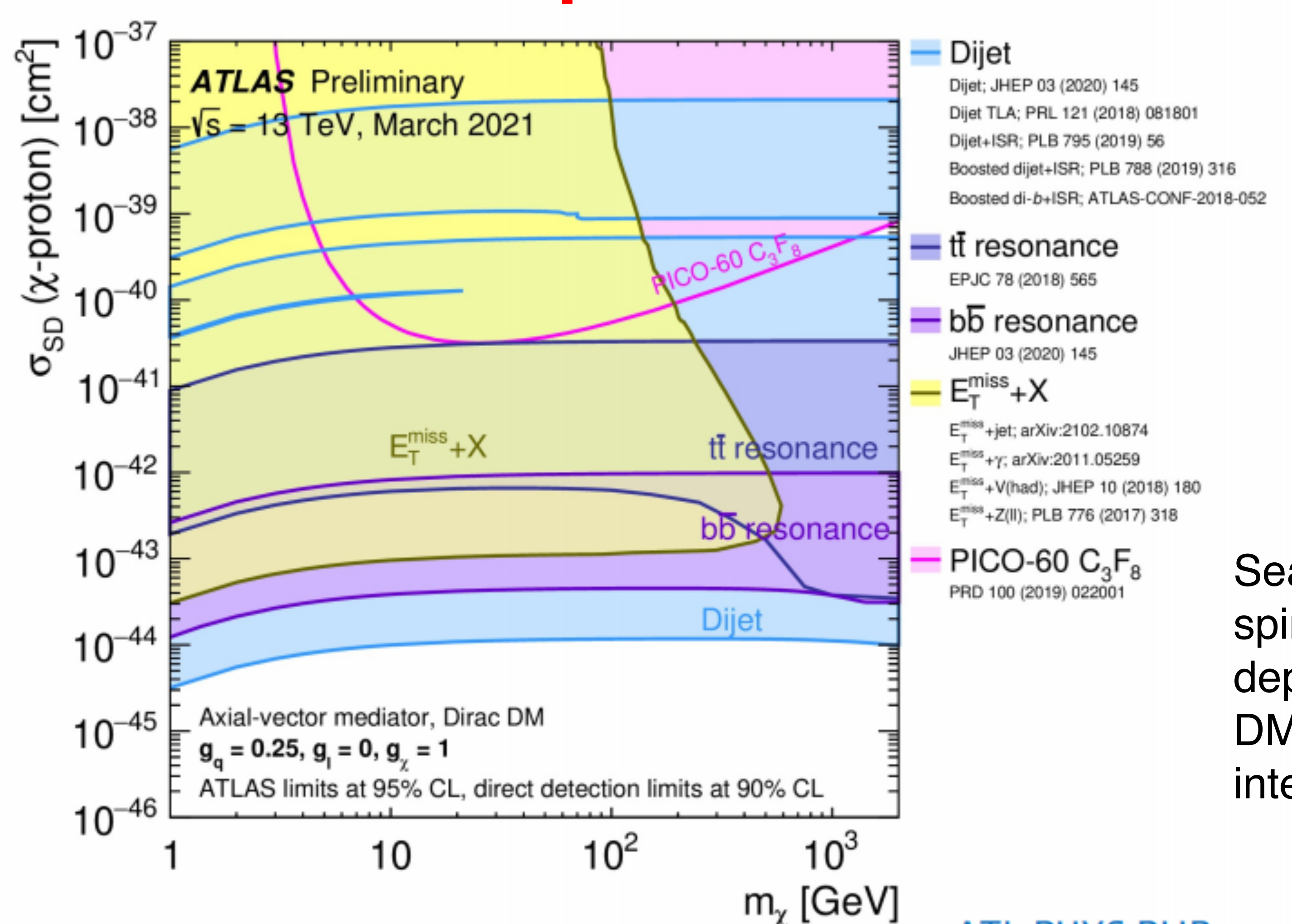

MG16 2021-07-09

Search for spin-dependent DM-nucleus interaction

ATL-PHYS-PUB-2021-006

Indirect detection of Cosmic Rays

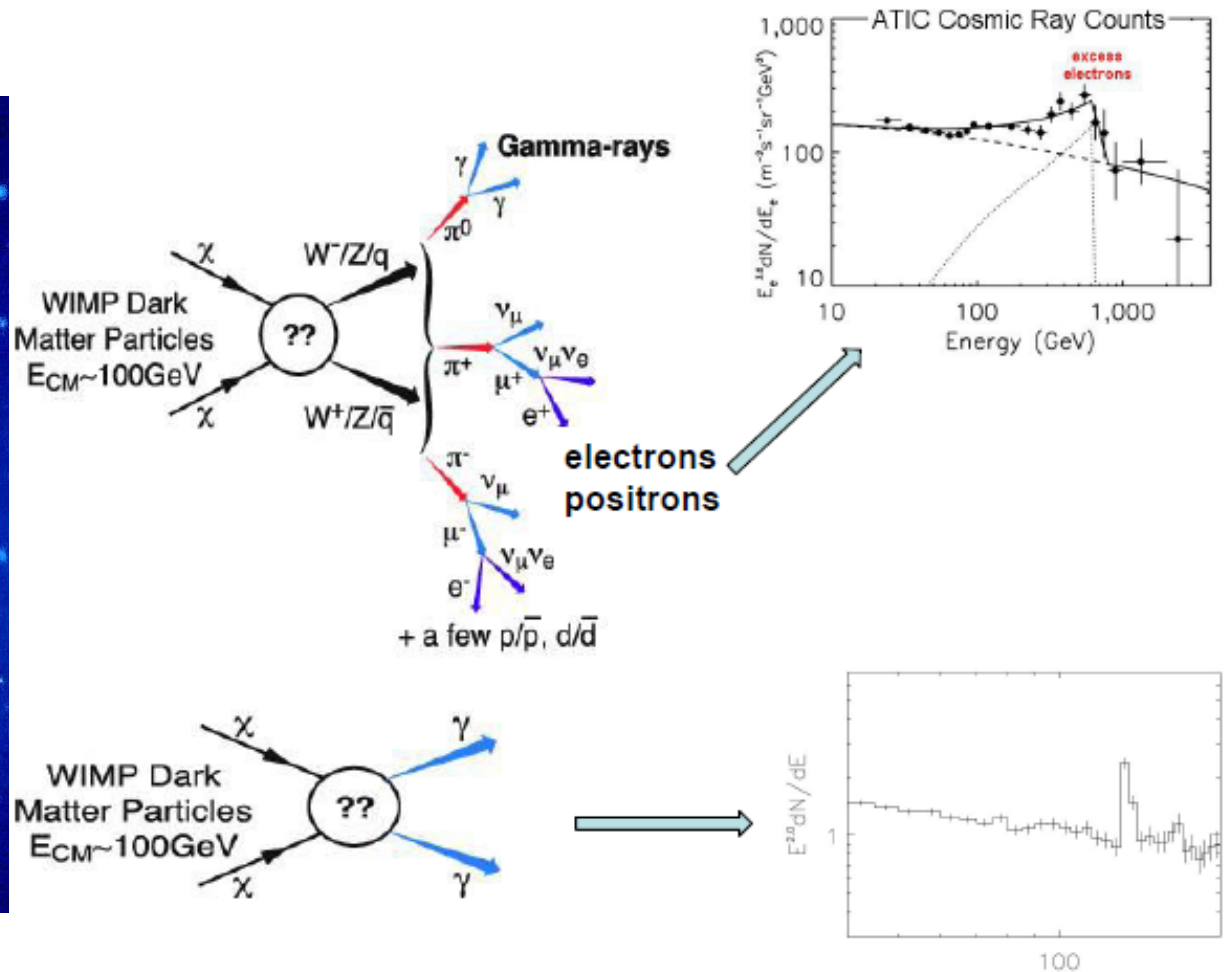

DM annihilate or decay into high energy particle and secondary radiation, contributing into the cosmic ray and gamma rays we observed.

Summary of cosmic ray detection

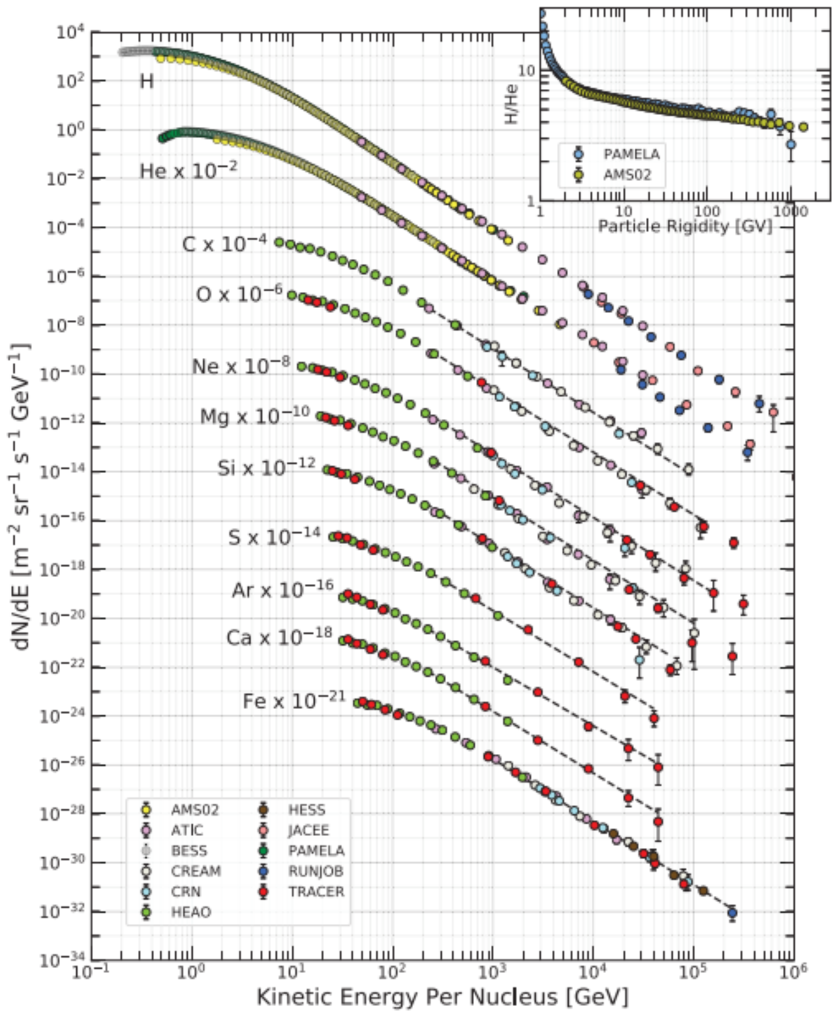

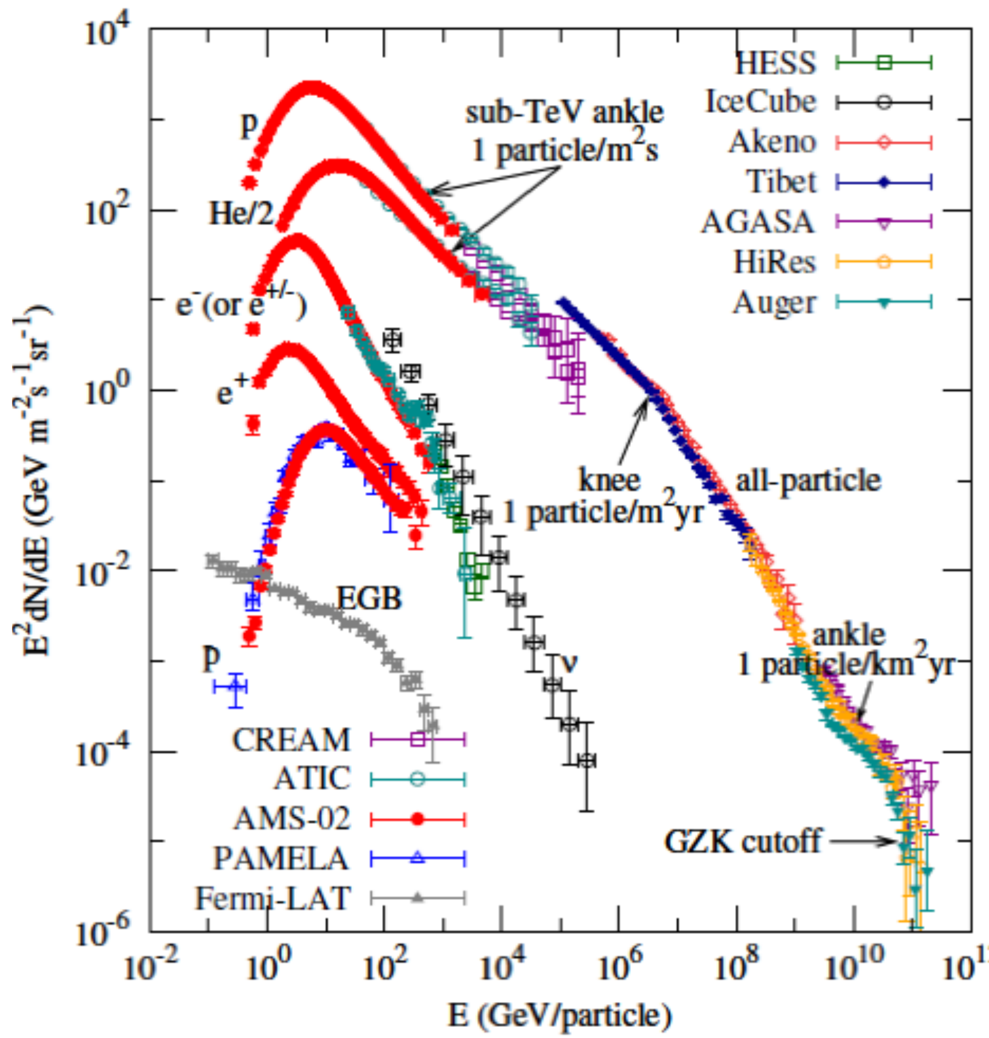

Signatures of DM indirect detection

- Gamma ray line spectrum: unique features
- Spatial distribution of gamma rays: tracing DM distribution
- Cosmic ray positrons and antiprotons: secondary products with low flux, and their flux can be predicted from cosmic ray models

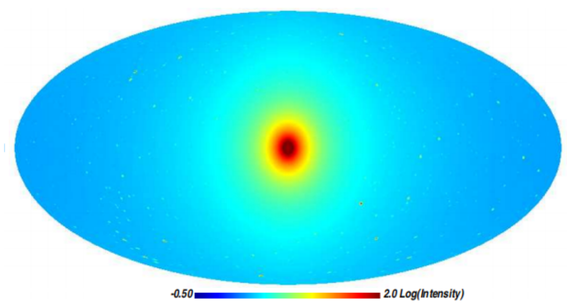

- Cosmic ray electrons: 10 times higher flux than positrons’. Good sensitivity for dark matter detection.

Spatial Indirect Search for DM

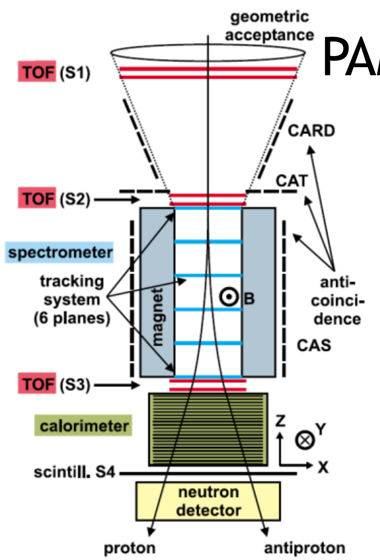

PAMELA

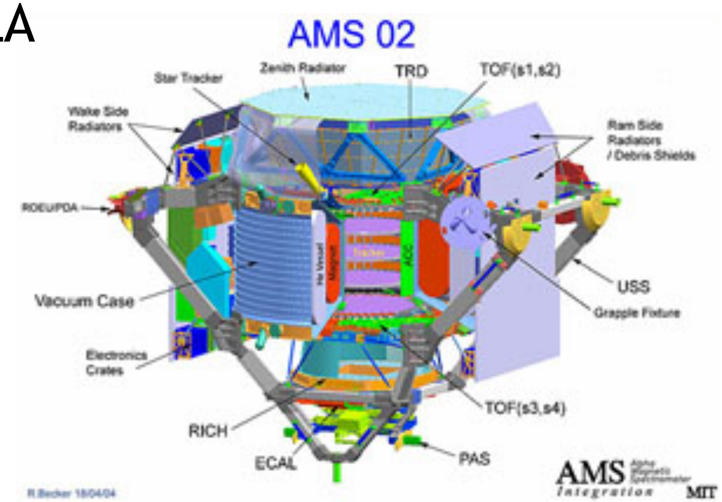

Fermi

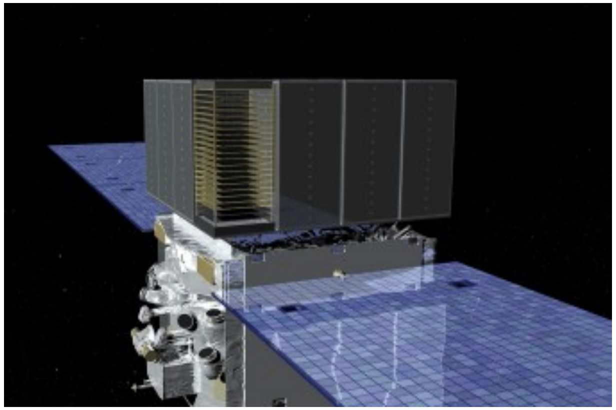

CALET

DAMPE

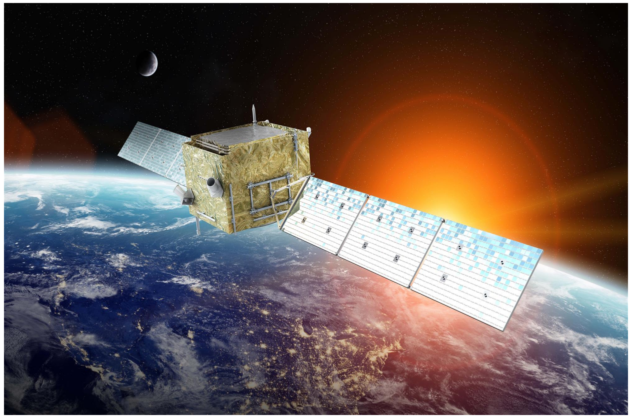

Possible gamma ray spectrum from Fermi

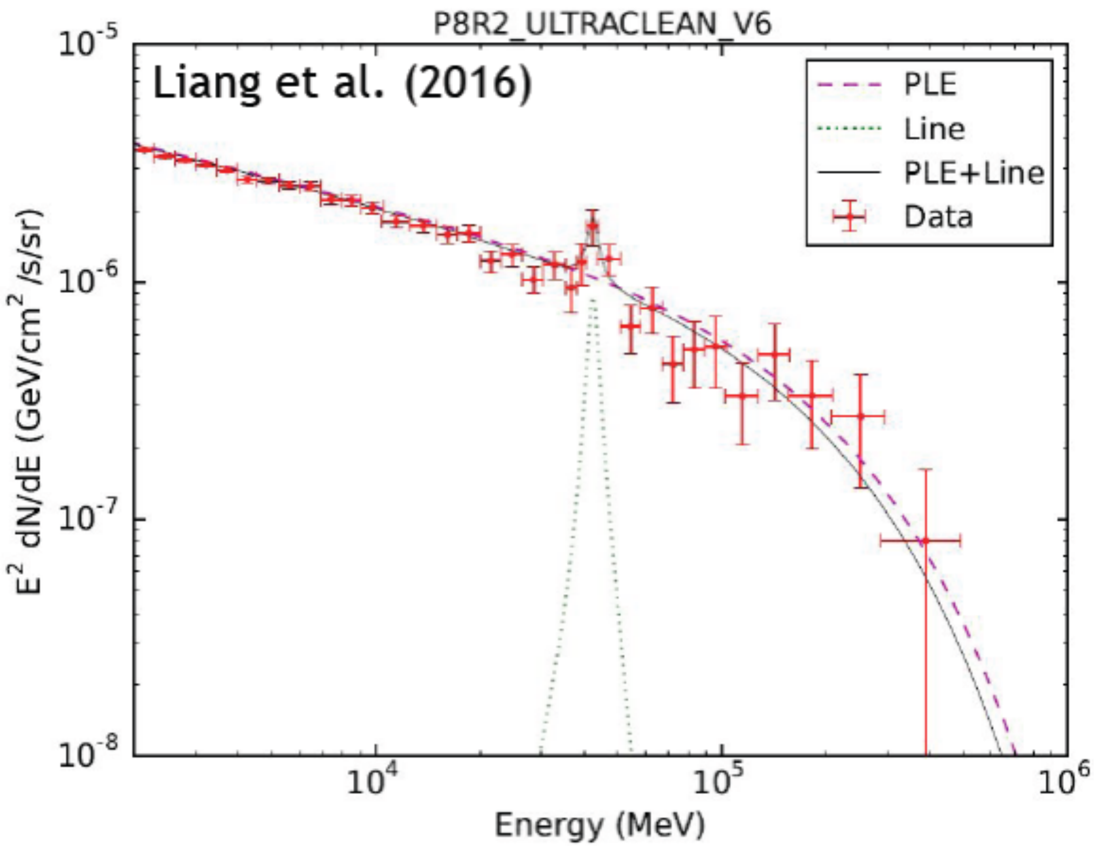

- E~43 GeV
- From a galaxy cluster
- No similar line spectrum radiation in places where dark matter is concentrated, such as the center of the Milky Way and dwarf spheroidal galaxies.
- Possibly statical fluctuation or instrument error?

Positron Excess

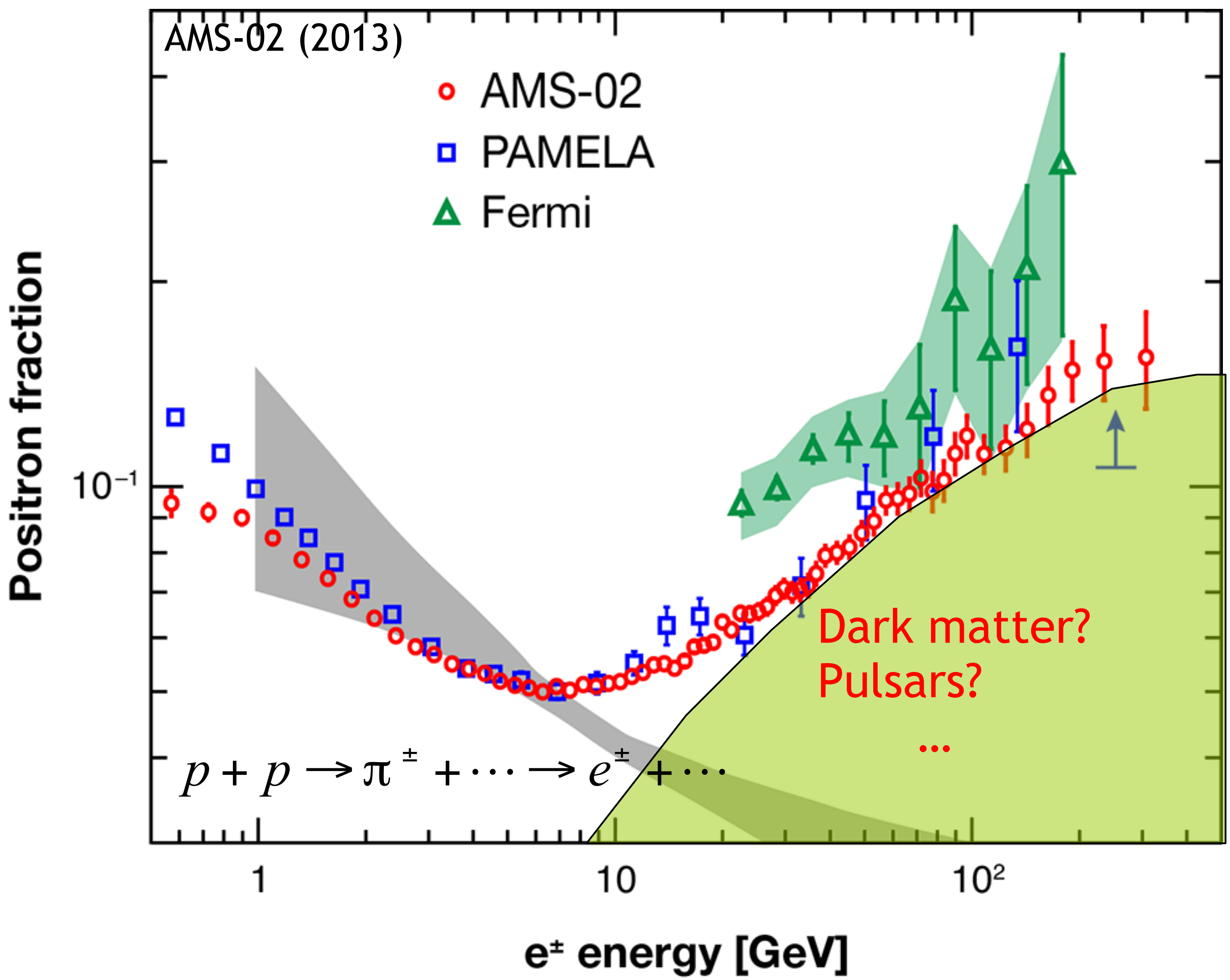

Gamma Ray Excess from Galactic Center

Gordon & Macias (2013)

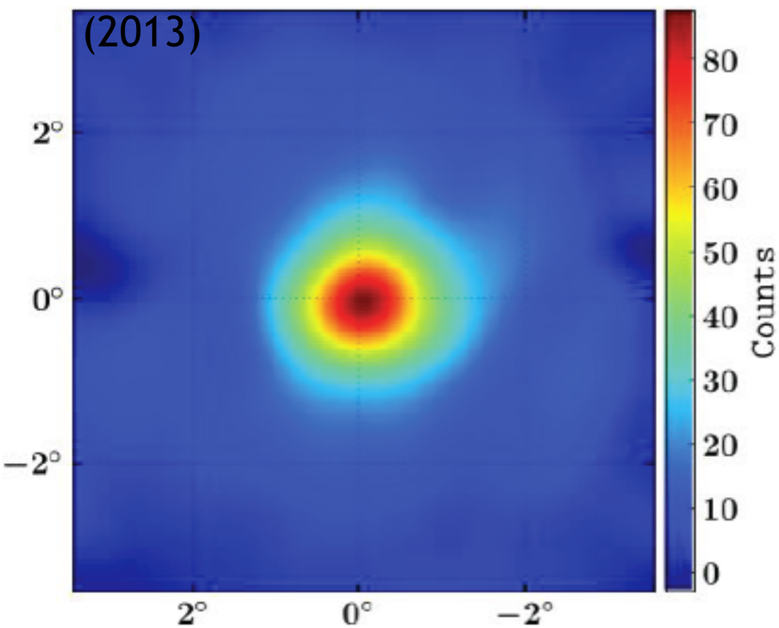

Calore et al. (2015)

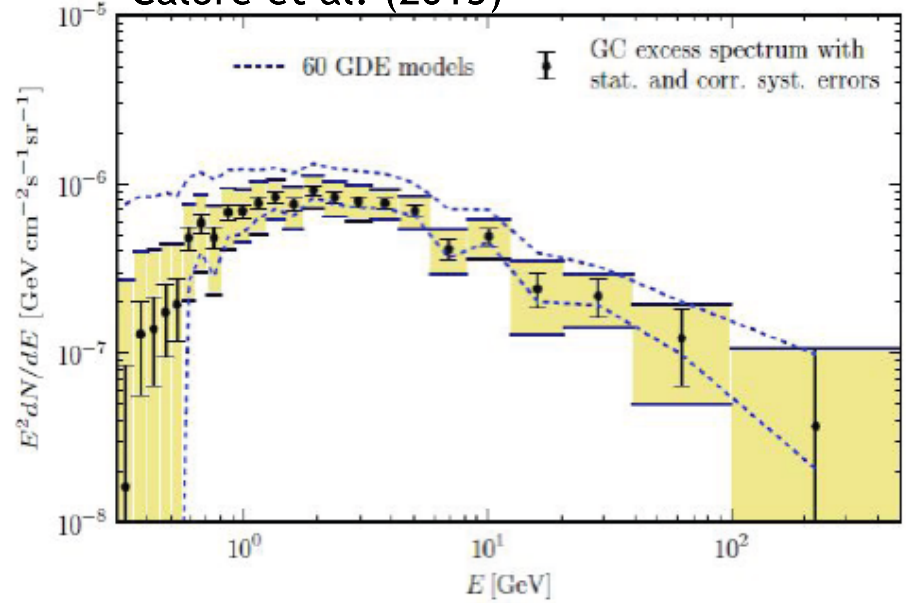

Goodenough & Hooper (2009)
Vitale & Morselli (2009)
Hooper & Goodenough (2011) ...

- Fermi gamma-ray observations of the Milky Way center reveal a circularly symmetric excess. Highly consistent with dark matter model expectations!
- DM model is not the only explanation.

Possible excess of anti-proton

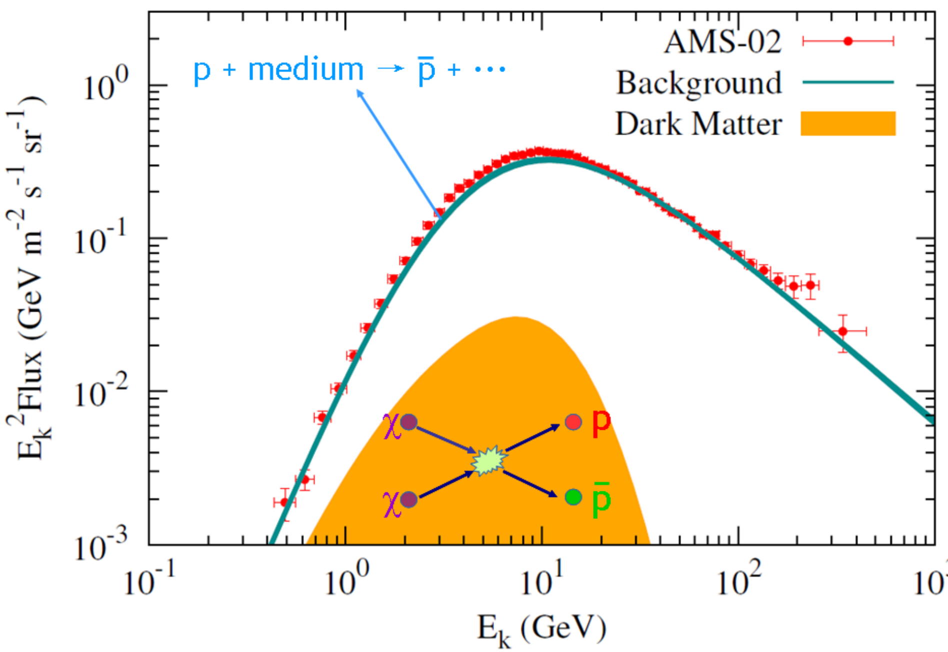

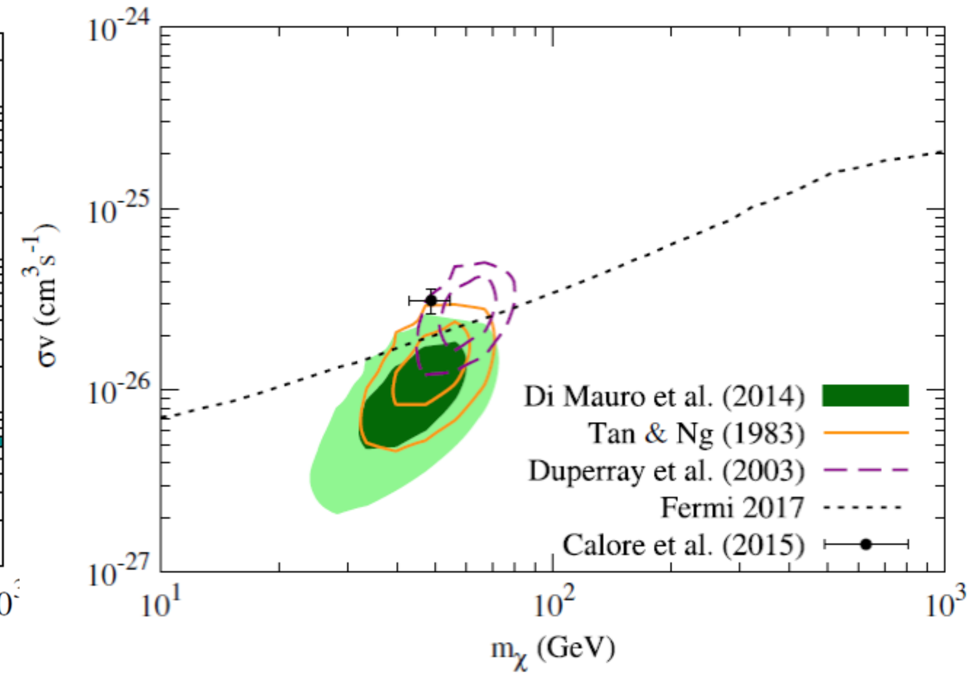

- ➢ Antiprotons from the secondary effects of cosmic rays is slightly lower than experiment. Could be resolved by DM, with highly consistent parameters with GC center excess!
- ➢ Still uncertainties in the antiproton production cross section and the modulation effect of the solar system on protons and antiprotons, calling for further research.

Cui et al. (2017); Cuoco et al. (2017)

Summary of DM detection

➢ Colliders： null results

➢ Direct Detection： null results

➢ Indirect detections：

1. Positron excess
2. GC gamma ray excess
3. Gamma Ray spectrum excess
4. Anti-proton excess

Large uncertainties from astronomy! Results still unclear!

➢ Astronomical observations discover dark matter through "invisibility"

➢ Physics experiments try to "see" dark matter, but so far no one has seen it

Detection Methods of DM

Wave-like DM Detection

Theorists' View of DM

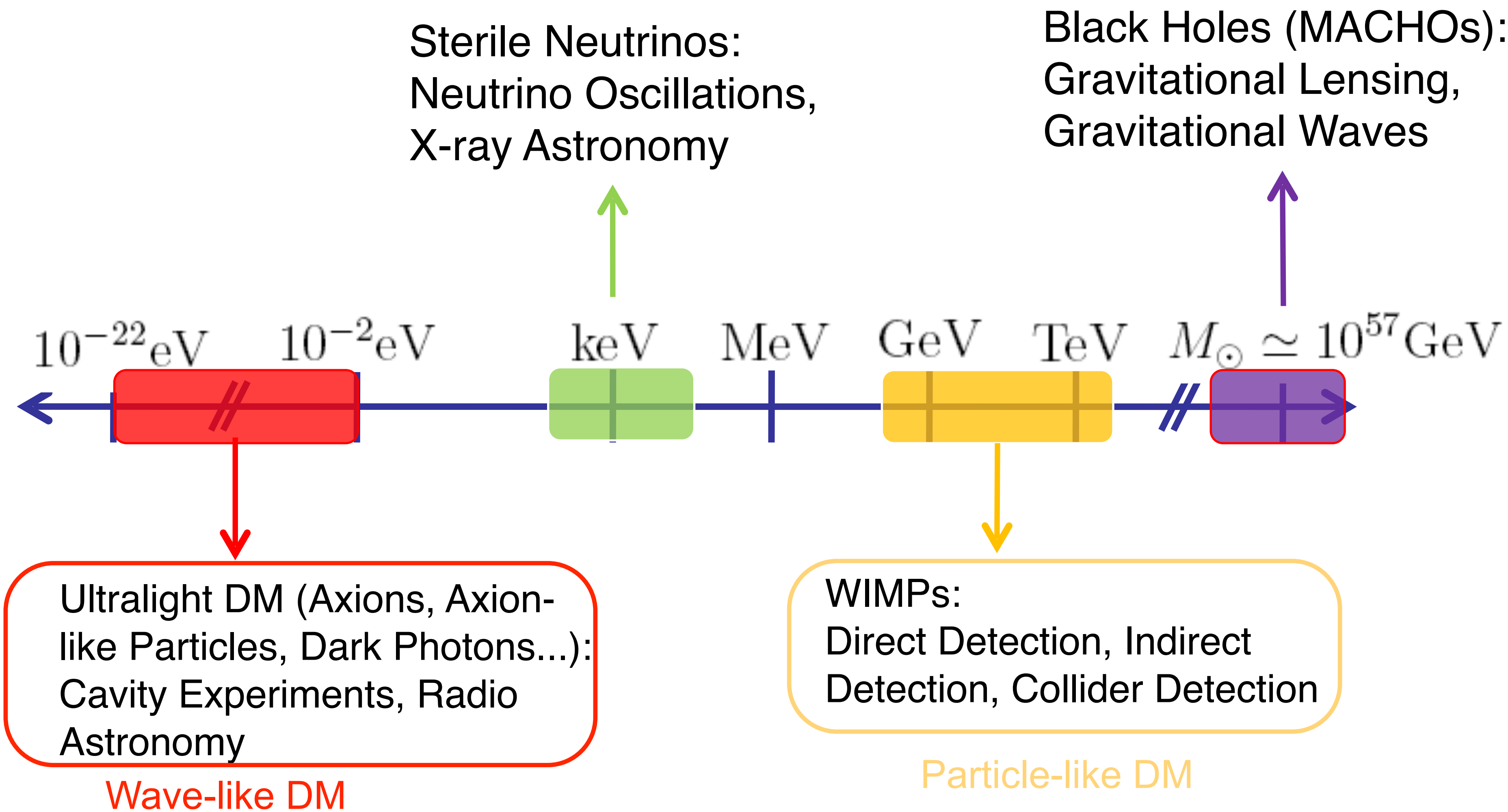

Theoretical possibilities for DM are numerous, spanning a wide range of masses and interaction cross-sections, making experimental detection highly challenging.

(Wavy) Ultra-light DM

Quantum Mechanics： Matter behave both like waves and particles

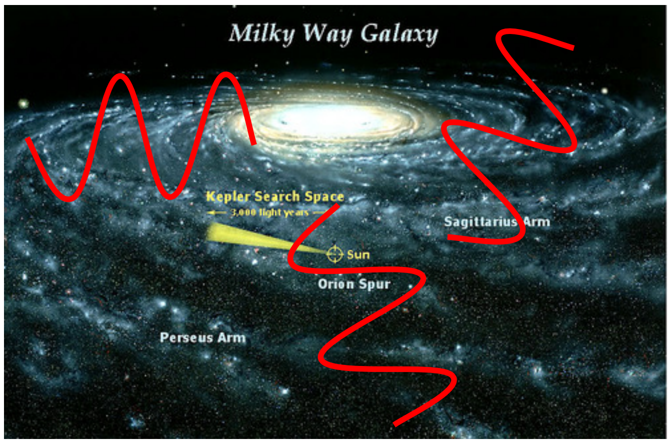

(m~10^{-22} eV)

de Broglie wavelength reaches galactic scales (kpc)

- Dependent on astrophysical observations (location, time)

Astrophysical experiments

Ultralight DM has a macroscopic wavelength, manifesting as a fluctuating background field on a macroscopic scale.

Unlike traditional DM detection (no longer based on particle scattering)

Huge potential for development

Similar to gravitational waves

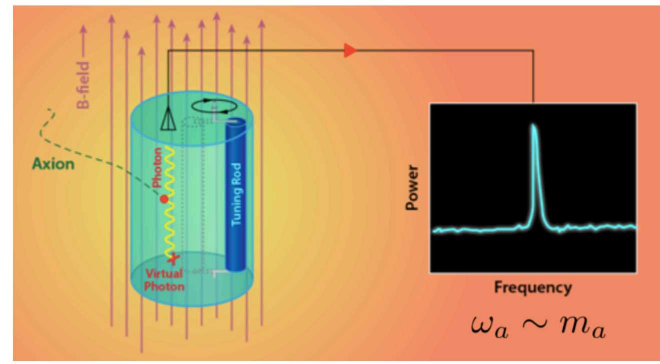

$m_a \sim \mathrm{GHz} \sim 10^{-6}\ \mathrm{eV}$

Compton wavelength is laboratory scale(m)

Resonant Cavity Quantum Amplifier

Propose new quantum detection method

Fussy DM

- Ultralight DM (bosons) can form Bose-Einstein condensates, resembling cold DM on large scales.
- On small scales (around kpc), it can addresse the cusp-core problem in dwarf galaxy observations.
- Core-Cusp problem of cold dark matter

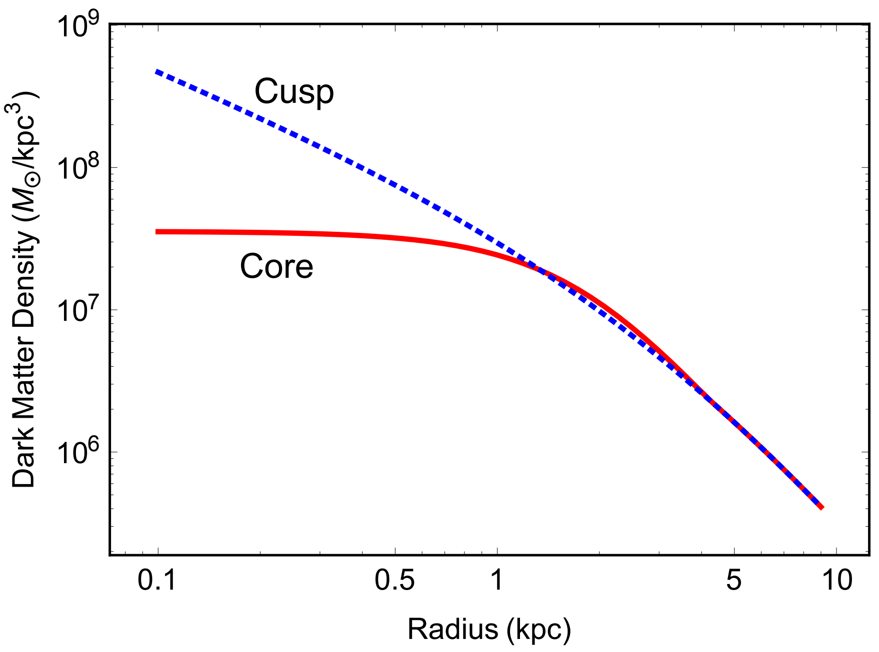

$$\rho(x) = \begin{cases} 0.019(\frac{m_a}{m_{a,0}})^{-2}(\frac{l_c}{1\mathrm{kpc}})^{-4} M_\odot \mathrm{pc}^{-3}, & \text{for } r < l_c \\ \frac{\rho_0}{r/R_H(1+r/R_H)^2}, & \text{for } r > l_c \end{cases}$$

Ultra-light DM candidate

Axion (ALP)： spin 0， CP odd

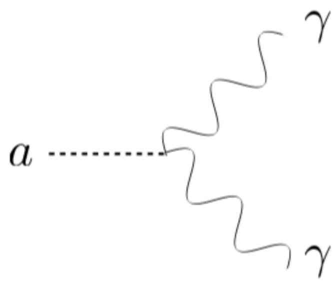

Inverse Primakoff effect

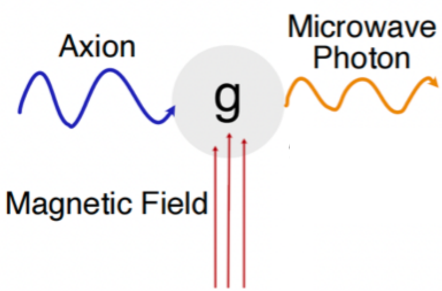

$$\nabla \times \mathbf{B} \simeq \partial_t \mathbf{E} + \mathbf{J} + \underline{g_{a\gamma\gamma} \mathbf{B}\, \partial_t a}$$

induces an effective current under strong magnetic field.

$$\vec{J}^a_{\rm eff} = g_{a\gamma} \omega_a a \vec{B}_0 .$$

Dark photon： spin 1

mili-charge particles?

kinetic mixing

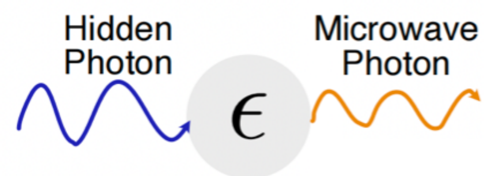

$$\mathscr{L} \supset -\tilde{A}_\mu \left(e J^\mu_{EM} - \varepsilon m^2_{A'} \tilde{A}'^\mu \right)$$

induces an effective current anyway.

$$J^{A'\,\mu}_{\rm eff} = \epsilon m^2_{A'} A'^\mu ,$$

QCD axion motivated by the Strong-CP Problem:
Why is the neutron electric dipole moment so small?

Naive estimate gives
nEDM ≈ 10^{-16} e-cm

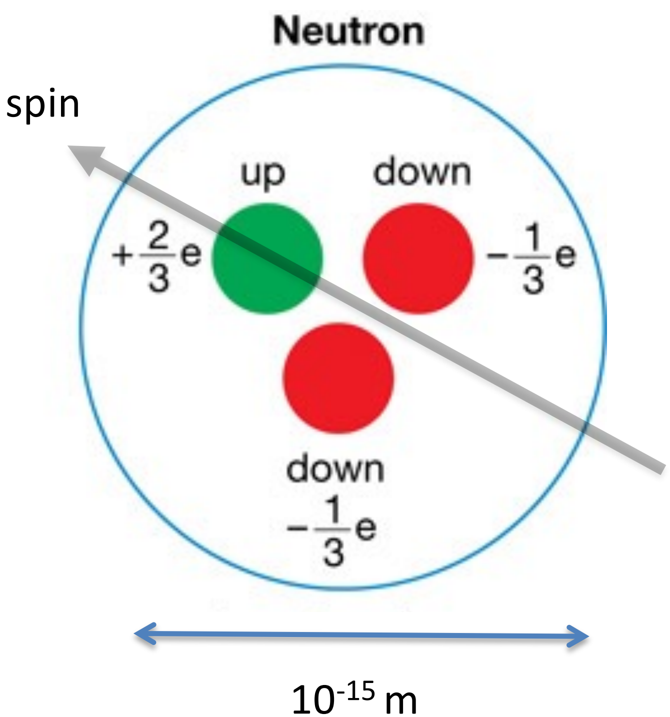

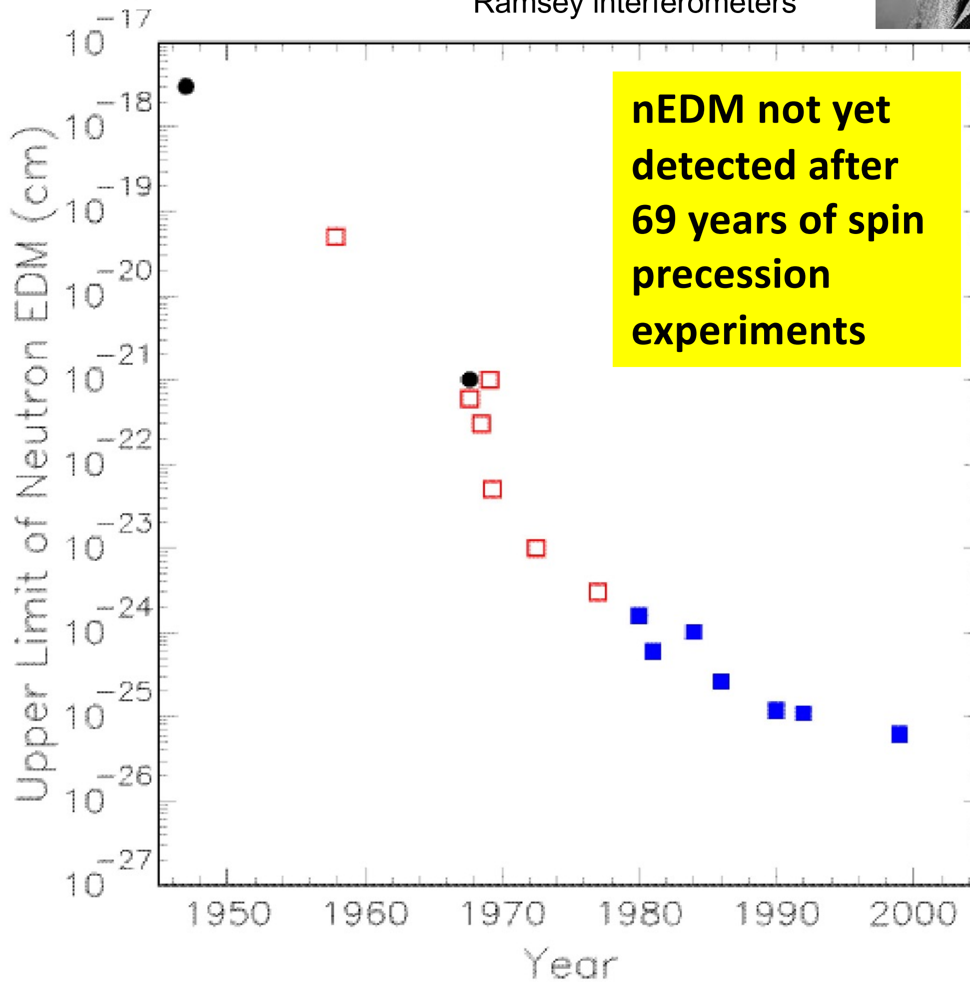

Norman Ramsey
Nobel Prize 1989.
Neutrino oscillation expts are "Ramsey interferometers"

The CP Problem of Strong Interactions

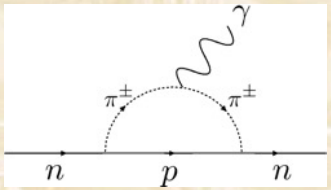

Characterizes degenerate QCD ground state (Θ vacuum)

Phase of Quark Mass Matrix

Standard QCD Lagrangian contains a CP violating term

$$L_{CP} = -\frac{\alpha_s}{8\pi}\underbrace{(\Theta - \arg\det M_q)}_{0\le\overline{\Theta}\le 2\pi}\,\mathrm{Tr}\,\tilde{G}_{\mu\nu}G^{\mu\nu}$$

Induces a neutron electric dipole moment (EDM) much in excess of experimental limits

$$d_n \approx \overline{\Theta}\, 10^{-16}\, e\,\mathrm{cm} \approx \frac{\overline{\Theta}}{10^2}\mu_n < 3\times 10^{-26}\, e\,\mathrm{cm}$$

$\overline{\Theta} \lesssim 10^{-10}$ **Why so small?**

Slide from G. Raffelt

The 1977 Peccei-Quinn solution to the strong-CP problem

Dirac Medal (2000)

- Promote theta to become a new **dynamical** scalar field which has a two-gluon coupling. (dynamical = can vary in space and time)

- Think like an electrical engineer: Use this field in a cosmological feedback loop to dynamically zero out any pre-existing CP-violating phase angles.

Natural potential energy function

$$V(A) = -f_a^2 A^2 + \frac{\lambda}{4!} A^4 + \left(\frac{g^2}{32\pi^2} \arg(A) - \frac{\alpha_s}{8\pi} \left(\theta_{QCD} + \theta_{quark} \right) \right) \langle G\tilde{G} \rangle$$

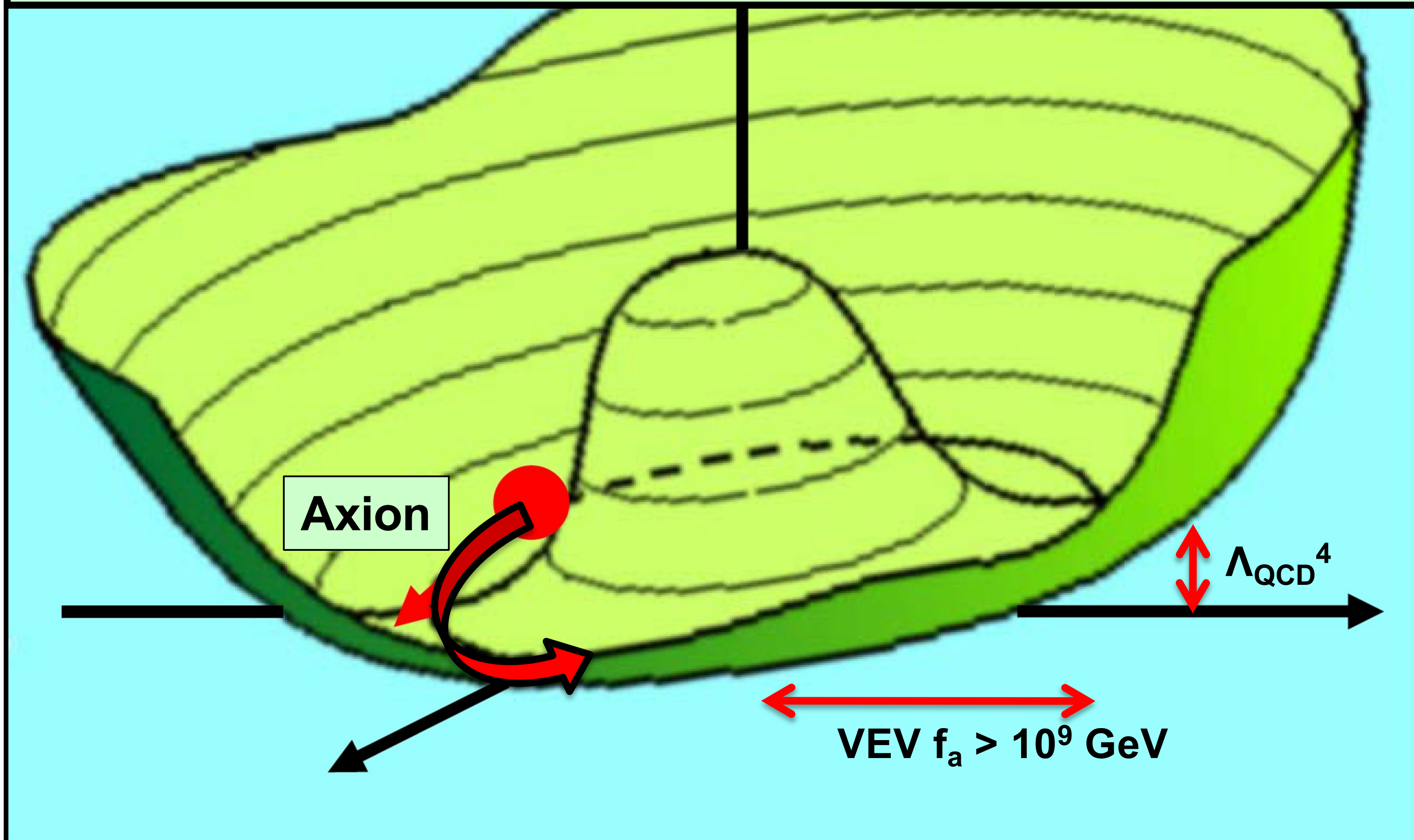

Natural potential energy function

$$V(A) = -f_a^2 A^2 + \frac{\lambda}{4!} A^4 + \left(\frac{g^2}{32\pi^2} \arg(A) - \frac{\alpha_s}{8\pi} \left(\theta_{QCD} + \theta_{quark} \right) \right) \langle G\tilde{G} \rangle$$

The axion field zeroes out any other CP-violating phases from the strong or electroweak quark sector.

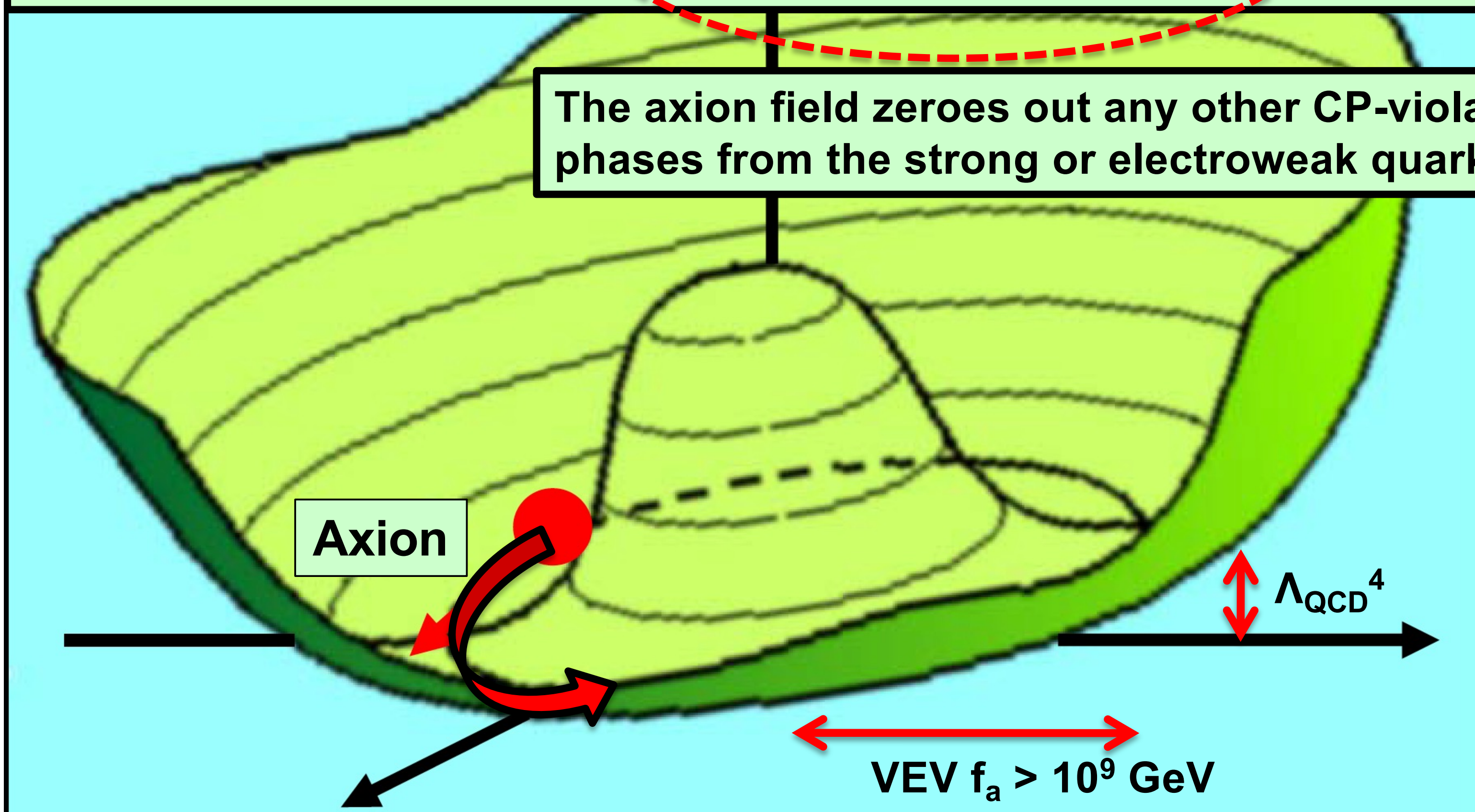

The neutron EDM vanishes, solving the **strong CP fine-tuning problem**.

Ultra-light DM: axion

Introduce a new global symmetry (PQ symmetry) broken at energ

$$\theta G\tilde{G} \longrightarrow \left(\theta + \frac{a}{f_a}\right) G\tilde{G}$$

breaking PQ shift symmetry

Potential energy term $\cos(\theta + a/f_a)$

At the minimum

$$\langle a \rangle = -\theta f_a$$

Self-adjust to 0

Axion mass = harmonic oscillator frequency

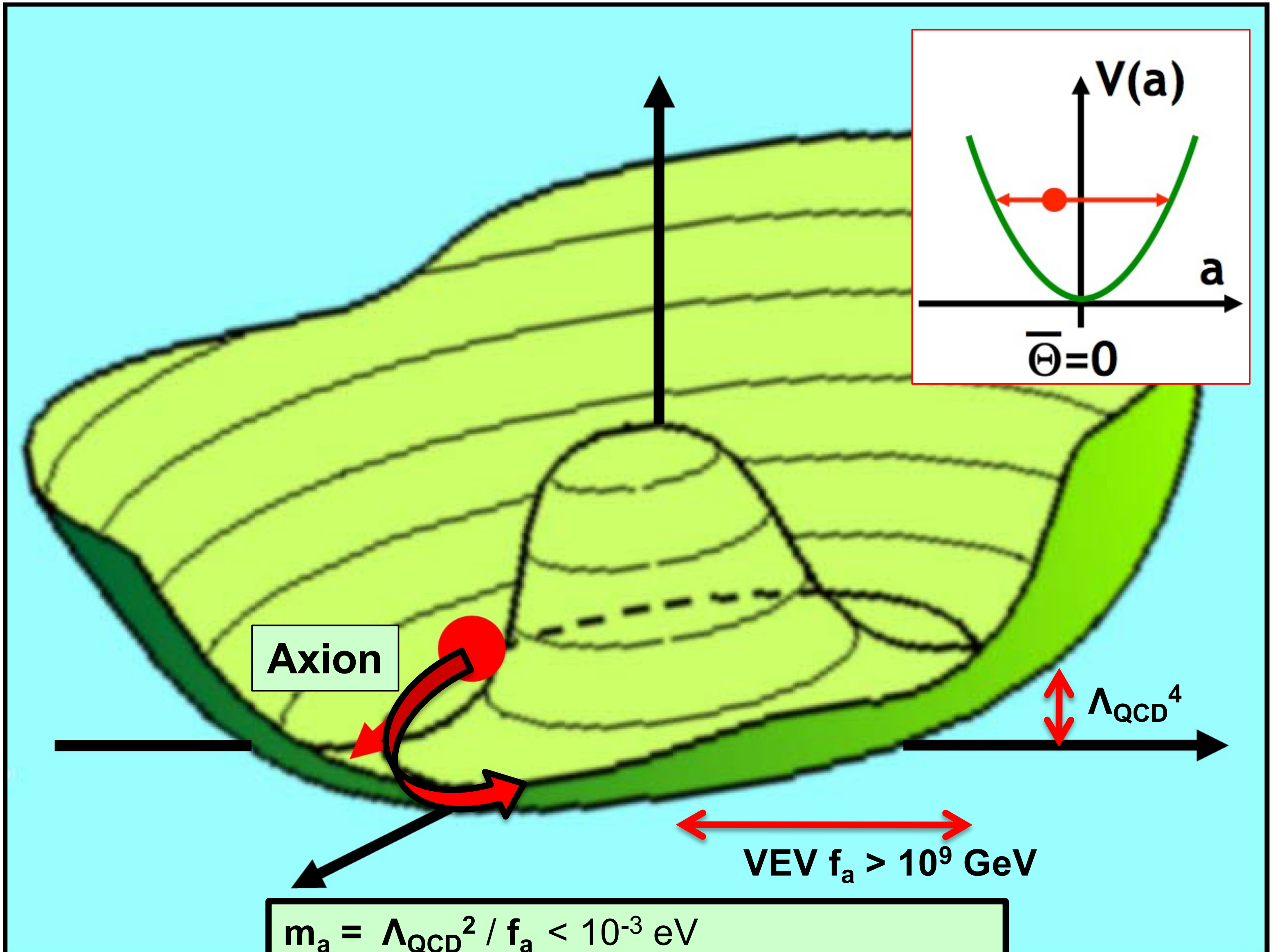

$m_a = \Lambda_{QCD}^2 / f_a < 10^{-3}$ eV
Single parameter model for axions

The initial potential energy density is released as ultracold dark matter

Abbott, Sikivie (1983)
Preskill, Wise, Wilczek (1983)
Dine, Fischler (1983)
…

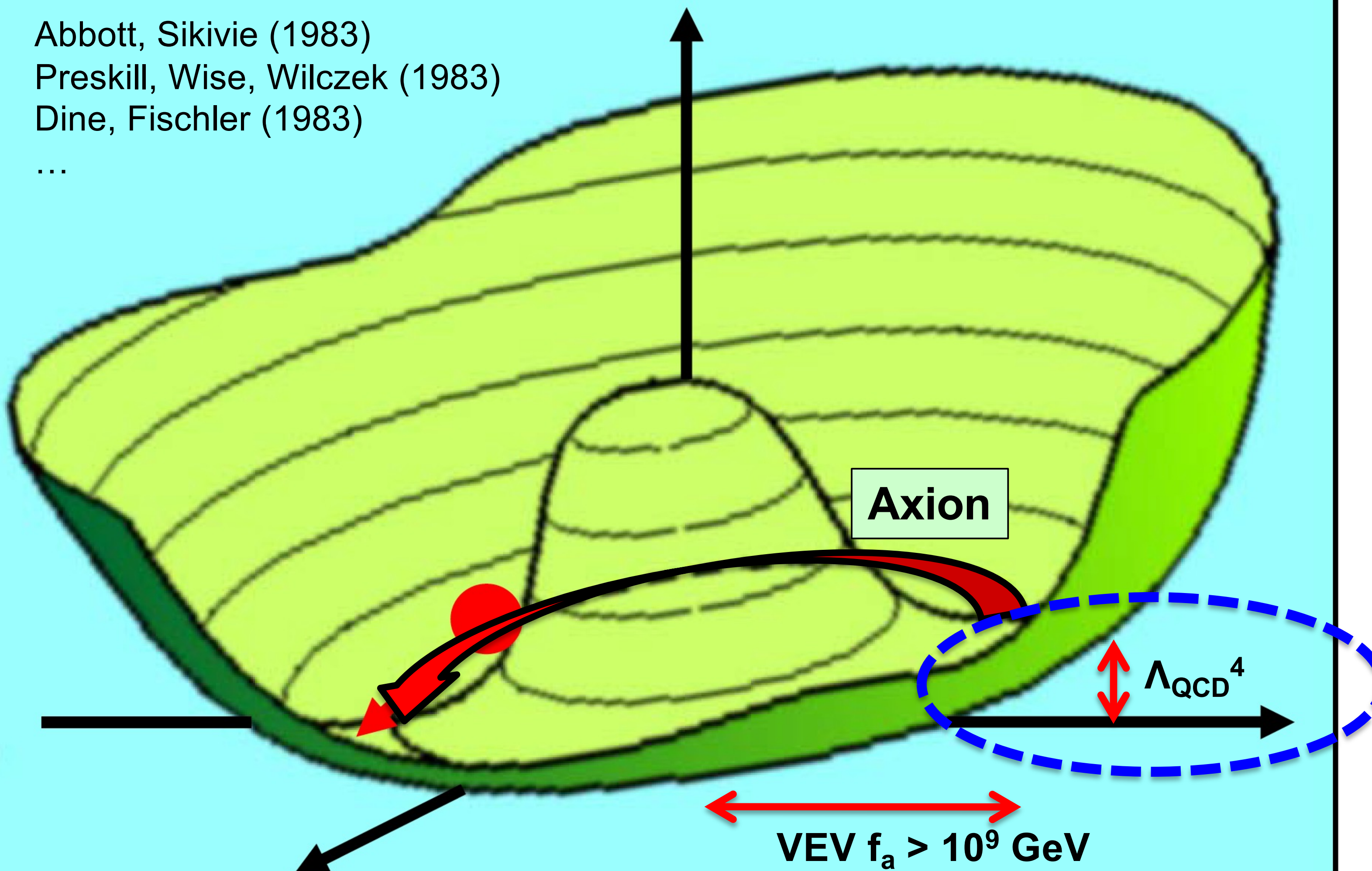

The initial azimuthal angle $\boldsymbol{\theta_0}$, determines the available potential energy to be released. **O(1)×**$\boldsymbol{\Lambda_{QCD}^4}$ of potential energy density is converted into **dark matter**.

The QCD axion and the Strong CP problem

$$\mathscr{L} \supset -\frac{\theta g_s^2}{32\pi^2} G\tilde{G} - \left(\bar{u}_L M_u u_R + \bar{d}_L M_d d_R + \text{h.c.}\right)$$

- The CKM matrix from $M_{u,d}$
  - CP violating phase θ_{CP} ~ 1.2 radian
- QCD induced CP violating phase, $\bar{\theta}$

$$\bar{\theta} = \theta + \arg\left[\det\left[M_u M_d\right]\right]$$

- $\bar{\theta}$ is invariant under quark chiral rotation $d^n_{\text{EDM}} \sim \theta \times 10^{-16}$ e cm
- According to neutron EDM experiment $d^n_{\text{exp}} < 10^{-26}$ e cm

$$\bar{\theta} \lesssim 1.3 \times 10^{-10} \text{ radian}$$

The Peccei-Quinn solution to Strong CP problem

- Experiment requires $\bar{\theta} = \theta + \arg\left[\det\left[M_u M_d\right]\right] \lesssim 10^{-1}\text{rad}$
- PQ: promote the constant $\bar{\theta}$ to a dynamical field, a
- Vafa-Witten theorem: vector-like theory (QCD) has ground state $\langle\theta\rangle = 0$
- Introduce a *global* PQ-symmetry $U(1)_{\text{PQ}}$, *anomalous* under the QCD
    - The massless Goldstone boson a is called *axion*
        - $a \to a + \kappa f_a \ \Rightarrow \mathcal{S} \to \mathcal{S} + \frac{\kappa}{32\pi^2}\int d^4x G\tilde{G}$, cancels $\bar{\theta}$
        - Low energy: $\mathscr{L} = \sum_q \bar{q}\left(iD_\mu\gamma^\mu - m_q\right)q - \frac{1}{4}GG + \frac{g_s^2}{32\pi^2}\frac{a}{f_a}G\tilde{G} + \frac{1}{2}\left(\partial_\mu a\right)^2 + \mathscr{L}_{\text{int}}[\partial_\mu a]$

https://arxiv.org/abs/hep-ph/0011376

Model independent visible axion properties

- For two flavor QCD, $q = (u, d)^T$
  - $\mathscr{L} \supset \frac{1}{2}\left(\partial_\mu a\right)^2 + \frac{g_s^2}{32\pi^2}\frac{a}{f_a}G\tilde{G} + \frac{1}{4}g^0_{a\gamma}F\tilde{F} - \bar{q}_L M_q q_R + \frac{\partial_\mu a}{2f_a}\bar{q}c^0_q\gamma^\mu\gamma_5 q + h.c.$
  - The three QCD related terms can be eliminated to 2 d.o.f.
  - Choose to eliminate $G\tilde{G}$ term by quark field redefinition in a-related chiral rotation

$q \to e^{i\alpha} q \qquad \bar{q} \to e^{-i\alpha}\bar{q}$

- A new quark field: $q' = \exp\left(i\frac{a}{2f_a}\gamma_5 Q_a\right)q$

anomalous U(1) axial transformation

a: transformation angle

- $\mathscr{L} \supset \frac{1}{2}\left(\partial_\mu a\right)^2 + \frac{1}{4}g_{a\gamma}F\tilde{F} - \bar{q}'_L M_{q'} q'_R + \frac{\partial_\mu a}{2f_a}\bar{q}' c_q\gamma^\mu\gamma_5 q' + h.c.$

Model independent visible axion properties

- In the new basis
    - $\mathscr{L} \supset \frac{1}{2}\left(\partial_\mu a\right)^2 + \frac{1}{4} g_{a\gamma} F\tilde{F} - \bar{q}'_L M_a q'_R + \frac{\partial_\mu a}{2f_a} \bar{q}' c_q \gamma^\mu \gamma_5 q' + h.c.$
    - $c_q = c_q^0 + Q_q\,,\; g_{a\gamma} = g_{a\gamma}^0 - 2N_c \frac{\alpha_{em}}{2\pi f_a} \mathrm{Tr}[Q_a Q^2]$
    - Quark mass is complex:

$$M_a = \exp\left(i\frac{a}{2f_a}Q_a\right) M_q \exp\left(i\frac{a}{2f_a}Q_a\right)$$

Induce cos(a) potential term

- There is a phase a in the mass if we define away $\frac{g_s^2}{32\pi^2}\frac{a}{f_a}G\tilde{G}$

The axion and Chiral Lagrangian

- The generic low energy Lagrangian is

$$\mathscr{L} \supset \frac{1}{2}\left(\partial_\mu a\right)^2 + \frac{1}{4} g_{a\gamma} F\tilde{F} - \bar{q}_L M_a q_R + \frac{\partial_\mu a}{2f_a}\bar{q} c_q \gamma^\mu \gamma_5 q + h.c.$$

Induce cos(a) potential term

- Two flavor quarks $q = (u, d)$; quark mass term $M_a = e^{i\frac{aQ_a}{2f_a}} M_q e^{i\frac{aQ_a}{2f_a}}$
- Below the QCD scale, one needs the chiral axion Lagrangian

$$\mathscr{L}_a^{\chi PT} = \frac{f_\pi^2}{4}\mathrm{Tr}\left[(D^\mu U)^\dagger D_\mu U + 2B_0(UM_a^\dagger + M_a U^\dagger)\right] + \frac{\partial^\mu a}{4f_a}\mathrm{Tr}[c_q \sigma^a] J_\mu^a$$

$$U \equiv e^{i\pi^a \sigma^a / f_\pi}$$

$$J_\mu^a \equiv e^{i\pi^a \sigma^a / f_\pi}$$

Axion mass and interaction with pions

$$\mathscr{L}_a^{\chi PT} = \frac{f_\pi^2}{4}\mathrm{Tr}\left[(D^\mu U)^\dagger D_\mu U + 2B_0(UM_a^\dagger + M_a U^\dagger)\right] + \frac{\partial^\mu a}{4f_a}\mathrm{Tr}[c_q\sigma^a]J_\mu^a$$

- Axion mass: $m_a^2 \simeq (Q_u + Q_d)^2 \frac{m_u m_d}{(m_u + m_d)^2}\frac{m_\pi^2 f_\pi^2}{f_a^2}$ $\quad m q_L \bar{q}_R + \mathrm{h.c.} \mapsto m e^{\mathrm{i}N\theta} q_L \bar{q}_R + \mathrm{h.c.}$
- Axion-π^0 mixing: $\theta_{a\pi} \simeq \frac{(Q_d m_d - Q_u m_u)}{(m_u + m_d)}\frac{f_\pi}{f_a}$
- Axion-pion couplings: $-\frac{3}{2}\frac{\epsilon}{f_a f_\pi}\partial_\mu a\left(2\partial^\mu\pi^0\pi^+\pi^- - \pi^0\partial^\mu\pi^+\pi^- - \pi^0\pi^+\partial^\mu\pi^-\right)$
  - Coefficient: $\epsilon = -\frac{1}{2}\left(\frac{Q_d m_d - Q_u m_u}{m_u + m_d} + c_d^0 - c_u^0\right)\frac{f_\pi}{f_a}$

All above are QCD axions, for ALPs, just follow the pNGB calculations

Experimental searches for Axion-Like Particles axion

$$\mathscr{L}_{\rm ALP} = g_{ag}\frac{a}{f_a}G\tilde{G} + g_{a\gamma}\frac{a}{f_a}F\tilde{F} + g_{af}\frac{\partial_\mu a}{2f_a}\bar{f}\gamma^\mu\gamma_5 f$$

- ALP couplings:

$$g_{a\gamma\gamma}aF_{\mu\nu}\epsilon^{\mu\nu\alpha\beta}F_{\alpha\beta} \sim g_{a\gamma\gamma}a\overrightarrow{E}\cdot\overrightarrow{B}$$

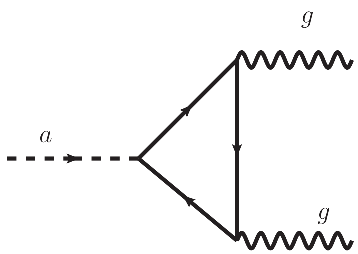

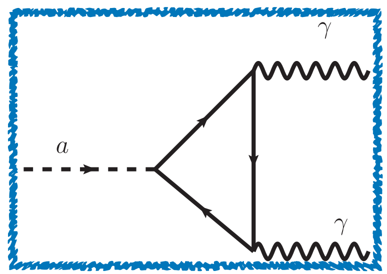

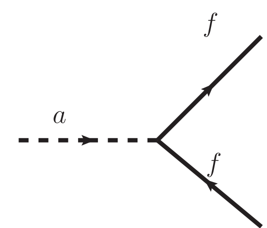

$$f = q, \ell, N$$

Dark Matter Cosmic Evolution

Axion DM

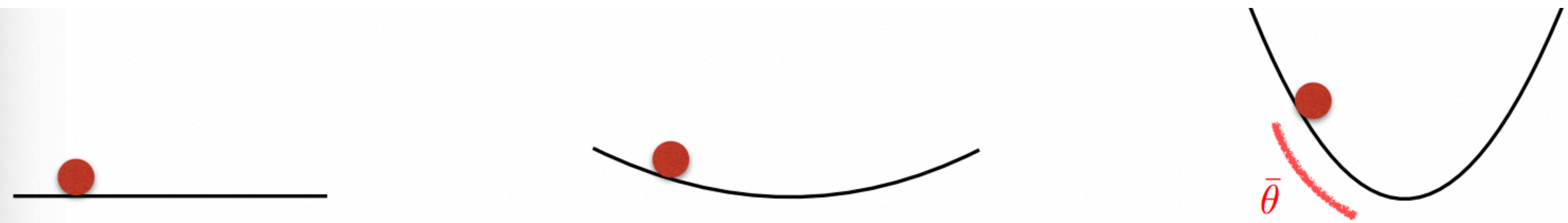

$$\theta \equiv a/f_a$$

$$\ddot{\theta} + 3H\dot{\theta} + m_a^2(T)\theta = 0$$

"Friction" "String"

Decay term

Dark Matter Mass Evolution

$$\ddot{\theta} + 3H\dot{\theta} + m_a^2(T)\theta = 0$$

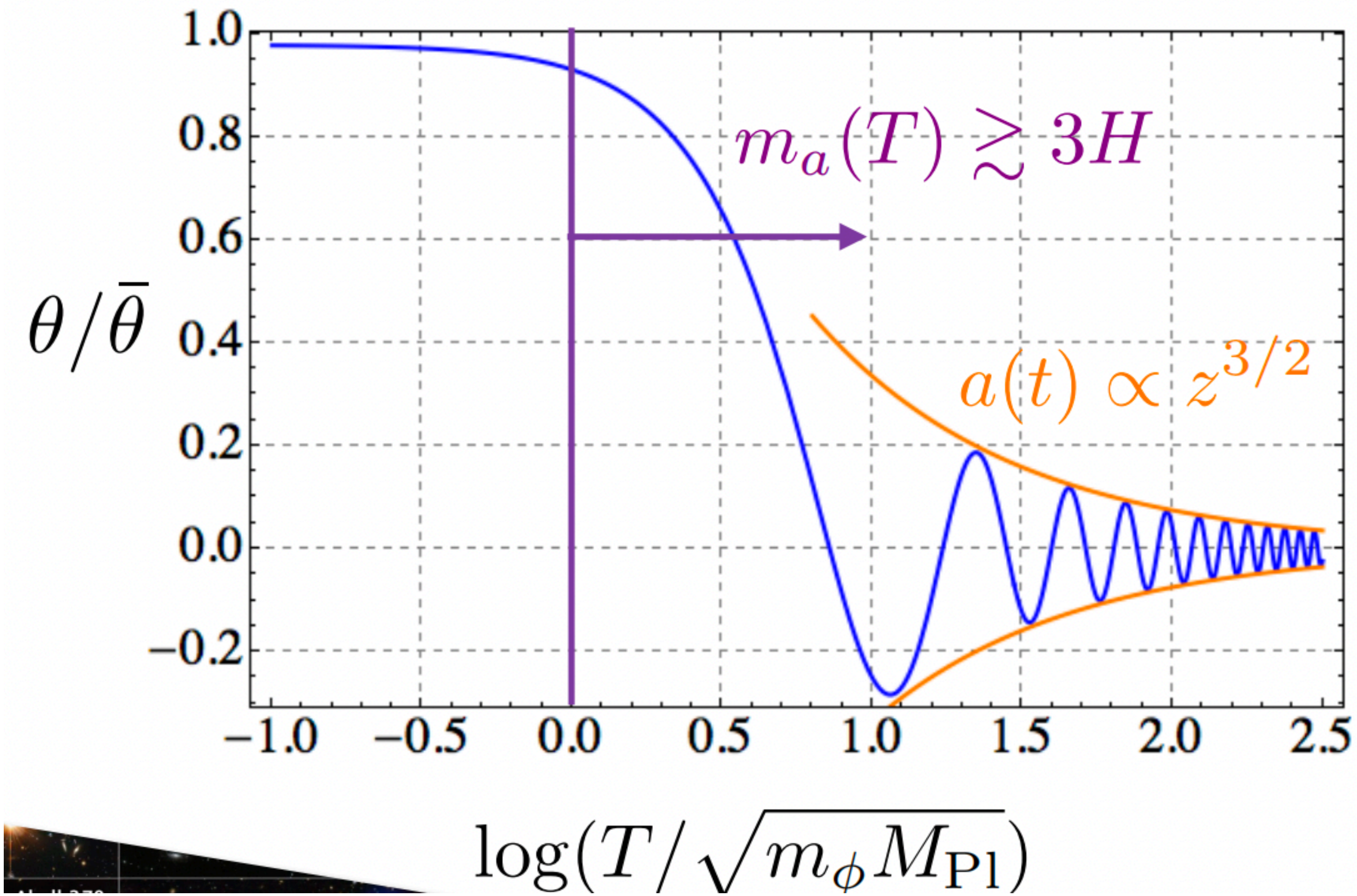

Dark Matter Mass Evolution

The number of ultralight DM particles within a unit de Broglie volume is enormous => must be bosons.

$$a(t) = \frac{\sqrt{2\rho_{\rm DM}}}{m_a}\cos(m_a t + \phi)$$

Gravitational virialization determines the correlation time and length of ultralight DM.

$$\tau_a \sim 1/m_a\langle v_{\rm DM}^2\rangle \sim Q_a/m_a \sim 10^6/m_a$$

$$\lambda_a \sim 1/m_a\sqrt{\langle v_{\rm DM}^2\rangle} \sim 10^3/m_a$$

Spectrum of Ultra-light Dark Matter

$$a(t) = \frac{\sqrt{2\rho_{\rm DM}}}{m_a}\cos(m_a t + \phi)$$

Frequency: $\omega_a \simeq \mathrm{GHz}\,\frac{m_a}{10^{-6}\ \mathrm{eV}}$

Coherence: $\tau_a \simeq \mathrm{ms}\,\frac{10^{-6}\ \mathrm{eV}}{m_a}$

Max Exp. Size: $\lambda_a \simeq 200\ \mathrm{m}\,\frac{10^{-6}\ \mathrm{eV}}{m_a}$

DM coherence time

$$\tau_a \sim 1/m_a\langle v_{\rm DM}^2\rangle \sim Q_a/m_a \sim 10^6/m_a$$

Energy Spectrum Width 10^{-6}

$$\lambda_a \sim 1/m_a\sqrt{\langle v_{\rm DM}^2\rangle} \sim 10^3/m_a$$

Momentum Width 10^{-3}

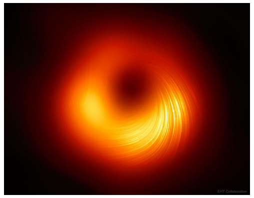

Ultra-light DM: Astrophysical Test

- Pulsar-Timing-Array search for ULDM

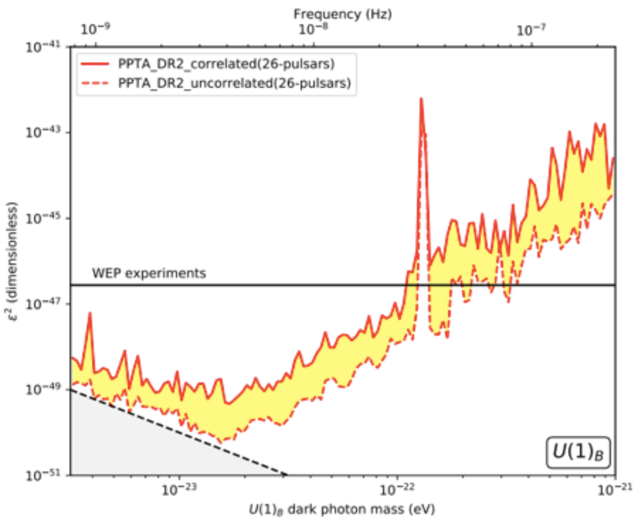

"No Man's Land", Best results now

China's FAST, future Square Kilometer Array (SKA)

- Using Event Horizon Telescope polarization observation to detect axion ULDM.

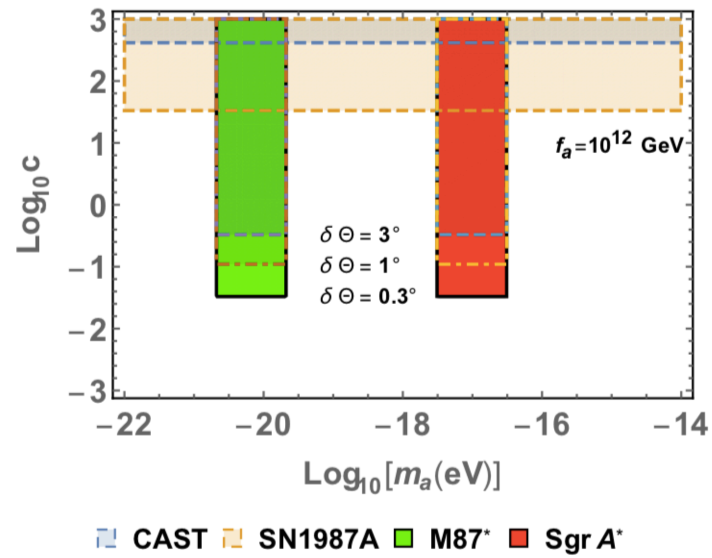

- Gaia satellite's precise measurement of stellar positions within the Milky Way.

- Accurate measurements of orbits in binary systems (Sun-Mercury, Earth-Moon, neutron star-white dwarf, etc.).

Pulsar

A pulsar is a highly magnetized rotating neutron star that emits strong electromagnetic radiation along its magnetic axis, periodically sending out pulse signals.

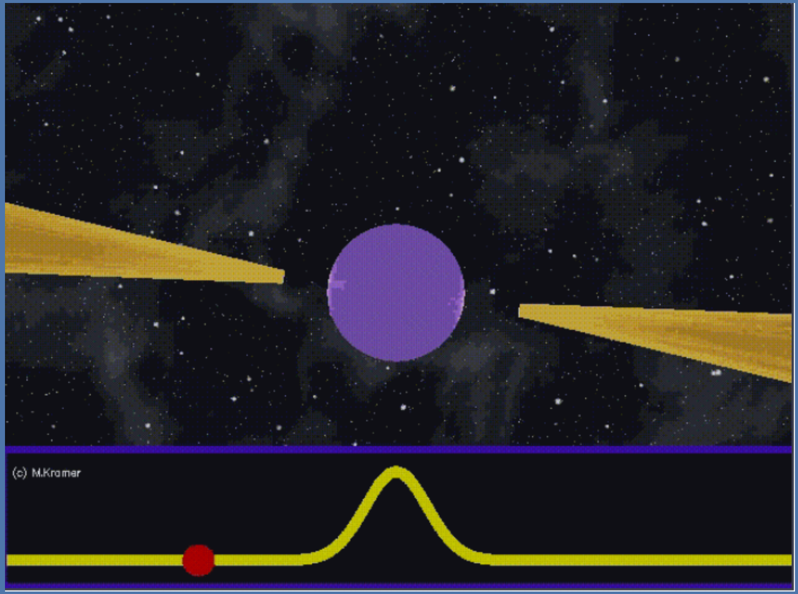

Pulsar-Timing-Array

PTA observation involves recording a series of pulsar pulse arrival times at a fixed observation frequency, referencing atomic time as a reference, compared with pulsar timing models.

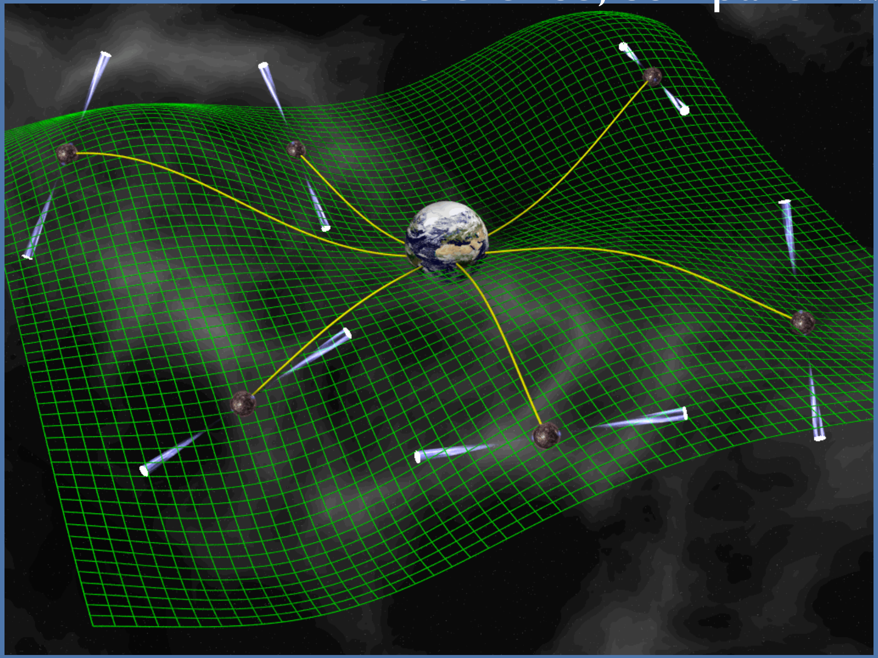

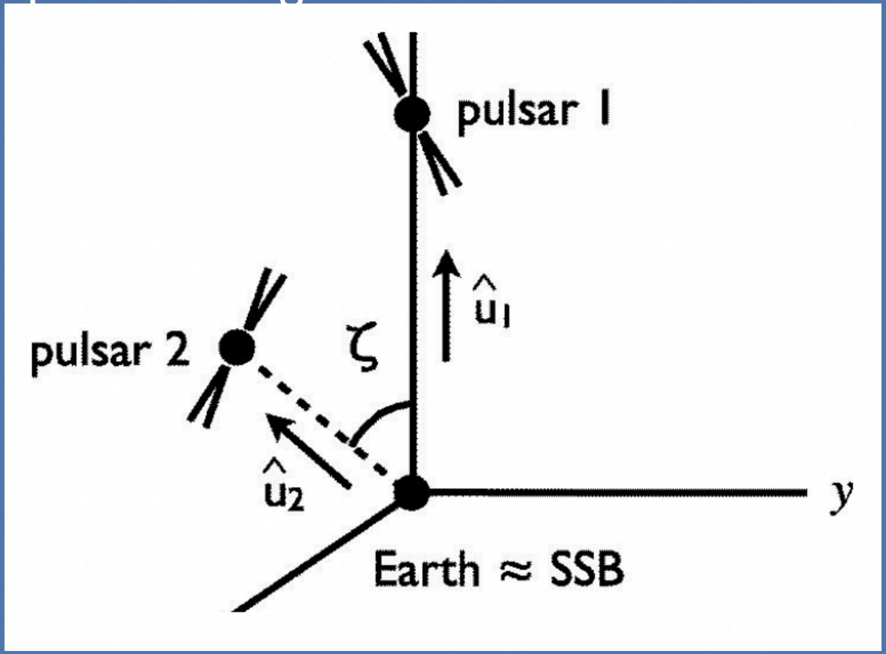

PTA measures the timing of pulses from multiple pulsars to analyze correlations between their signals.

The pulsar timing array (PTA)

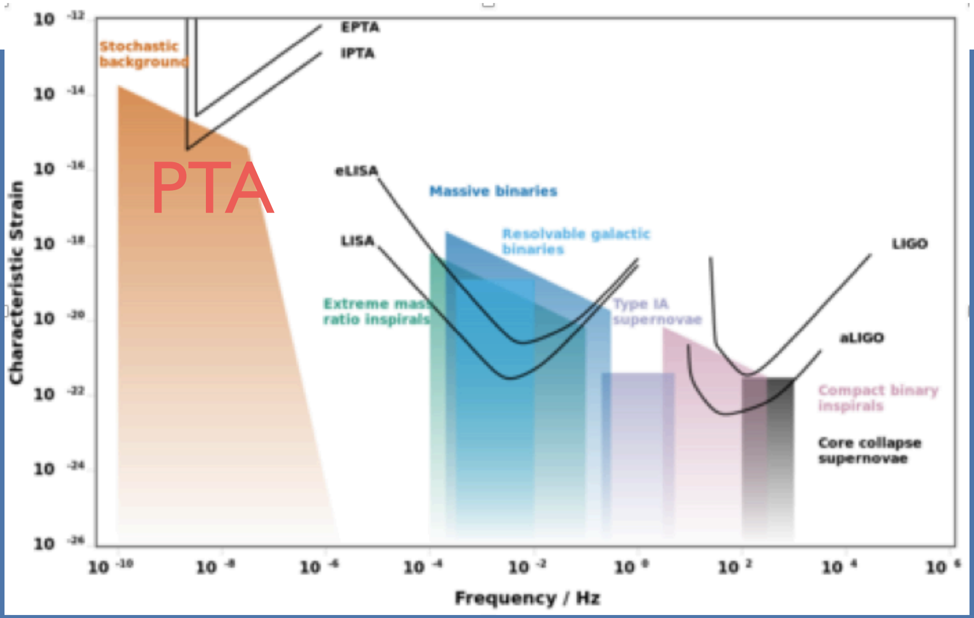

Precise measurement of pulsar pulse timing can detect gravitational waves in the nHz range and can also be used to measure ultralight DM.

PPTA, EPTA, IPTA, NanoGrav, CPTA(FAST)?

Ultra-light DM: Astrophysical Test

FAST in China

Observing Pulsars, binaries, etc.

future Square Kilometer Array (SKA)

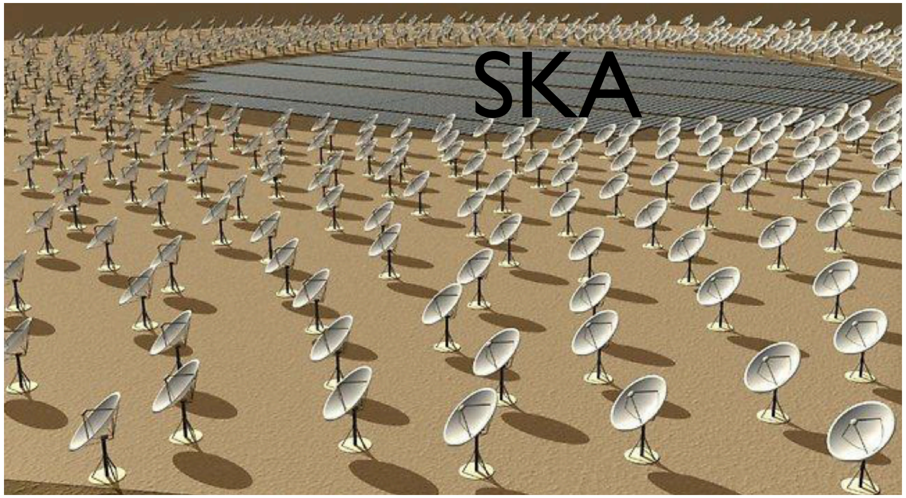

FAST & SKA?

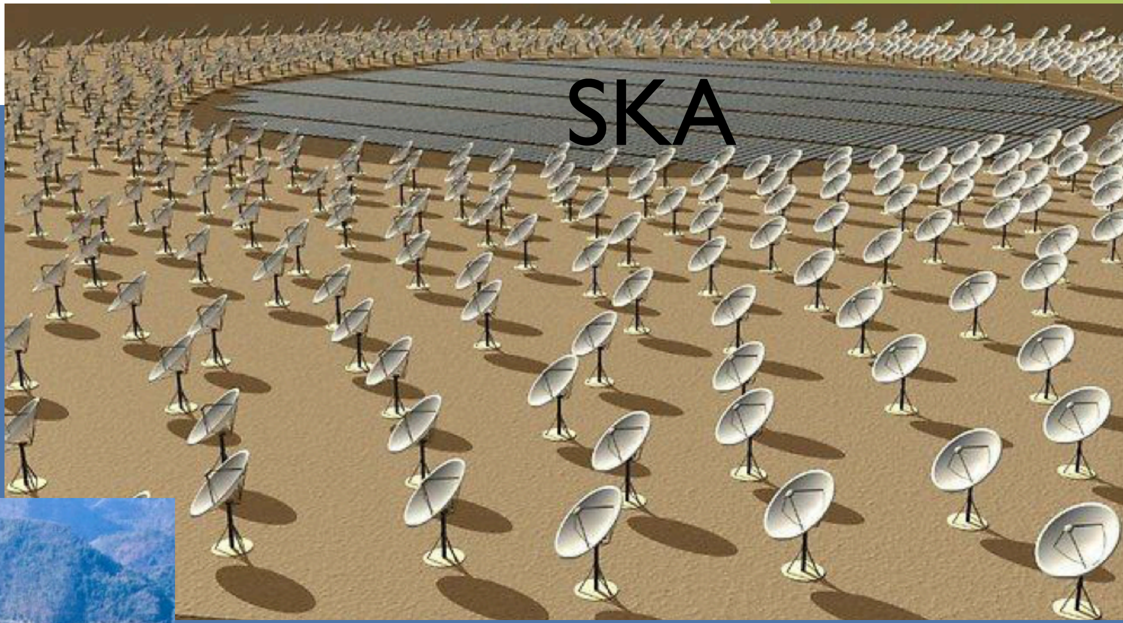

PPTA search for scalar fuzzy DM

Parkes Pulsar Timing Array constraints on ultralight scalar-field dark matter

Nataliya K. Porayko,[1,*] Xingjiang Zhu,[2,3,4,†] Yuri Levin,[5,6,2] Lam Hui,[5] George Hobbs,[7] Aleksandra Grudskaya,[8] Konstantin Postnov,[8,9] Matthew Bailes,[10,4] N. D. Ramesh Bhat,[11] William Coles,[12] Shi Dai,[7] James Dempsey,[13] Michael J. Keith,[14] Matthew Kerr,[15] Michael Kramer,[1,14] Paul D. Lasky,[2,4] Richard N. Manchester,[7] Stefan Osłowski,[10] Aditya Parthasarathy,[10] Vikram Ravi,[16] Daniel J. Reardon,[10,4] Pablo A. Rosado,[10] Christopher J. Russell,[17] Ryan M. Shannon,[10,4] Renée Spiewak,[10] Willem van Straten,[18] Lawrence Toomey,[7] Jingbo Wang,[19] Linqing Wen,[3,4] and Xiaopeng You[20]
(The PPTA Collaboration)

1810.03227

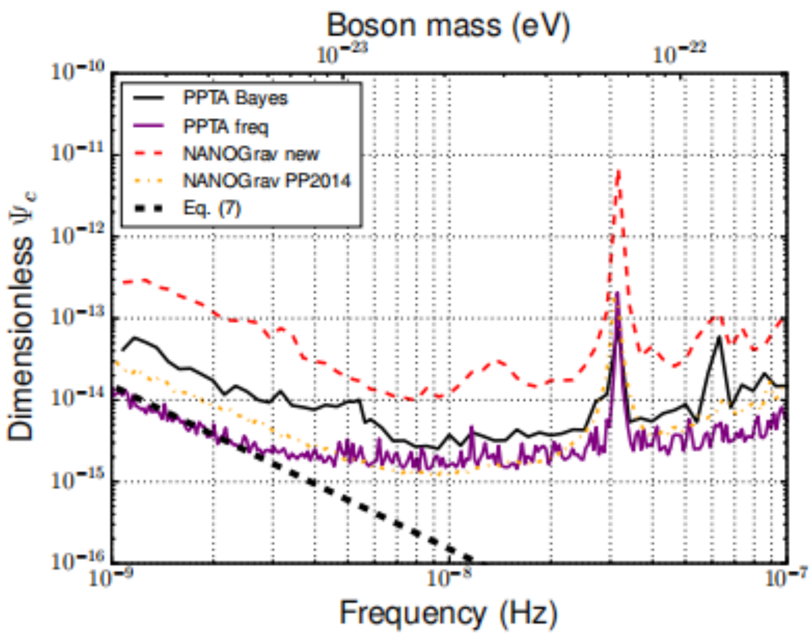

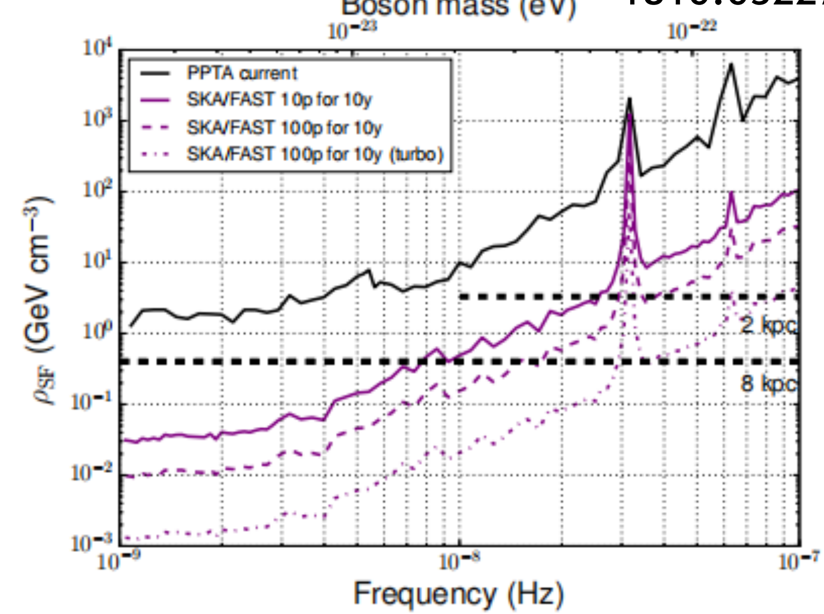

Future SKA can have much better results!

Effects of Gravity from ULDM

The gravitational potential of oscillating DM fields will alter the surrounding energy-momentum tensor, thereby changing the gravitational deflection of incoming electromagnetic pulses.

Scalar DM:

$$s(t) = \frac{\Psi_c}{\pi f} \sin(\alpha_e - \theta_p) \cos(2\pi f t + \alpha_e + \theta_p)$$

Vector DM:

$$\begin{aligned} R_V = &\quad R_\Psi + R_h \\ = &\quad \frac{h_{\rm osc}}{\pi f} \left\{ \frac{1}{2} \left[(\hat{p} \cdot \hat{l})^2 + (\hat{p} \cdot \hat{n})^2 - 2(\hat{p} \cdot \hat{k})^2 \right] - \frac{1}{8} \right\} \\ &\quad \sin(\alpha_e - \alpha_p) \cos\left(2\pi f t + \alpha_e + \alpha_p\right) \end{aligned}$$

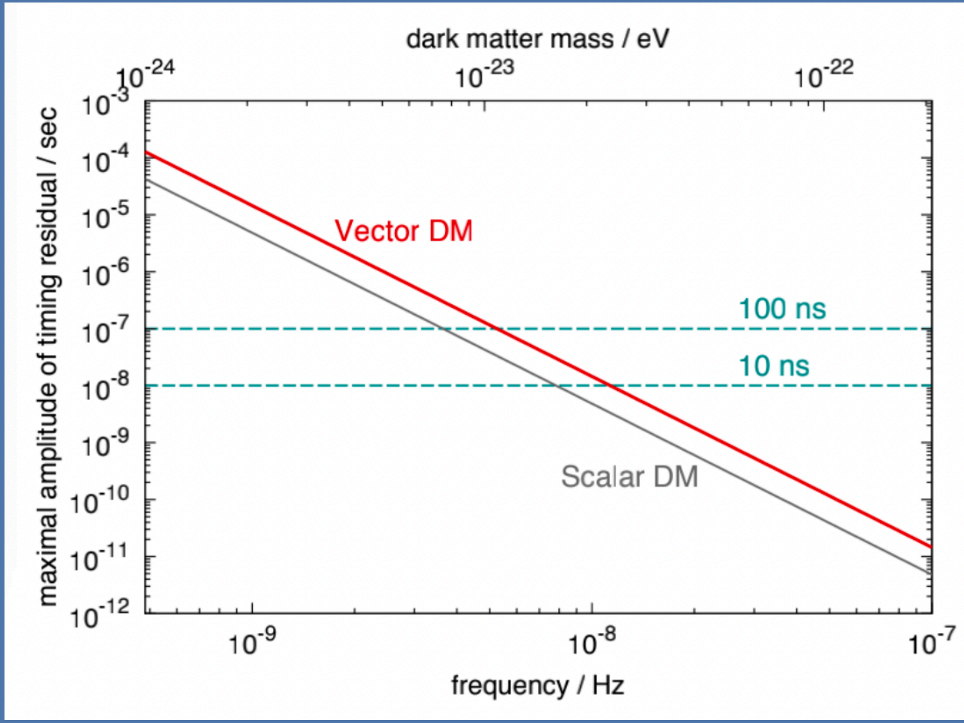

Effects of ULDM's Direct Coupling with Matter

ULDM can directly interact with matters to produce acceleration

$$\boldsymbol{a}(t,\boldsymbol{x}) \simeq \epsilon e \frac{q}{m} m_A \boldsymbol{A}_0 \cos\left(m_A t - \boldsymbol{k}\cdot\boldsymbol{x} + \alpha(\boldsymbol{x})\right),$$

Acceleration induce displacement

$$\Delta\boldsymbol{x}(t,\boldsymbol{x}) = -\frac{\epsilon e q}{m m_A} \boldsymbol{A}_0 \cos\left(m_A t - \boldsymbol{k}\cdot\boldsymbol{x} + \alpha(\boldsymbol{x})\right).$$

(A) Completely uncorrelated: The phases and amplitudes of dark photon background for each pulsar are independent.

(B) Completely correlated: The phases are independent phases but with a common amplitude.

Change of pulsar timing series

$$\Delta t^{(B)}_{\mathrm{DPDM}} = -\frac{\epsilon e}{m_A}\left(\frac{q_p^{(B)}}{m_p}\boldsymbol{A_0}^p \cos\left(m_A t + \alpha_p\right) - \frac{q_e^{(B)}}{m_e}\boldsymbol{A_0}^e \cos\left(m_A t + \alpha_e\right)\right)\cdot\boldsymbol{n},$$

$$\Delta t^{(B-L)}_{\mathrm{DPDM}} = -\frac{\epsilon e}{m_A}\left(\frac{q_p^{(B-L)}}{m_p}\boldsymbol{A_0}^p \cos\left(m_A t + \alpha_p\right) - \frac{q_e^{(B-L)}}{m_e}\boldsymbol{A_0}^e \cos\left(m_A t + \alpha_e\right)\right)\cdot\boldsymbol{n},$$

Parkes PTA data

64m Parkes telescope in Australia

Pulsars	N_{obs}	T(years)	$\overline{\sigma} \times 10^{-6}(s)$	$\log_{10} A_{SN}$	γ_{SN}	$\log_{10} A_{DM}$	γ_{DM}
J0437-4715	29262	15.03	0.296	$-15.76^{+0.17}_{-0.18}$	$6.63^{+0.17}_{-0.13}$	$-13.05^{+0.10}_{-0.08}$	$2.26^{+0.32}_{-0.44}$
J0613-0200	5920	14.20	2.504	$-14.63^{+0.77}_{-0.68}$	$4.93^{+1.33}_{-1.61}$	$-13.02^{+0.08}_{-0.08}$	$0.95^{+0.33}_{-0.31}$
J0711-6830	5547	14.21	6.197	$-12.85^{+0.14}_{-0.16}$	$0.97^{+0.64}_{-0.55}$	$-14.54^{+0.72}_{-0.89}$	$4.43^{+1.68}_{-1.72}$
J1017-7156	4053	7.77	1.577	$-12.89^{+0.07}_{-0.07}$	$0.54^{+0.53}_{-0.37}$	$-12.72^{+0.06}_{-0.06}$	$2.18^{+0.45}_{-0.44}$
J1022+1001	7656	14.20	5.514	$-12.79^{+0.12}_{-0.13}$	$0.54^{+0.55}_{-0.37}$	$-13.04^{+0.10}_{-0.12}$	$0.58^{+0.47}_{-0.36}$
J1024-0719	2643	14.09	4.361	$-14.28^{+0.27}_{-0.20}$	$6.51^{+0.35}_{-0.60}$	$-14.53^{+0.54}_{-0.56}$	$5.22^{+1.14}_{-1.18}$
J1045-4509	5611	14.15	9.186	$-12.75^{+0.24}_{-0.40}$	$1.58^{+1.28}_{-0.93}$	$-12.18^{+0.09}_{-0.08}$	$1.86^{+0.36}_{-0.32}$
J1125-6014	1407	12.34	1.981	$-12.64^{+0.11}_{-0.12}$	$0.51^{+0.55}_{-0.37}$	$-13.14^{+0.19}_{-0.21}$	$3.36^{+0.73}_{-0.66}$
J1446-4701	508	7.36	2.200	$-16.46^{+2.88}_{-3.17}$	$2.74^{+2.49}_{-1.89}$	$-13.49^{+0.32}_{-1.87}$	$2.48^{+1.92}_{-1.45}$
J1545-4550	1634	6.97	2.249	$-17.33^{+2.50}_{-2.55}$	$3.25^{+2.45}_{-2.18}$	$-13.40^{+0.24}_{-0.38}$	$3.90^{+1.61}_{-1.09}$
J1600-3053	7047	14.21	2.216	$-17.63^{+2.10}_{-2.29}$	$3.28^{+2.34}_{-2.15}$	$-13.27^{+0.12}_{-0.13}$	$2.79^{+0.43}_{-0.40}$
J1603-7202	5347	14.21	4.947	$-12.82^{+0.14}_{-0.16}$	$1.01^{+0.67}_{-0.60}$	$-12.66^{+0.10}_{-0.09}$	$1.44^{+0.40}_{-0.38}$
J1643-1224	5941	14.21	4.039	$-12.32^{+0.08}_{-0.09}$	$0.51^{+0.42}_{-0.34}$	$-12.27^{+0.07}_{-0.07}$	$0.55^{+0.32}_{-0.29}$
J1713+0747	7804	14.21	1.601	$-14.09^{+0.25}_{-0.38}$	$2.98^{+1.00}_{-0.64}$	$-13.35^{+0.08}_{-0.08}$	$0.53^{+0.32}_{-0.31}$
J1730-2304	4549	14.21	5.657	$-17.39^{+2.39}_{-2.51}$	$3.05^{+2.59}_{-2.12}$	$-14.11^{+0.40}_{-0.57}$	$4.22^{+1.42}_{-1.04}$
J1732-5049	807	7.23	7.031	$-16.51^{+3.04}_{-2.97}$	$3.29^{+2.37}_{-2.97}$	$-13.38^{+0.54}_{-0.84}$	$4.07^{+1.96}_{-1.93}$
J1744-1134	6717	14.21	2.251	$-13.39^{+0.14}_{-0.15}$	$1.49^{+0.66}_{-0.57}$	$-13.35^{+0.09}_{-0.09}$	$0.86^{+0.40}_{-0.33}$
J1824-2452A	2626	13.80	2.190	$-12.56^{+0.13}_{-0.12}$	$3.61^{+0.41}_{-0.39}$	$-12.18^{+0.11}_{-0.10}$	$1.64^{+0.46}_{-0.59}$
J1832-0836	326	5.40	1.430	$-16.47^{+2.63}_{-3.09}$	$3.66^{+2.33}_{-2.52}$	$-13.07^{+0.24}_{-0.63}$	$3.77^{+2.00}_{-1.05}$
J1857+0943	3840	14.21	5.564	$-14.76^{+0.74}_{-0.50}$	$5.75^{+0.91}_{-1.53}$	$-13.40^{+0.20}_{-0.25}$	$2.66^{+0.83}_{-0.67}$
J1909-3744	14627	14.21	0.672	$-13.60^{+0.13}_{-0.12}$	$1.60^{+0.43}_{-0.46}$	$-13.48^{+0.09}_{-0.08}$	$0.69^{+0.38}_{-0.35}$
J1939+2134	4941	14.09	0.468	$-14.38^{+0.22}_{-0.18}$	$6.24^{+0.49}_{-0.62}$	$-11.59^{+0.07}_{-0.07}$	$0.13^{+0.19}_{-0.10}$
J2124-3358	4941	14.21	8.863	$-14.79^{+0.82}_{-0.67}$	$5.07^{+1.37}_{-1.97}$	$-13.35^{+0.18}_{-0.33}$	$0.95^{+1.11}_{-0.66}$
J2129-5721	2879	13.88	3.496	$-15.48^{+1.92}_{-3.54}$	$2.91^{+2.29}_{-1.83}$	$-13.31^{+0.13}_{-0.14}$	$1.07^{+0.65}_{-0.65}$
J2145-0750	6867	14.09	5.086	$-12.82^{+0.10}_{-0.11}$	$0.62^{+0.50}_{-0.40}$	$-13.33^{+0.14}_{-0.16}$	$1.38^{+0.54}_{-0.55}$
J2241-5236	5224	8.20	0.830	$-13.40^{+0.09}_{-0.08}$	$0.44^{+0.40}_{-0.30}$	$-13.79^{+0.10}_{-0.10}$	$1.42^{+0.61}_{-0.59}$

Results from Parkes PTA in Australia

Results for ULDM $U(1)_B$ and ULDM $U(1)_{B-L}$

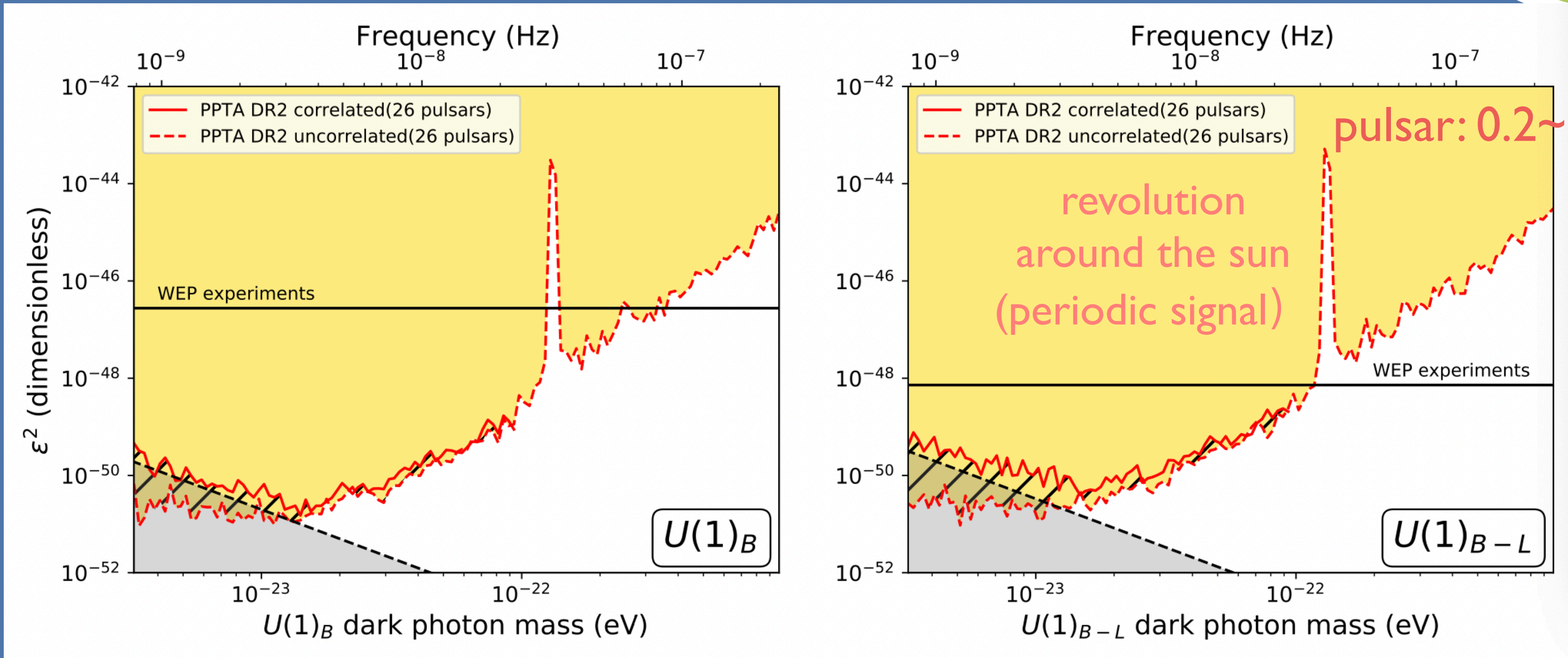

X. Xiao, Z-j. Xia, J. Shu., Q. Yuan, Y. Zhao, X-j. Zhu, with PPTA collaboration, Phys.Rev.Res. 4 (2022) 1, L012022

Gaia Stellar Position Measurements

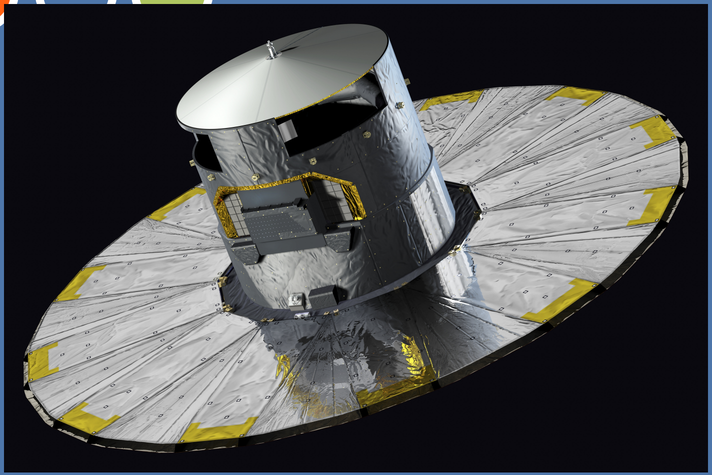

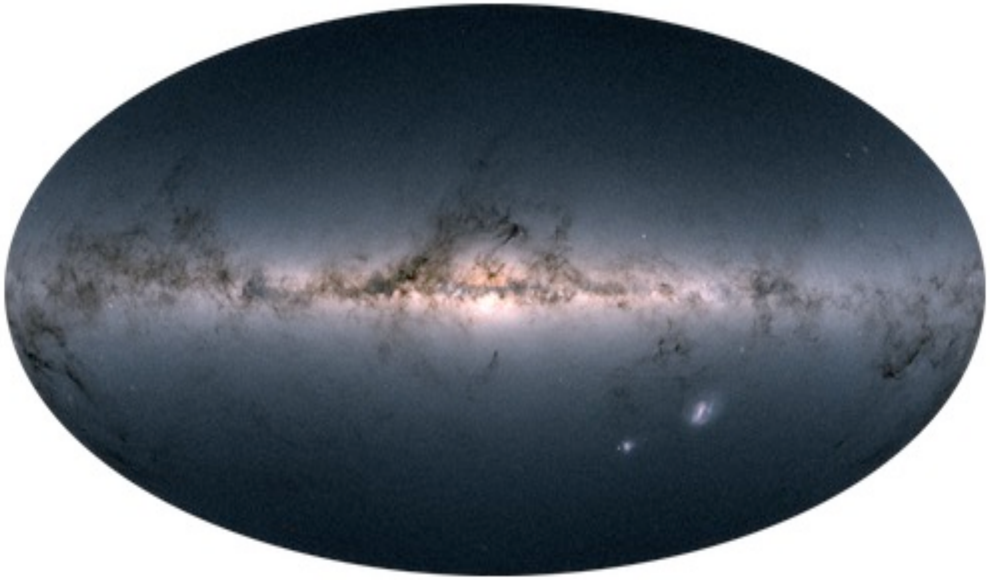

The Gaia satellite (launched in 2003) precisely measures the positions and velocities of ~1% of stars within the Milky Way (~10^9 stars).

Study the structure of the Milky Way, stellar evolution, new planets, fundamental physics, etc.

DPDM detection from astrometry

(Gaia Satellite) experiences a dragging effect under an ultralight DM background field.

$$\boldsymbol{a}(t,\boldsymbol{x}) \simeq \epsilon e \frac{q}{m} m_A \boldsymbol{A}_0 \cos(m_A t - \boldsymbol{k}\cdot\boldsymbol{x})$$

Acceleration causes periodic changes in velocity, leading to changes in the observed angle.

$$\Delta \boldsymbol{v}(t,\boldsymbol{x}) \simeq \epsilon e \frac{q}{m} \boldsymbol{A}_0 \sin(m_A t - \boldsymbol{k}\cdot\boldsymbol{x}).$$

$$\Delta\theta \simeq -\Delta v \sin\theta$$

Lower precision in the radial direction.

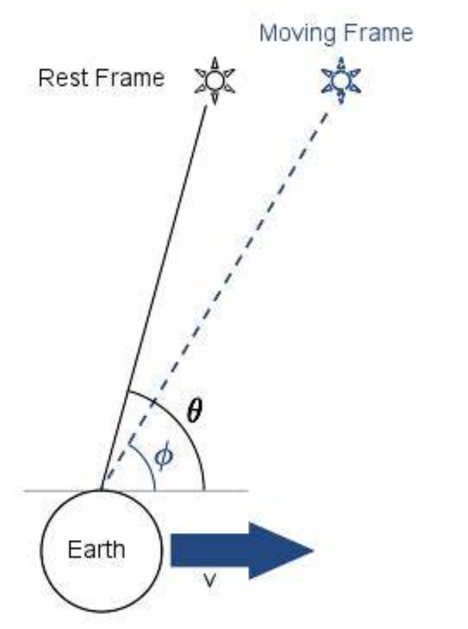

Global Periodically changes on star position

Neglecting star position changes

Search for ULDM with Gaia

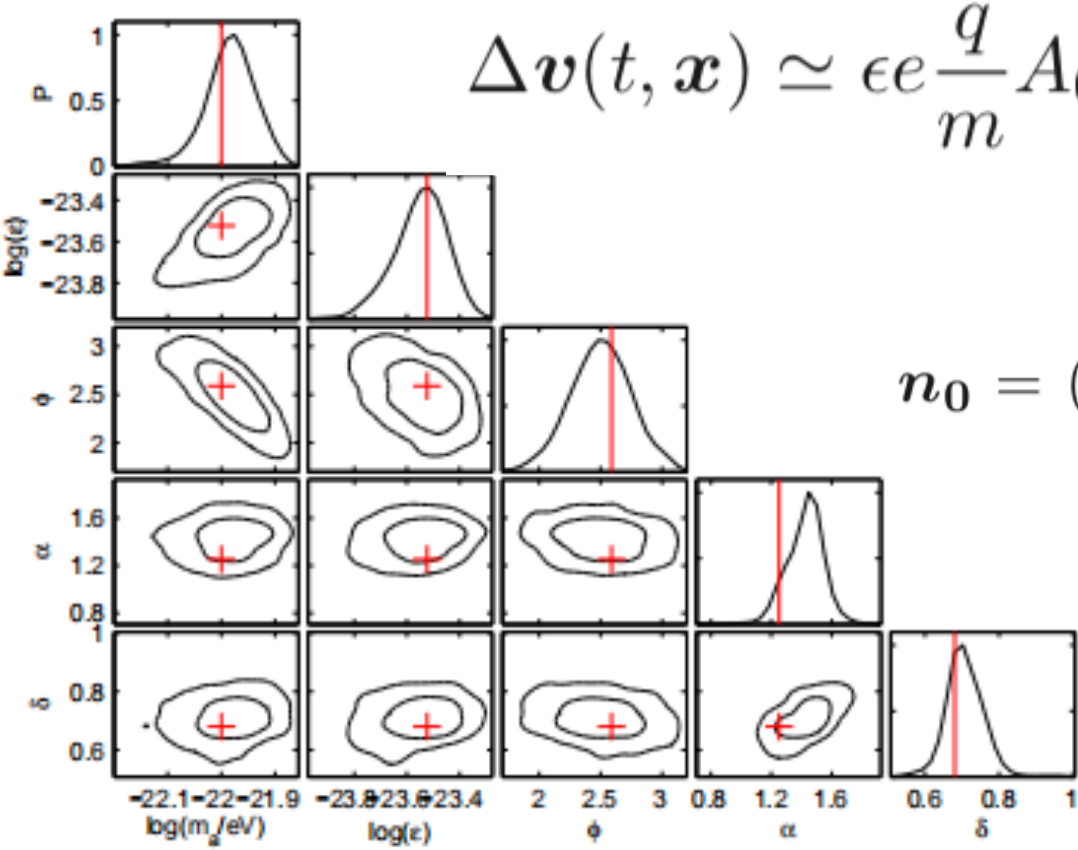

$$\Delta \boldsymbol{v}(t, \boldsymbol{x}) \simeq \epsilon e \frac{q}{m} A_0 \boldsymbol{n_0} \sin[m_A(t - t_0) + \phi],$$

equatorial coordinate (α, δ)

$$\boldsymbol{n_0} = (\cos\delta\cos\alpha,\ \cos\delta\sin\alpha,\ \sin\delta),$$

Data Processing
Compression

$$\sigma = 100\ \mu\text{as}/\sqrt{10^5}.$$

mock data

H-k. Guo, Y-q. Ma, J. Shu., X. Xiao, Q. Yuan, Y. Zhao, JCAP 1905 (2019) 015

$$(m_A, \epsilon, \phi, \alpha, \delta) = (10^{-22}\ \text{eV}, 3 \times 10^{-24}, 2.59, 1.25, 0.68).$$

Search for ULDM with Gaia

95% C.L. Exclusion Line (Expected Value)

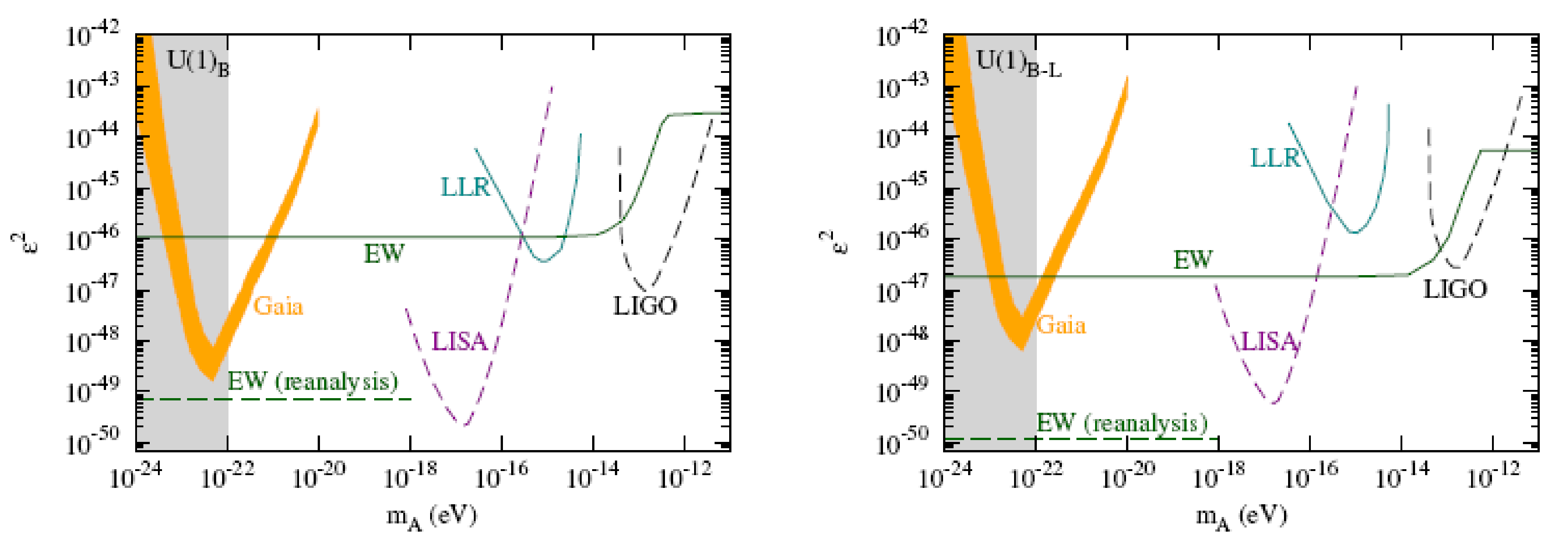

H-k. Guo, Y-q. Ma, J. Shu., X. Xiao, Q. Yuan, Y. Zhao, JCAP 1905 (2019) 015

Gaia's 2025 data release includes temporal variations, which can be used for actual measurements.

M87* Black Hole Polarization Observations

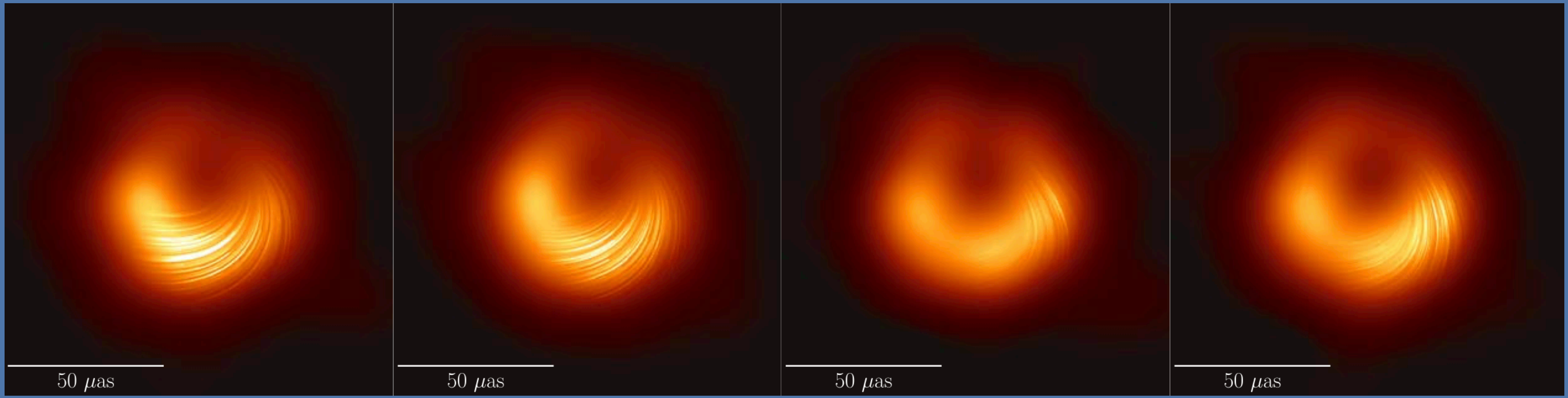

4 days of polarimetry observation of *M87**

Event Horizon Telescope

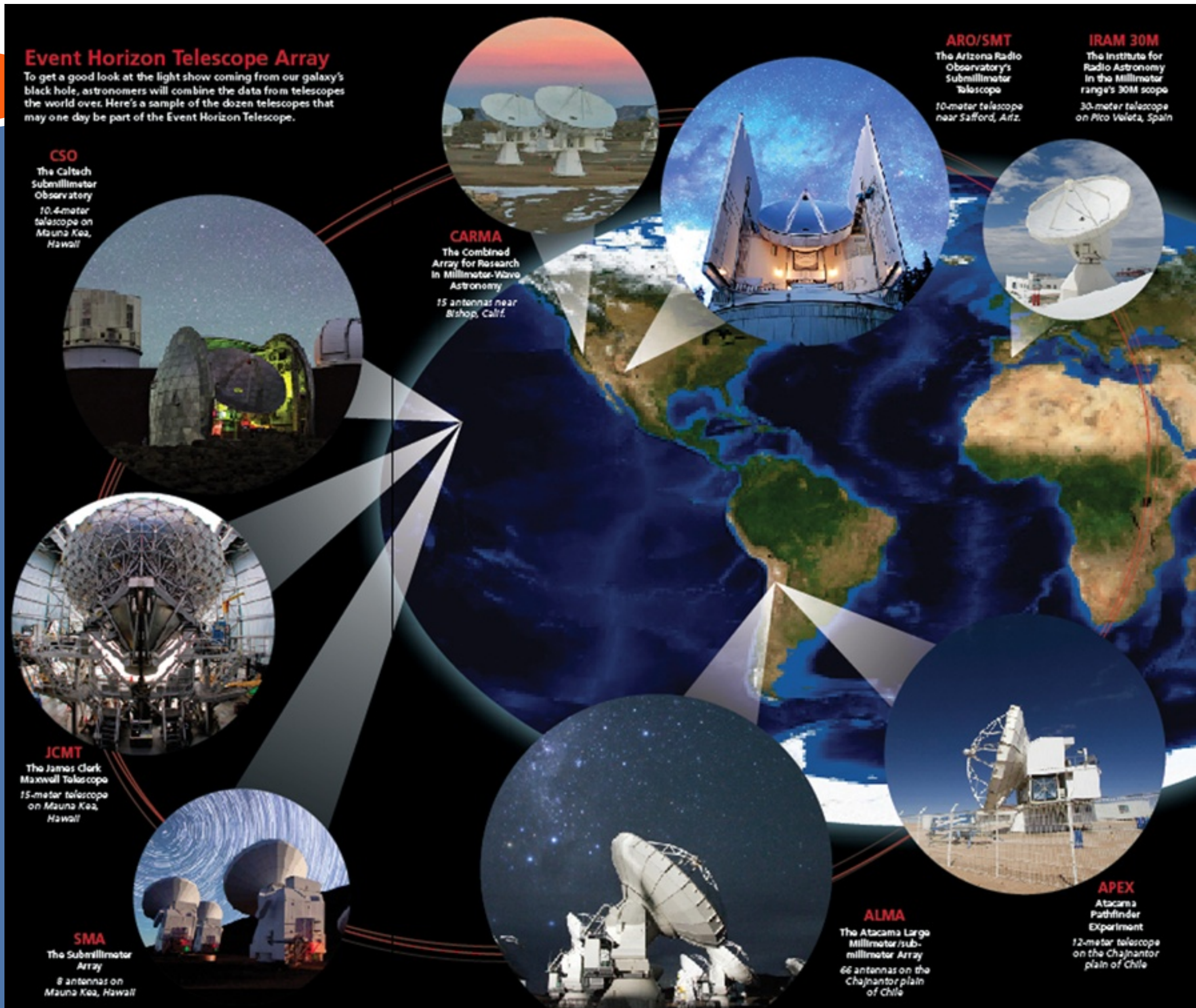

Western Hemisphere mm-Wave Telescope Array

mm-Wave Band is Suitable for Precise Polarization Angle Measurements

Axion-Electromagnetic Equation

Axion-induced bi-refringence effect

$$\mathcal{L} = -\frac{1}{4}F_{\mu\nu}F^{\mu\nu} - \frac{1}{2}g_{a\gamma}aF_{\mu\nu}\tilde{F}^{\mu\nu} + \frac{1}{2}\nabla^{\mu}a\nabla_{\mu}a - V(a),$$

$$\nabla\cdot\boldsymbol{E} = g\nabla\varphi\cdot\boldsymbol{B}, \quad \nabla\times\boldsymbol{E} + \frac{\partial\boldsymbol{B}}{\partial t} = 0,$$

$$\nabla\times\boldsymbol{B} - \frac{\partial\boldsymbol{E}}{\partial t} = g\left(\boldsymbol{E}\times\nabla\varphi - \boldsymbol{B}\frac{\partial\varphi}{\partial t}\right),$$

$$\nabla\cdot\boldsymbol{B} = 0,$$

$$\Box\varphi = \frac{\partial^2\varphi}{\partial t^2} - \nabla^2\varphi = -g\boldsymbol{E}\cdot\boldsymbol{B}.$$

The CP-odd axion field affects the phase velocity of left and right circularly polarized electromagnetic waves.

Maxwell's equations with axion field

Bi-refringence Effect

Axion-induced **bi-refringence effect**

$$\Box A_\pm = \pm 2 i g_{a\gamma}[\partial_z a \dot{A}_\pm - \dot{a}\partial_z A_\pm],$$

$$\omega_\pm \approx k \pm \tfrac{1}{2} g \left(\frac{\partial \varphi}{\partial t} + \nabla\varphi \cdot \frac{\boldsymbol{k}}{k} \right)$$

different phase velocities for +/- helicities

For linear-polarized photons

$$\begin{aligned} \Delta\Theta &= g_{a\gamma} \Delta a(t_{\rm obs}, \mathbf{x}_{\rm obs}; t_{\rm emit}, \mathbf{x}_{\rm emit}) \\ &= g_{a\gamma} \int_{\rm emit}^{\rm obs} ds\, n^\mu\, \partial_\mu a \\ &= g_{a\gamma}[a(t_{\rm obs}, \mathbf{x}_{\rm obs}) - a(t_{\rm emit}, \mathbf{x}_{\rm emit})], \end{aligned}$$

The polarization angle shift is the difference between the initial and final expectation values of the axion field.

Therefore, precise measurements of the polarization angle is needed.

Superradiance

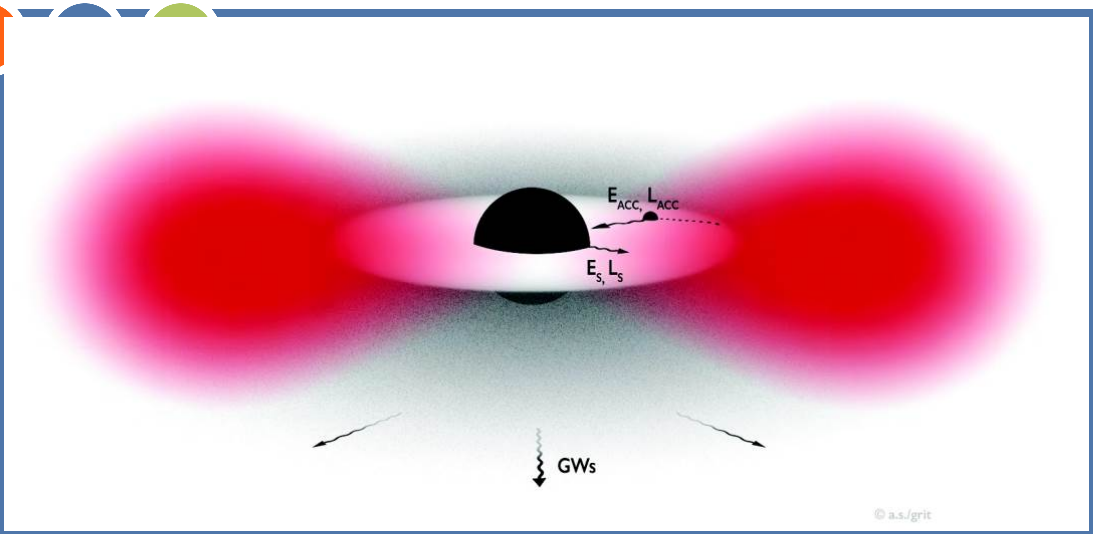

Superradiance condition

$$\omega < \omega_c = \frac{a_J m}{2r_+}$$

Rapidly rotating black holes lose energy and angular momentum by radiating axion fields.

Axion cloud induced near the black hole

Effective Frequency range for Superradiance: when the axion wavelength is comparable to the black hole's event horizon.

$$\frac{r_g}{\lambda_C} = \mu M \equiv \alpha \in (0.1, 1),$$

The energy of the axion cloud could be comparable to that of the black hole.

Superradiance Field Equation Solution

Axion Could

K-G equation solution under kerr background

Similar to hydrogen atom energy level (non-relativistic):

$$a(x^\mu) = e^{-i\omega t} e^{im\phi} S_{lm}(\theta) R_{lm}(r)$$

$$\alpha \equiv \mu M$$

$$\mathrm{Re}(\omega) \simeq \left(1 - \frac{\alpha^2}{2\bar{n}^2}\right)\mu$$

Reduce to spherical harmonics Y_{lm} in the non-relativistic limit.

The imaginary part of the field provides superradiance conditions.

Axion cloud production is more effective in lower l-modes

Black Hole Superradiance

Radial Solution

$$r_\pm = r_g \left(1 \pm \sqrt{1 - a_J^2}\right)$$

The brightest position of the electromagnetic radiation ring observed by EHT is approximately where the radial solution reaches its maximum.

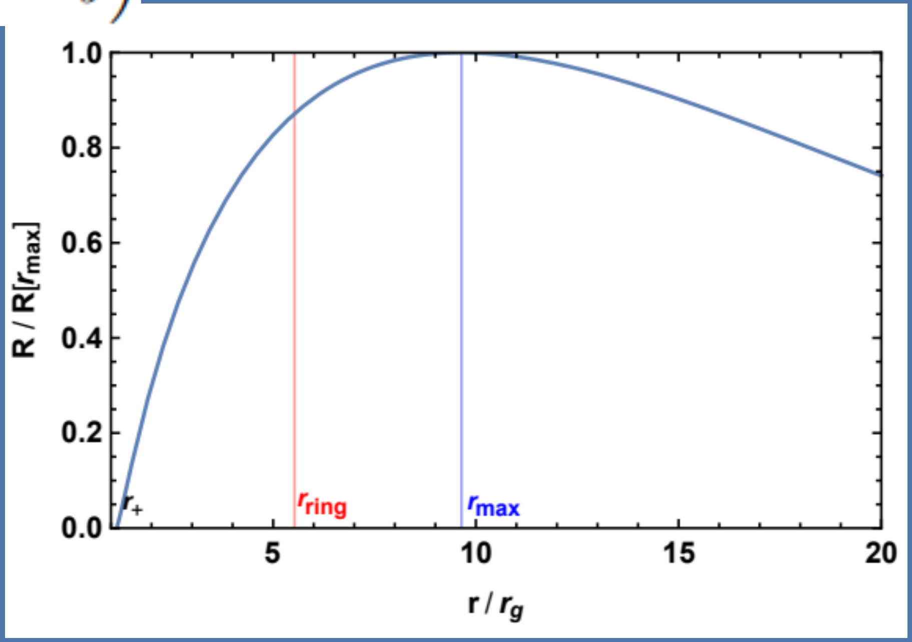

Y-f. Chen, J. Shu., X. Xiao, Q. Yuan, Y. Zhao, Phys.Rev.Lett. 124 (2020) 061102

Self-Interaction of Axion Cloud

Besides gravity, the self-interaction of ultralight DM field matters.

$$S = \int d^4x\sqrt{-g}[-\frac{1}{2}(\nabla a)^2 - \mu^2 f_a^2(1-\cos\frac{a}{f_a})]$$

Ansatz: $$a = \frac{1}{\sqrt{2\mu}}(e^{-i\mu t}\psi + e^{i\mu t}\psi^*)$$

Simulation results suggest that axion clouds can stably exist.

Gravity potential

$$S_{\rm NR} = \int d^4x \left(i\psi^*\partial_t\psi - \frac{1}{2\mu}\partial_i\psi\partial_i\psi^* - \frac{\alpha}{r}\psi^*\psi + \frac{(\psi^*\psi)^2}{16 f_a^2} \right)$$

Self-interaction

Position angle change

We use $a_0 \approx f_a$ and $\omega \approx \mu$

Neglect the axion field near earth

$$\Delta\Theta_{\max} \simeq -b g_{a\gamma} f_a \cos\left[\mu t_{\rm emit} + \beta(|\mathbf{x}_{\rm emit}| = r_{\max})\right],$$

$$b \equiv a_{max}/f_a$$

$$\Delta\Theta(t, r, \theta, \phi) \approx -\frac{b g_{a\gamma} f_a R_{11}(r)}{R_{11}(r_{\max})} \sin\theta \cos\left[\omega t - m\phi\right]. \quad (17)$$

Spatial and temporal resolution

$$g_{a\gamma} \equiv \frac{c}{2\pi f_a} \equiv \frac{c_\gamma \alpha_{em}}{4\pi f_a},$$

fermion loop $c_\gamma \sim NQ^2.$

clockwork $c_\gamma \sim 2Q^2 q^{N-M}.$

Huge

Expected Limit

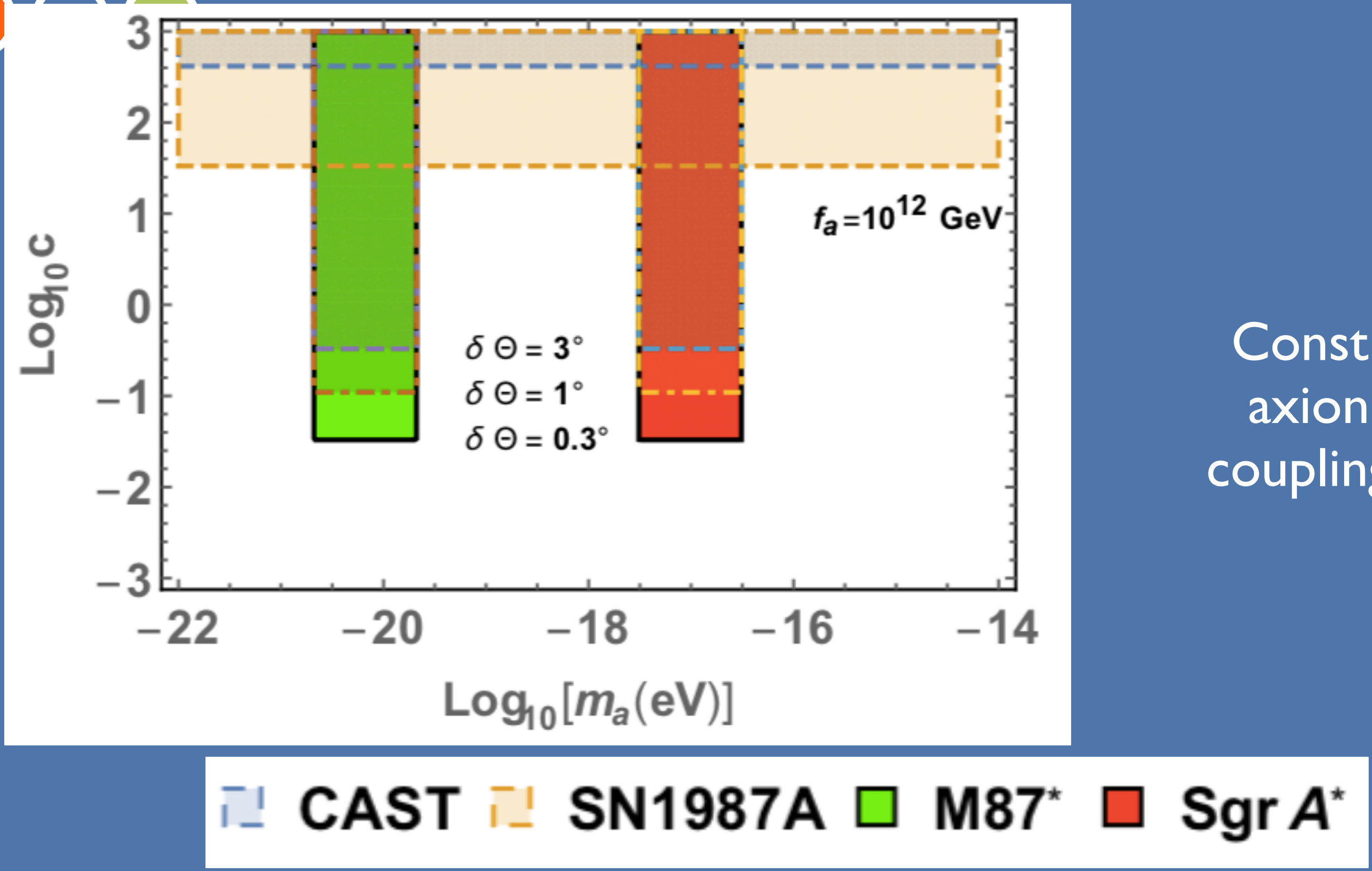

Constraints on axion-photon coupling strength

Y-f. Chen, J. Shu., X. Xiao, Q. Yuan, Y. Zhao, Phys.Rev.Lett. 124 (2020) 061102

Polarization Parameters

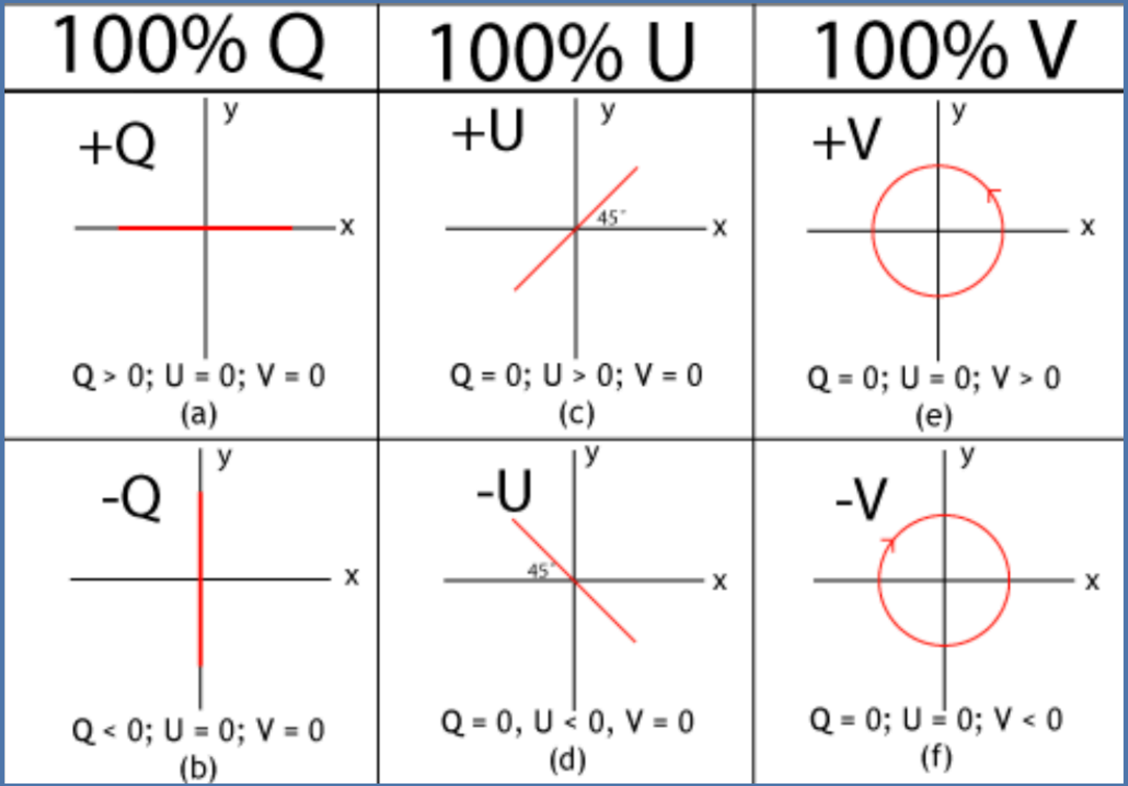

4 Stokes parameters *(I, Q, U,V):*

I: total intensity;
Q, U: linear polarization;
V: circular polarization.

Radiative Transfer

$$\frac{d}{ds}\begin{pmatrix} I \\ Q \\ U \\ V \end{pmatrix} = \begin{pmatrix} j_I \\ j_Q \\ j_U \\ j_V \end{pmatrix} - \begin{pmatrix} \alpha_I & \alpha_Q & \alpha_U & \alpha_V \\ \alpha_Q & \alpha_I & \rho_V & \rho_U \\ \alpha_U & -\rho_V & \alpha_I & \rho_Q \\ \alpha_V & -\rho_U & -\rho_Q & \alpha_I \end{pmatrix}\begin{pmatrix} I \\ Q \\ U \\ V \end{pmatrix}$$

Considering curved spacetime and plasma effects, we use Stokes parameters for radiative transformation. The axion birefringence effect is similar to the Faraday rotation effect (without periodic time variation).

$$\rho_V = \rho_V^{\mathrm{FR}} - 2g_{a\gamma}\frac{da}{ds},$$

EVPA $\chi \equiv \frac{1}{2}\arg(Q + iU).$

Change of EVPA

RIAF model

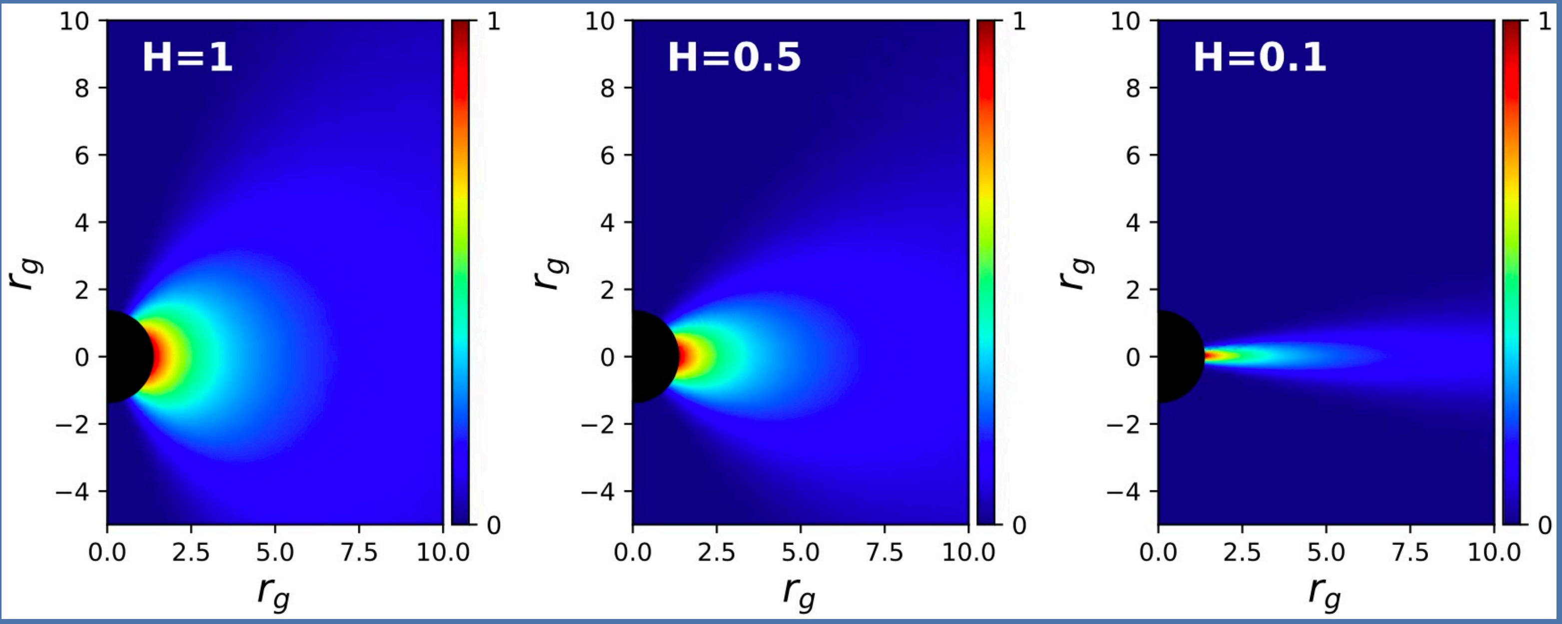

Color indicate the electron number density

H stands for the average thickness of the accretion disk

RIAF Model, thin accretion disk give smaller background

Demonstration

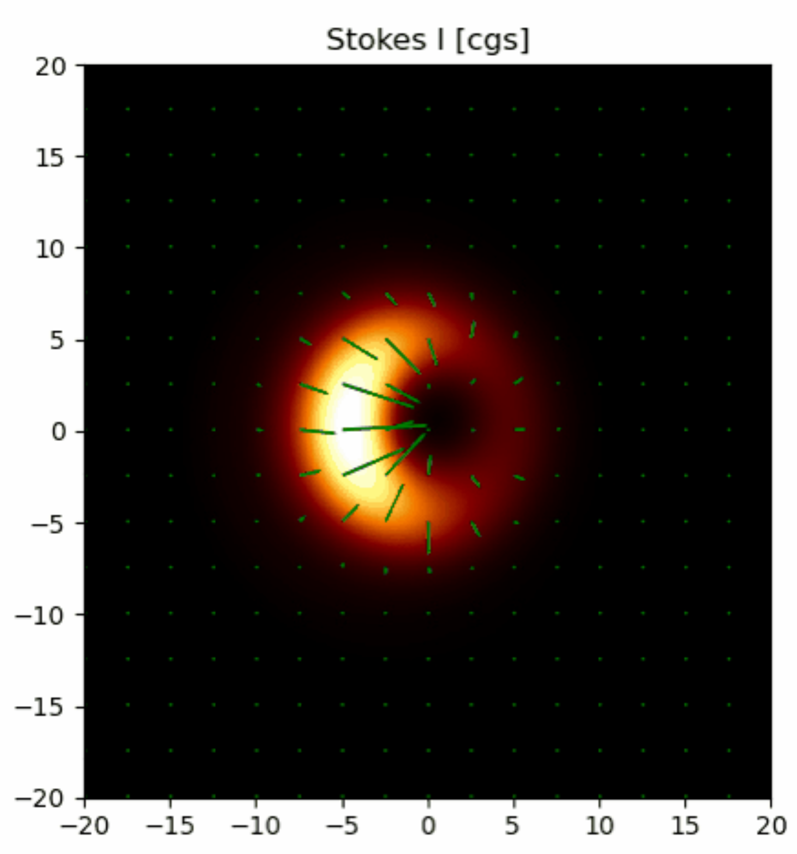

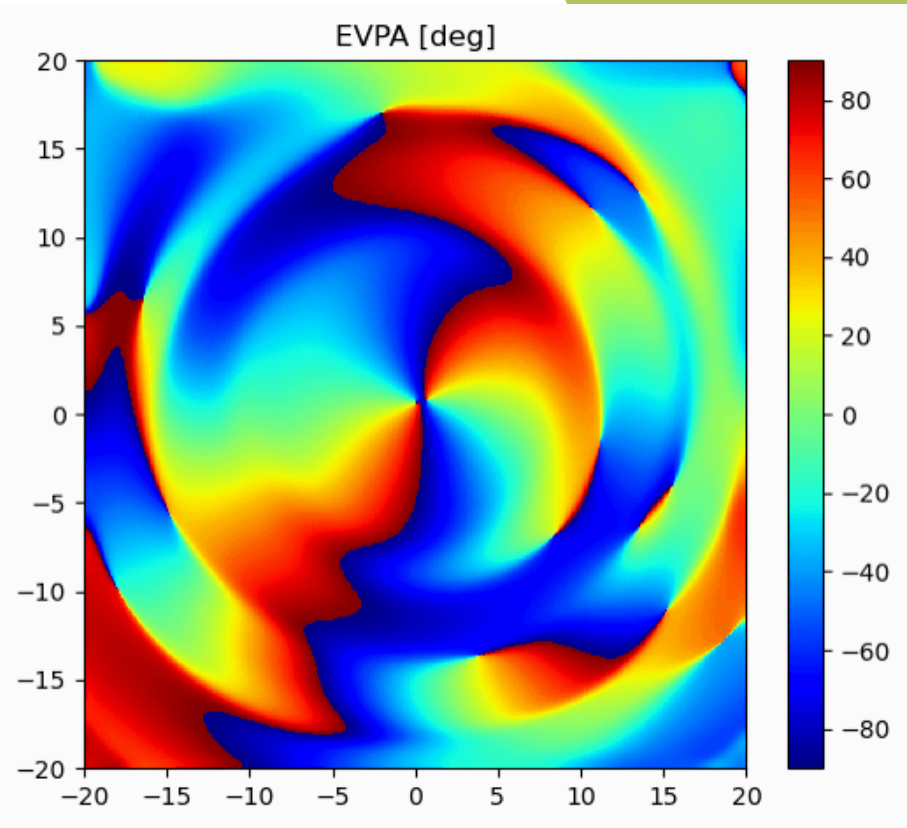

Numerical results from analytical RIAF model

Y-f. Chen, Y-x. Liu, R-s. Lu, Y. Mizauno, J. Shu., X. Xiao, Q. Yuan, Y. Zhao, Nature Astronomy

EHT’s Observation

Polarization Data released on March, 2021

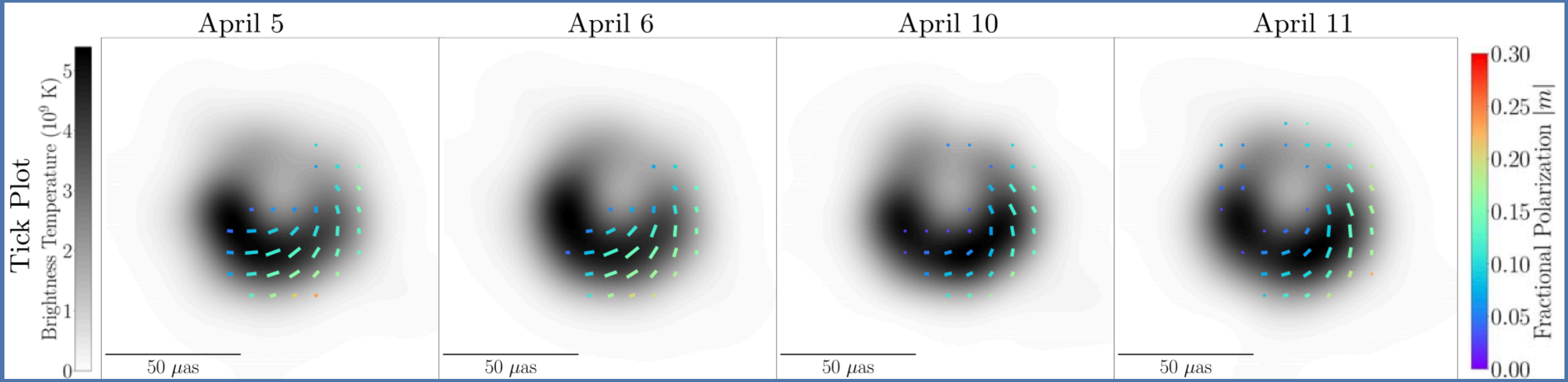

4 days of Polarization Data

Results

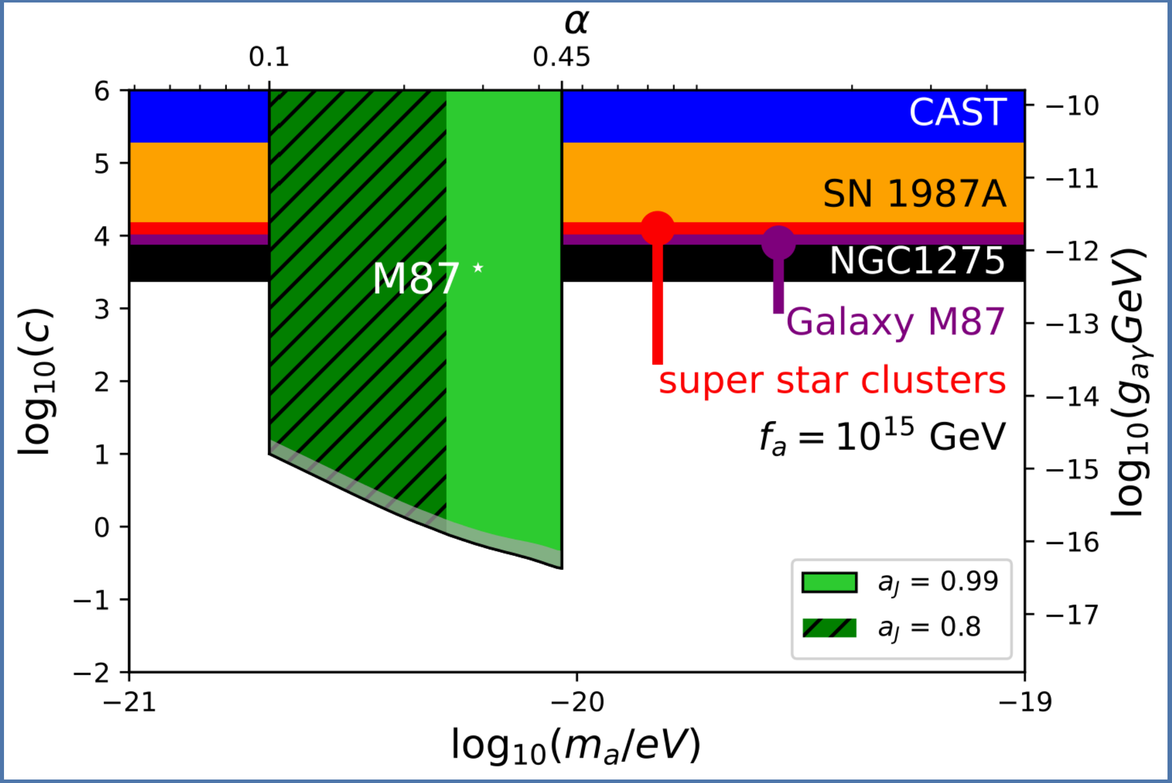

Smaller mass,
longer wavelength,
longer period.

Long periods, with smaller amplitude changes over four days of subtraction, reducing sensitivity.

Y-f. Chen, Y-x. Liu, R-s. Lu, Y. Mizuno, J. Shu., X. Xiao, Q. Yuan, Y. Zhao, Nature Astronomy 2022

Current status

- Axon dark matter detection competition :
  - Traditional resonant cavity: ADMX, CAPP, HAYSTACK
  - LC circuit: DM Radio, ABRACADABRA
  - Nuclear Magnetic Resonance: CASPER, Spin amplifier (USTC) …

- The main experimental limits come from the resonant cavity, CAST, and stellar cooling.

A huge parameter space to be explored!

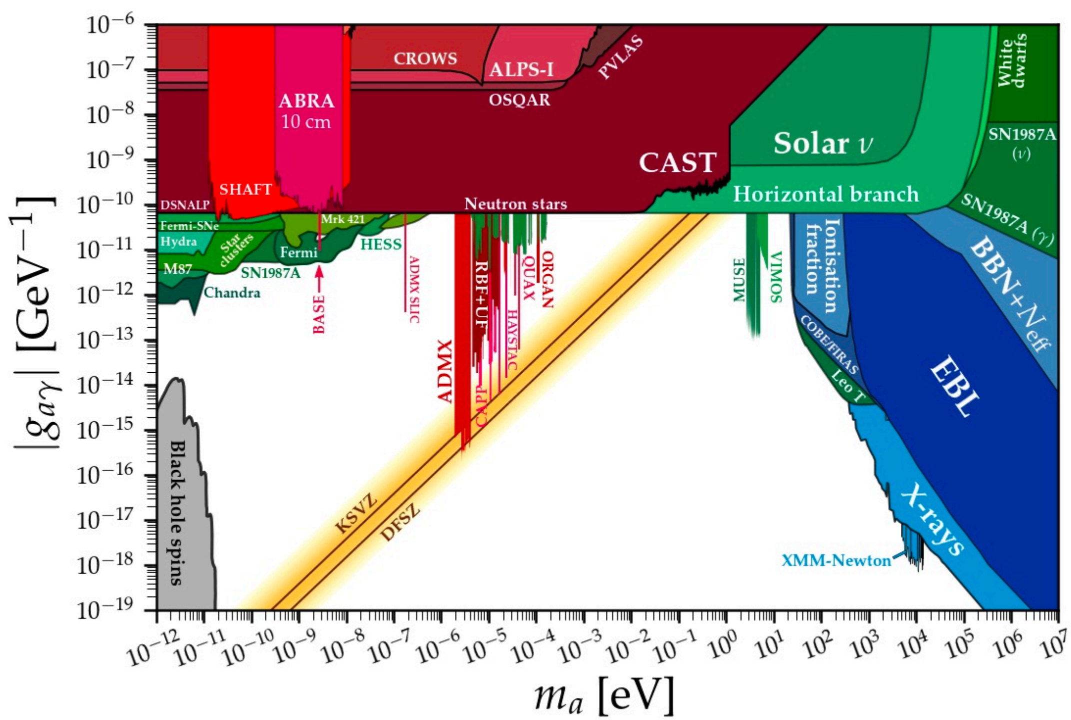

Inverse Primakoff Effect

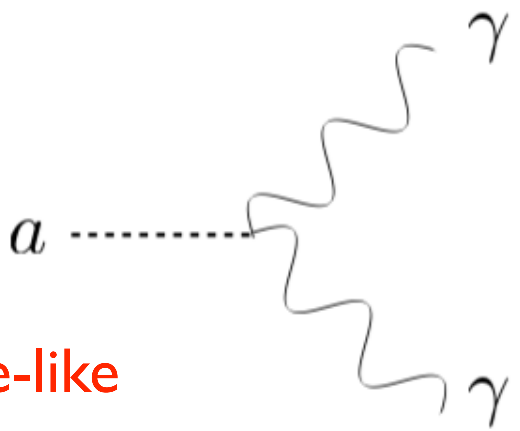

Wave-like dark matter

Under strong magnetic field background

$$g_{a\gamma\gamma} a F_{\mu\nu} \epsilon^{\mu\nu\alpha\beta} F_{\alpha\beta} \sim g_{a\gamma\gamma} a \vec{E} \cdot \vec{B}$$

$$\nabla \times \mathbf{B} \simeq \partial_t \mathbf{E} + \mathbf{J} + \underline{g_{a\gamma\gamma} \mathbf{B}\, \partial_t a}$$

Axion dark matter induces an effective current under strong magnetic field.

$$J_{\rm eff}(t) \sim g_{a\gamma\gamma} B_0(t) \sqrt{\rho_{\rm DM}} \cos m_a t$$

Cavity with static B field

$$\left(\partial_t^2 + \frac{m_a}{Q_1}\partial_t + m_a^2\right)\mathbf{E}_1 \sim m_a \cos m_a t$$

$$Q_a \sim 10^6$$

Quantum amplifier to readout the signal.

$$m_a \sim \text{GHz} \sim 10^{-6}\ \text{eV}$$

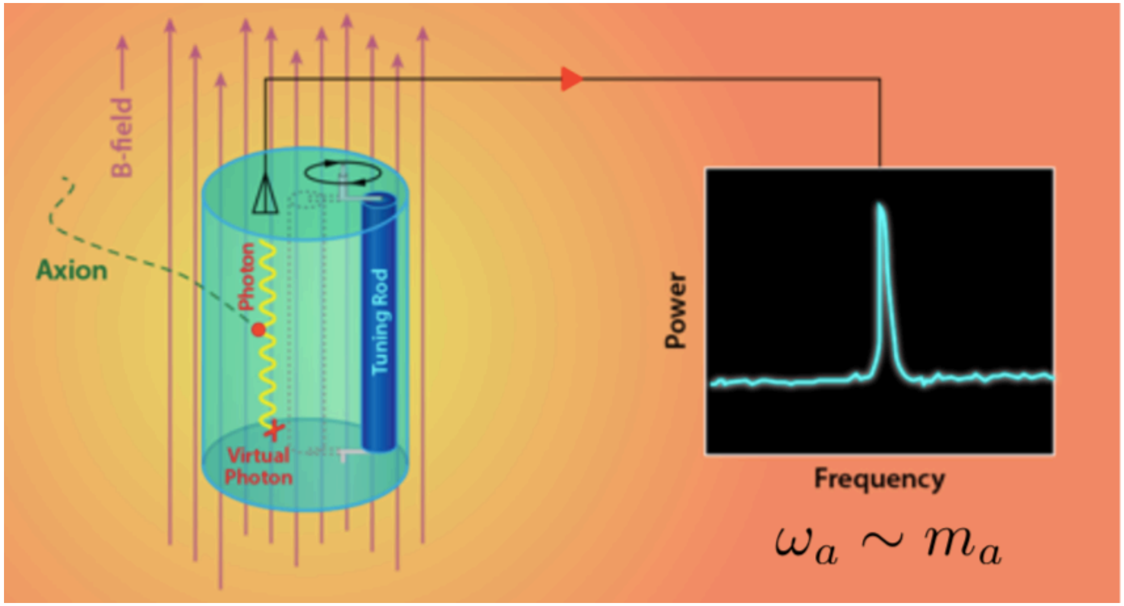

Cavity size ~ (axion mass)^-1

Signal power decreases with axion mass

e.g. ADMX, HAYSTACK

$$g_{a\gamma\gamma} a F_{\mu\nu}\epsilon^{\mu\nu\alpha\beta}F_{\alpha\beta} \sim g_{a\gamma\gamma} a \vec{E}\cdot\vec{B}$$

Resonant EM detection of axion dark matter

Cavity mode equation

Source: **a**
(almost monochromatic)

$$\sum_n \left(\partial_t^2 + \frac{\omega_n}{Q_n}\partial_t + \omega_n^2\right)\mathbf{E}_n = g_{a\gamma\gamma}\partial_t(\mathbf{B}\partial_t a)$$

Signal Mode: $\mathbf{E}_n$

Pump Mode: **B**

- Traditional resonant detection matches axion mass with the resonant frequency by using a static B field.

$$\omega_1 \simeq m_a \qquad \partial_t(\mathbf{B}) \simeq 0$$

$$\left(\partial_t^2 + \frac{m_a}{Q_1}\partial_t + m_a^2\right)\mathbf{E}_1 = g_{a\gamma\gamma}\mathbf{B}\sqrt{\rho_{\rm DM}}m_a\cos m_a t$$

The Dark Matter Haloscope:
Classical axion wave drives RF cavity mode

Pierre Sikivie,
Sakurai Prize 2019

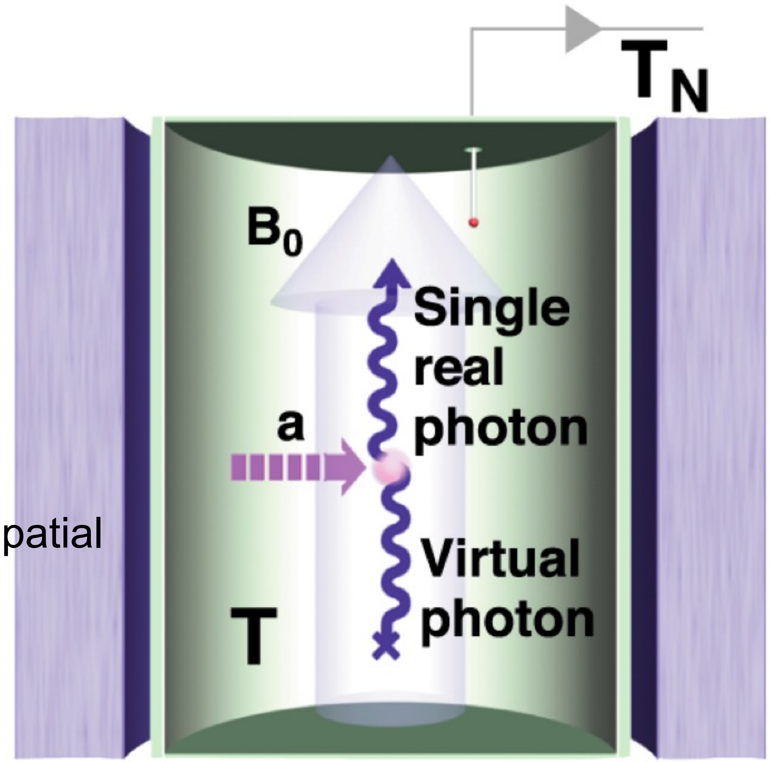

- In a constant background B_0 field, the oscillating axion field acts as an exotic, space-filling current source

$$\vec{J}_a(t) = -g\theta \vec{B}_0 m_a e^{i m_a t}$$

Ignore the spatial derivative

which drives E&M via Faraday's law:

$$\vec{\nabla} \times \vec{H}_r - \frac{d\vec{D}_r}{dt} = \vec{J}_a$$

- Periodic cavity boundary conditions extend the coherent interaction time **(cavity size ≈ 1/m_a)** → the exotic current excites standing-wave RF fields.

A spatially-uniform cavity mode can **optimally** extract power from the dark matter wave

$$P_a(t) = \int \vec{J}_a(t) \cdot \vec{E}_r(t)\, dV$$

Axions vs WIMPs:

Resonant scattering requires size of scattering target = 1/(momentum transfer)

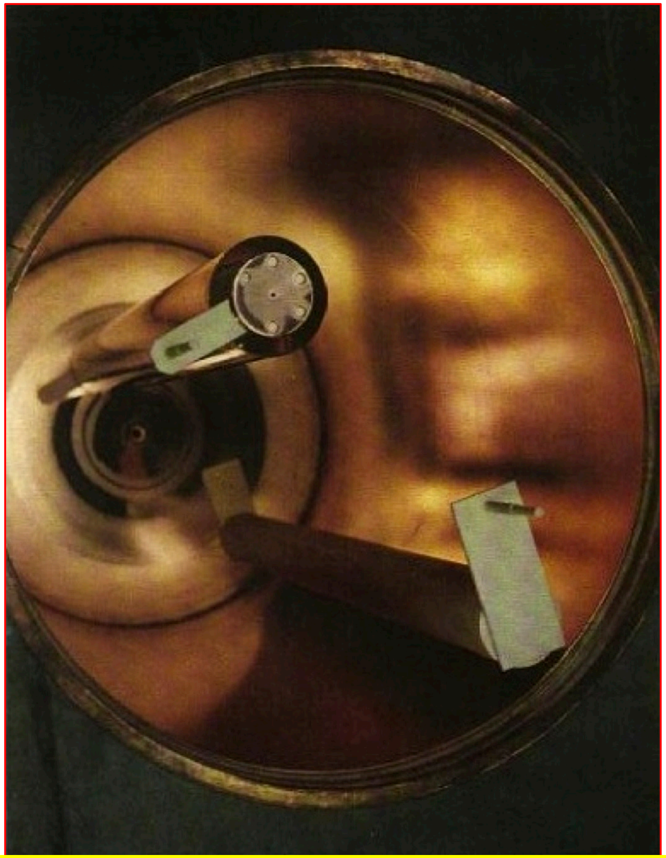

4 μeV mass axions scatter on 50cm size microwave cavities

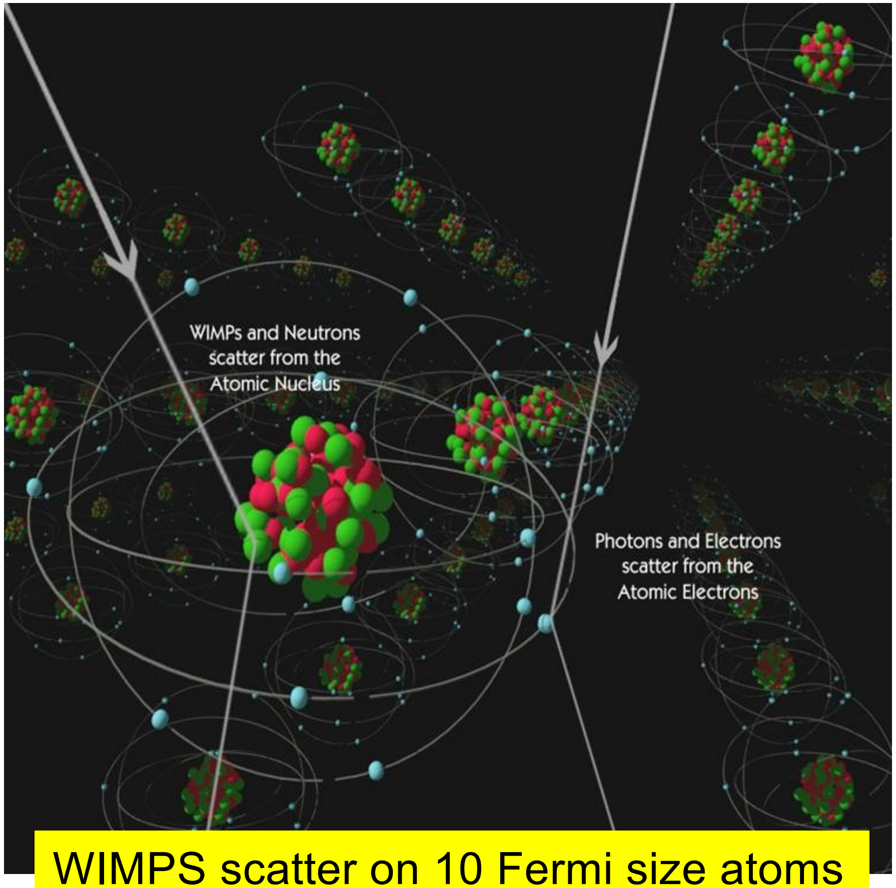

WIMPS scatter on 10 Fermi size atoms

Spectral analysis of output voltage time series

Discrete Fourier transform

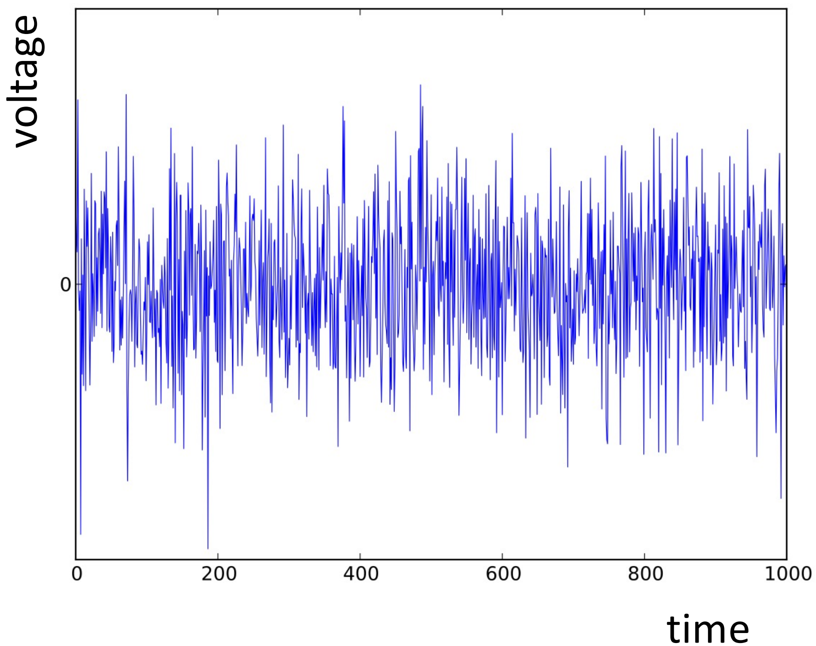

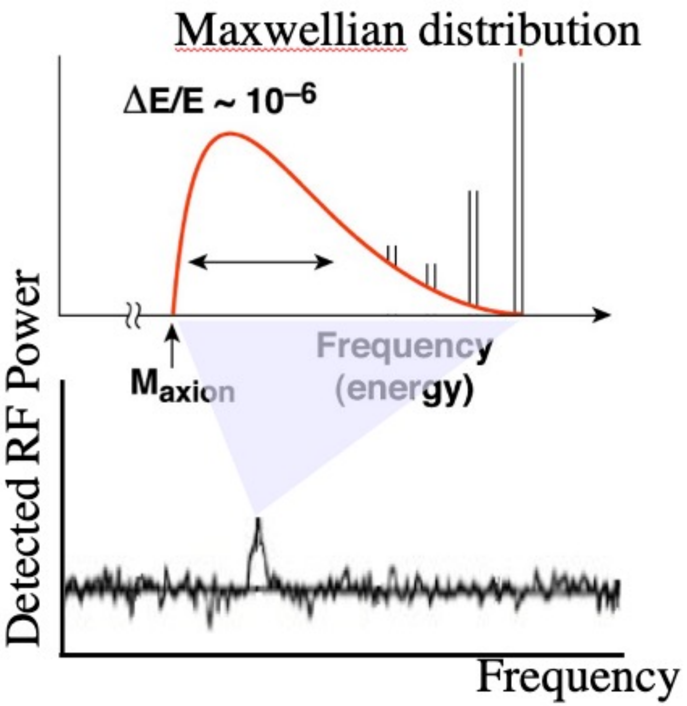

Digitization rate f_{dig} gives maximum resolvable "Nyquist" frequency $f_{dig}/2$.
Duration Δt of acquired time series gives frequency resolution $\Delta f = 1/2\Delta t$.

Dark matter signal = excess above white noise backgrounds.

LC Circuit with static B field

- Resonant conversion happens when

$$m_a = \omega = \frac{1}{\sqrt{LC}}$$

- Scan the mass from 100 Hz to 100 MHz by tuning the capacitor C

Much broader detection frequency

e.g. DM radio, ADMX-SLIC

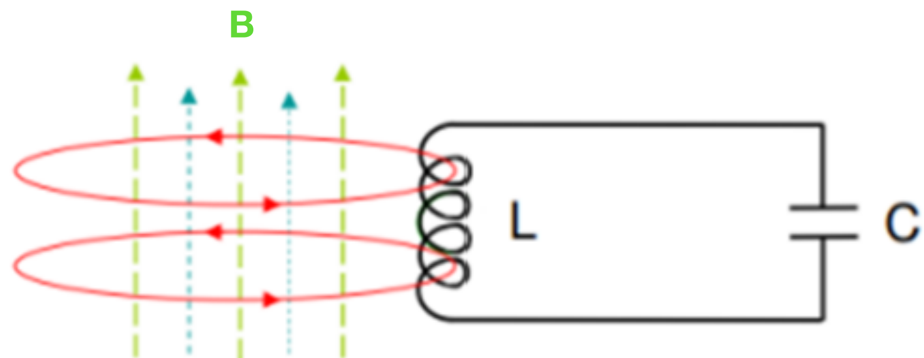

DM Radio science: axions

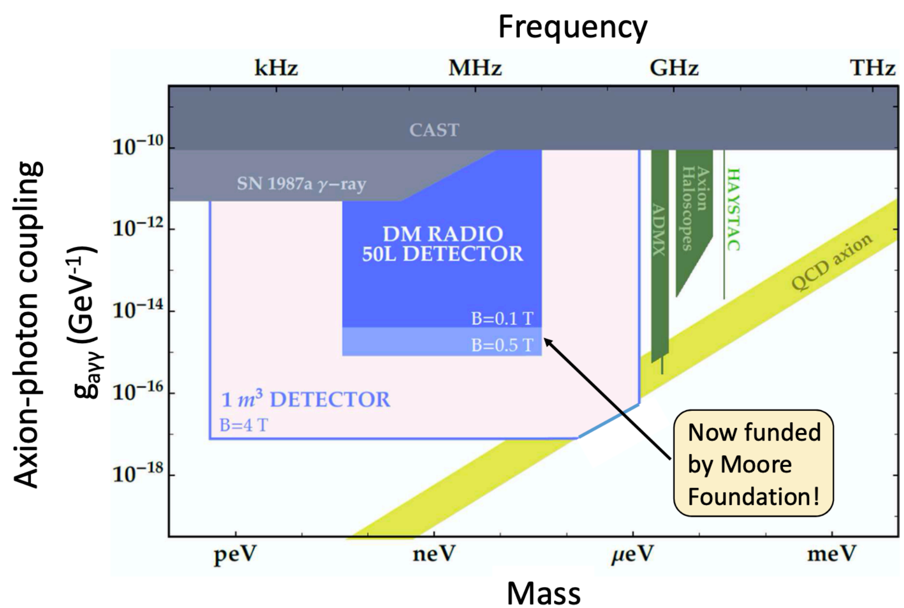

Assumptions: T=10 mK, Q=10^6, 3.5 year integration time, quantum-limited readout

Broadband Detection

- ABRACADABRA: no capacitor, **simultaneous scan of broad frequencies using SQUID**. [Y.Kahn, B. Safdi, J. Thaler 16']

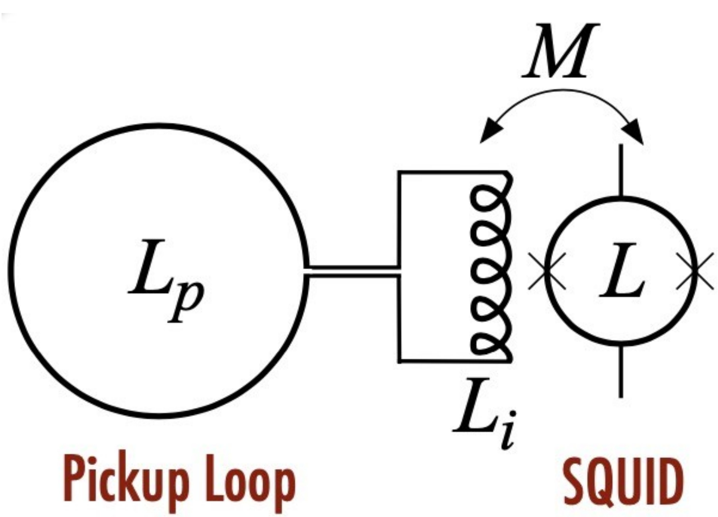

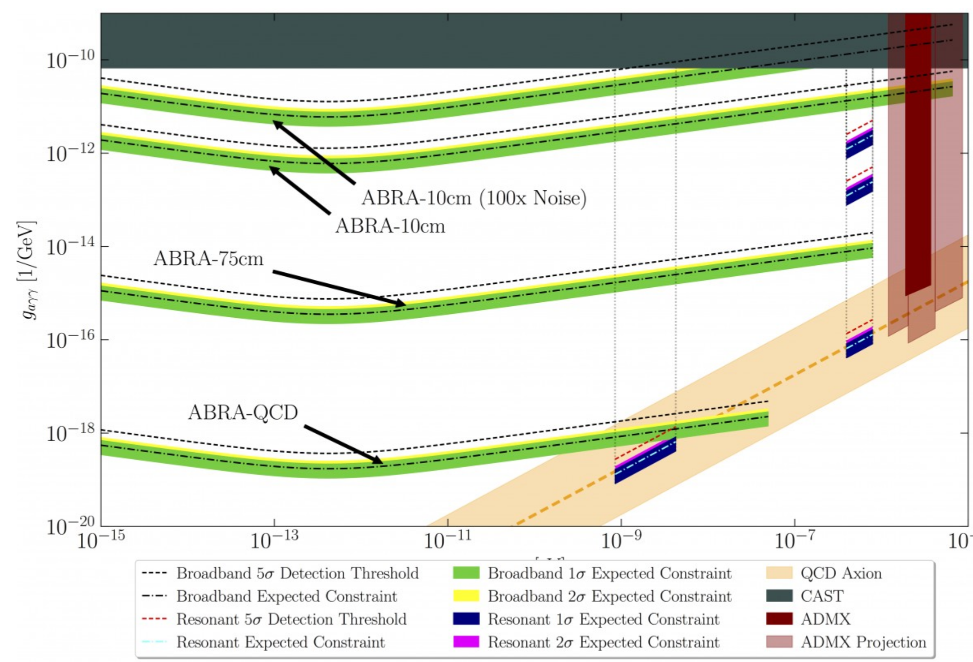

Higher Frequency Electromagnetic Resonant Detection

1 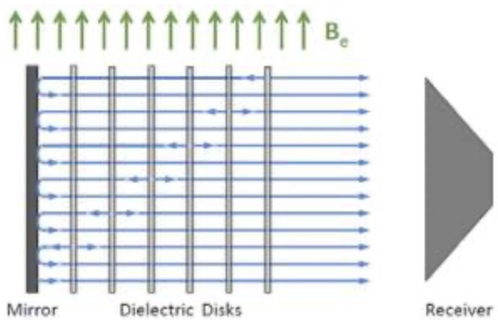

2 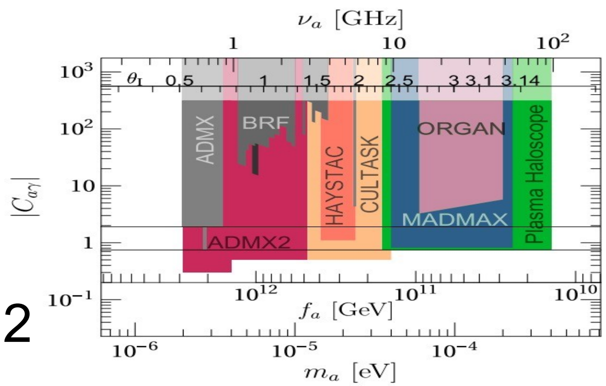

3 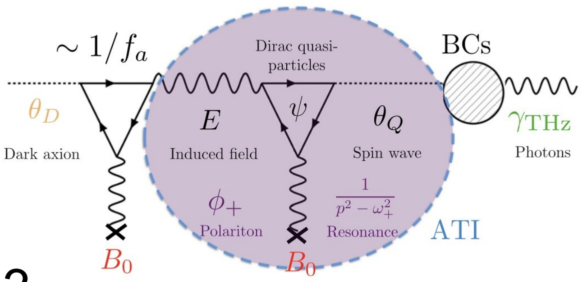

- 1 **Dielectric Haloscope**: discontinuity of E-field leads to coherent emission of photons from each surface, up to 50 GHz. [A.Caldwell et al 17']

- **2.Plasma Haloscope**: using tunable cryogenic plasma to match axion mass, up to 100 GHz. [M.Lawson et al 19']

- **3.Topological Insulator**: quasiparticle in it mixing with E field becomes polariton whose frequency can be tuned by magnetic field, up to THz. [D.J.E.Marsh et al 19']

Birefringent effect

Axion induced birefringent effect

$$\Box A_{\pm} = \pm 2 i g_{a\gamma} [\partial_z a \dot{A}_{\pm} - \dot{a} \partial_z A_{\pm}],$$

$$\omega_{\pm} \approx k \pm \tfrac{1}{2} g \left(\frac{\partial \varphi}{\partial t} + \nabla \varphi \cdot \frac{\boldsymbol{k}}{k} \right)$$

different phase velocities for +/- helicities

For linearly polarized photons

$$\begin{aligned} \Delta\Theta &= g_{a\gamma} \Delta a(t_{\rm obs}, \mathbf{x}_{\rm obs}; t_{\rm emit}, \mathbf{x}_{\rm emit}) \\ &= g_{a\gamma} \int_{\rm emit}^{\rm obs} ds\, n^{\mu}\, \partial_{\mu} a \\ &= g_{a\gamma} [a(t_{\rm obs}, \mathbf{x}_{\rm obs}) - a(t_{\rm emit}, \mathbf{x}_{\rm emit})], \end{aligned}$$

Measure the change of the position angle:

Requires polarimetric measurements

GW Interferometers and Birefringent Cavity

- Interferometer: using vertically polarized laser and measuring the horizontal component, resonant when baseline matches λ_c. [DeRocco, Hook 18']

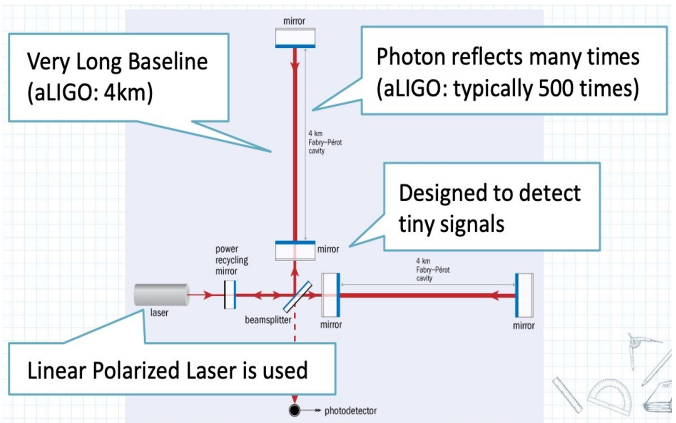

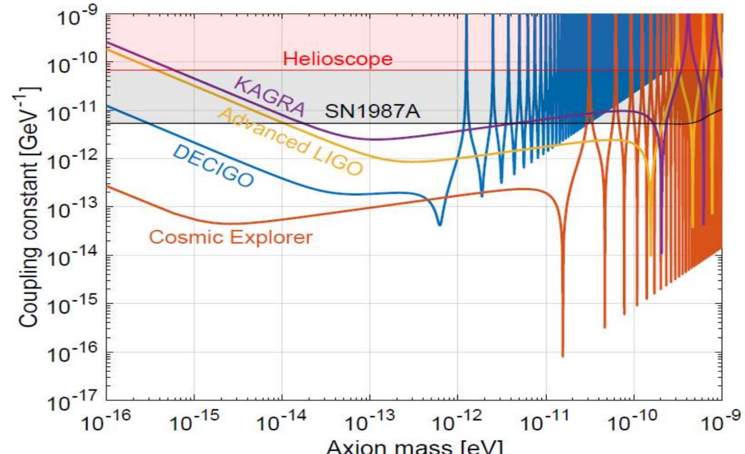

- Birefringent cavity: using mirror to accumulate the axion induced sideband. [Liu, Elwood et al 18']

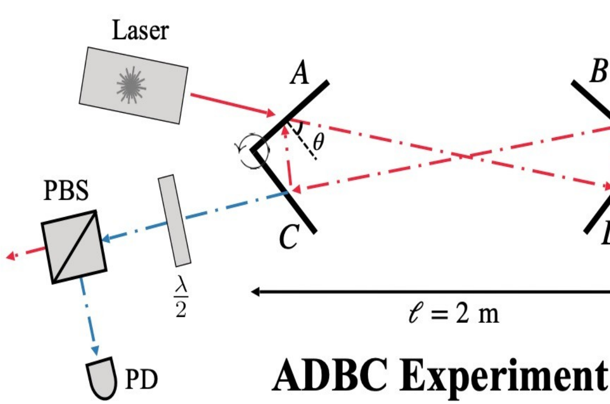

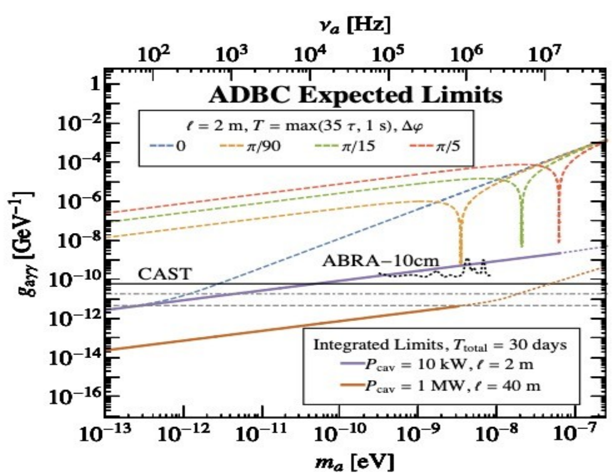

Light Shining Through Walls [Redondo, Ringwald 10']

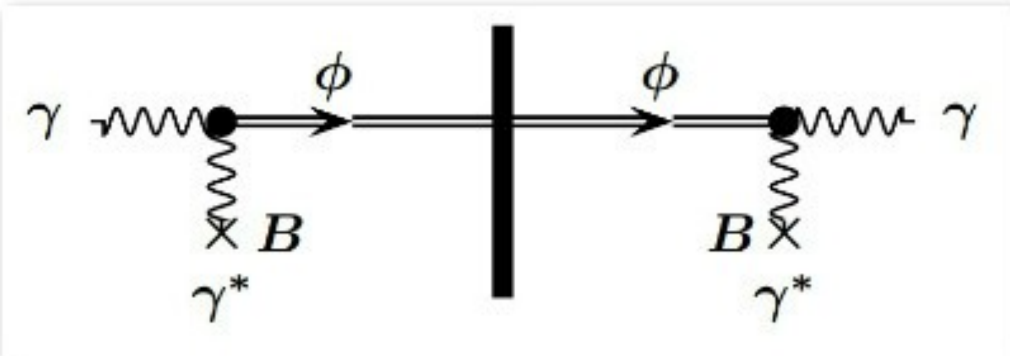

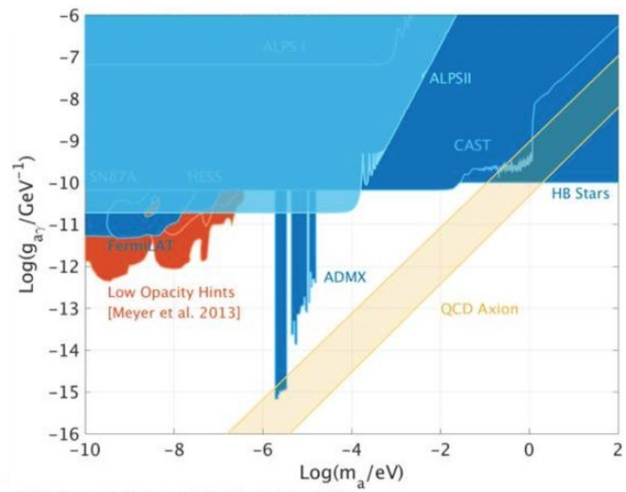

- Photons **convert into axions in B field, pass through a wall and convert back into photons.**

- Both optical and SRF cavity [Janish et al 19'].

- Not dependent on if axion is the major dark matter.

Nuclear Magnetic Resonance [Budker, Graham et al 13']

- **CASPEr Electric**: axion gluon coupling leads to oscillating EDM.
- **CASPEr-Wind:** axion nucleons coupling ~ **∇a · σ_N leads to precession of the spin, proportional to axion DM velocity (wind).**

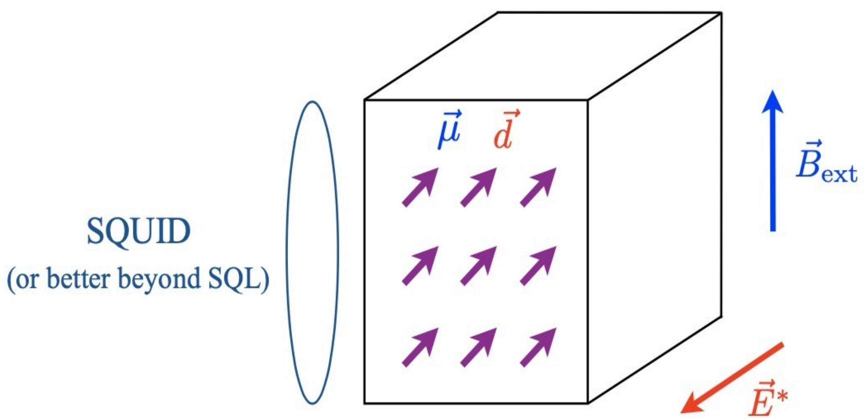

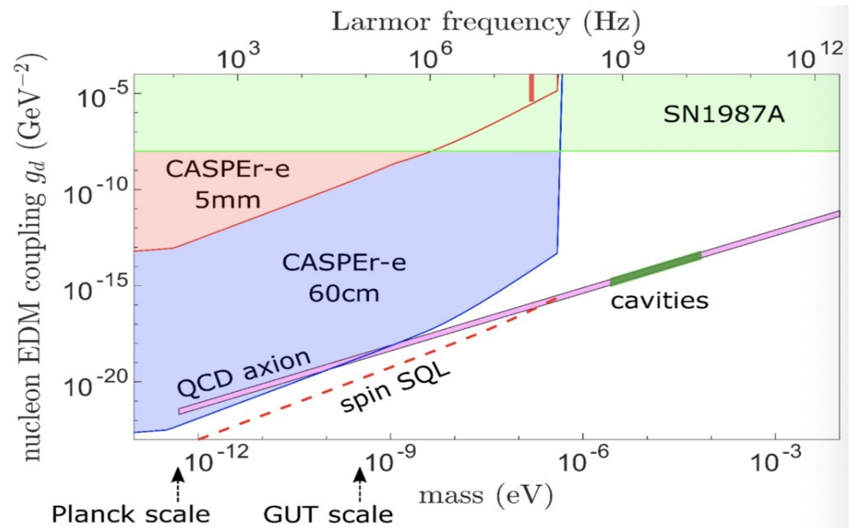

Larmor frequency $2\,\mu B_{ext} = m_a$ leads to NMR-like resonant enhancement.

Axion-Induced Fifth Force [Moody, Wilczek, 84']

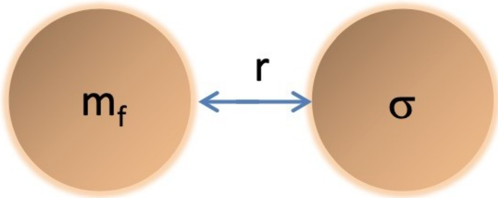

Monopole-Dipole axion exchange

Axion-mediated **monopole-dipole interaction** between nucleons:

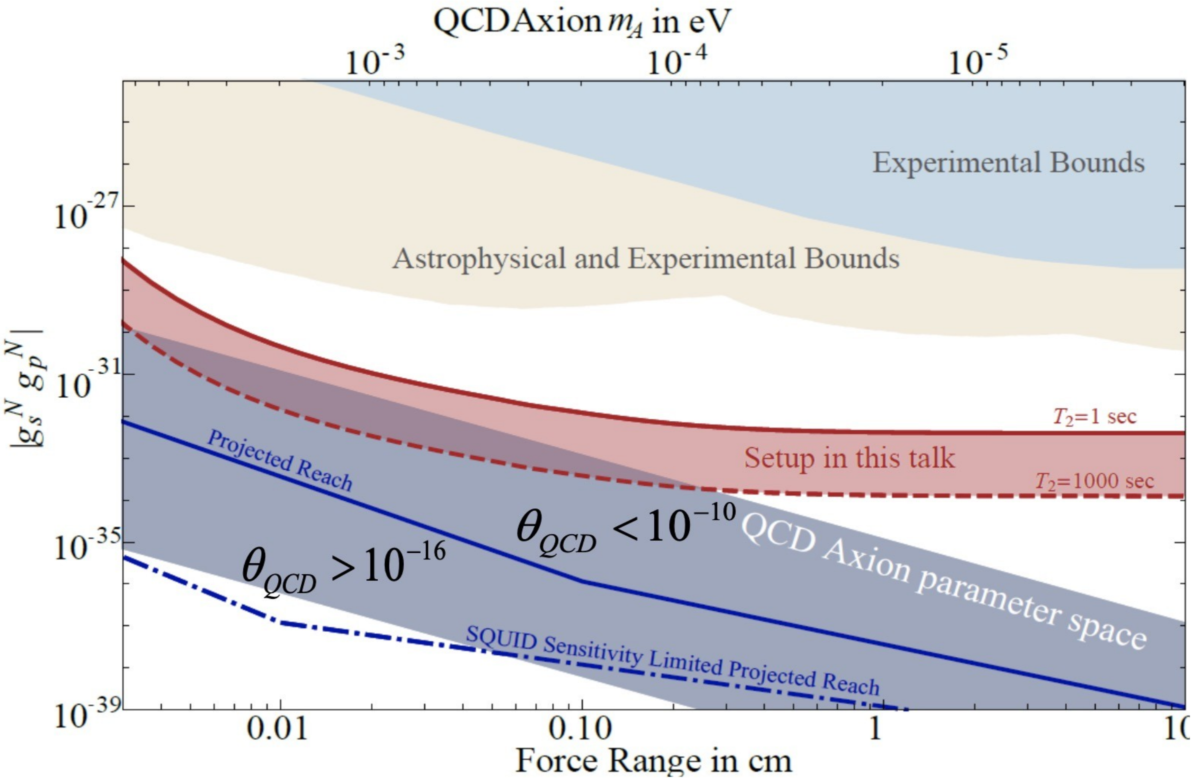

[ARIADNE 14']

Current DPDM search

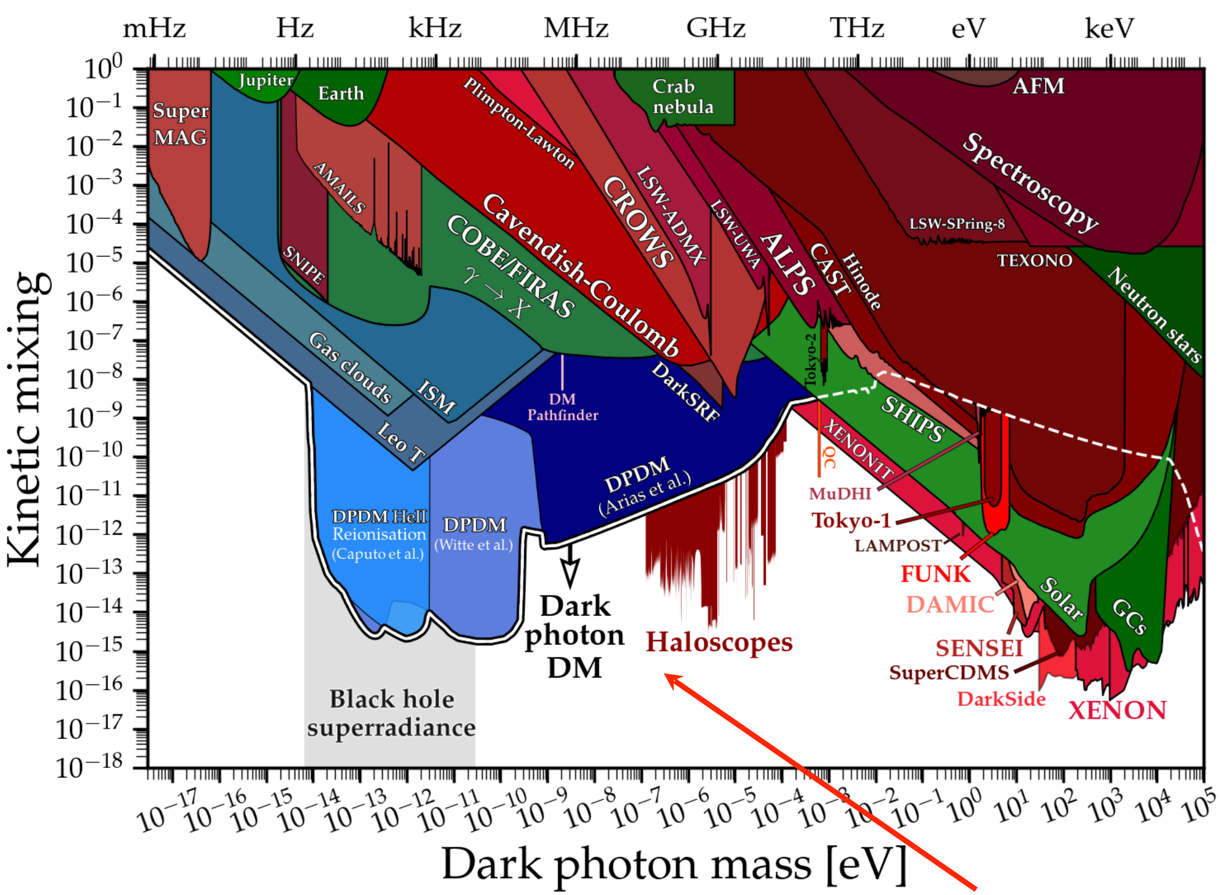

Still a lot of room to detect

Haloscope sensitivity largely depends on Q: Superconducting cavity has Q~10^{10}

how to make use it? 5 orders more than traditional cavity.

Axion limit webpage: https://github.com/cajohare/AxionLimits/blob/master/docs/dp.md

SRF search for DPDM (2022)

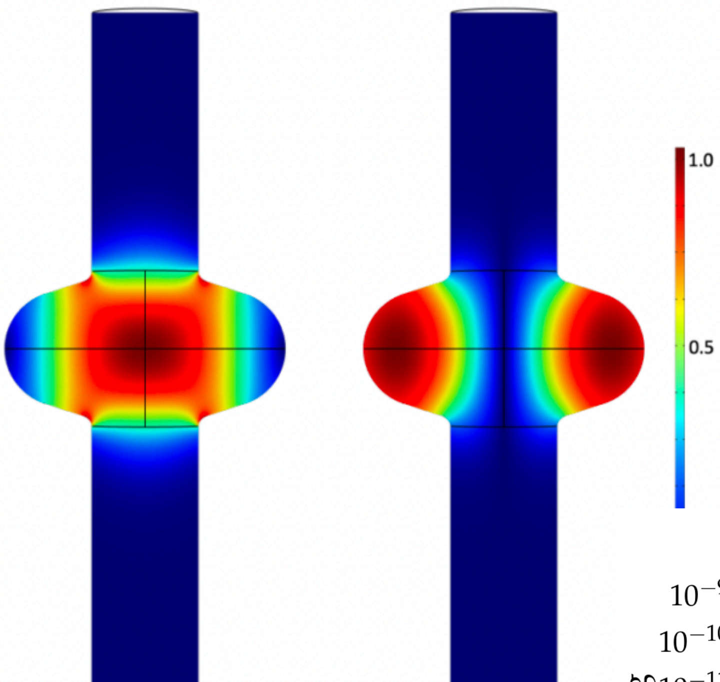

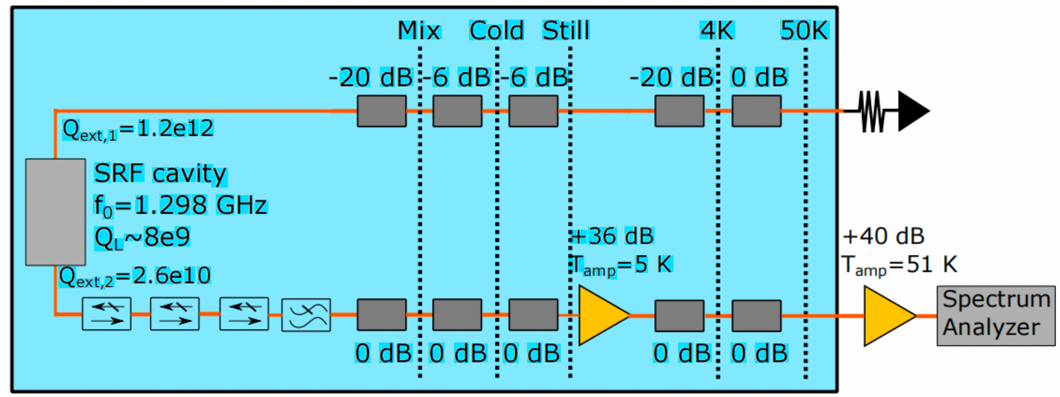

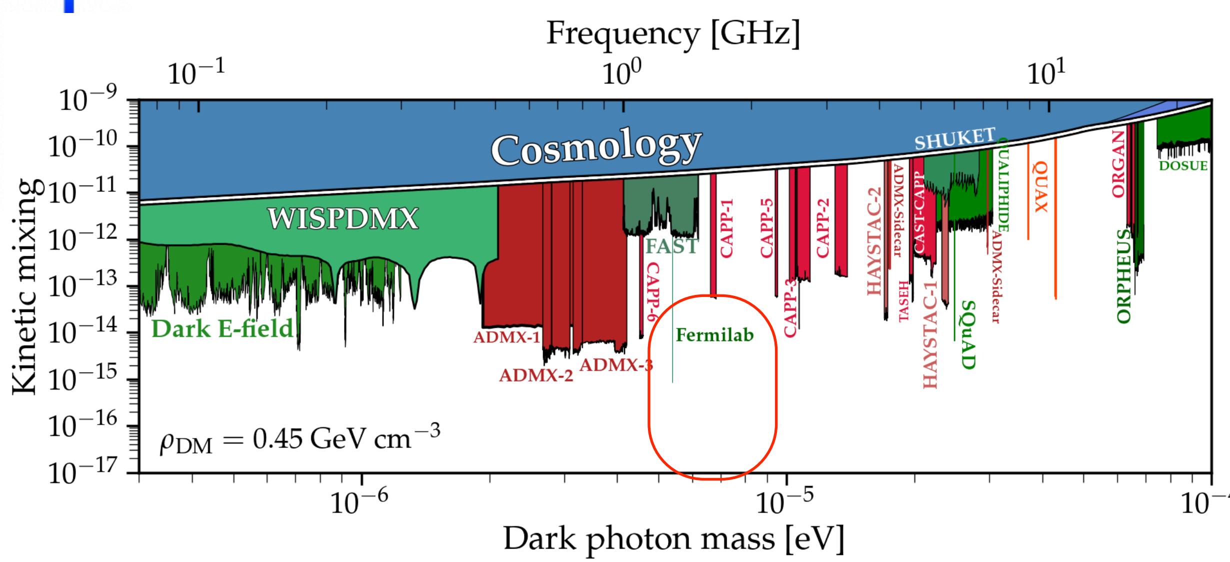

Highest sensitivity

Q~8.7*10^9

R. Cervantes,[1,*] C. Braggio,[2,3] B. Giaccone,[1] D. Frolov,[1] A. Grasselino,[1] R. Harnik,[1] O. Melnychuk,[1] R. Pilipenko,[1] S. Posen,[1] and A. Romanenko[1]

2203.03183

DPDM searches

Haloscope detail

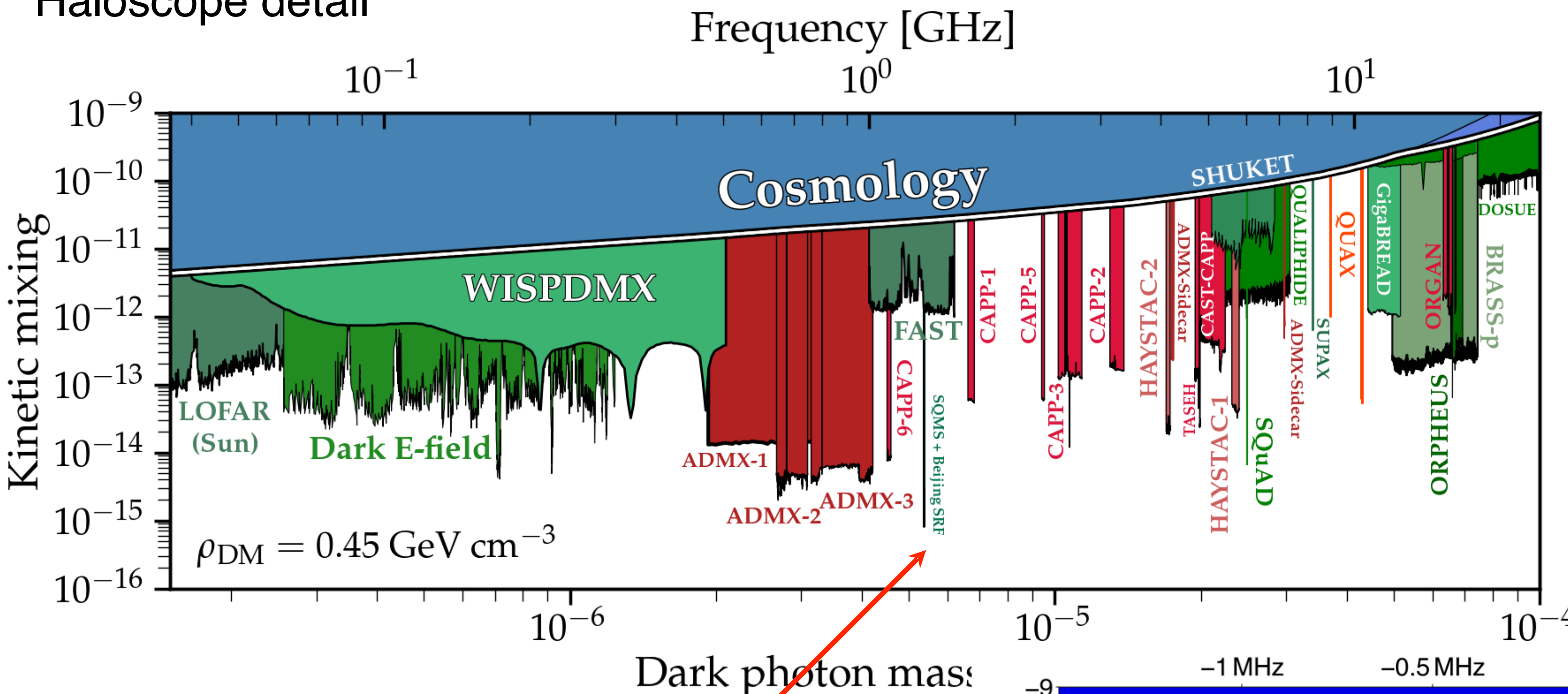

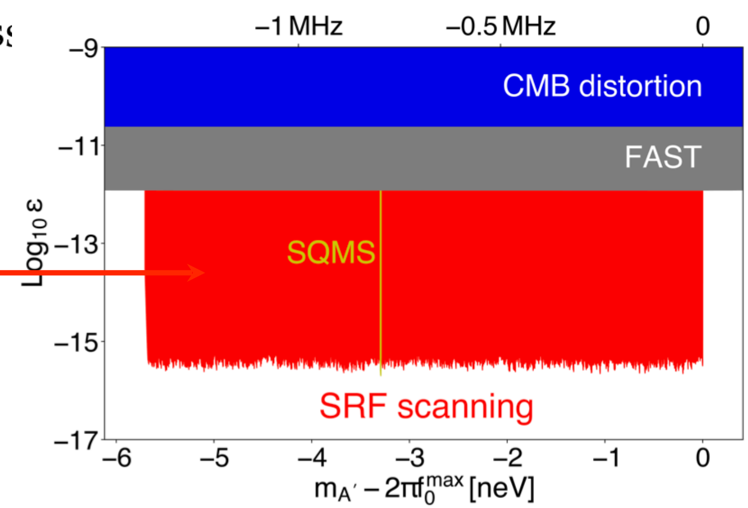

First tunable results with deepest exclusion limit

SHANHE collaboration,
arxiv: 2305.09711, (Accepted by PRL)

SHANHE collaboration

中国科学院高能物理研究所
Institute of High Energy Physics Chinese Academy of Sciences

supportive collaborations

中國科學院物理研究所
Institute of Physics, Chinese Academy of Sciences

北京量子信息科学研究院
Beijing Academy of Quantum Information Sciences

量子科学与工程研究院
Institute for Quantum Science and Engineering

Superconducting cavity for High-frequency gravitational wave, Axion, and other New particles in High energy physics.

Ph.D.: UChicago

Boya distinguished professor: PKU

Both theory and experimentalist

Looking for international collaboration
if people get interested

SRF Experimental facilities In PKU

Liquid helium system

2K pumping system

Vertical Dewar

Cavity suspension

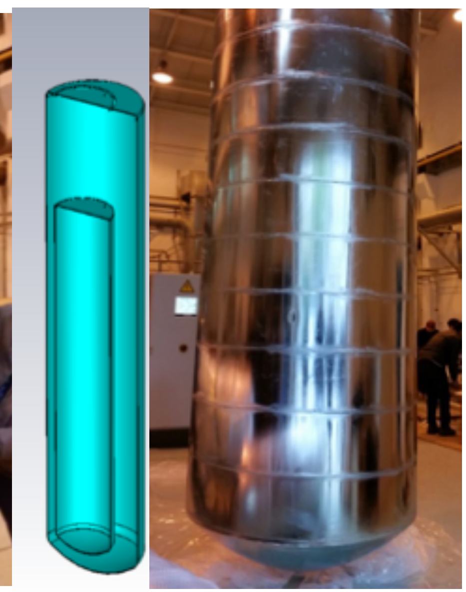

Magnetic shielding

- residual magnetism<10 mGs
- Static heat leak: < 1 W
- Cooling power: >200W@2K

SRF in IHEP

中国科学院高能物理研究所

Institute of High Energy Physics Chinese Academy of Sciences

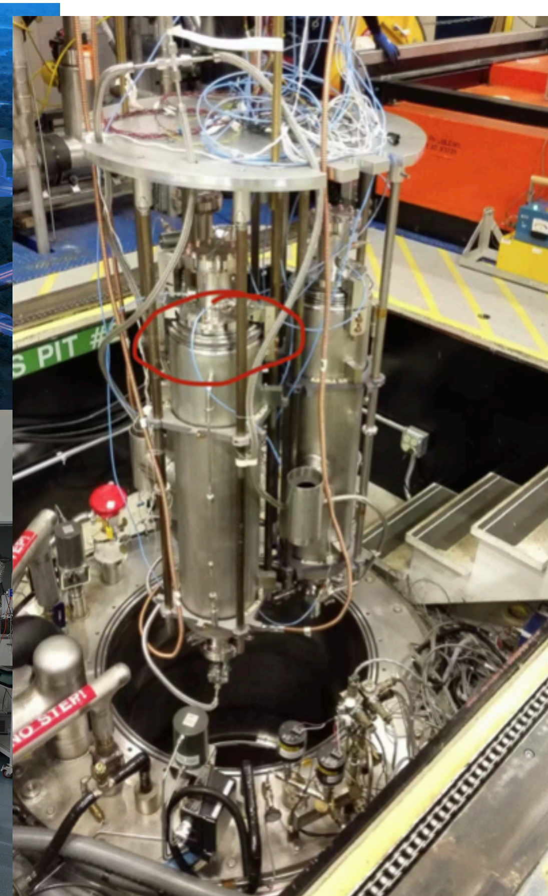

SRF used for Beijing & Shanghai Synchrotron Radiation Facility and future CEPC

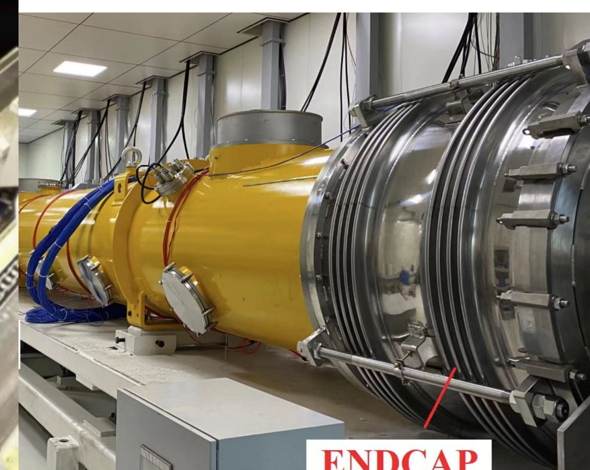

SRF with AC B field

Signal Mode: $\mathbf{E}_1$

Source: **a**
(almost monochromatic)

$$\sum_n \left(\partial_t^2 + \frac{\omega_n}{Q_n}\partial_t + \omega_n^2 \right) \mathbf{E}_n = g_{a\gamma\gamma}\partial_t(\mathbf{B}\partial_t a)$$

Pump Mode: $\mathbf{B}_0$

Static $\mathbf{B}_0$:

$$\omega_1 \simeq m_a \qquad \partial_t(\mathbf{B}) \simeq 0$$

$$\mathbf{E}_1 \sim \frac{m_a g_{a\gamma\gamma}\sqrt{\rho_{\mathrm{DM}}}\mathbf{B}}{m_a^2 - \omega_1^2 + i\frac{m_a \omega}{Q_1}}$$

Oscillating $\mathbf{B}_0$:

$$\omega_1 \simeq \omega_0 + m_a \qquad \partial_t(\mathbf{B}) \simeq i\omega_0\mathbf{B}$$

$$\mathbf{E}_1 \sim \frac{\omega_0 g_{a\gamma\gamma}\sqrt{\rho_{\mathrm{DM}}}\mathbf{B}}{(\omega_0 + m_a)^2 - \omega_1^2 + i\frac{(\omega_0 + m_a)\omega}{Q_1}}$$

Signal enhancement at low frequency $m_a << \omega_0$

A.Berlin, R.T. D'Agnolo, et al, JHEP07(2020)no.07, 088.

SRF with AC B field

Signal Mode: $\mathbf{E}_1$

Source: **a**
(almost monochromatic)

$$\sum_n \left(\partial_t^2 + \frac{\omega_n}{Q_n}\partial_t + \omega_n^2\right)\mathbf{E}_n = g_{a\gamma\gamma}\partial_t(\mathbf{B}\partial_t a)$$

Pump Mode: $\mathbf{B}_0$

Oscillating $\mathbf{B}_0$:

$$\omega_1 \simeq \omega_0 + m_a \qquad \partial_t(\mathbf{B}) \simeq i\omega_0\mathbf{B}$$

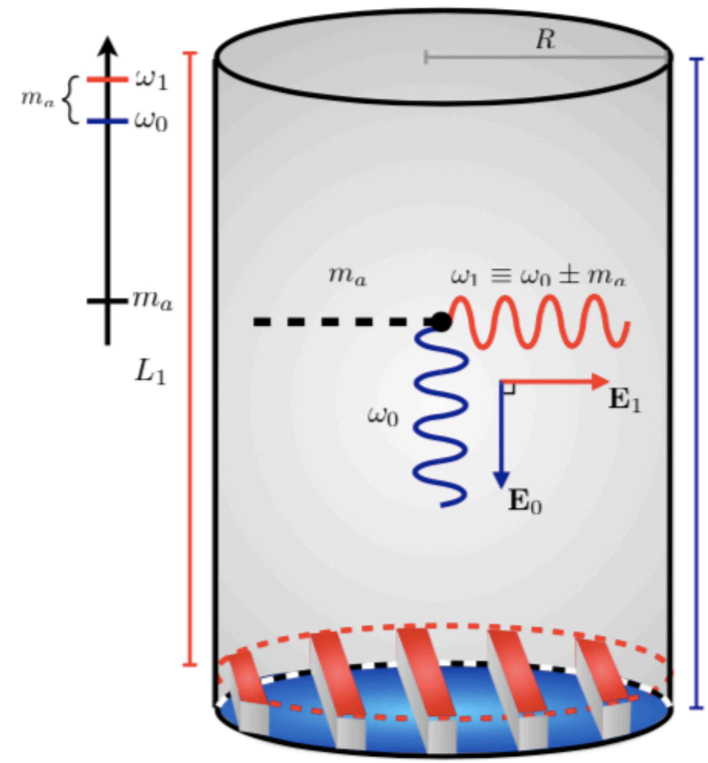

Scanning the axion mass by tuning the differences between two quasi-degenerate modes

A.Berlin, R.T. D'Agnolo, et al, JHEP07(2020)no.07, 088.

SRF with AC B field

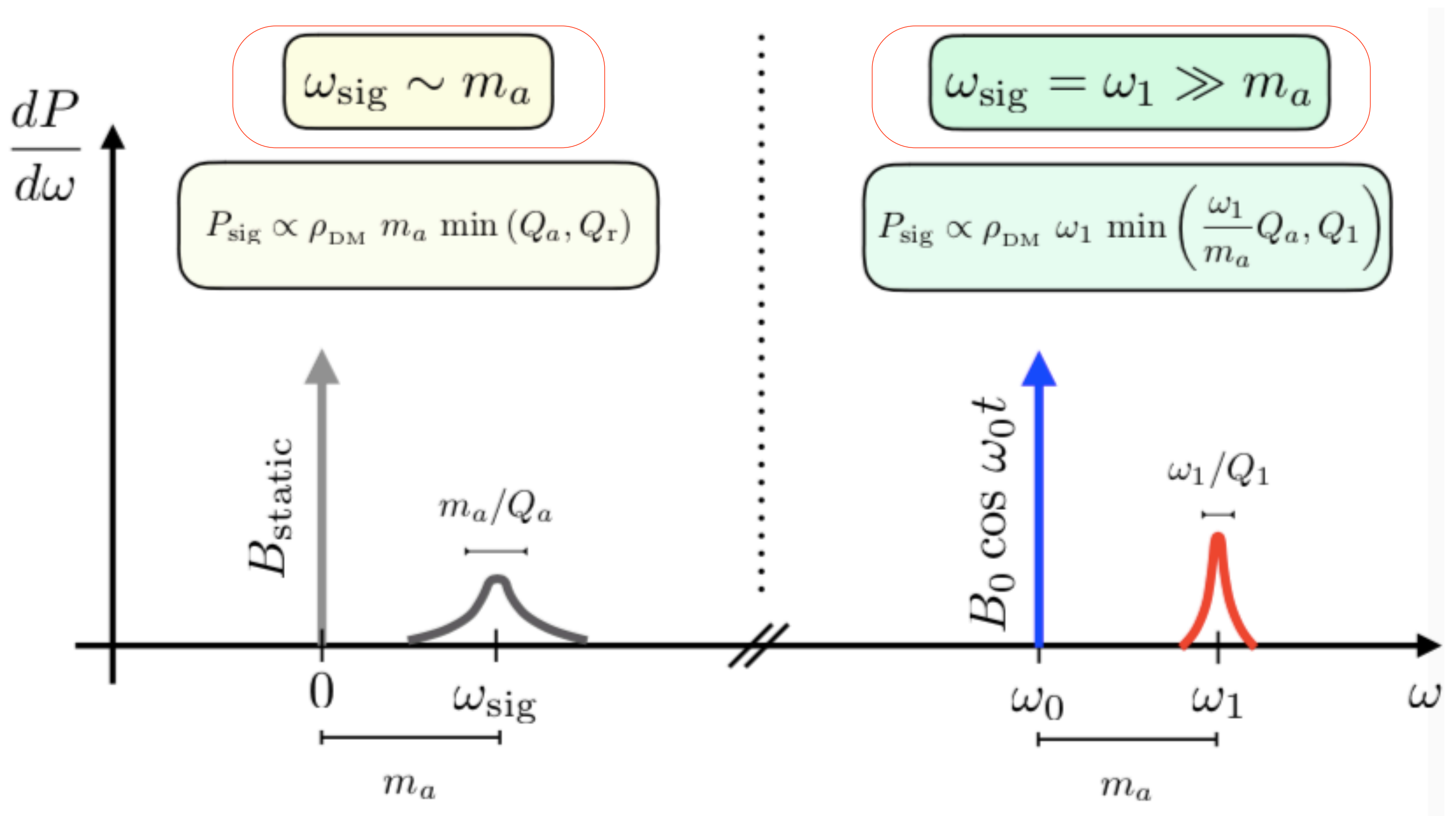

Main differences: signal power

$$P_{\rm sig}^{(\rm r)} \sim \frac{\mathcal{E}_a^2}{R} \min\left(1, \frac{\tau_a}{\tau_{\rm r}}\right) \sim \omega_{\rm sig}^2\, B_a^2 V \min(Q_{\rm r}/\omega_{\rm sig}, Q_a/m_a)$$

A.Berlin, R.T. D'Agnolo, et al, JHEP07(2020)no.07, 088.

Axion Dark Matter Detection Using SRF

Hard to scan for a broad mass window in traditional cavity!

$\omega_1 \simeq m_a \qquad \partial_t(\mathbf{B}) \simeq 0$

narrow mass window due to size of the cavity

$\omega_1 \simeq \omega_0 + m_a \qquad \partial_t(\mathbf{B}) \simeq i\omega_0 \mathbf{B}$

The AC magnetic field inside the SRF and two nearly degenerate modes enable the scan of axion mass from the frequency splitting.

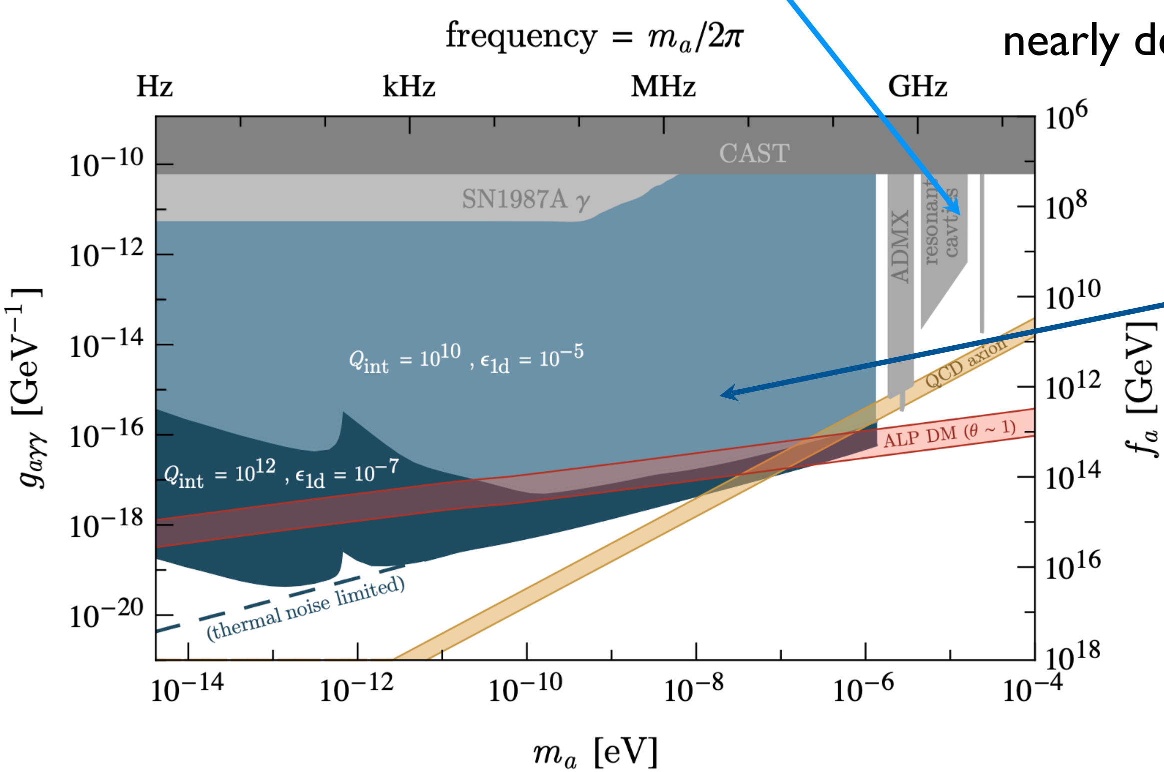

Much broader detection mass window at lower frequency.

Only gray region is excluded. Large unexplored parameter space!

A.Berlin, R.T. D'Agnolo, et al, JHEP07(2020)no.07, 088.

ULDM： Quantum Detection Schemes

Traditional resonant cavity detection suffers that DM mass must match the cavity's resonant frequency, depending on the cavity size.

$\omega_1 \simeq m_a \qquad \partial_t(\mathbf{B}) \simeq 0$

$\omega_1 \simeq \omega_0 + m_a \qquad \partial_t(\mathbf{B}) \simeq i\omega_0 \mathbf{B}$

Cavities cannot be very large or very small, leading to a narrow detection range.

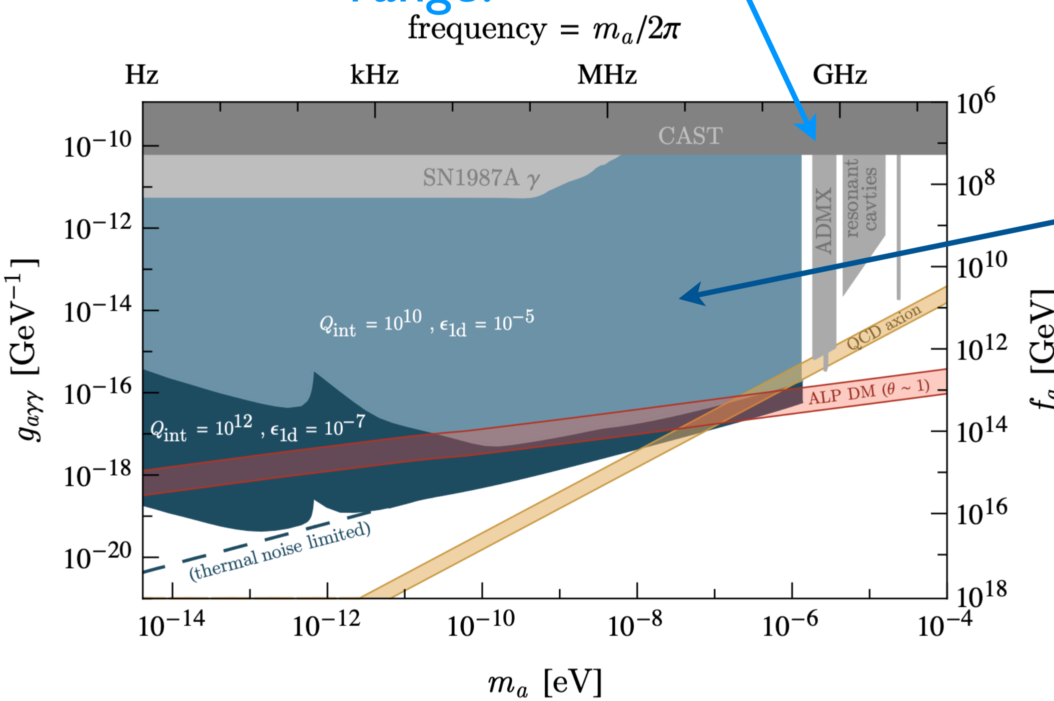

The alternating magnetic field in a superconducting cavity means DM mass depends on the frequency difference.

With the quasi-degenerate energy levels superconducting cavity, the DM mass range is much broader in the lighter region.

The gray area represents the already detected regions, with nearly no current detection!

Broadband case

For ultra-light axion, $\omega_1 = \omega_0 + m_a \simeq \omega_0$

Two degenerate and transverse modes can reach the ultra-light region!

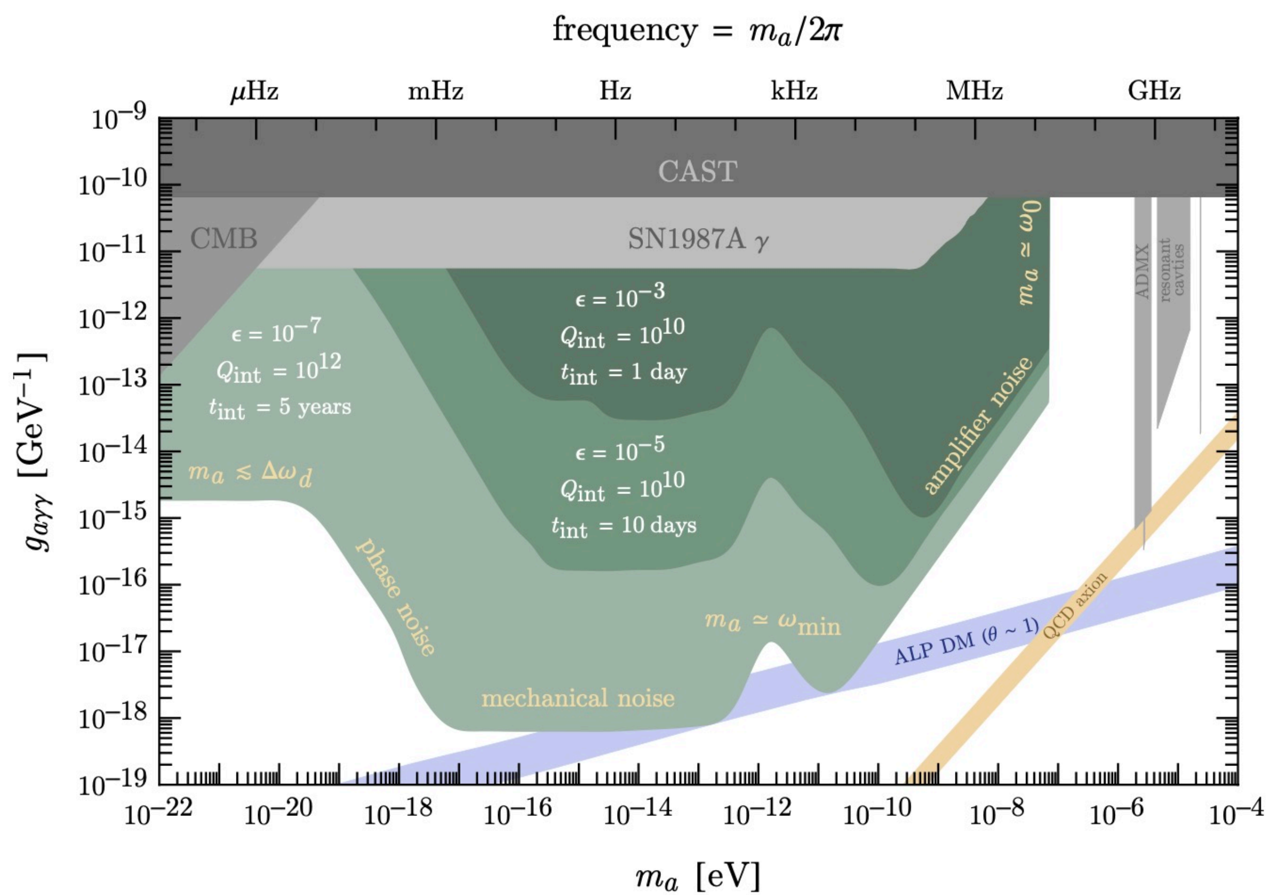

A.Berlin, R.T. D'Agnolo, et al, [arXiv:2007.15656 [hep-ph]].

Under preparation

TDR like

Fermilab

arXiv:2207.11346

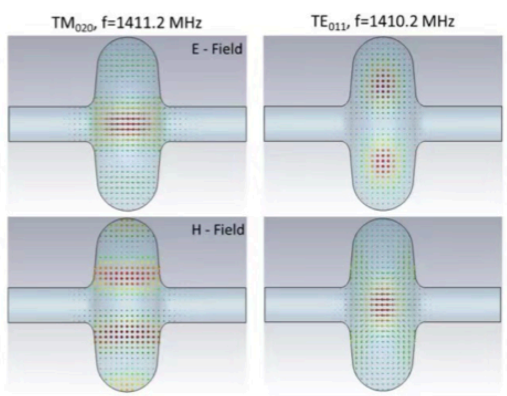

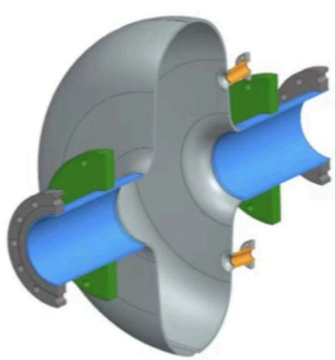

SHANHE collaboration

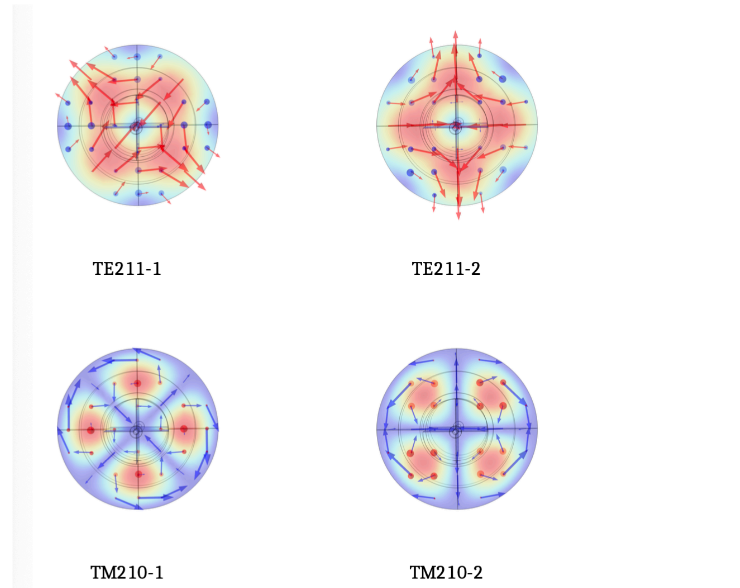

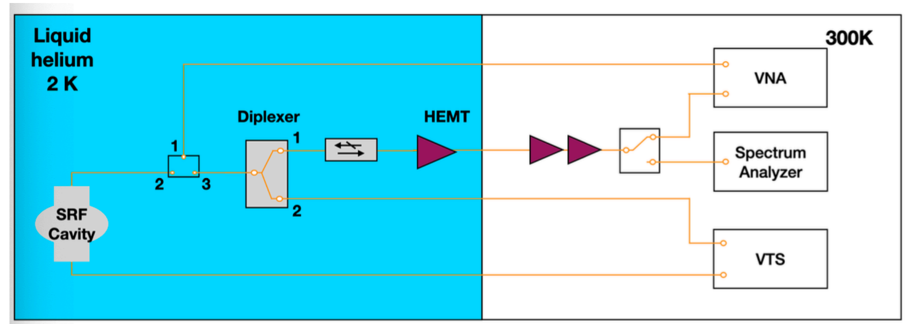

Will be operating this summer

Other searches using SRF

- **Fermilab SQMS**

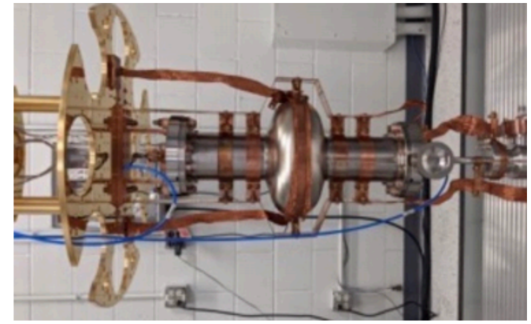

•SERAPH:
Single-bin search and ongoing scan

•Dark SRF:
Light-shining-wall search for dark photon.

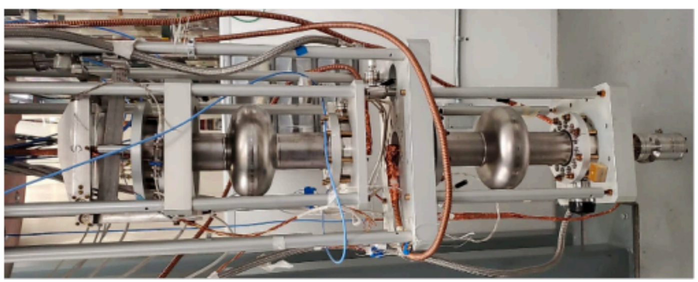

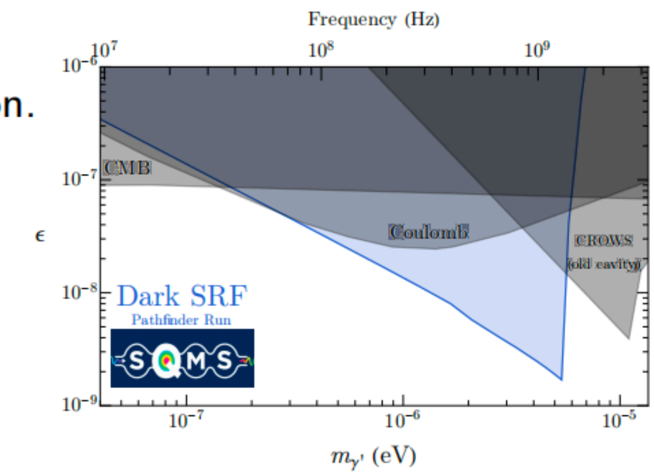

- **DESY**:

•MAGO 2.0
Mode transition from GW-induced cavity deformation.

Clever test of wave-like DM (beyond SQL?)

Targeting higher axion masses predicted in cosmological scenarios with *high energy scale* cosmic inflation

These simple inflation models also produce detectable primordial B-mode polarization patterns in the cosmic microwave background – science target for CMB-S4.

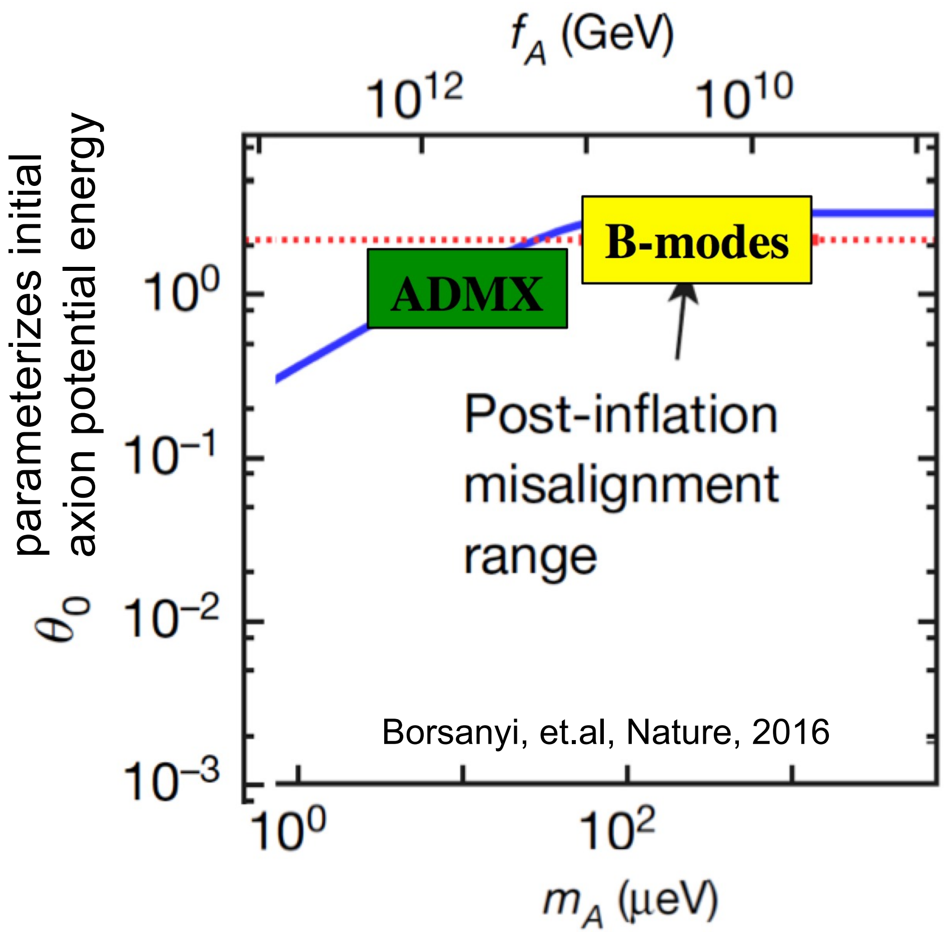

Higher axion mass allows early release of QCD vacuum energy. Avoids overproduction of dark matter.

What prevents us from immediately going to higher frequencies?

The predicted axion DM signal/noise ratio plummets as the axion mass increases → SQL readout is not scalable.

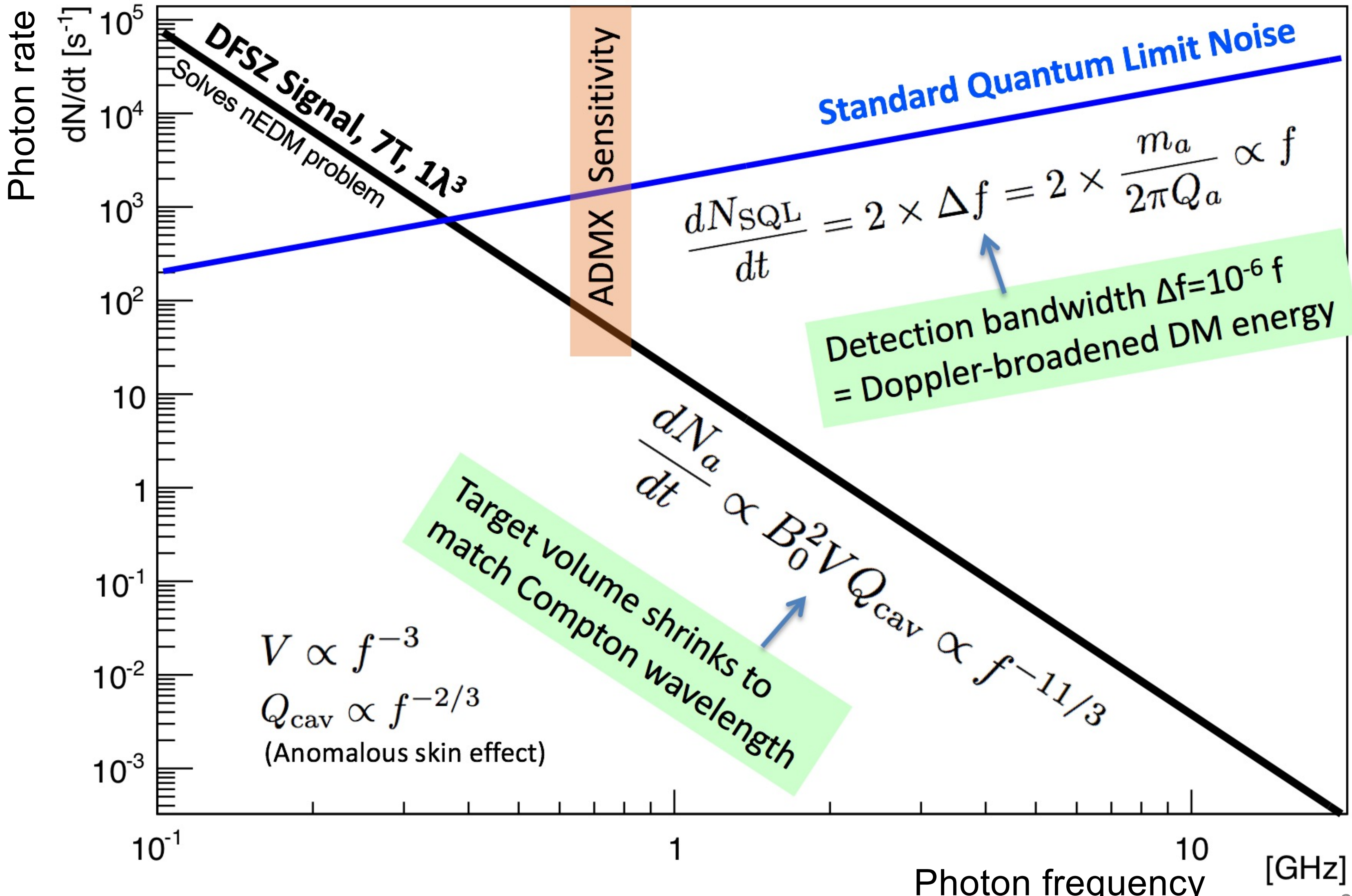

Aaron S. Chou, QSFP lecture 2021

Heisenberg uncertainty principle
= quantization of (internal) phase space area

Wigner pseudo-probability distributions for the endpoint of the phasor:

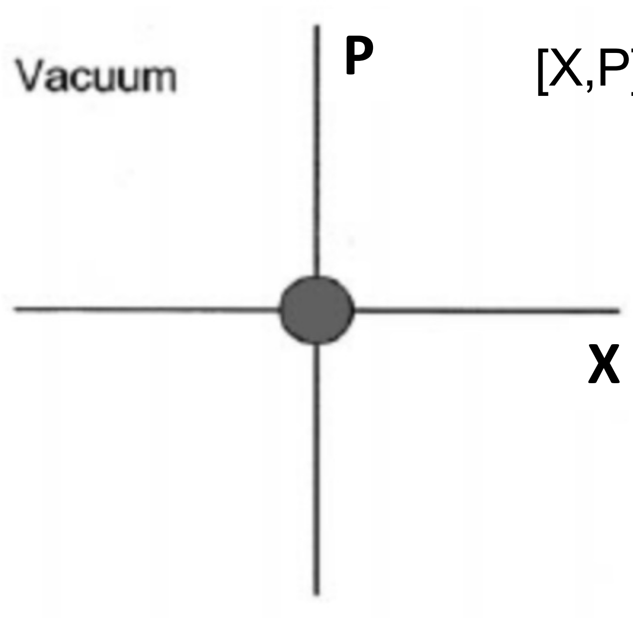

$[X,P]=i$ so $\Delta X \cdot \Delta P = \frac{1}{2}$

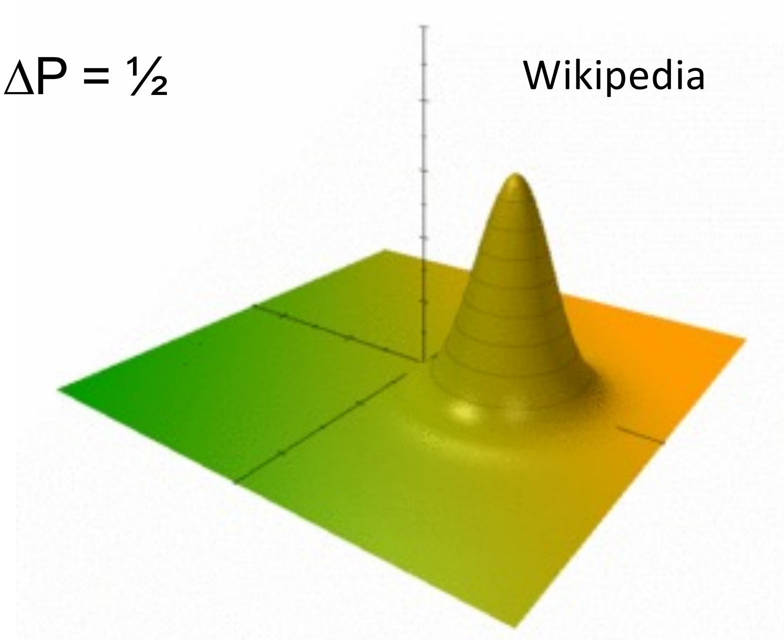

The vacuum state of the oscillator is a zero length phasor which still exhibits **zero-point noise**.

Sine wave with quantum uncertainty included. The Gaussian width in the radial direction manifests as Poisson **shot noise**.

In polar coordinates, Heisenberg becomes number-phase uncertainty: $\Delta N \times \Delta \varphi \geq \frac{1}{2}$

Lecture 2 review:

Creation/annihilation operators are just translation operators in phase space

$$p = i\frac{d}{dx}$$

Generates translations in position

$$x = i\frac{d}{dp}$$

Generates translations in momentum

$$a^\dagger = x + ip$$
$$a = x - ip$$

Generate translations in an arbitrary direction in x-p phase space

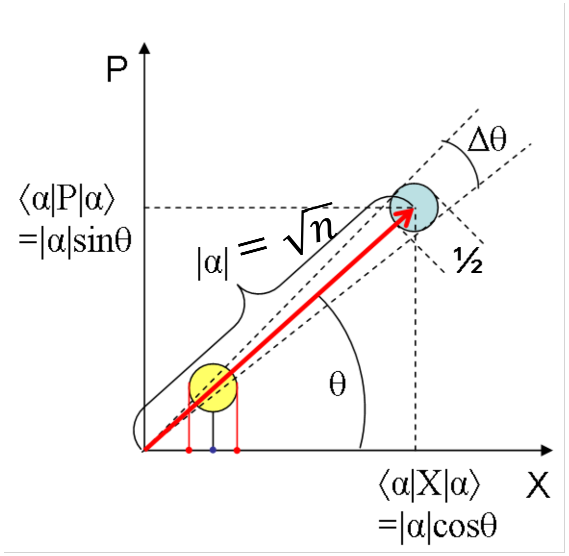

Exponentiate differential operator to get finite translation α in complex plane:

$$\hat{D}(\alpha) = \exp\left(\alpha\hat{a}^\dagger - \alpha^*\hat{a}\right)$$

Phasor of amplitude α is generated as:

$$D(\alpha)\,|0\rangle = |\alpha\rangle$$

"Coherent state" describing a classical sine wave

Lecture 2 review:

Classical sine waves have intrinsic Poisson noise

Coherent states form a Poisson distribution in the number state basis:

$$|\alpha\rangle = e^{-\frac{|\alpha|^2}{2}} e^{\alpha \hat{a}^\dagger} |0\rangle = e^{-\frac{|\alpha|^2}{2}} \sum_{n=0}^{\infty} \frac{\alpha^n}{\sqrt{n!}} |n\rangle$$

$$P(n) = |\langle n|\alpha\rangle|^2 = e^{-\langle n\rangle} \frac{\langle n\rangle^n}{n!}$$

$$\langle n\rangle = \langle \hat{a}^\dagger \hat{a}\rangle = |\alpha|^2$$

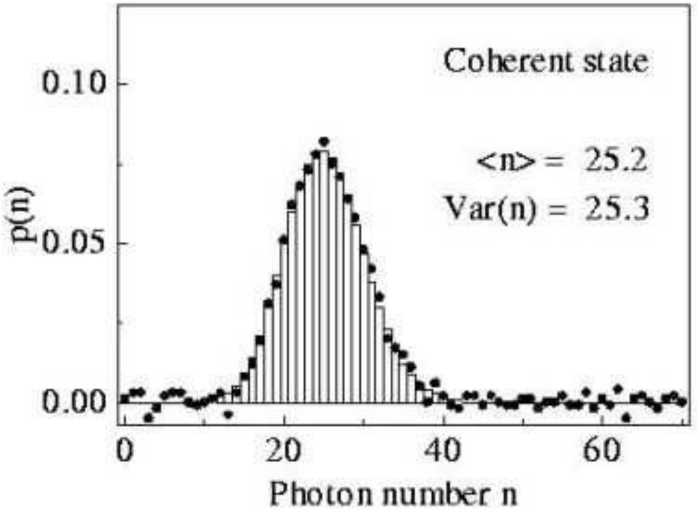

Like the zero-point fluctuations, the Poisson shot noise in classical wave intensity is a consequence of the Heisenberg uncertainty principle.

Lecture 2 review:

The resolution of a probe to displacement signals is given by its phase space distribution

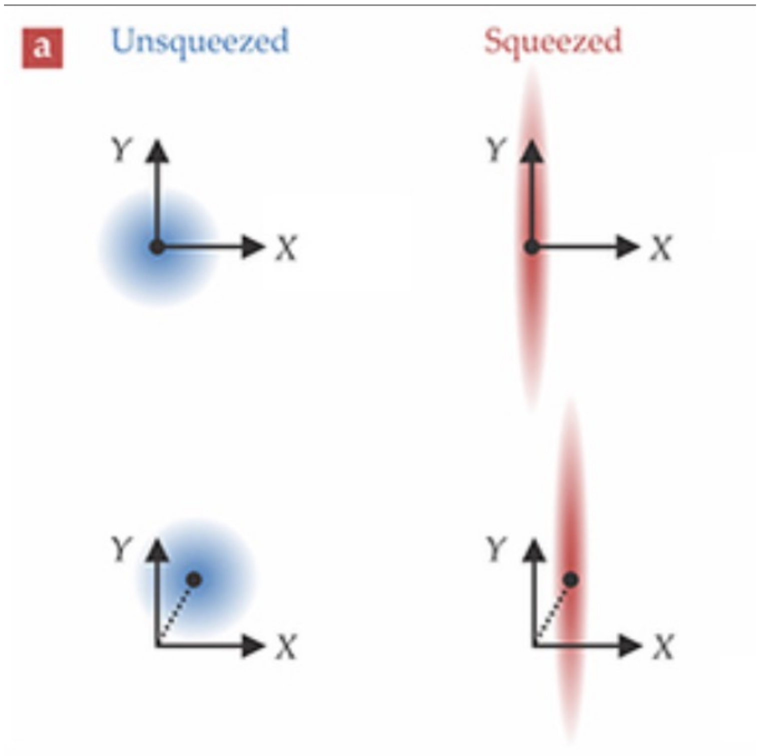

Amplifiers = scattering process via nonlinear 4-*wave mixing*

Ex. Josephson Traveling Wave Parametric Amplifier uses Josephson waveguide

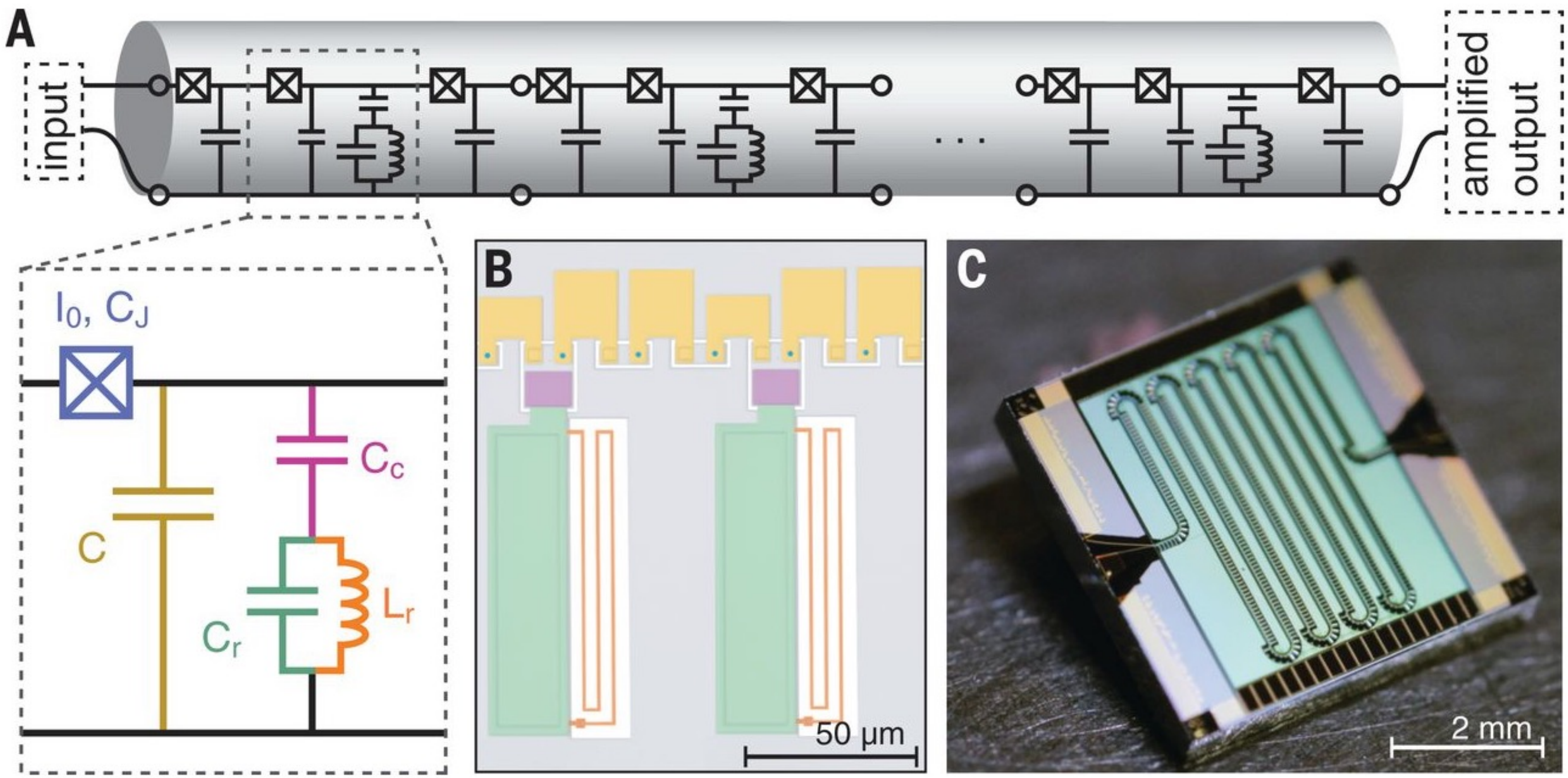

When signal and idler frequencies coincide → noiseless single quadrature amplification → squeezed states.

Inject squeezed vacuum state into the open port of the cavity.

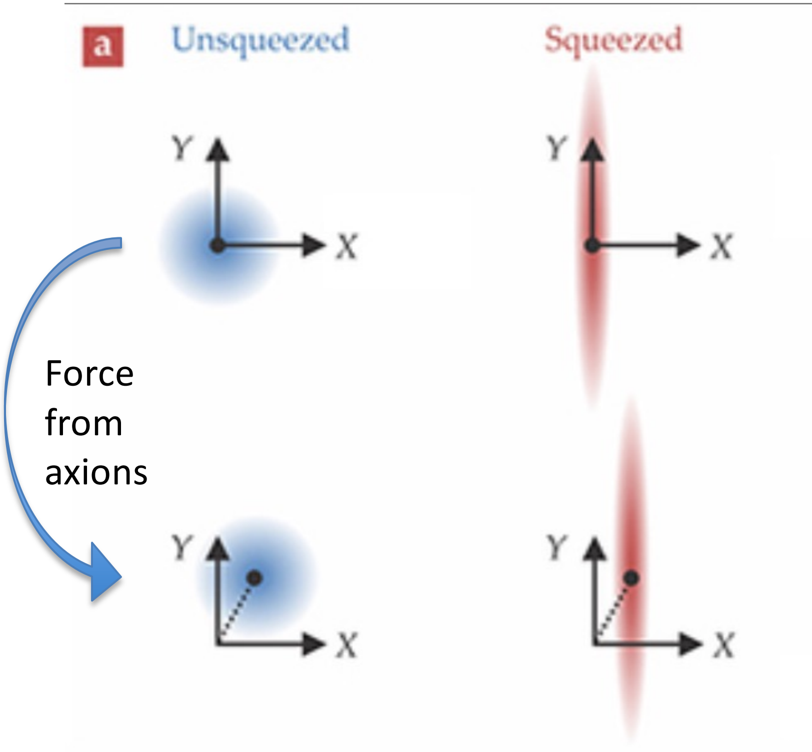

HAYSTAC Collaboration, Nature 590 (2021)

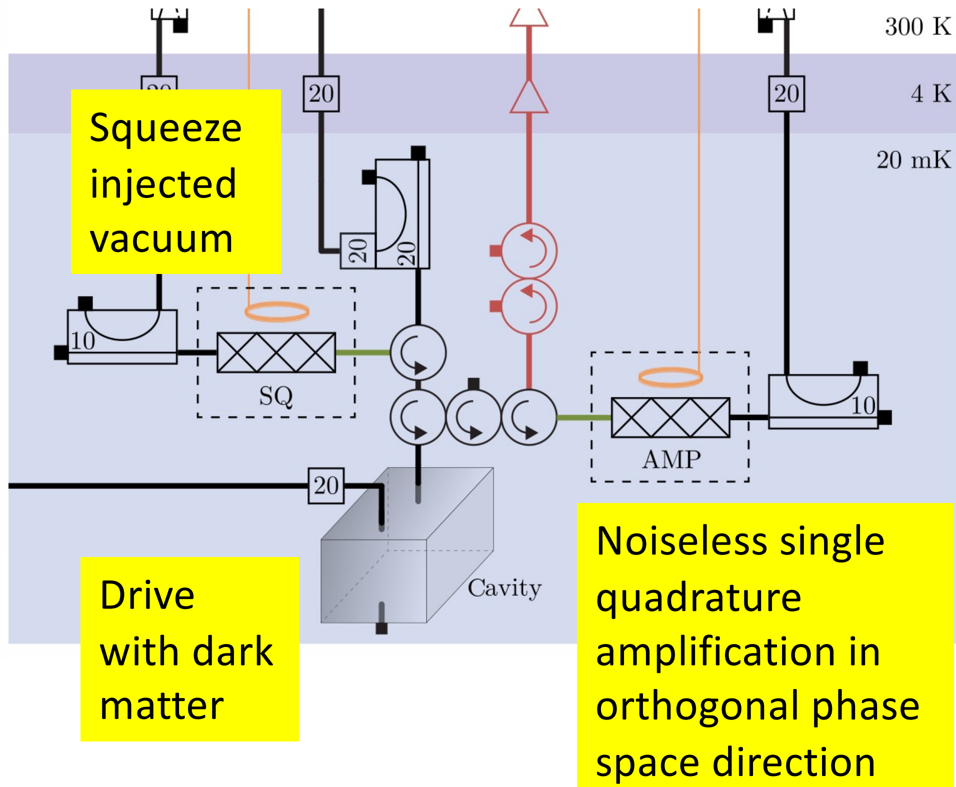

Again, think of the phase space distribution of the probe as its resolution function.

Quantum Noise Limit for EM Resonant Detection

- **Standard quantum limit for power law detection**:
  [Chaudhuri, Irwin, Graham, Mardon 18']

Noise PSD: resonant intrinsic noise $S_{\rm int}$ + flat readout noise $S_{\rm r}$.

- Sensitivity to $S_{\rm sig}$ and $S_{\rm int}$ is the same.

  SNR^2 ∝ range where $S_{\rm int}$ dominates over $S_{\rm r}$.

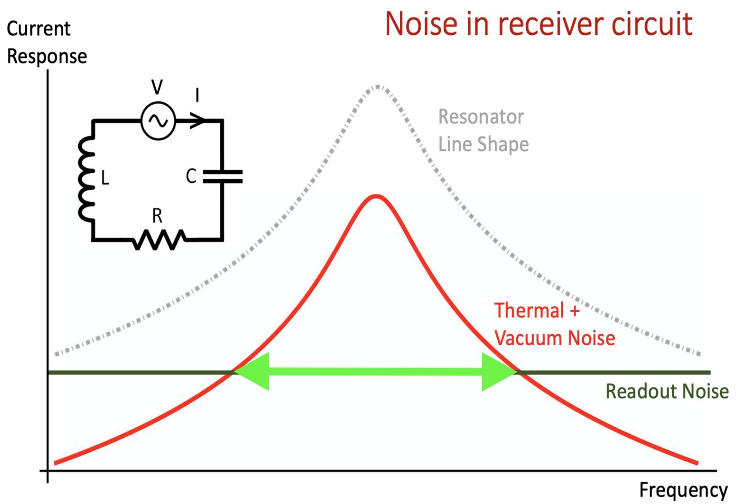

$S_{\rm int}$ ∝ Cauchy distribution

- **Beyond quantum limit**:

  Squeezing $S_{\rm r}$, e.g., HAYSTACK.

Increasing the sensitivity to $S_{\rm sig}$, e.g., white light cavity in optomechanics/GW detection [Miao, Ma, Zhao, Chen 15'].

PT-symmetric haloscope

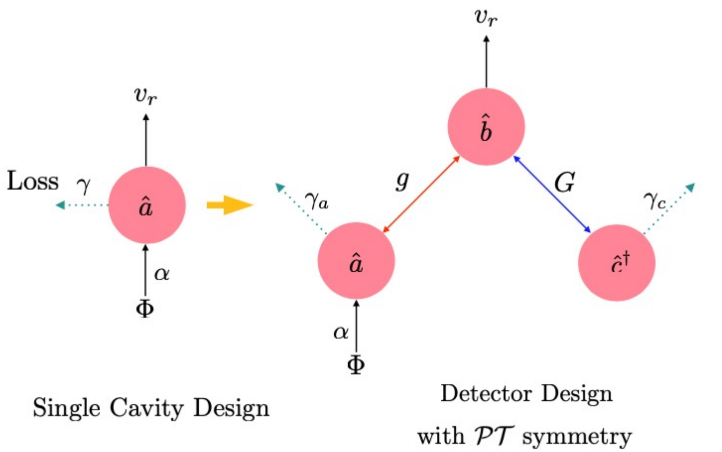

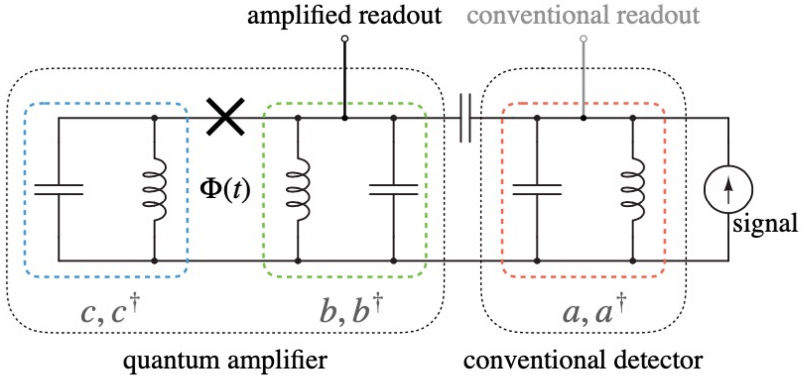

Probing mode: $\hbar\alpha(\hat{a} + \hat{a}^\dagger)\Phi$

- **Beam-splitting**: $\hbar g(\hat{a}\hat{b}^\dagger + \hat{a}^\dagger\hat{b})$.
- **Non-degenerate parametric interaction**: $\hbar G(\hat{b}\hat{c} + \hat{b}^\dagger\hat{c}^\dagger)$.
- **$\mathcal{PT}$-symmetry ($\hat{a} \leftrightarrow \hat{c}^\dagger$) emerges** when $g = G$.

$$\begin{aligned} (\dot{\hat{a}} + \dot{\hat{c}}^\dagger) &= -i(g - G)\hat{b} - i\alpha\Phi + \cdots ; \\ \dot{\hat{b}} &= -\gamma_r\hat{b} - ig(\hat{a} + \hat{c}^\dagger) + \cdots . \end{aligned}$$

- Coherent cancellation leads to **double resonance**.
  $S_{\rm sig}$ is largely enhanced when $g \gg$ **intrinsic dissipation** γ:

$$S_{\rm sig}^{\rm WLC}(\Omega) = \frac{2\gamma_r\alpha^2 S_\Phi(\Omega)}{(\gamma + \gamma_r)^2 + \Omega^2}\left(\frac{g^2}{\gamma^2 + \Omega^2}\right).$$

Readout coupling γ_r

Sensitivity and Physics Reach

- Optimized $\text{SNR}^2[\gamma_r, g - G] \propto$ range where S_{int} dominates over S_r $\propto 2^n \left(\frac{g}{\gamma n_{\text{occ}}}\right)^{\frac{2n}{2n+1}}$, where $g/\gamma \to Q_{\text{int}}$.

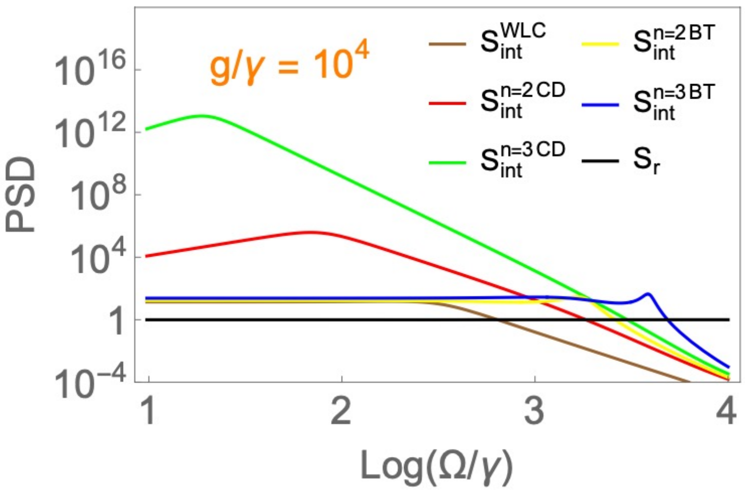

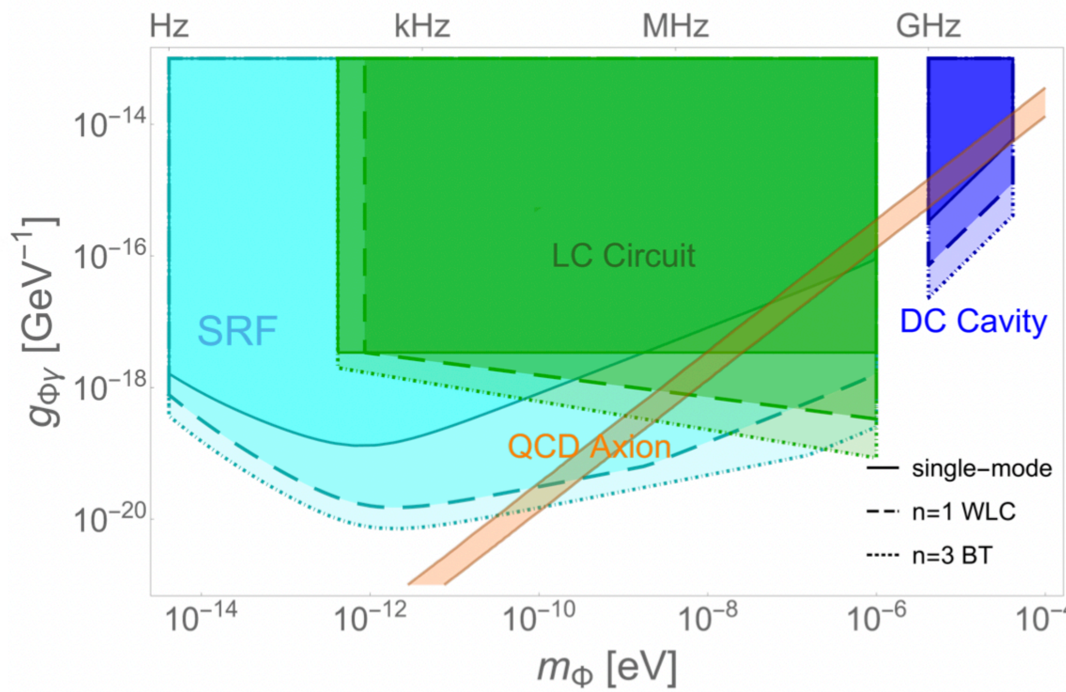

- Resonant and, at the same time, broadband.

Y-f. Chen, M-y. Jiang, Y-q Ma, J. Shu., Y-t. Yang, Phys.Rev.Res. 4 (2022) 2, 023015

- LC circuit: ineffective at low frequency due to large n_{occ}.
- High Q_{int} of SRF with BT can cover $m_\Phi >$ kHz QCD axion dark matter.

Increase the scan speed by 1000 times

Accelerated scan rate

Other models with similar effects has been proposed later

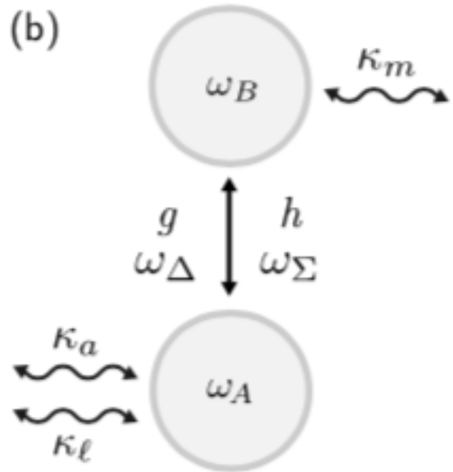

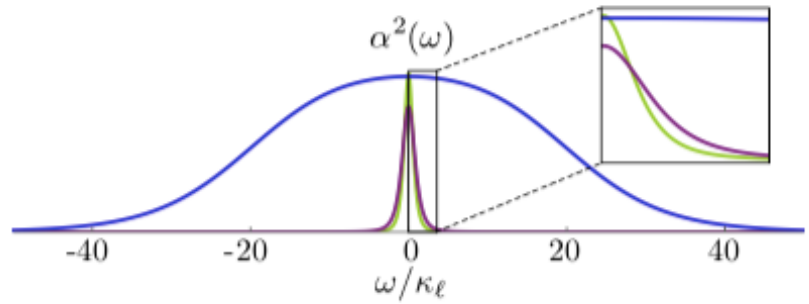

K. Wurtz, B. M. Brubaker, Y. Jiang, E. P. Ruddy, D. A. Palken and K. W. Lehnert, PRX Quantum 2 (2021) 4, 040350

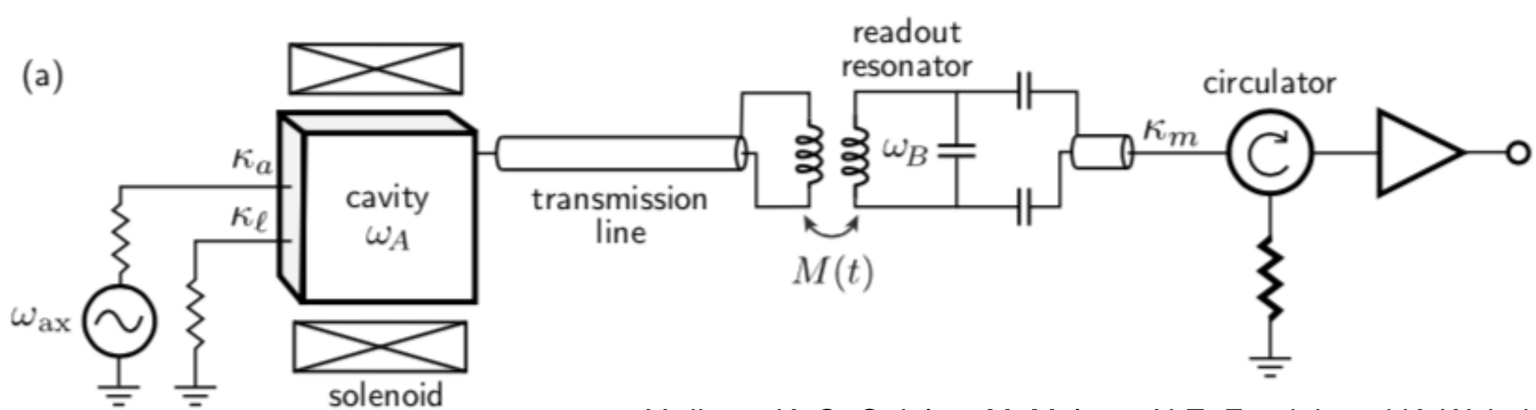

Y. Jiang, K. O. Quinlan, M. Malnou, N.E. Frattini, and K. W. Lehnert, PRX Quantum 4 (2023) 4, 020302

When squeezing the amplifier noise, the effective filter bandwidth of the cavity can be increased to many linewidths while maintaining constant Signal/(Cavity Noise) ratio

Cavity filters both signal and its own noise by the same Lorentzian transfer function.

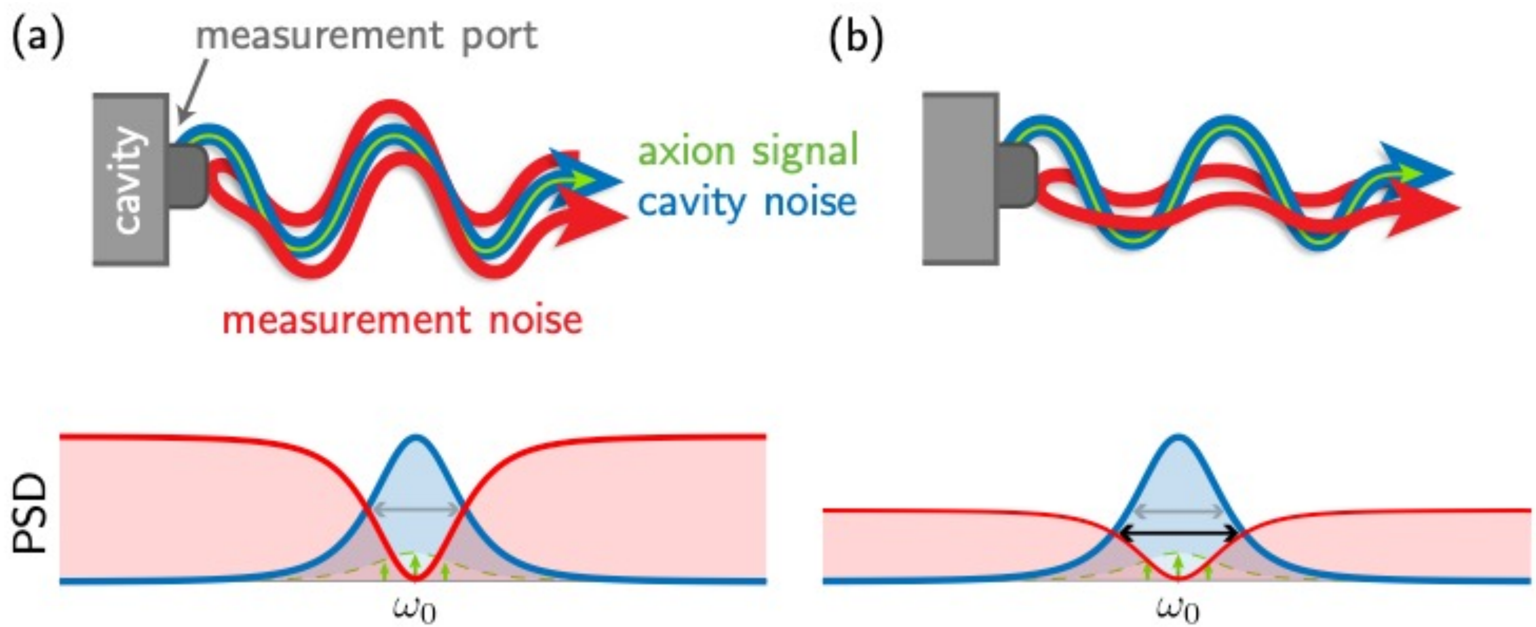

Figure from K.Wurtz, et.al, arXiv:2107.04147

Speeds up the radio scan rate since more frequencies can be simultaneously checked.

Quantum non-demolition “off-shell” sensors transduce photon occupation numbers into atomic frequency shifts

Index of refraction diagrams:

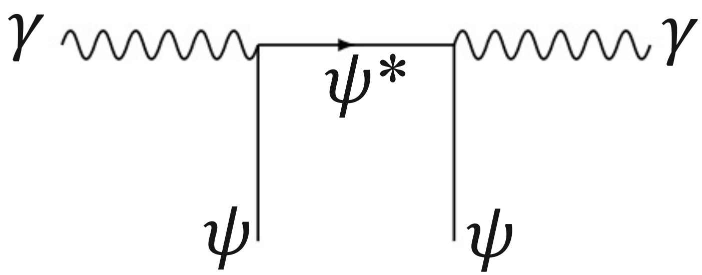

Photons slow down when passing through a dielectric medium

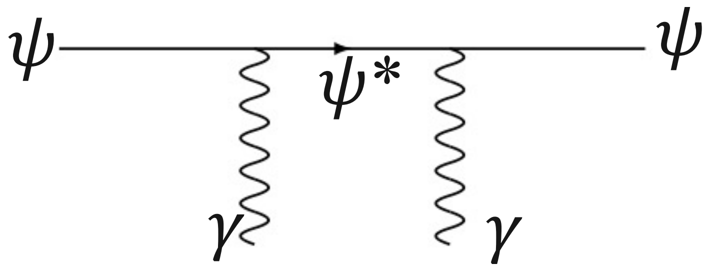

Atomic clocks slow down when interacting with a bath of background photons

The photon occupation number of the cavity mode is encoded as a frequency shift of the probe atom.

Being far off-resonance of ψ^* results in **no net absorption** of photons.

Quantum non-demolition: indirectly measure the same photon many times (via atom’s frequency shift) to achieve higher measurement fidelity.

Cavity QED again:
Use another cavity mode to measure atom's final state

Linear cavity
Bosonic oscillator,
Number operator = $a^\dagger a$

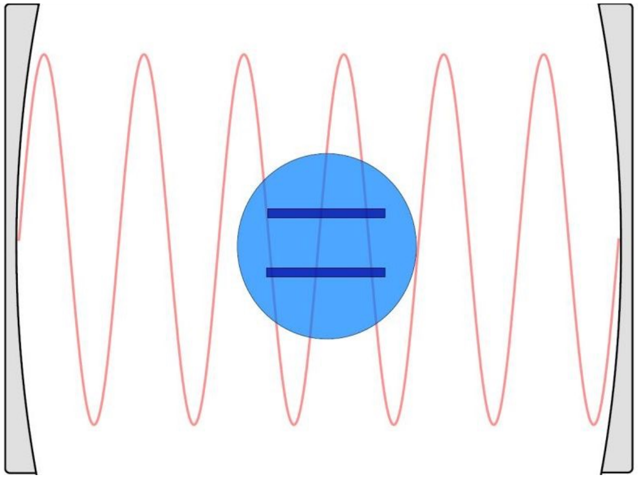

2-level "atom"
Fermionic oscillator,
Number operator = σ_z

$$g \approx \vec{d} \cdot \vec{E}_0 \approx d\sqrt{\omega/V}$$

$\Delta = \omega_r - \omega_a$

$$H \approx \hbar\omega_\mathrm{r}\left(a^\dagger a + 1/2\right) + \frac{\hbar}{2}\left(\omega_\mathrm{a} + \frac{2g^2}{\Delta}a^\dagger a + \frac{g^2}{\Delta}\right)\sigma_\mathrm{z}$$

Rewrite as:

$$H \approx \hbar\left(\omega_\mathrm{r} + \frac{g^2}{\Delta}\sigma_\mathrm{z}\right)\left(a^\dagger a + 1/2\right) + \frac{\hbar}{2}\left(\omega_\mathrm{a} + \frac{g^2}{\Delta}\right)\sigma_\mathrm{z}$$

The cavity mode's frequency also depends on the atom's occupation number (0 or 1)!
Measure cavity's frequency shift with many probe photons without disturbing the atom.

Quantum non-demolition measurements using atoms

Electric field of even a single trapped photon can “stretch” the atom and change its frequency. Just like tightening a violin string.

Serge Haroche 2012 Nobel prize: Measure the same photon with 100’s of atoms using Ramsey phase-shift interferometry

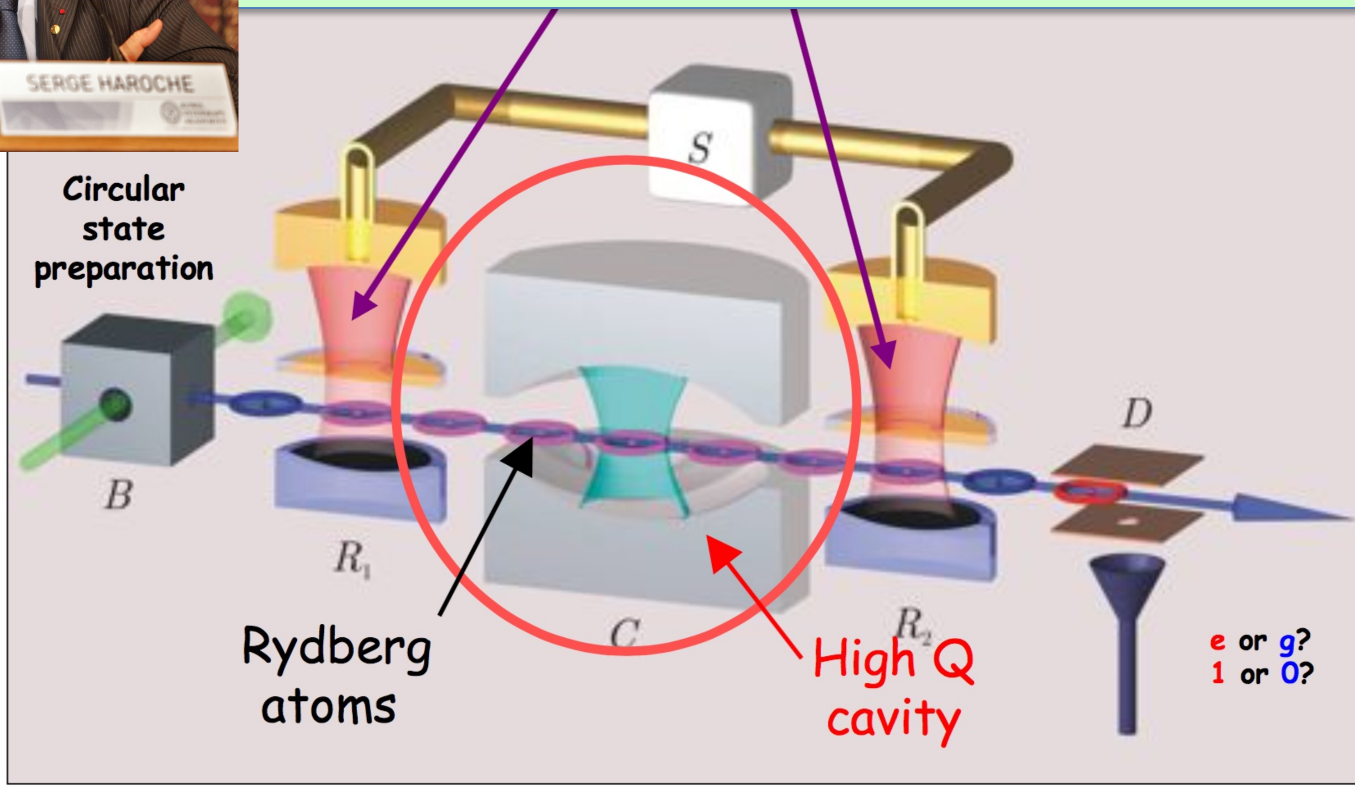

An atomic clock delayed by photons trapped inside

Quantum computing terminology: controlled phase (parity) gate

Any anharmonic oscillator exhibits 2-level system behavior and acts as a fermionic artificial atom

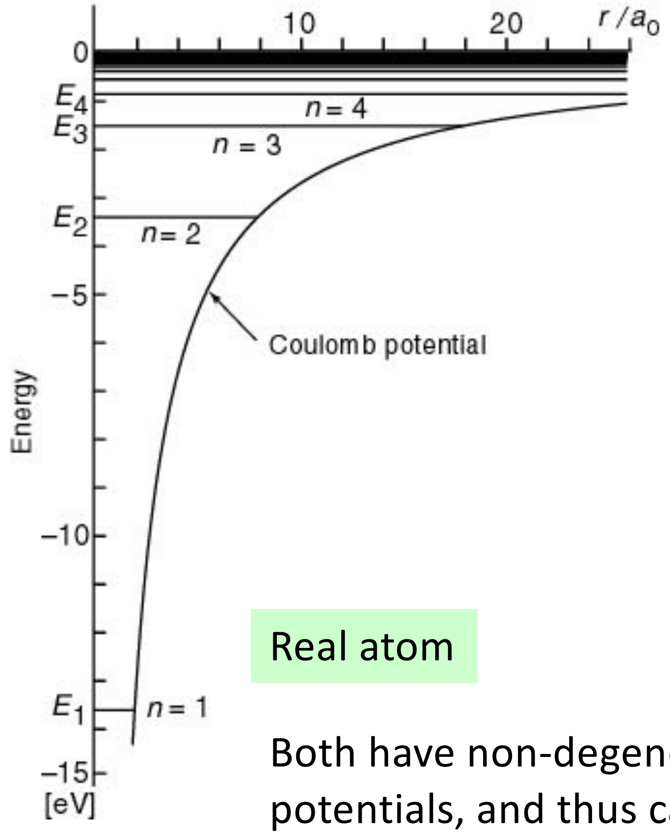

Real atom

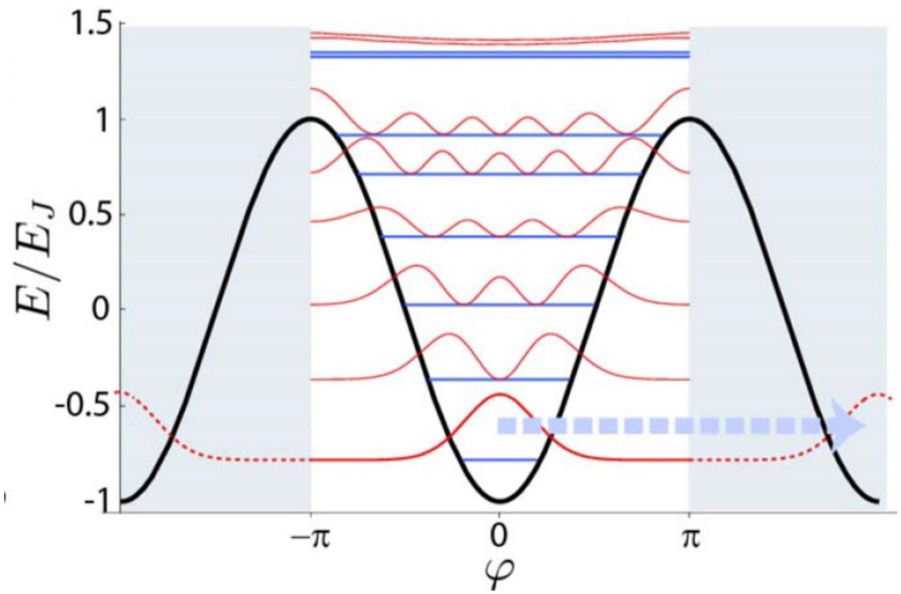

Artificial atom (Josephson junction oscillator)

Both have non-degenerate energy level spacings due to the nonlinear potentials, and thus can act as fermionic 2-level systems.

Jostling of the nonlinear oscillator due to electric fields from background photon fields result in frequency shifts as the restoring force changes for larger amplitude motion

→ Lamb shift from zero-point fluctuations

→ **quantized AC Stark shift from finite background photon occupation number**

Use artificial atoms made of superconducting “transmon” qubits to nondestructively sense photons

A.S. Chou, Dave Schuster, Akash Dixit, Ankur Agrawal, …

$$H \approx \hbar\omega_r a^\dagger a + \frac{\hbar}{2}(\omega_a' + 2\chi a^\dagger a)\sigma_z$$

Funded by

HEISING-SIMONS FOUNDATION

DOE QuantISED

Fermilab LDRD

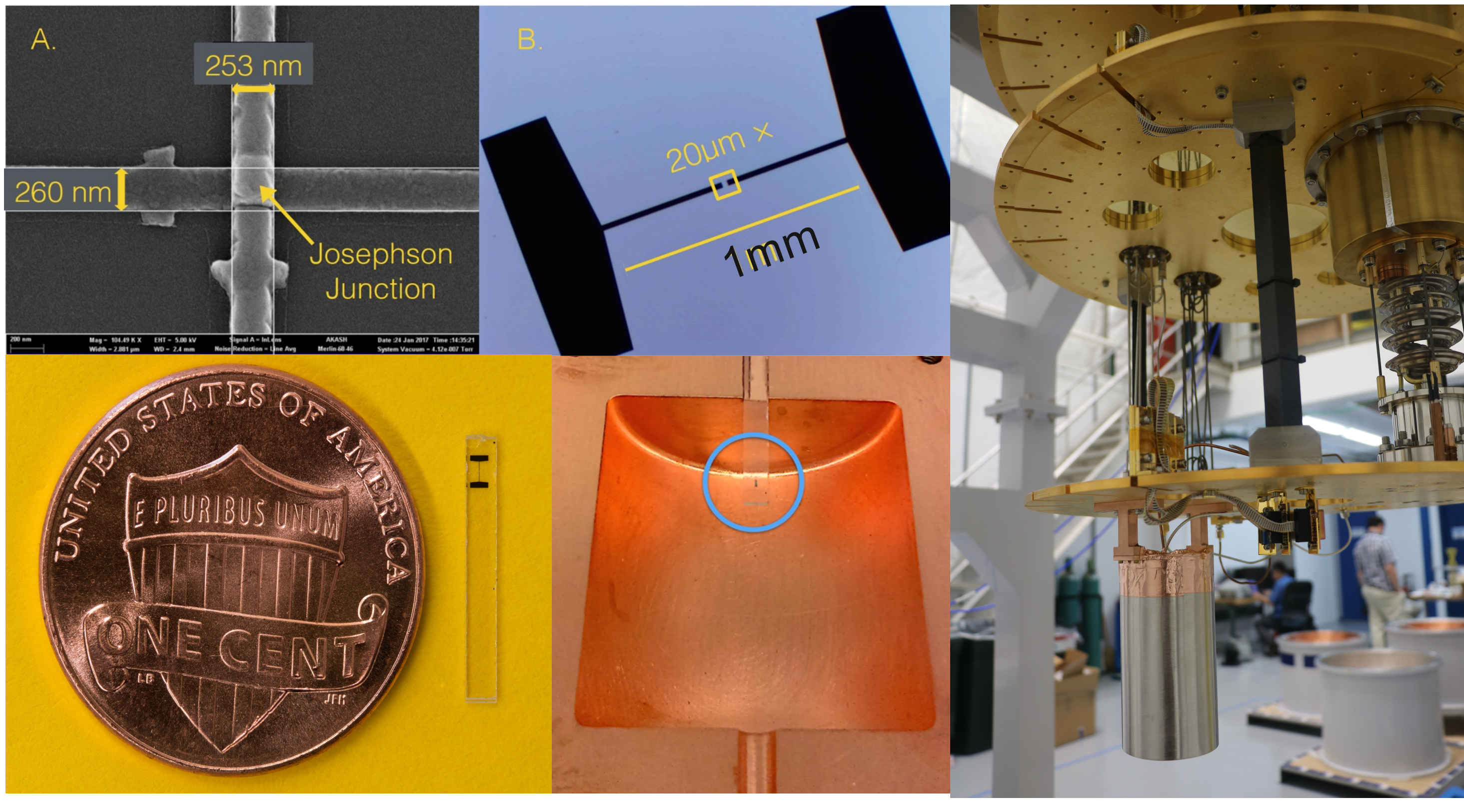

The electric field of individual photons exercises the nonlinear inductance of the Josephson junction. **Photon number is transduced into frequency shifts of the $|g\rangle \rightarrow |e\rangle$ transition.** Same as Lamb shift, but for finite photon number.

Single photon resolution:

Measure qubit $|g\rangle \rightarrow |e\rangle$ transition frequencies while weakly driving the primary cavity mode into a Glauber state with <n>=1

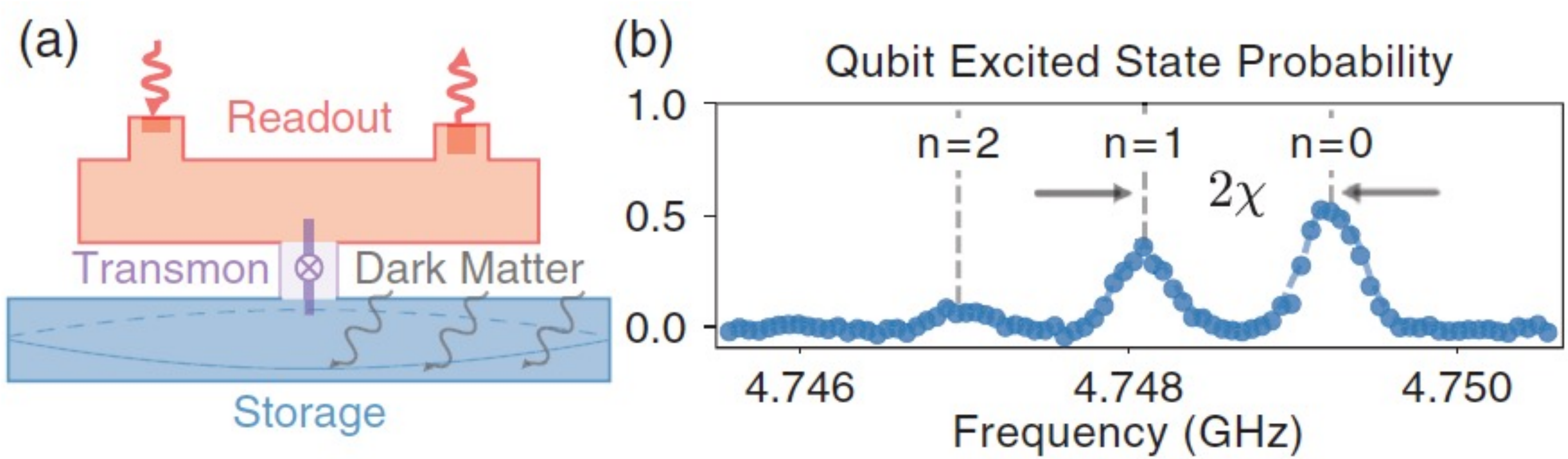

After displacing cavity with a sinusoidal drive, the measured qubit spectrum exhibits a distribution of resonances which are in 1-1 correspondence with the Poisson distribution of the cavity's coherent state.

Non-destructively count photons by measuring the qubit's quantized frequency shift.

Perform Ramsey interferometry with the oscillating qubit "clock" to measure cavity photon number parity

Just like asking in an oscillation experiment, do the neutrinos see "matter effects" or not?
If there is a photon, the clock runs slow. If no photon, the clock runs fast.

Bloch sphere:
Map qubit states
to spin ±1/2

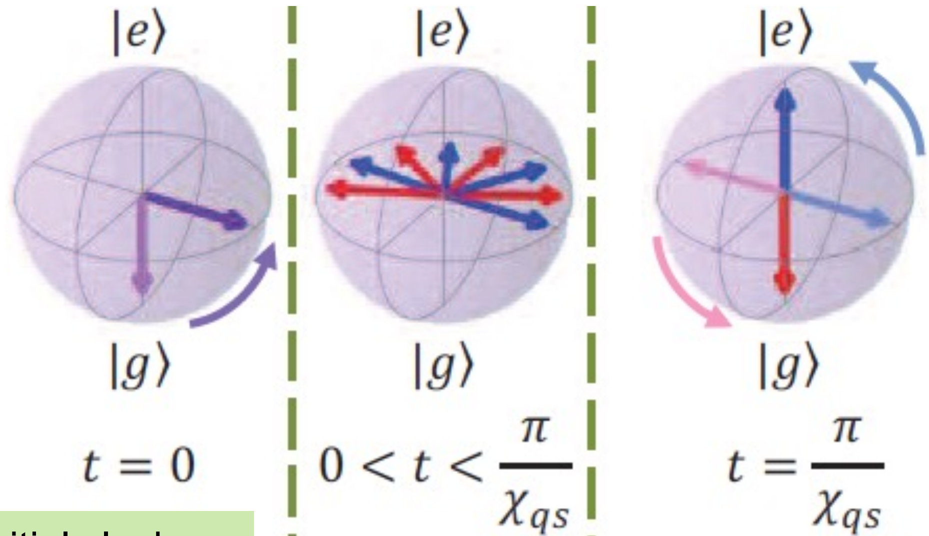

Prepare initial clock state with $\pi/2$ pulse to give $|g\rangle + |e\rangle$ state

Evolve system to accumulate π phase difference over Stark period

Analyze with final $\pi/2$ pulse to map:
Even N → $|g\rangle$
Odd N → $|e\rangle$

The qubit's "spin" flips only if a cavity photon is present.

Measure final qubit state $|g\rangle$ *or* $|e\rangle$ via freq. shift of an auxiliary cavity mode.

Parity measurement maps cavity state onto qubit

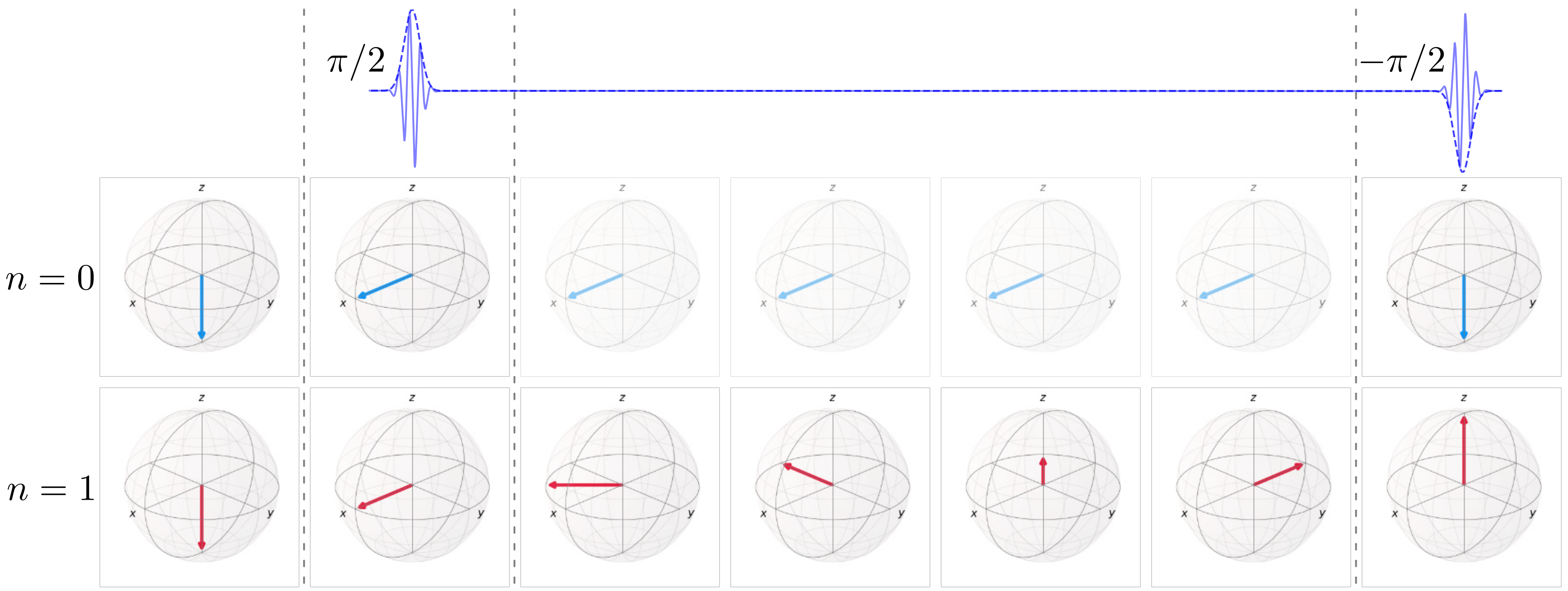

Signature of a single signal photon is many sequential successful qubit "spin-flips" from $|g\rangle \leftrightarrow |e\rangle$

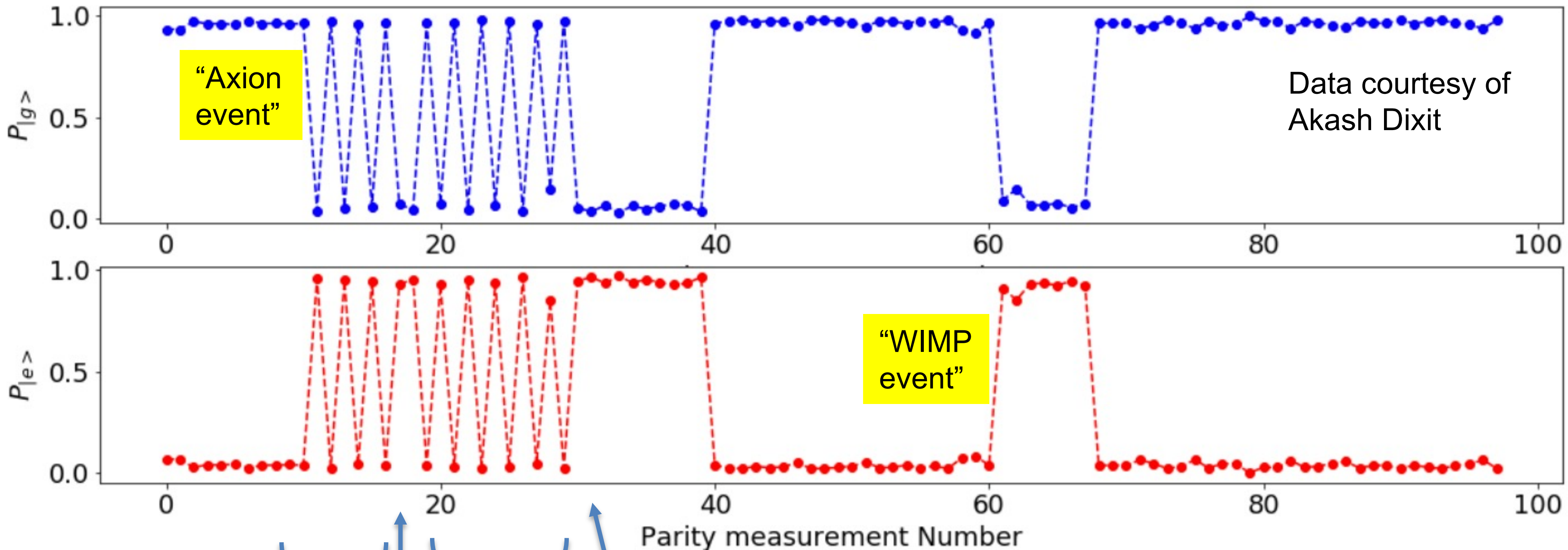

Single photon injected, repeated successful qubit spin flips

Failed spin-flip = readout error

More successful readouts

Photon decays, qubit stuck in $|e\rangle$ state

Qubit decays

Many failed spin-flips indicate that no photon is present.

Qubit spontaneously excited and then decays. Does not mimic photon event since subsequent spin-flip attempts fail.

Trigger on photons by placing threshold on MCMC probability ratio Prob(γ)/Prob(no γ) for observed spin-flip sequence

Akash V. Dixit, et.al, Phys.Rev.Lett. 126, 141302 (2021)

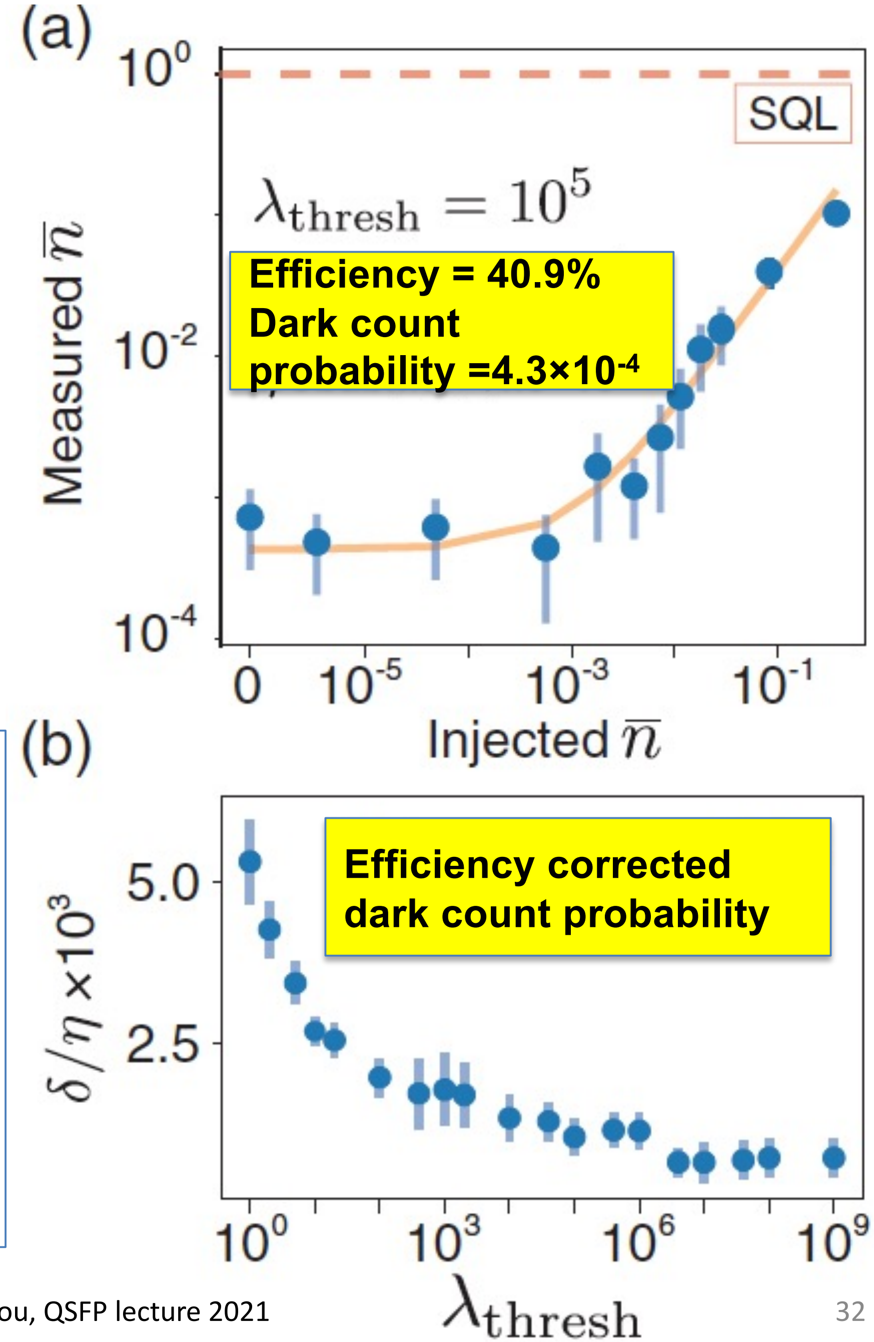

Background = few 10^{-3} of leakage photons per measurement.

Compare to amplifier readout which gives +/- 1 photon of zero-point variance per measurement.

Noise equivalent of 15.7 dB of squeezing!

Vacuum state 2008.12231

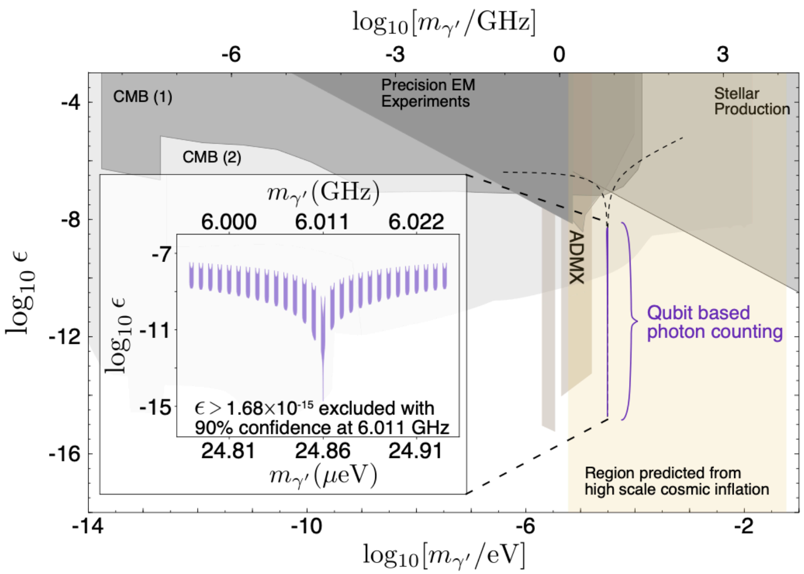

Improved SRF Q by 1 order by using Nb instead of Al

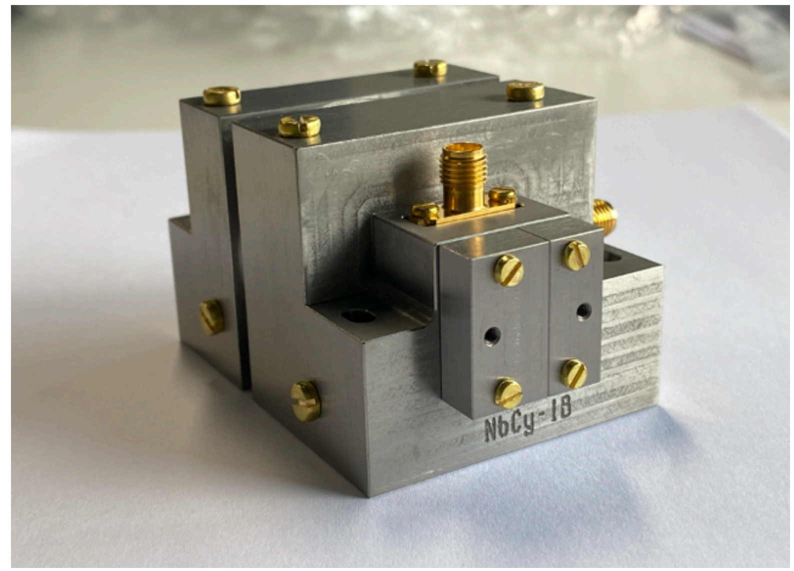

Fock state 2305.03700

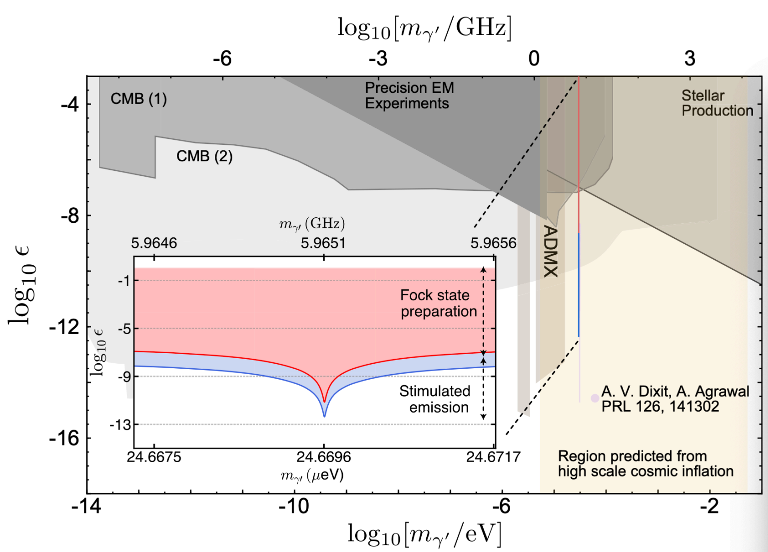

Better measurements by using the cat-like states

Our new results ~ 10^{-16}

So what do we do for even higher frequencies?

Figure adapted from DOE "Small Dark Matter" BRN Study, 2018

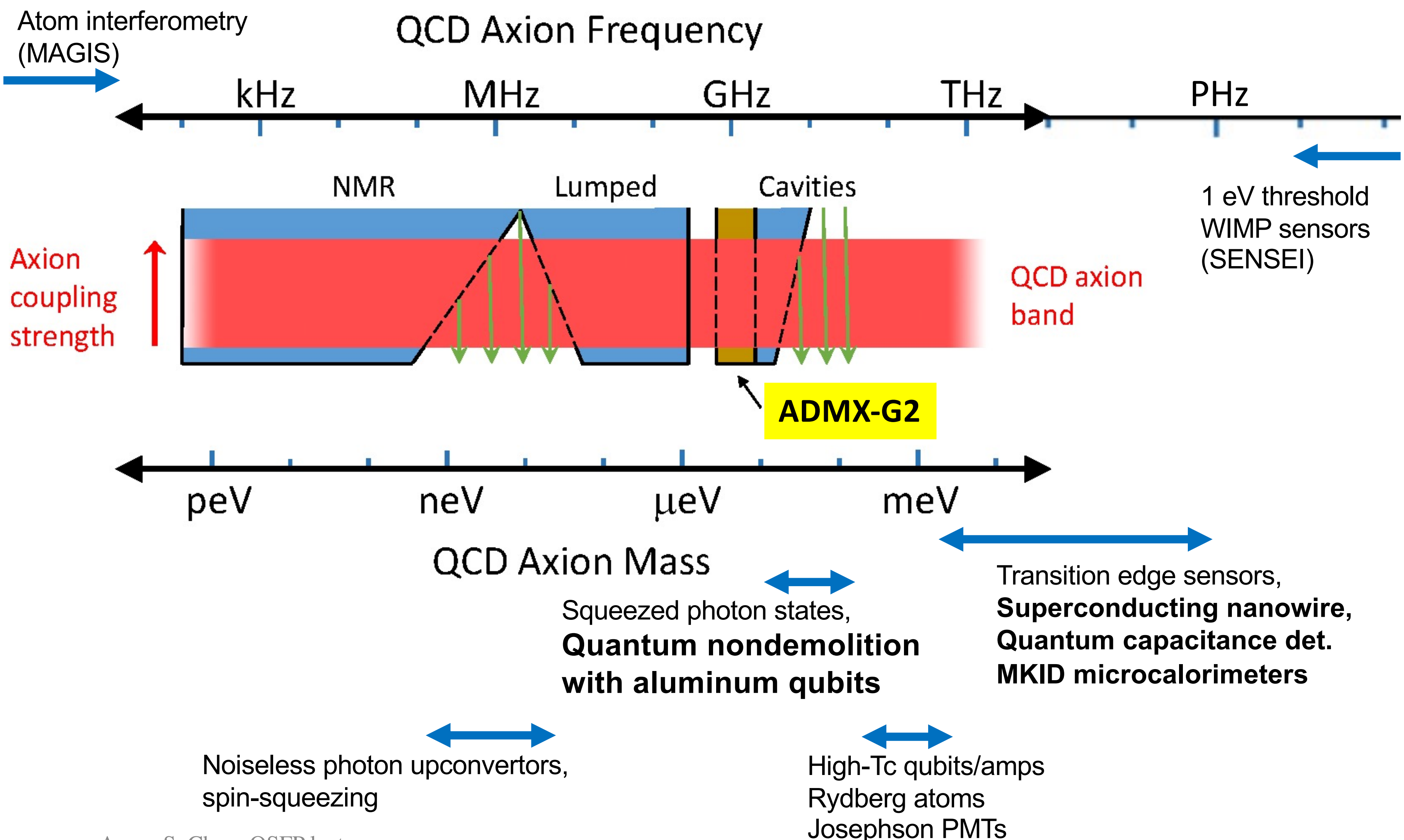

One can instead use a huge dish antenna whose area contains many wavelength-squared pixels

D. Horns, et.al, JCAP 1304, 016 (2013)

This is like having an array of N cavities, where each cavity only gets 1 bounce.

Axion emits transition radiation upon impedance mismatch.

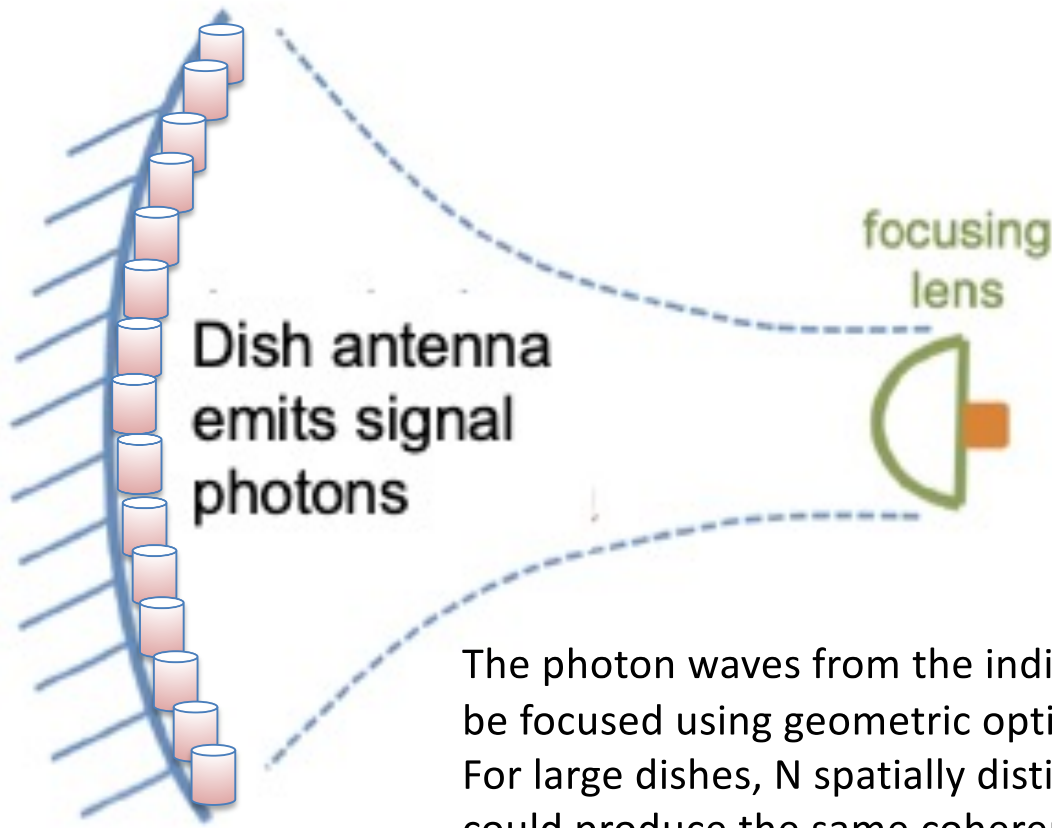

The photon waves from the individual pixels can be focused using geometric optics.
For large dishes, N spatially distinct emitters could produce the same coherent sum as that of Q bounces inside a resonant cavity.

Since the axion can convert into photons when encountering any interface which breaks translation symmetry, we can also use many dielectric plates

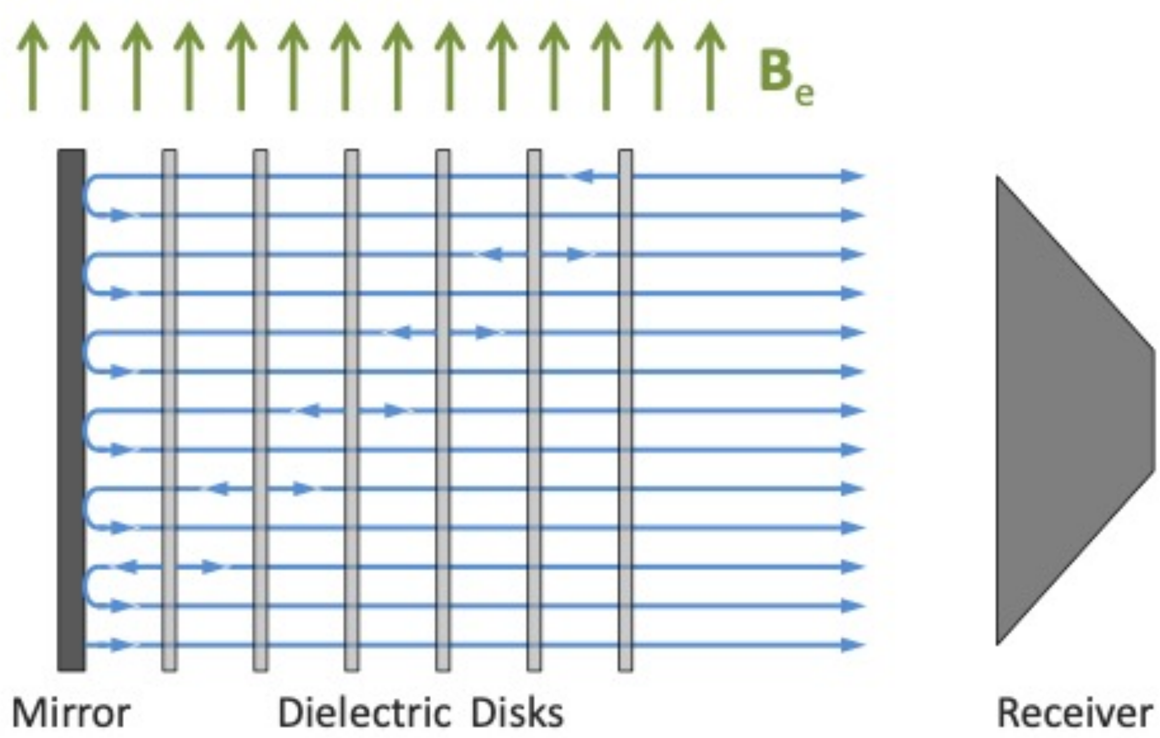

MADMAX idea,
A. Caldwell, et.al, Phys. Rev. Lett. 118, 091801 (2017)

However, for achievable magnetic fields, the photon signal rate is low

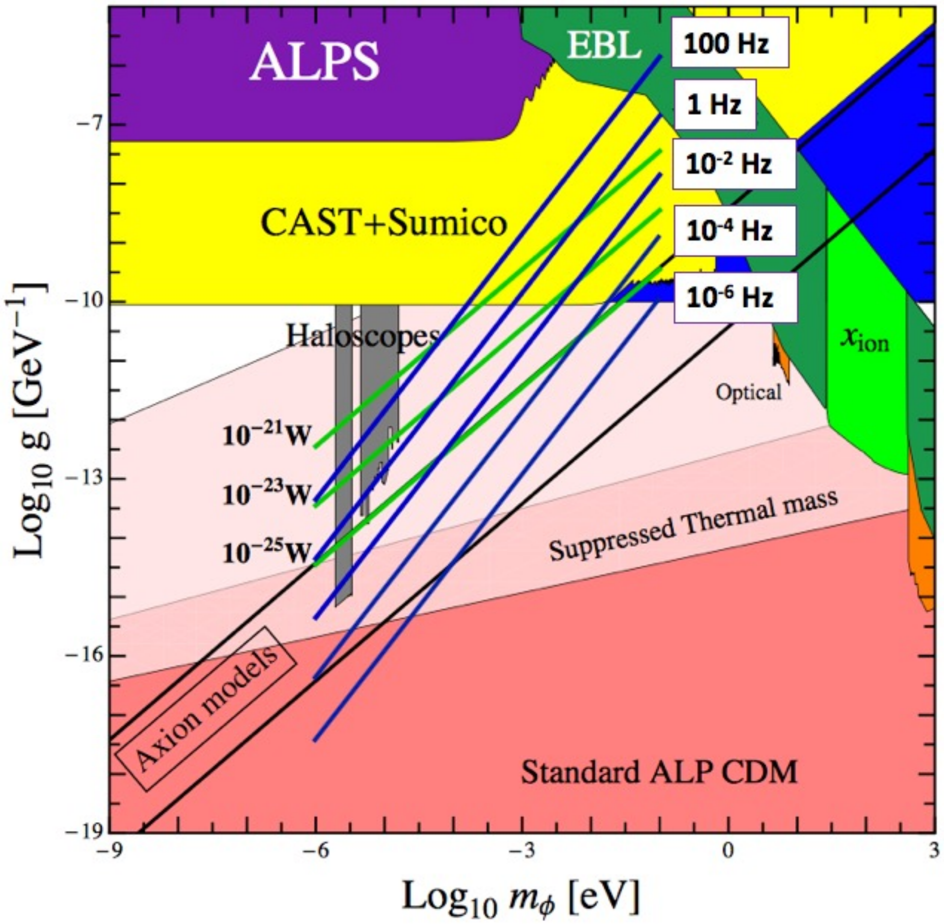

Figure adapted from Horns et.al (2012)

These will be long duration experiments, and we do not yet have the single photon detection technology with sufficiently low dark rates.

Cavity detectors (e.g. ADMX)

1 eV threshold particle detectors (e.g. SENSEI)

Need better sensors

Aaron S. Chou, QSFP lecture 2021

Dark counts probably not cosmic rays – observed 10^{-2} Hz rate in qubit CPU's is too low

Resolving catastrophic error bursts from cosmic rays in large arrays of superconducting qubits

Matt McEwen,[1,2] Lara Faoro,[3] Kunal Arya,[2] Andrew Dunsworth,[2] Trent Huang,[2] Seon Kim,[2] Brian

M. McEwen, et.al, arXiv:2104.05219

Google Sycamore chip already functions as a phonon detector with 100% chip-wide failure in response to ionizing radiation events which can be localized in both space and time

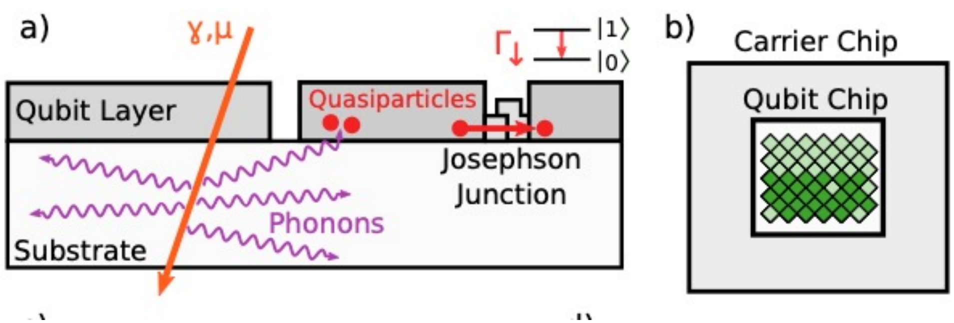

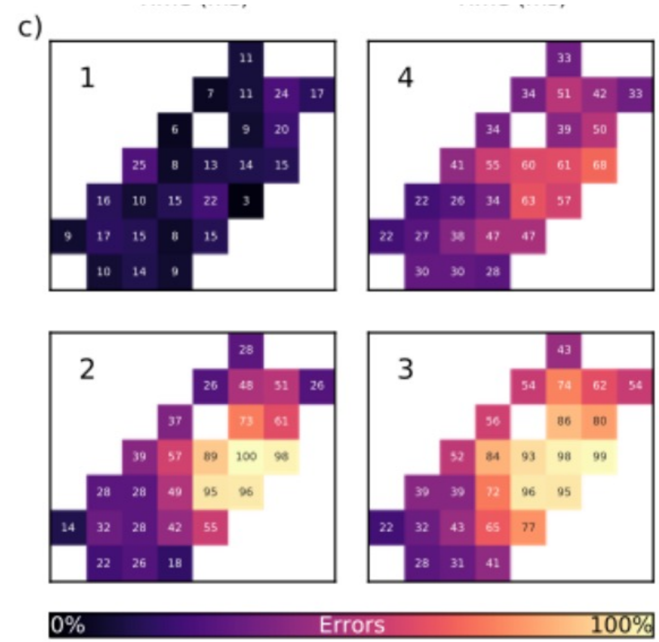

Figure 3. **Localization and spread of error.** (a-b) Time-

Eventually axion experiments will have to move underground just like WIMP experiments, but cosmic rays are not currently the dominant background.

Superconducting devices all suffer from mysterious non-equilibrium quasiparticle population

These now appear to be created in discrete, time-resolved events.

E.T. Mannila, et.al, arXiv:2102.00484 *(2021)*

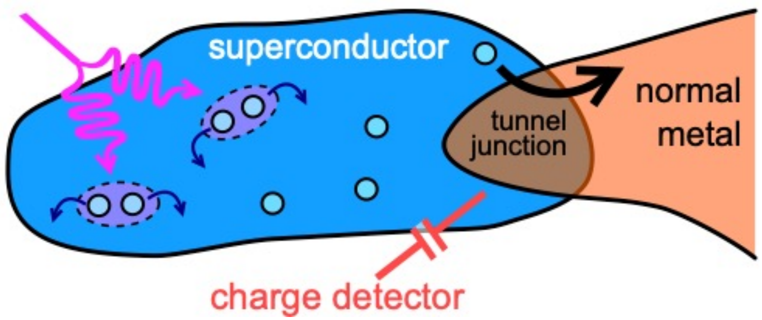

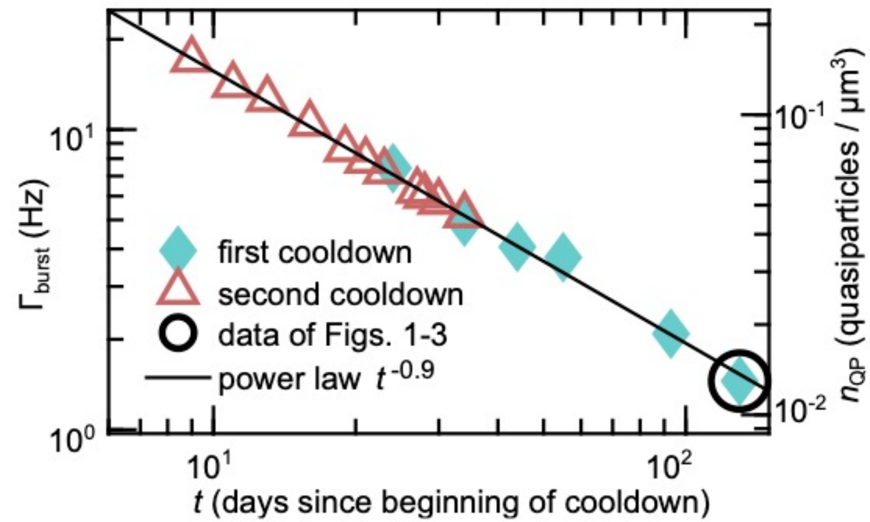

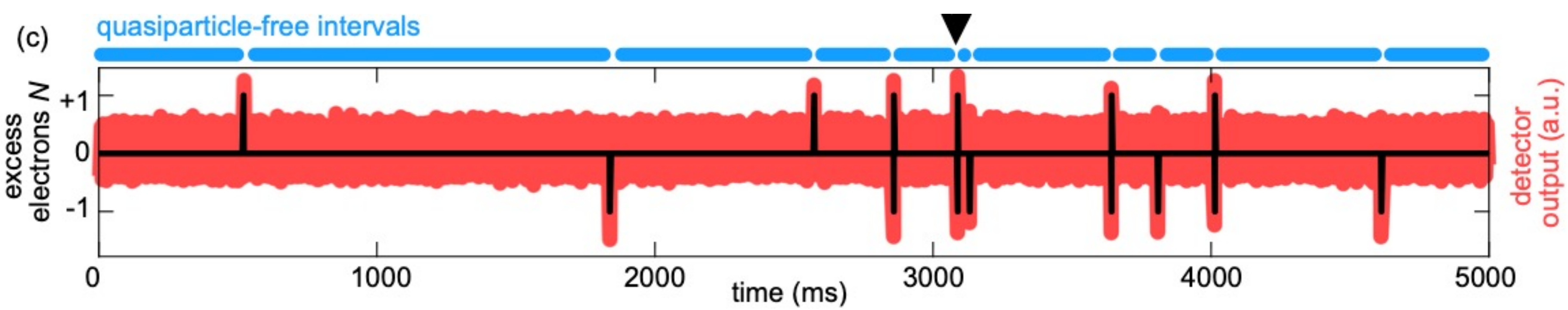

Origins of events still a 20-year-old mystery….

Cosmic ray detection from Q Qbits

Nature 584, 551-556 (2020)

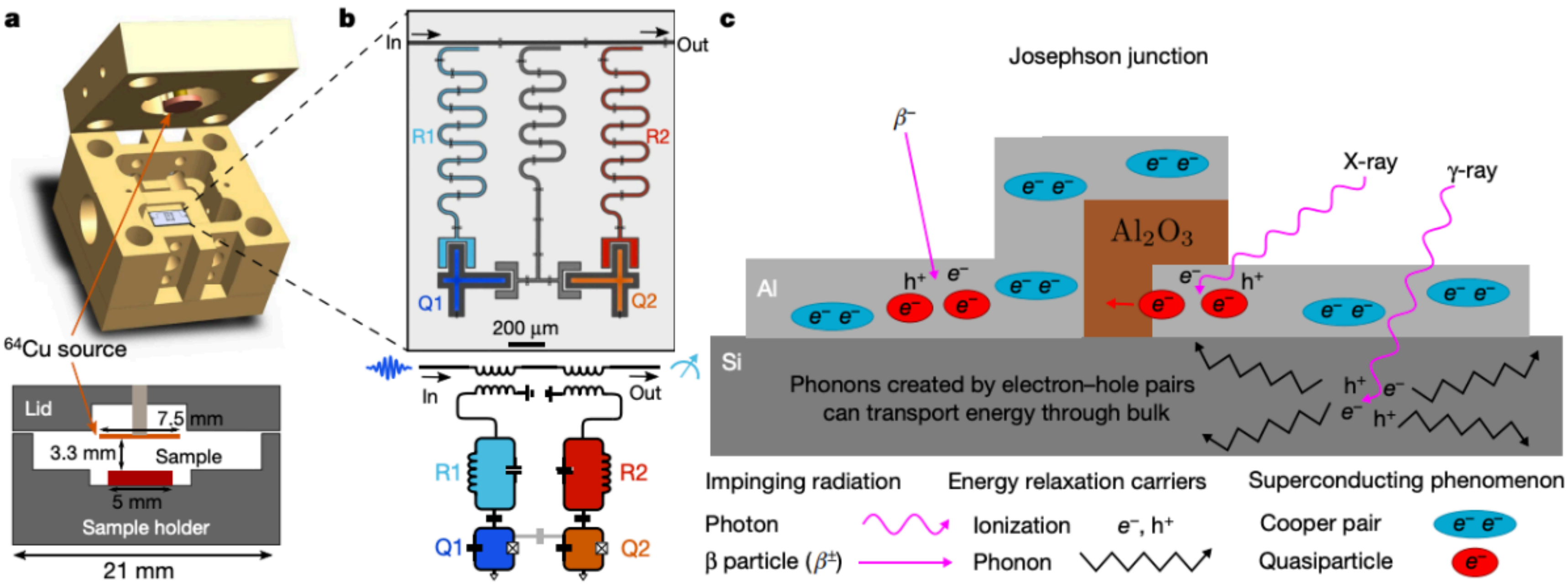

Cosmic rays ionize the substrate to produce electron-hole pairs, which subsequently generate phonons.

These phonons in superconducting materials break Cooper pairs to produce quasiparticles, and the tunneling of these quasiparticles generates signals in quantum bits.

Q Qbit signals

Charge-parity jumps

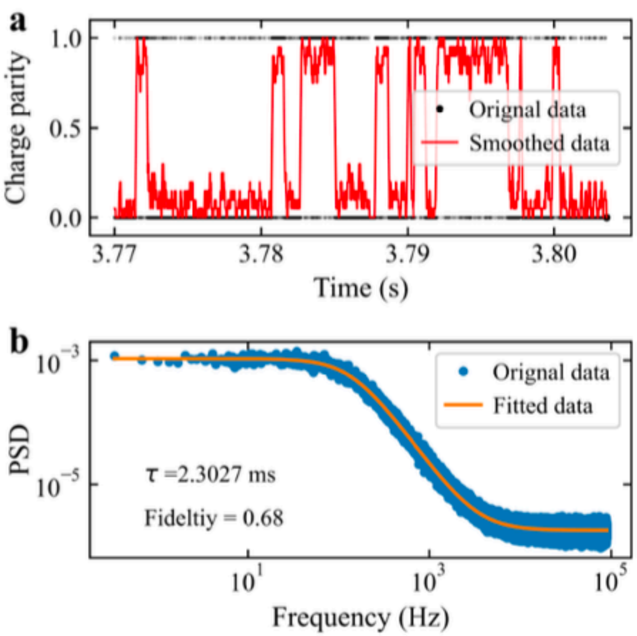

Quasiparticle tunneling causes a change in the charge parity on both sides of the Josephson junction.

Spin flips

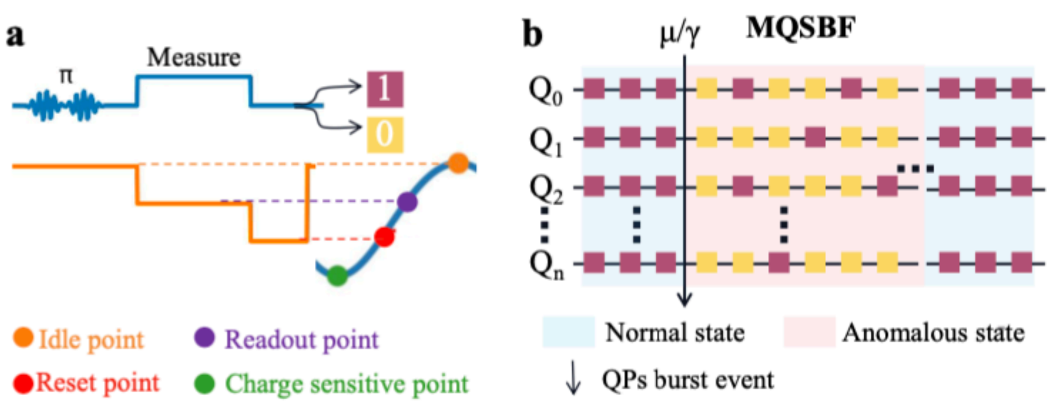

Quasiparticle tunneling also induces a change in the eigenstates of the quantum bit.

Signals

Cosmic rays are all signals

Signal are not all cosmic rays

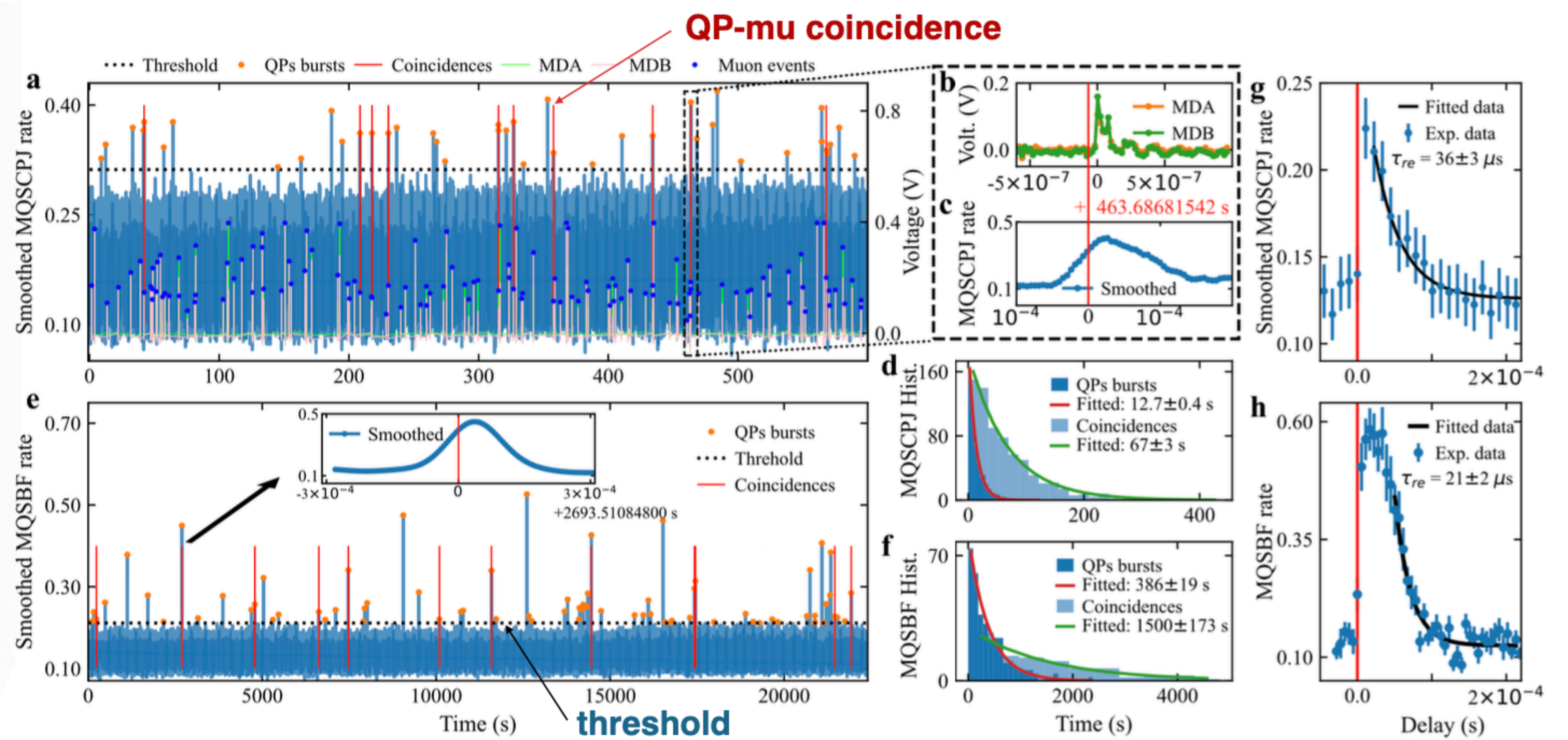

Dark matter and quantum qubits

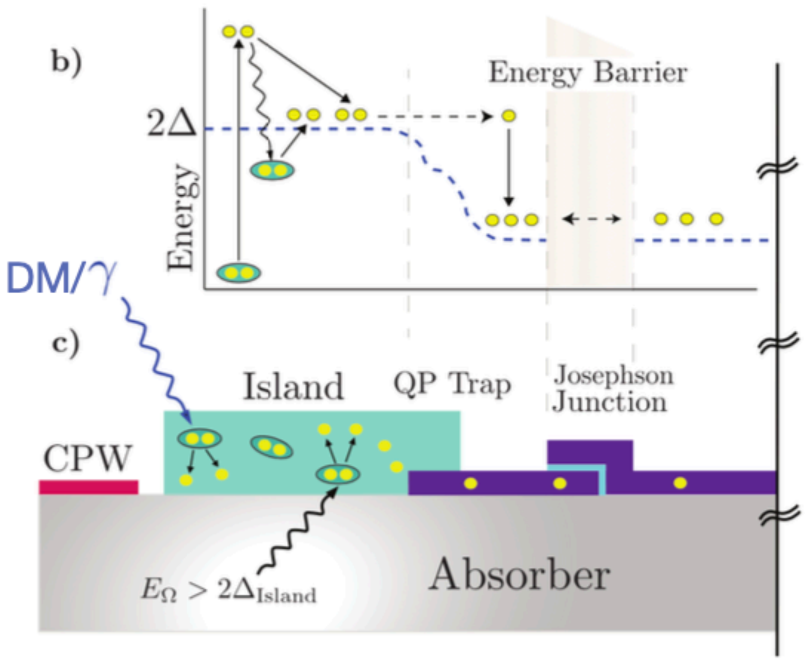

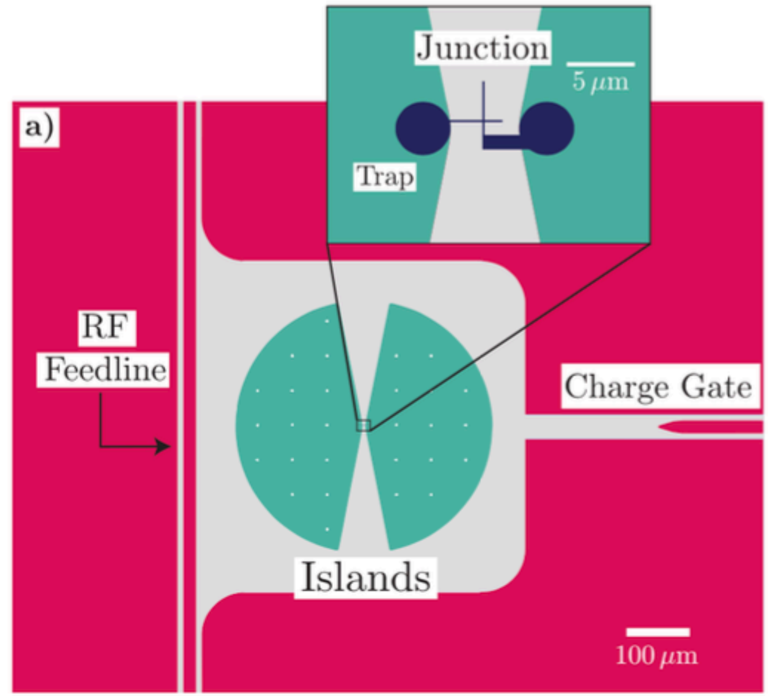

Dark matter scatters in the substrate to produce phonons, which in turn generate quasiparticles in the superconducting film. The tunneling of these quasiparticles generates signals in the quantum bit.

Dark counts in deep underground

Evaluating radiation impact on transmon qubits in above and underground facilities

Francesco De Dominicis,[1,2,*] Tanay Roy *,[3,†] Ambra Mariani,[4,‡] Mustafa Bal,[3] Nicola Casali,[4]
Ivan Colantoni,[4] Francesco Crisa,[5] Angelo Cruciani,[4] Fernando Ferroni,[1,4] Dounia L Helis,[2]
Lorenzo Pagnanini,[1,2] Valerio Pettinacci,[4] Roman M Pilipenko,[3] Stefano Pirro,[2] Andrei Puiu,[2]
Alexander Romanenko,[3] David v Zanten,[3] Shaojiang Zhu,[3] Anna Grassellino,[3] and Laura Cardani[4]

[1] *Gran Sasso Science Institute*
[2] *INFN, Laboratori Nazionali del Gran Sasso*
[3] *Superconducting Quantum Materials and Systems Division, Fermi National Accelerator Laboratory (FNAL), Batavia, IL 60510, USA*
[4] *INFN, Sezione di Roma*
[5] *Illinois Institute of Technology*
(Dated: May 29, 2024)

Fermilab SQMS to Gran Sasso Laboratory (INFN-LNGS, Italy).

Still there are unknown dark counts…..

中国锦屏地下实验室
China Jinping Underground Laboratory
CJPL
清华大学 · 雅砻江流域水电开发有限公司

北京量子信息科学研究院
Beijing Academy of Quantum Information Sciences

Aiming for low threshold quantum qubits DM detection

Proposed spin flip measurements under Jinping underground laboratory.

Collaboration of JinPing Deep Underground Quantum Instrument Experimental (CJPDUQIE)

Summary and Outlooks

Summary

- Astronomers discovered the "dark matter problem" nearly a century ago, but what DM is remains an unsolved mystery.

- Exploring the physical nature of DM is a long and challenging journey. (Enjoyable as a scientist?)

- Discovering the existence or non-existence of DM would both be a significant breakthrough, likely triggering a new revolution in physics (fundamental science).

Thanks!

Modern astronomy plays an increasingly prominent role in science

Since 1936, 28 people in the field of astrophysics have won the Nobel Prize in Physics 13 times in 17 categories

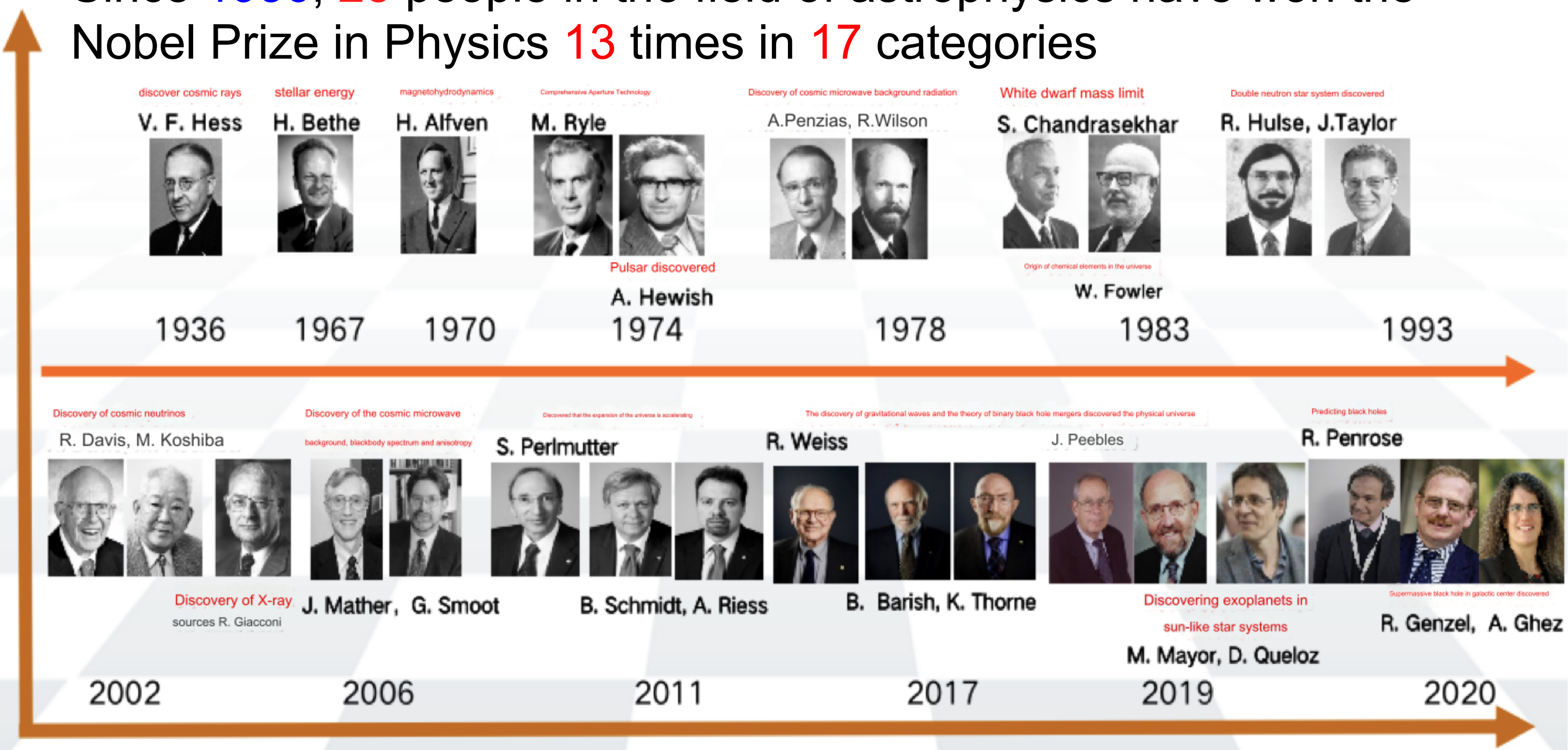

Can we expect the discovery of DM? Or something else?

Backup slice